



US010646130B2

(12) **United States Patent**
Chen et al.

(10) **Patent No.:** **US 10,646,130 B2**
(45) **Date of Patent:** **May 12, 2020**

(54) **METHOD FOR RECOGNIZING POINT QUANTIFICATION STANDARD ELEVATION OR DEPRESSION NEAR THE EQUIPOTENTIAL LINE OF EACH HEARTBEAT**

(71) Applicants: **Guangren Chen**, Acadia, CA (US);
Rong Yang, Porter Ranch, CA (US)

(72) Inventors: **Guangren Chen**, Acadia, CA (US);
Rong Yang, Porter Ranch, CA (US)

(*) Notice: Subject to any disclaimer, the term of this patent is extended or adjusted under 35 U.S.C. 154(b) by 148 days.

(21) Appl. No.: **16/114,025**

(22) Filed: **Aug. 27, 2018**

(65) **Prior Publication Data**
US 2019/0015006 A1 Jan. 17, 2019

(63) **Related U.S. Application Data**
Continuation-in-part of application No. 15/998,487, filed on Aug. 16, 2018, which is a (Continued)

(51) **Int. Cl.**
A61B 5/04 (2006.01)
A61B 5/0408 (2006.01)
A61B 5/0402 (2006.01)
A61B 5/044 (2006.01)
A61B 5/00 (2006.01)
(Continued)

(52) **U.S. Cl.**
CPC *A61B 5/0408* (2013.01); *A61B 5/044* (2013.01); *A61B 5/04012* (2013.01); *A61B 5/04023* (2013.01); *A61B 5/0452* (2013.01); *A61B 5/725* (2013.01); *A61B 5/7257* (2013.01); *A61B 5/0245* (2013.01); *A61B 5/0456* (2013.01); *A61B 5/0464* (2013.01); *A61B 5/0468* (2013.01);
(Continued)

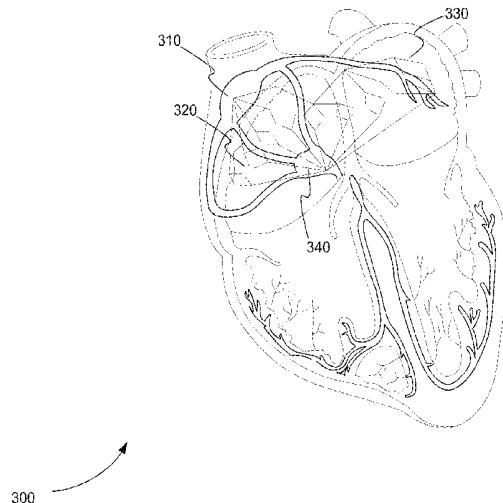
(58) **Field of Classification Search**
CPC *A61B 5/0245*; *A61B 5/04012*; *A61B 5/04023*; *A61B 5/0408*; *A61B 5/044*; *A61B 5/0452*; *A61B 5/0456*; *A61B 5/0464*; *A61B 5/0468*; *A61B 5/0472*; *A61B 5/6823*; *A61B 5/725*; *A61B 5/7257*; *A61B 5/7267*
See application file for complete search history.

(56) **References Cited**
U.S. PATENT DOCUMENTS
2009/0112106 A1* 4/2009 Zhang *A61B 5/0452* 600/509
* cited by examiner

Primary Examiner — George Manuel
(74) *Attorney, Agent, or Firm* — John R. Kasha; Kelly L. Kasha; Kasha Law LLC

(57) **ABSTRACT**
An ECG system measures and annotates the P-point of an ECG waveform from harmonic waveforms. Electrical impulses are received from a beating heart. The electrical impulses are converted to an ECG waveform. The ECG waveform is converted to a frequency domain waveform, which, in turn, is separated into two or more different frequency domain waveforms, which, in turn, are converted into a plurality of time domain cardiac electrophysiological subwaveforms and discontinuity points between these subwaveforms. The plurality of subwaveforms and discontinuity points are compared to a database of subwaveforms and discontinuity points for normal and abnormal patients. A discontinuity point is identified as the P-point of the ECG waveform from the comparison. Similar measurements are made for the P'-point, I-point, J-point, and T'-point. Distances from these points to the equipotential line are calculated and used to detect blockages leading to myocardial infarction.

20 Claims, 82 Drawing Sheets



Related U.S. Application Data

- continuation-in-part of application No. 15/961,952, filed on Apr. 25, 2018, now Pat. No. 10,092,201, which is a continuation-in-part of application No. 15/904,543, filed on Feb. 26, 2018, now Pat. No. 10,085,663, which is a continuation-in-part of application No. 15/393,135, filed on Dec. 28, 2016, now Pat. No. 9,999,364, which is a continuation-in-part of application No. 14/749,697, filed on Jun. 25, 2015, now Pat. No. 9,538,930, which is a continuation-in-part of application No. 14/662,996, filed on Mar. 19, 2015, now Pat. No. 9,339,204, which is a continuation of application No. PCT/US2015/020828, filed on Mar. 16, 2015.
- (60) Provisional application No. 62/008,435, filed on Jun. 5, 2014, provisional application No. 62/017,185, filed on Jun. 25, 2014, provisional application No. 62/271,699, filed on Dec. 28, 2015, provisional application No. 62/271,704, filed on Dec. 28, 2015, provisional application No. 62/463,662, filed on Feb. 26, 2017, provisional application No. 62/489,540, filed on Apr. 25, 2018, provisional application No. 62/546,461, filed on Aug. 16, 2017, provisional application No. 62/551,759, filed on Aug. 29, 2017.
- (51) **Int. Cl.**
A61B 5/0452 (2006.01)
A61B 5/0456 (2006.01)
A61B 5/0472 (2006.01)
A61B 5/0464 (2006.01)
A61B 5/0245 (2006.01)
A61B 5/0468 (2006.01)
- (52) **U.S. Cl.**
CPC *A61B 5/0472* (2013.01); *A61B 5/6823* (2013.01); *A61B 5/7267* (2013.01)

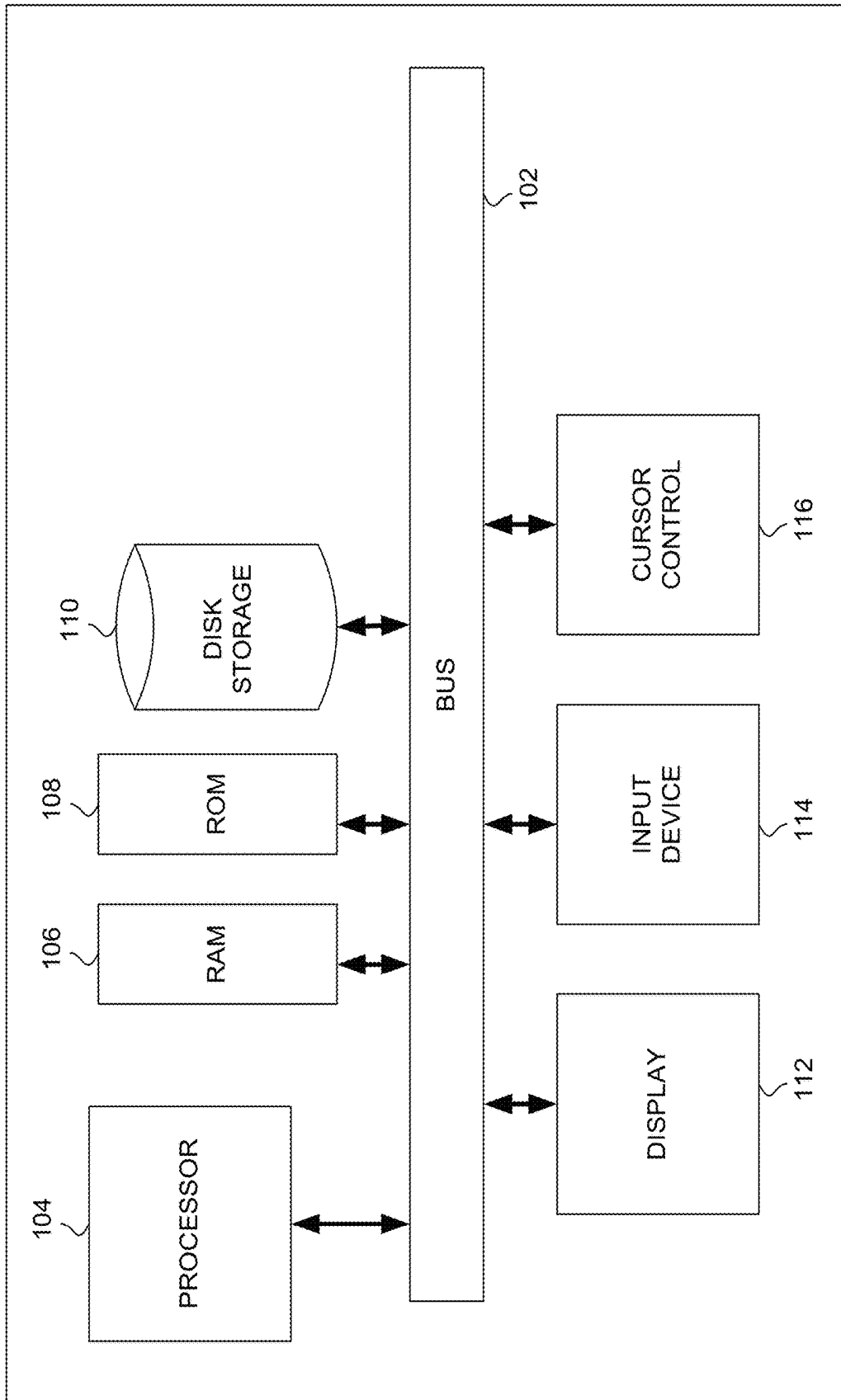
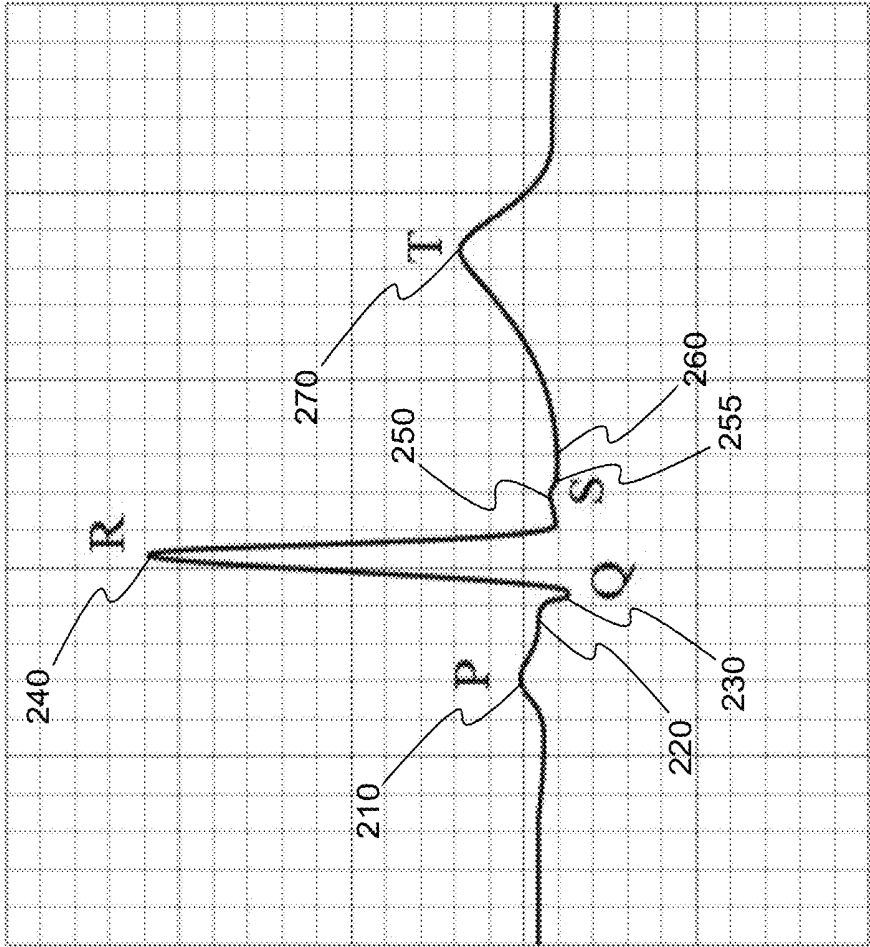


FIG. 1

100



(PRIOR ART)

FIG. 2

200

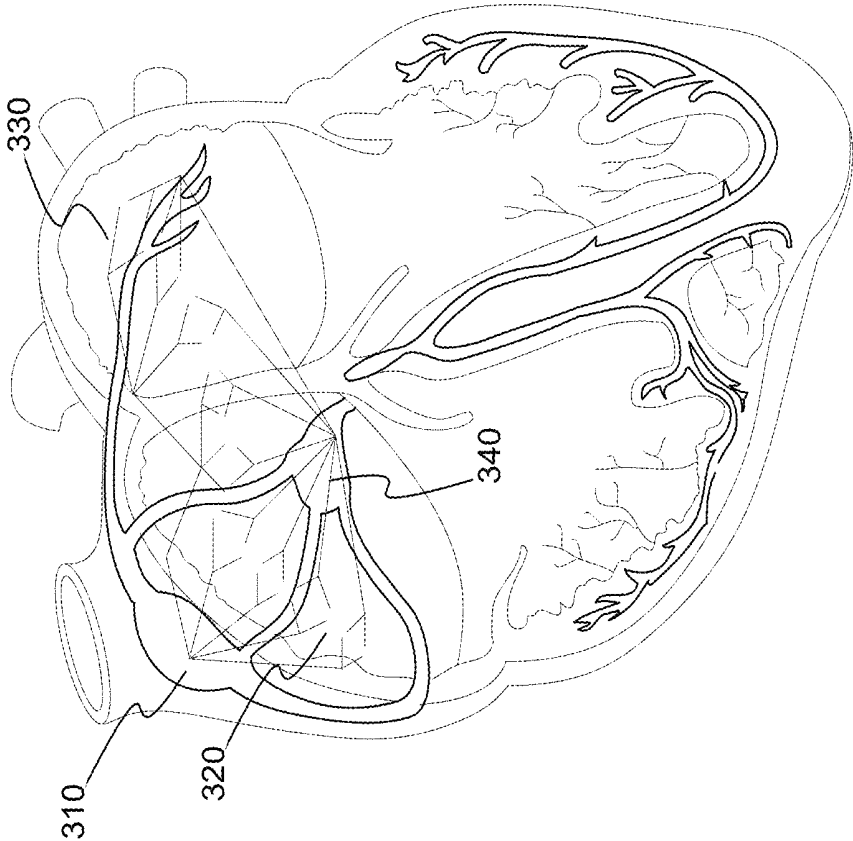


FIG. 3



300

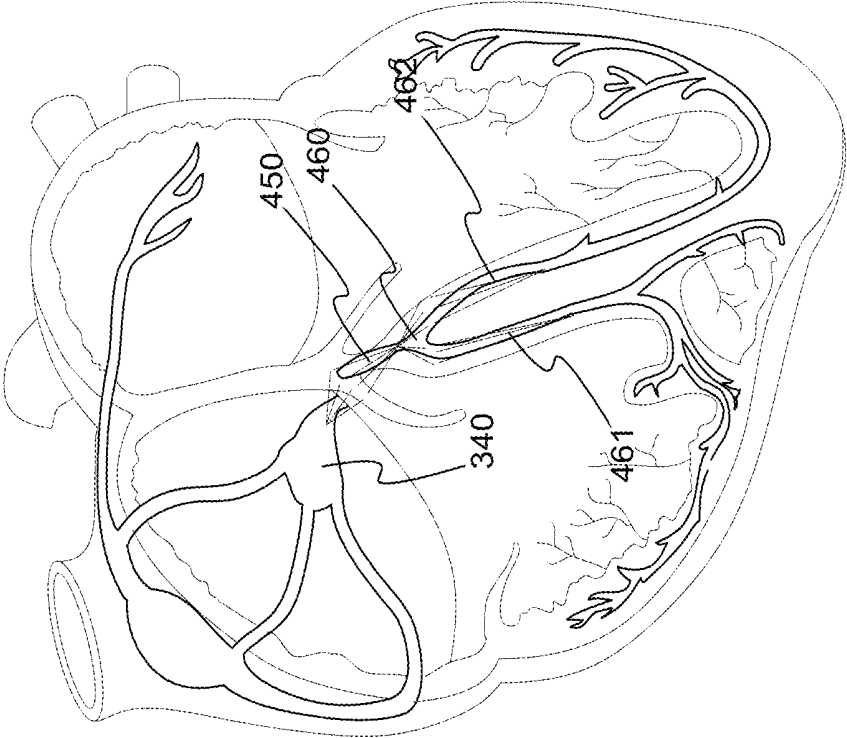


FIG. 4



400

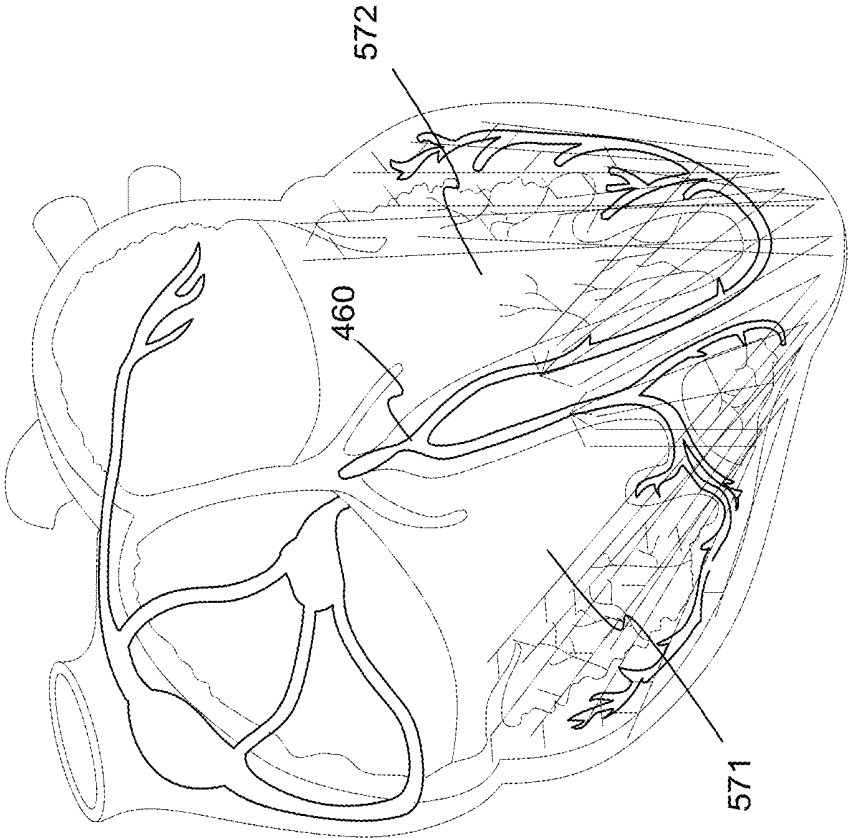


FIG. 5



500

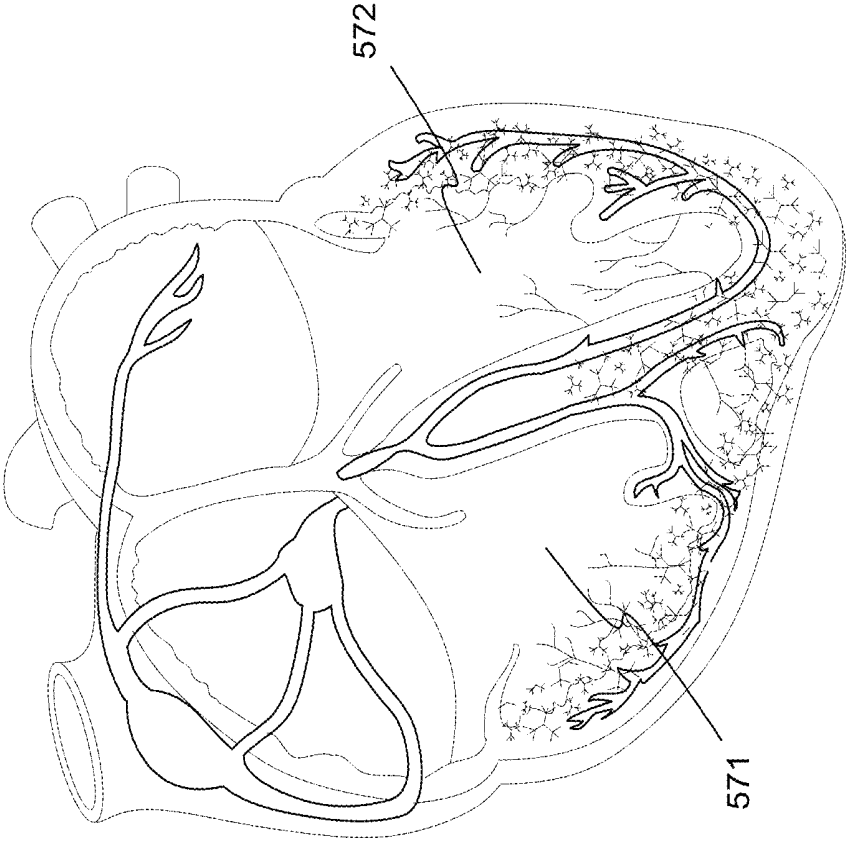
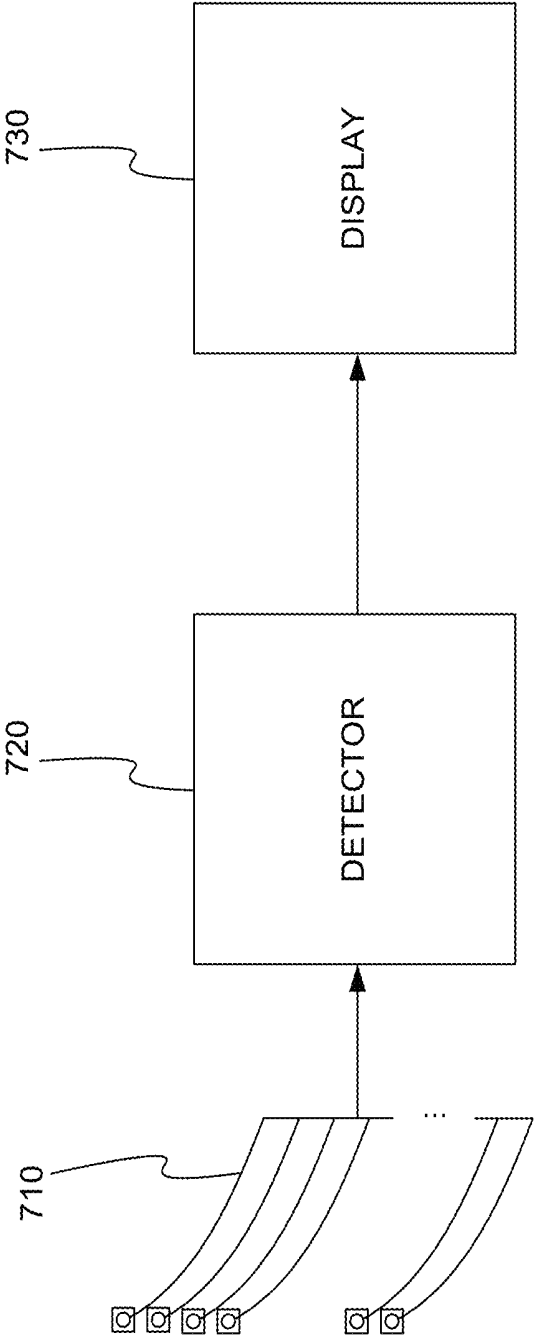


FIG. 6





(PRIOR ART)

FIG. 7

700

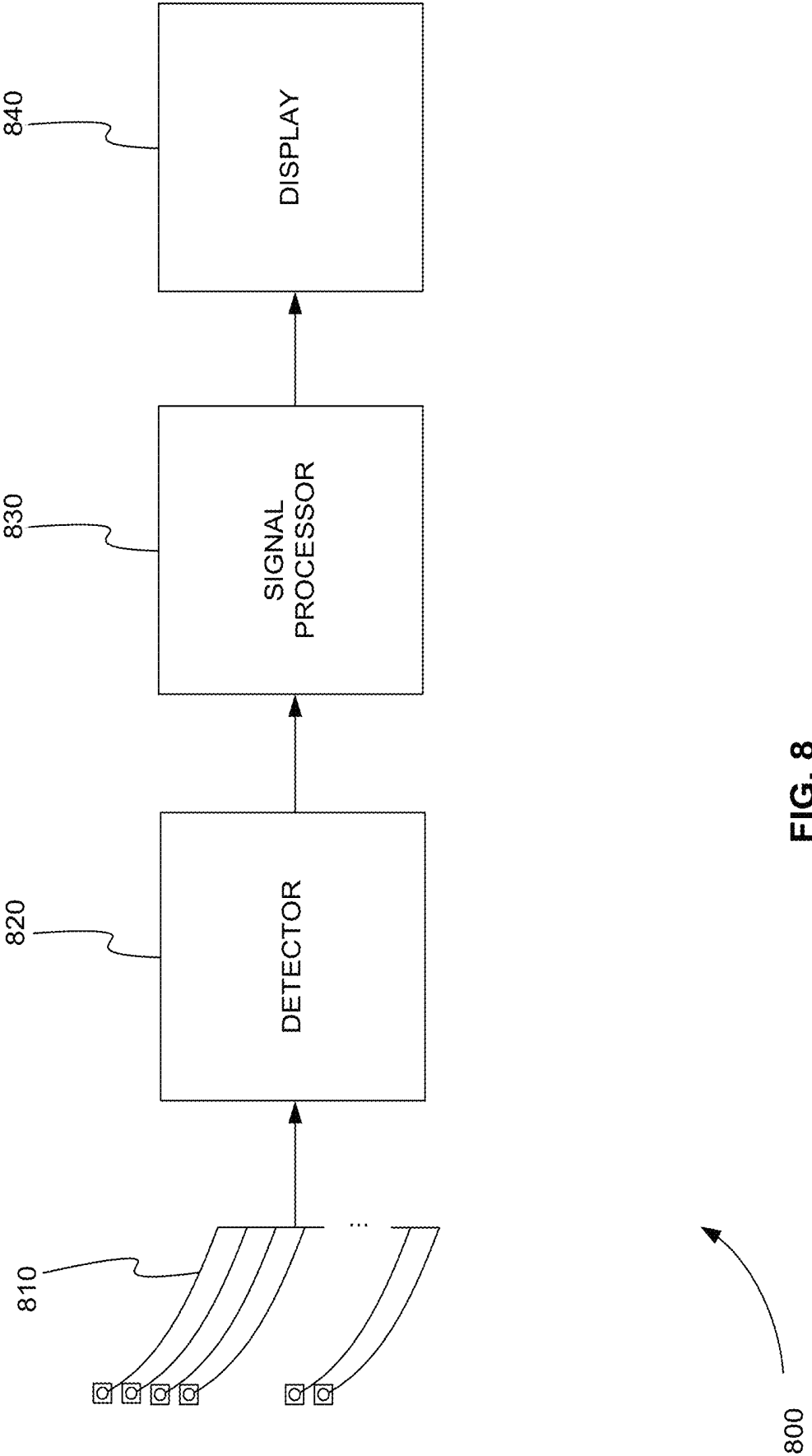


FIG. 8

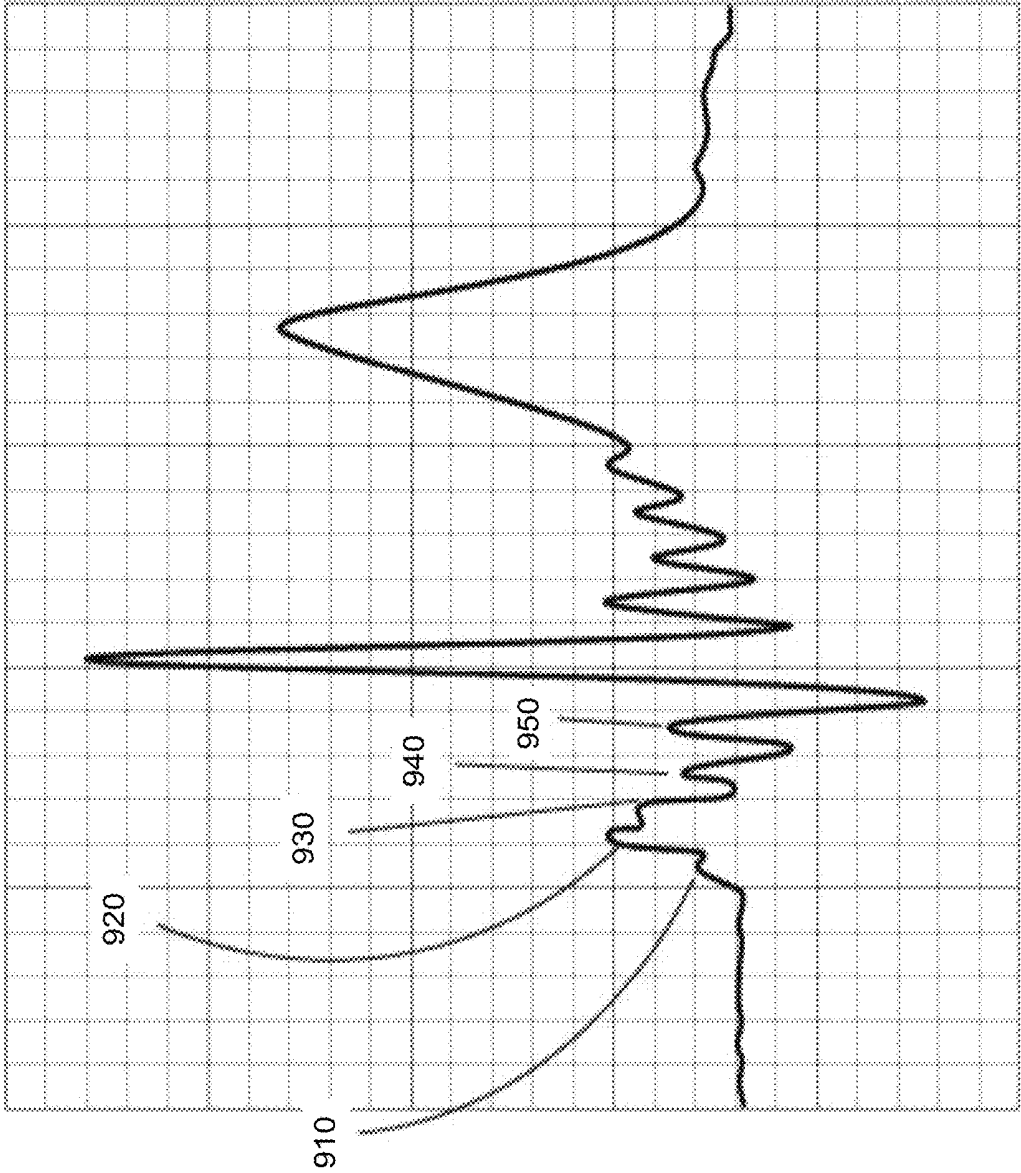


FIG. 9

900

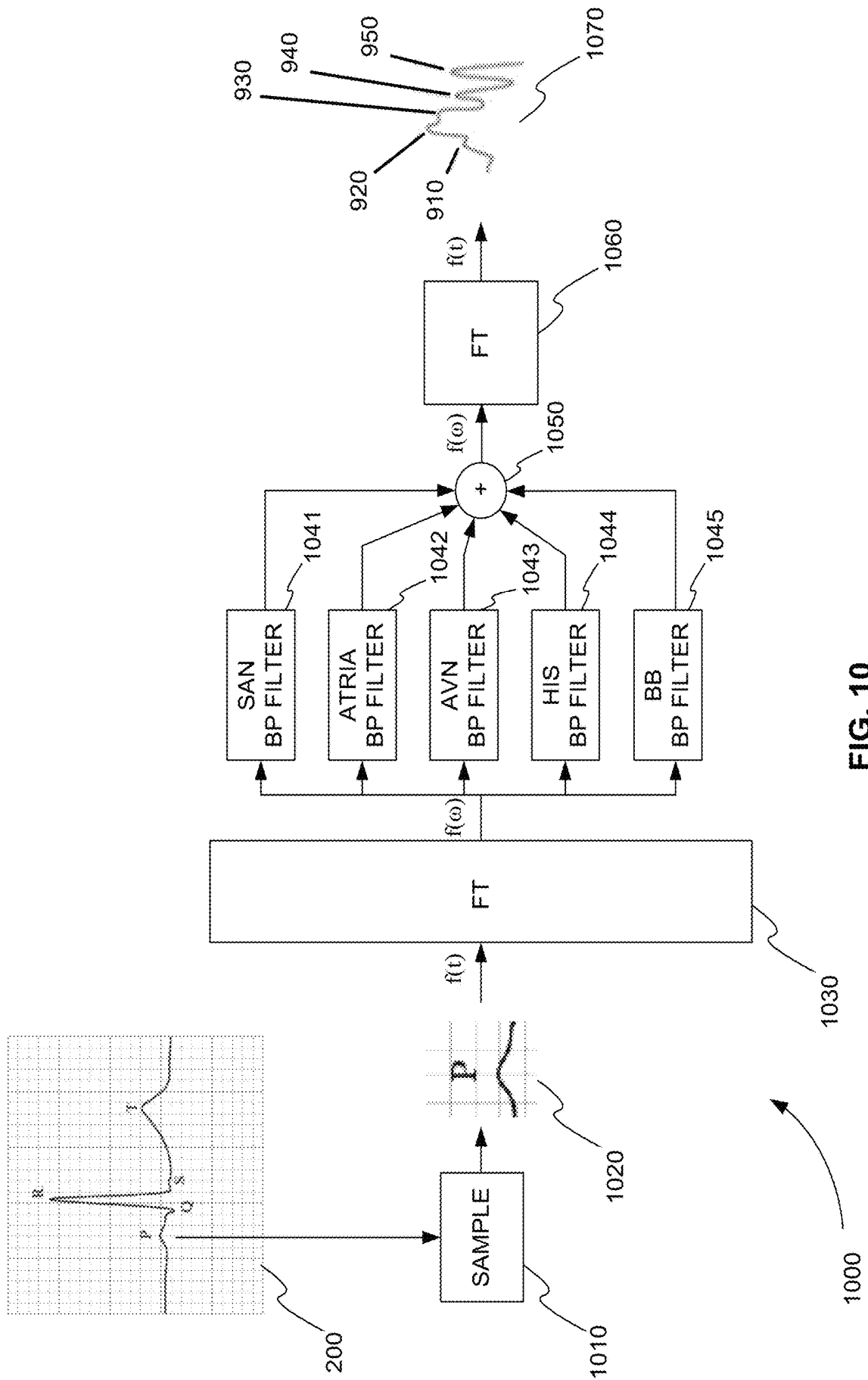


FIG. 10

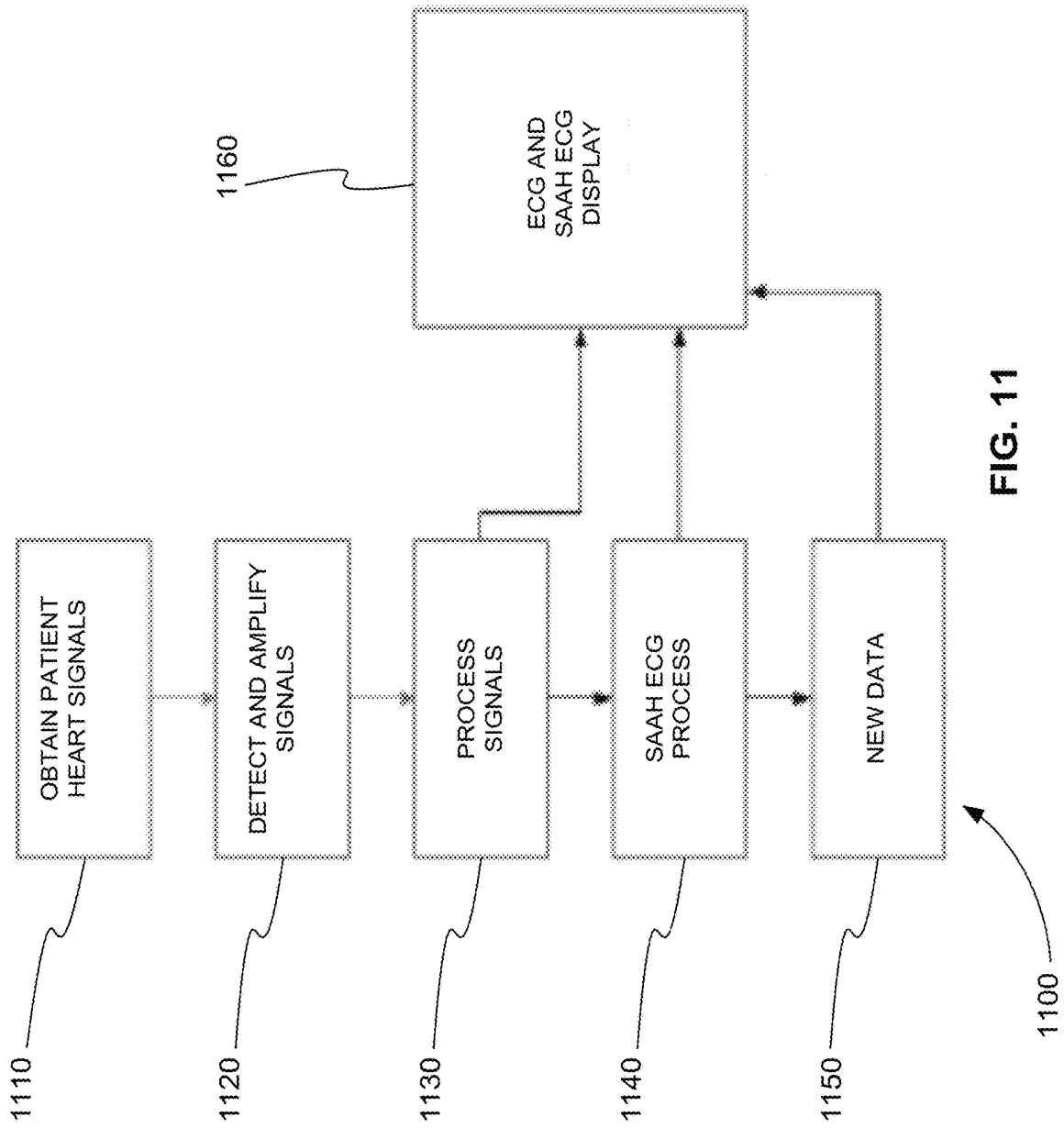
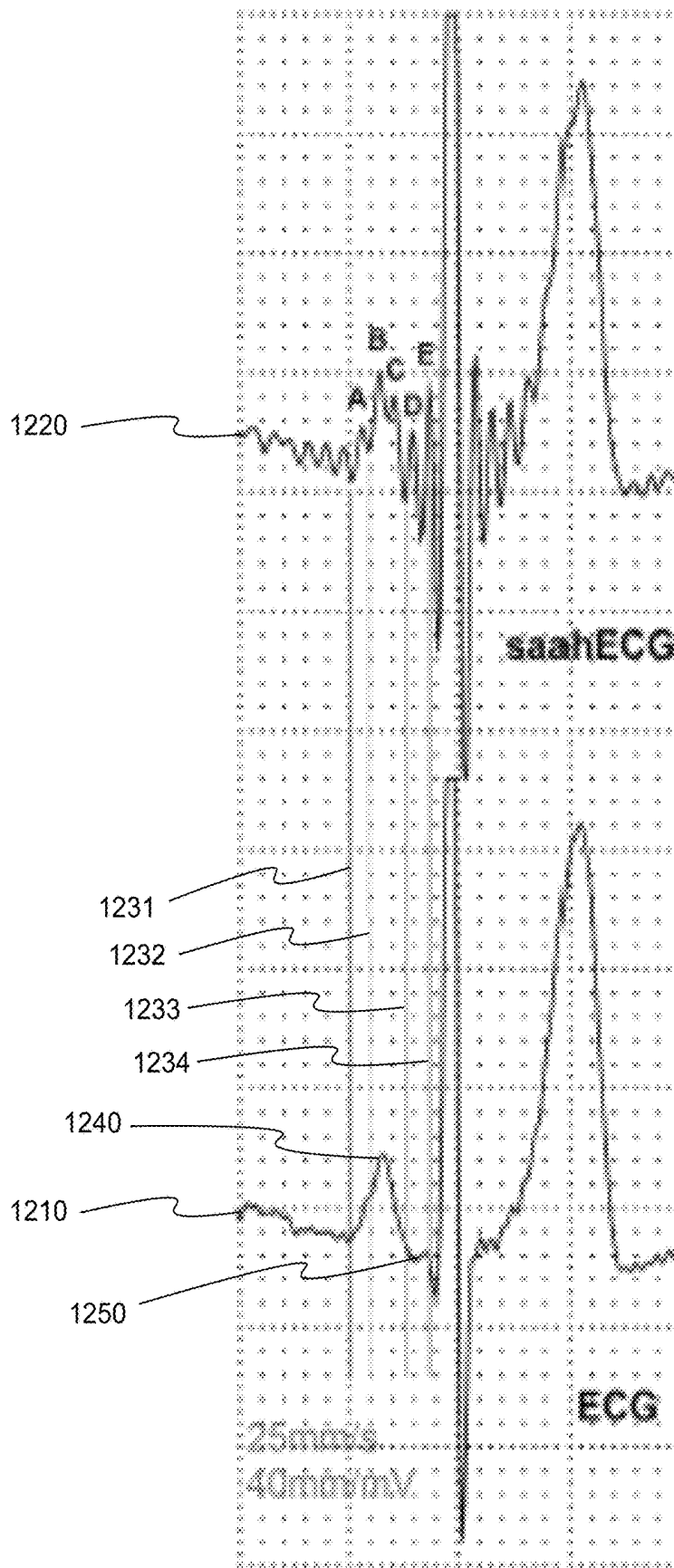
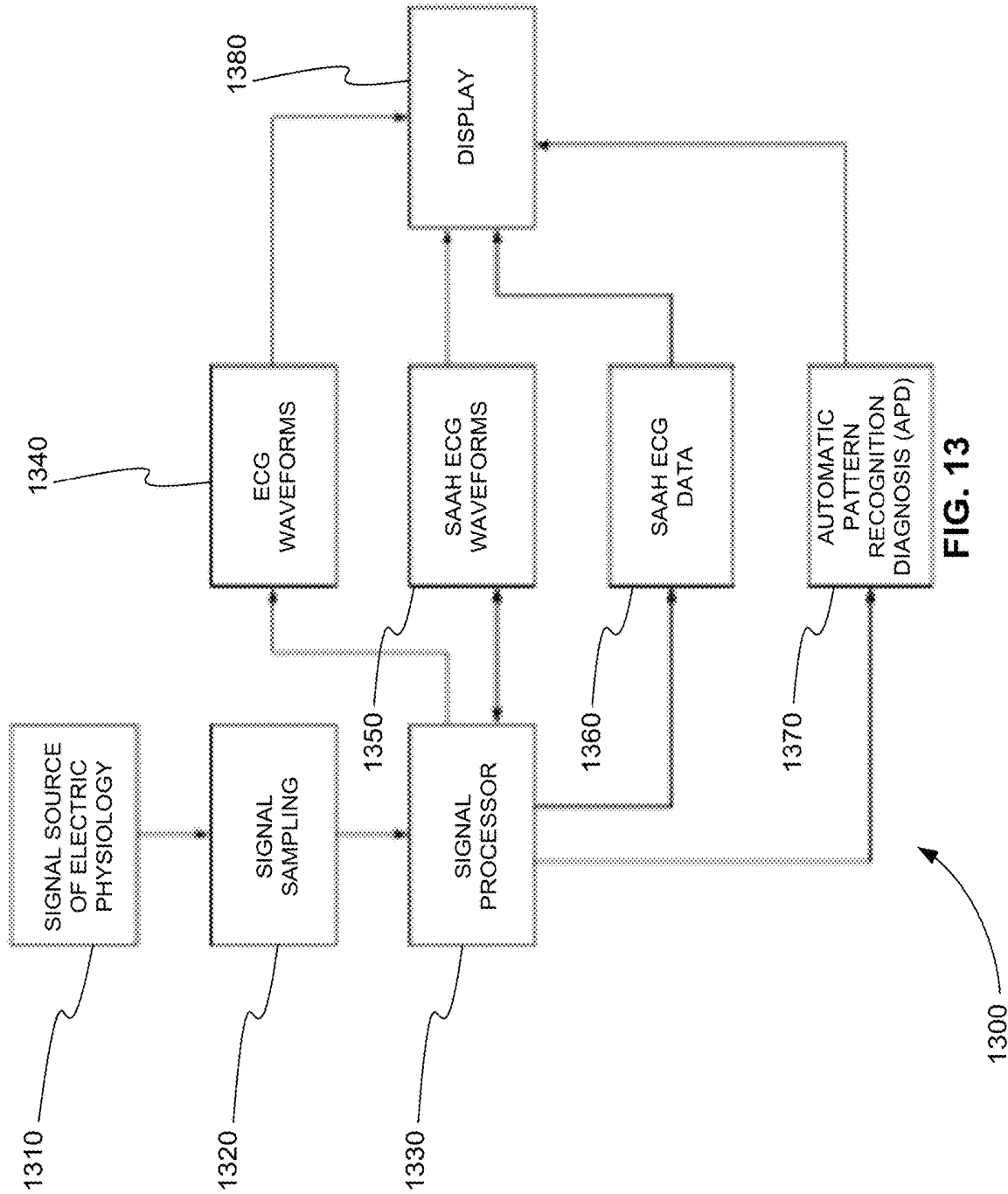


FIG. 11



1200

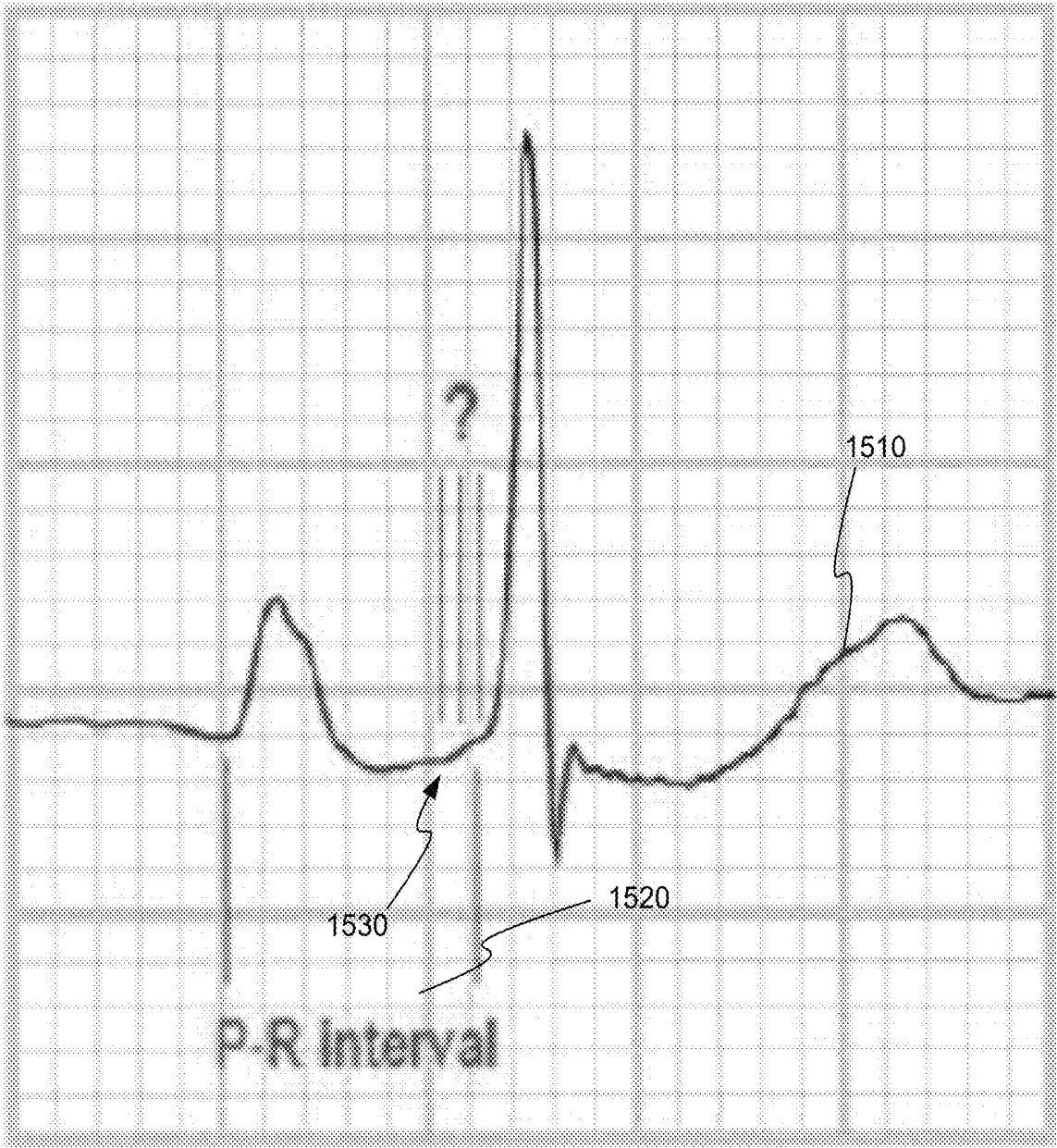
FIG. 12





1400 →

FIG. 14



1500 →

FIG. 15

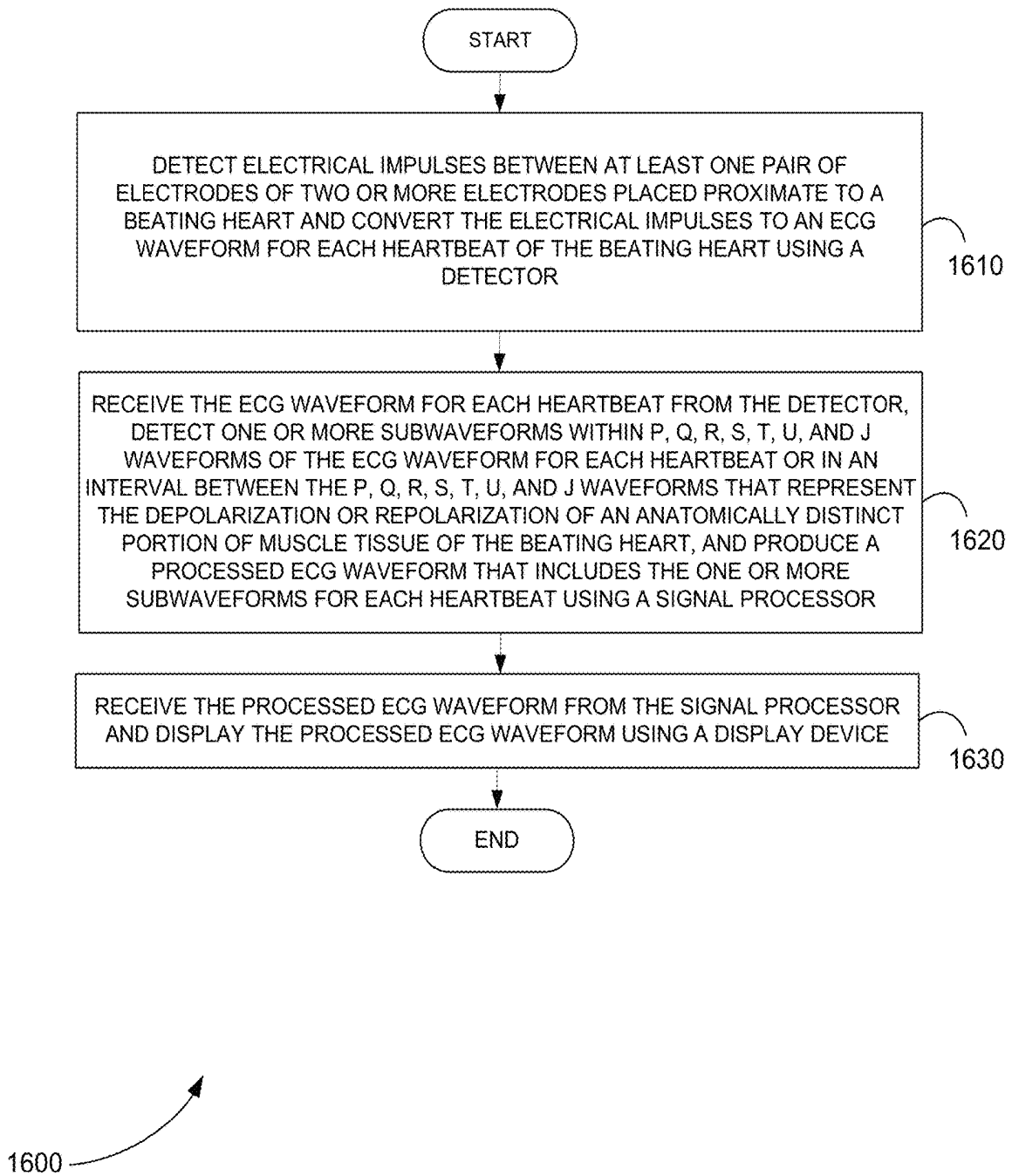


FIG. 16

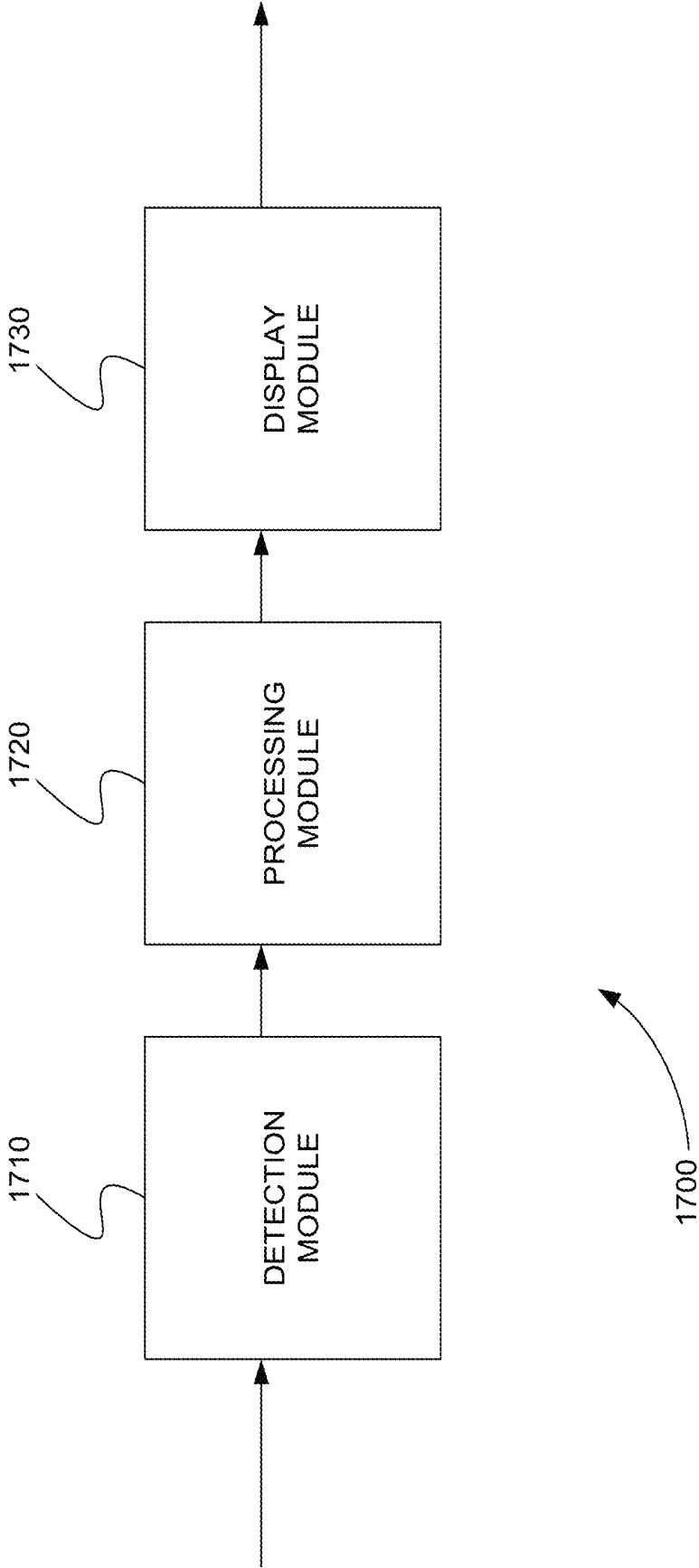
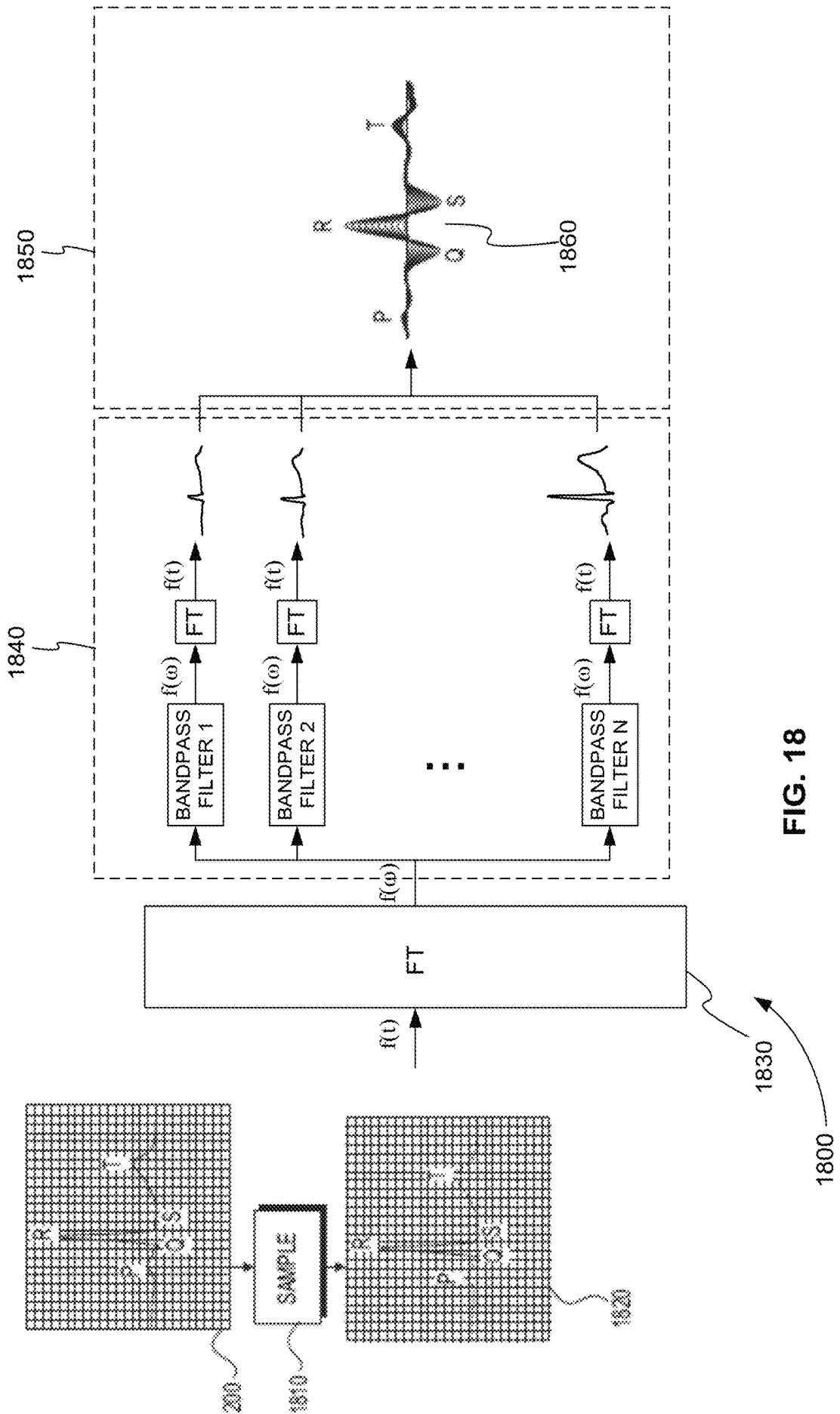


FIG. 17



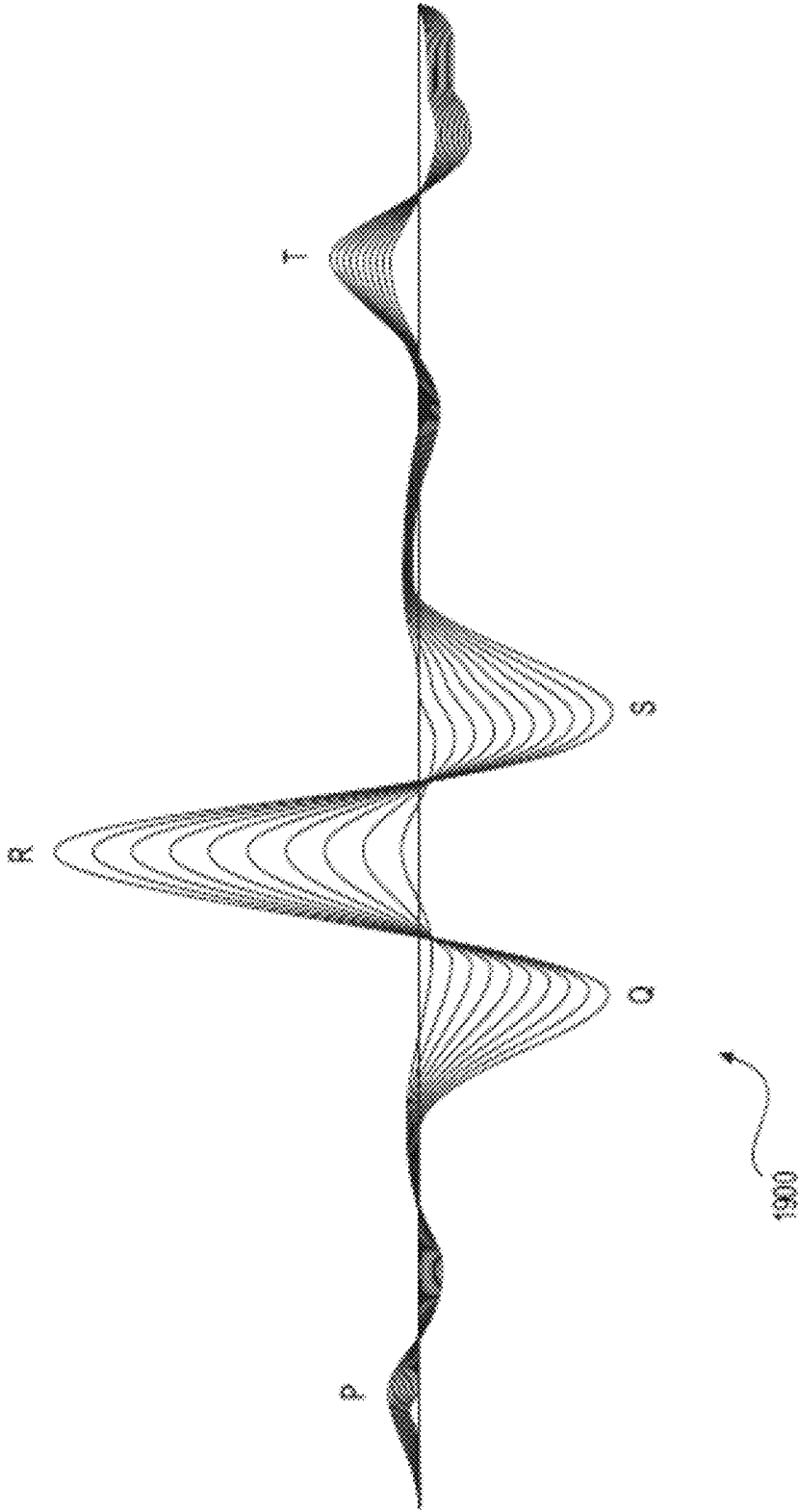
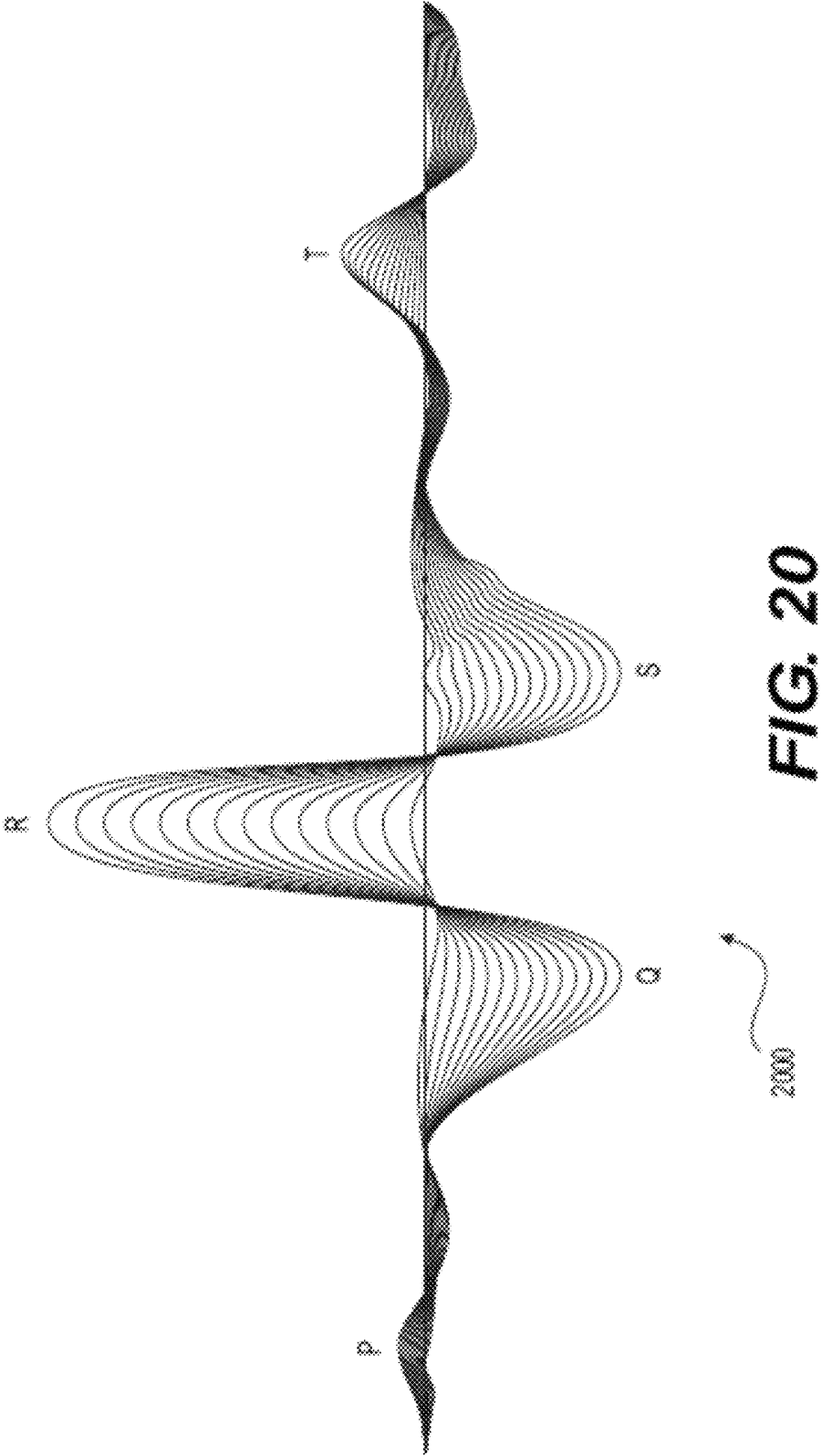
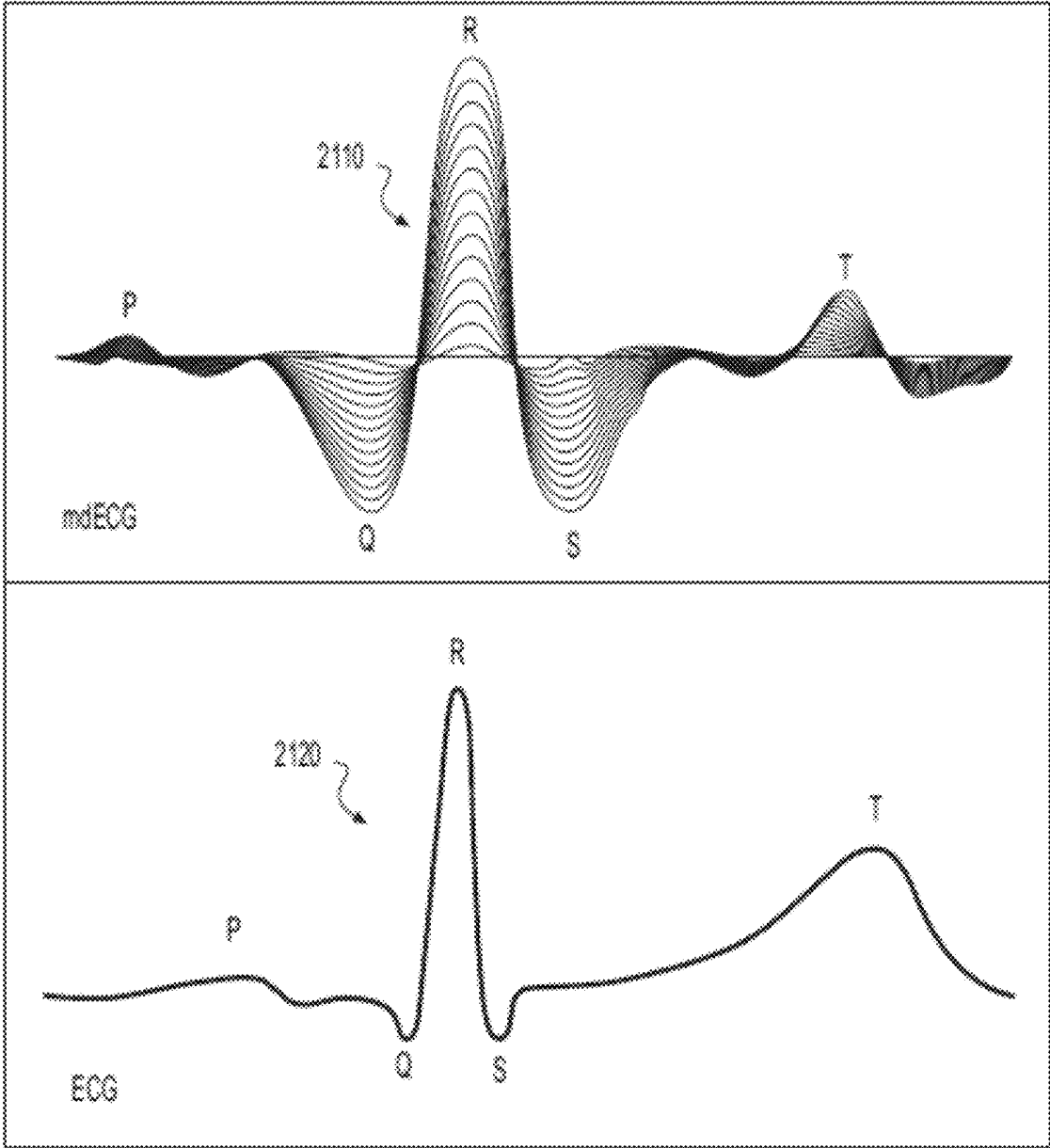


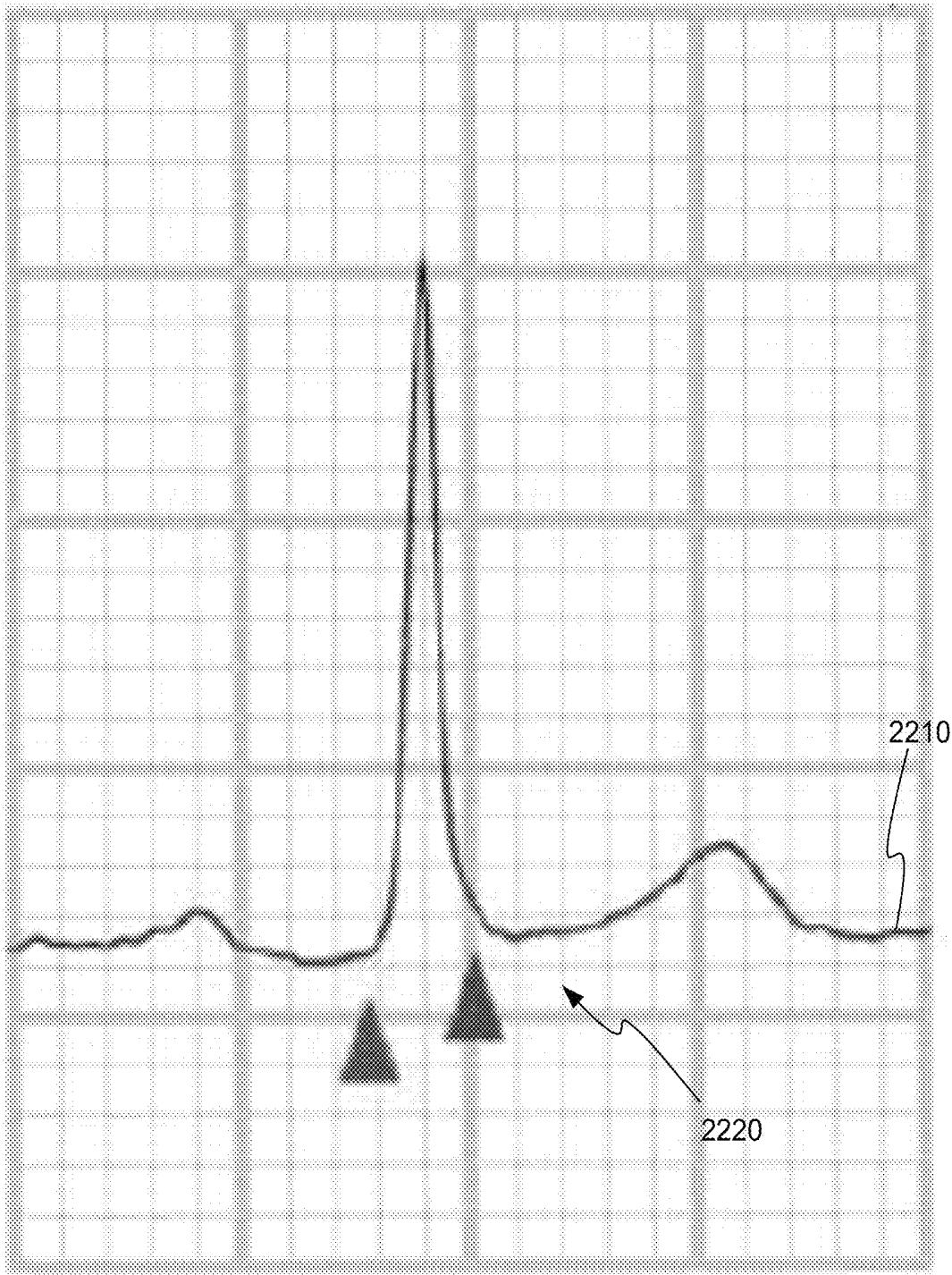
FIG. 19





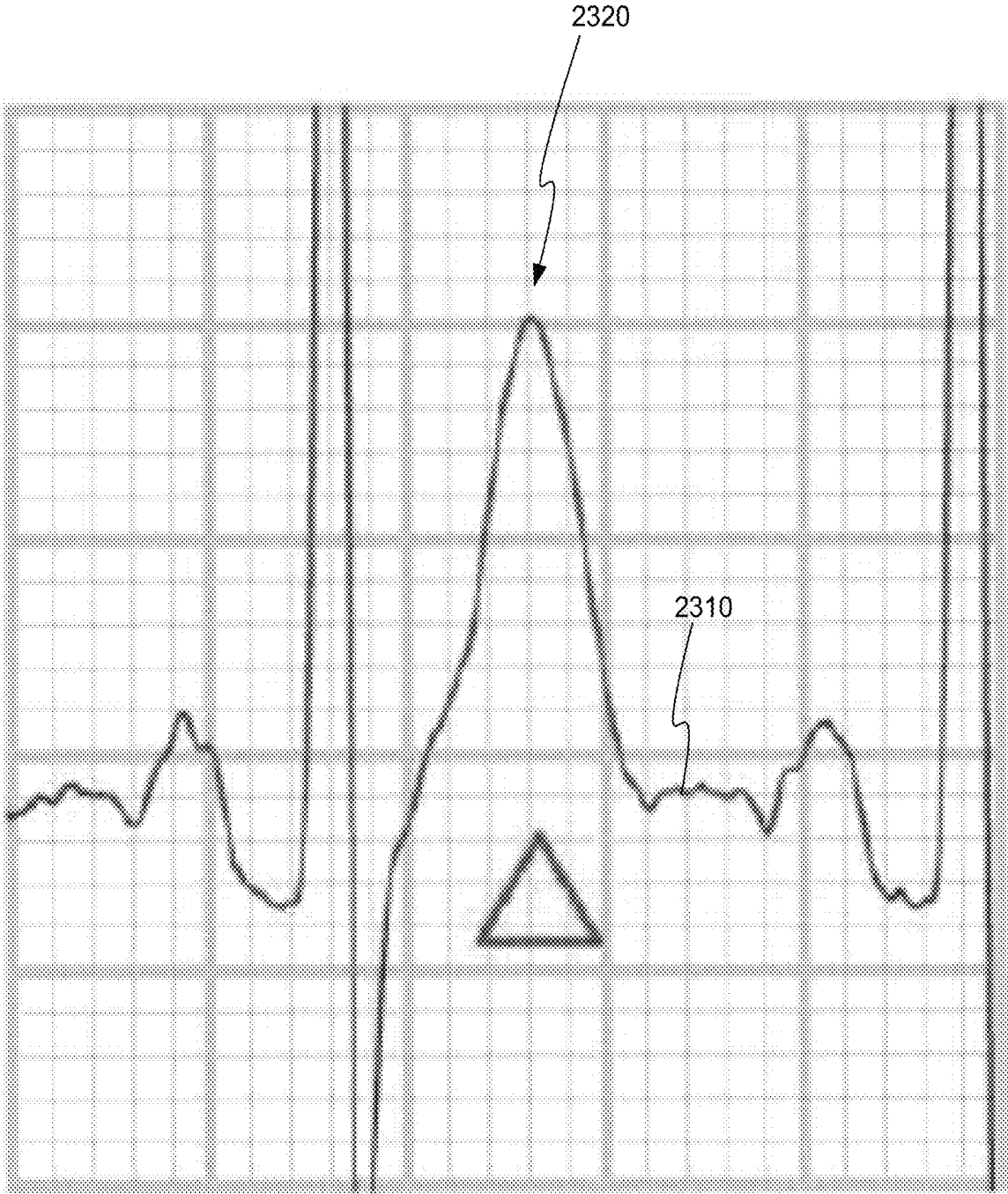
2100

FIG. 21



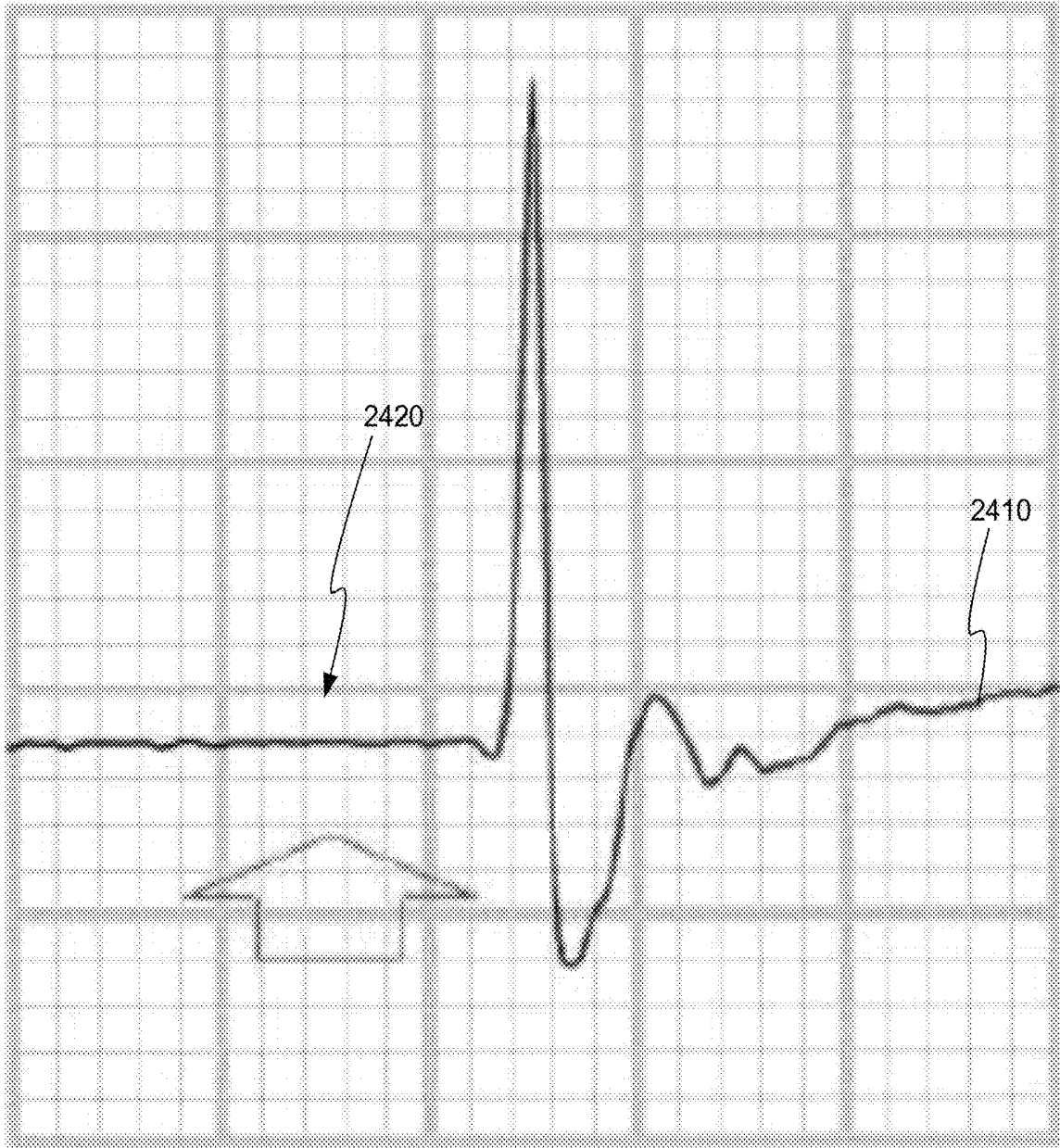
2200 →

FIG. 22



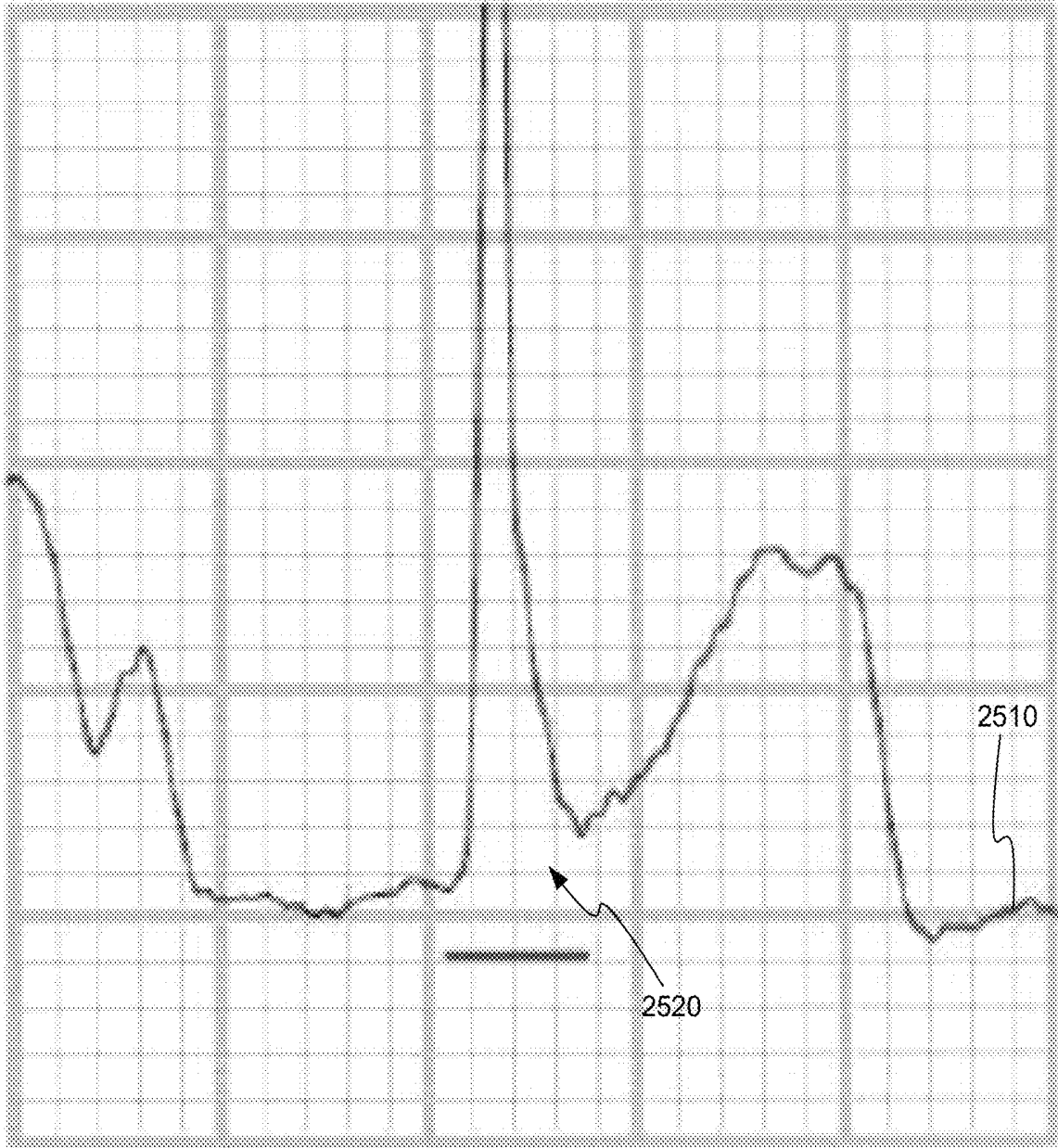
2300

FIG. 23



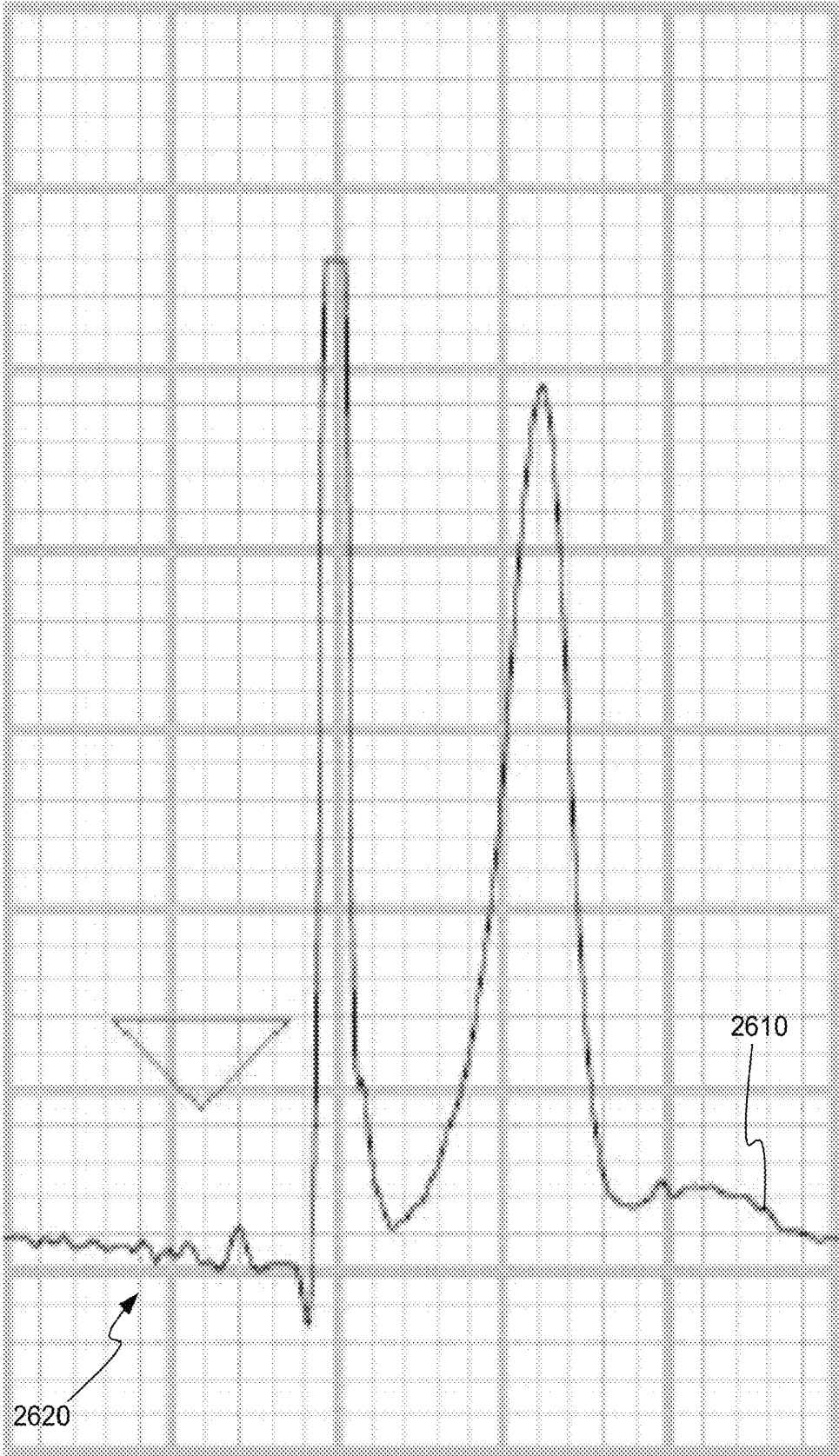
2400 →

FIG. 24



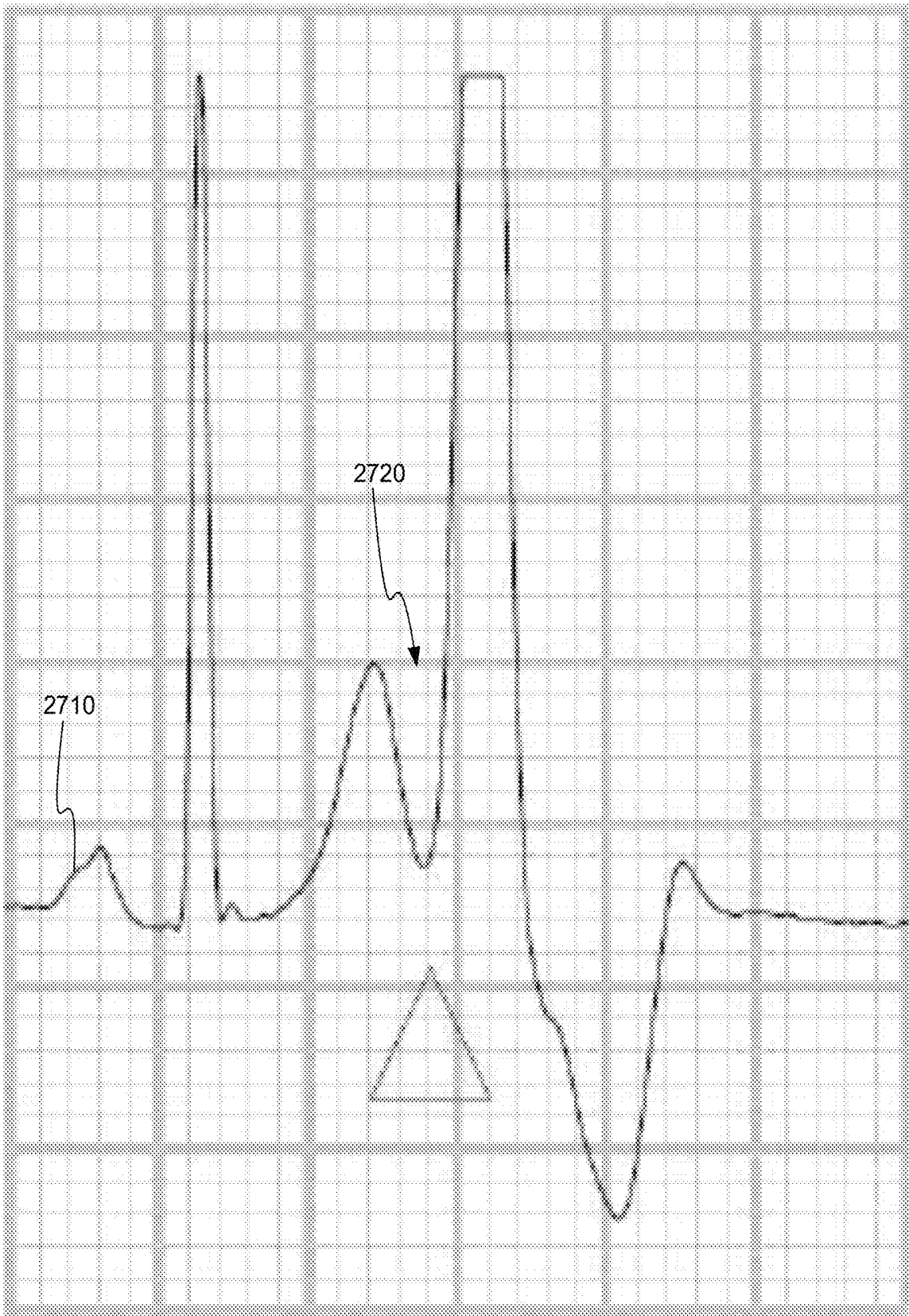
2500 →

FIG. 25



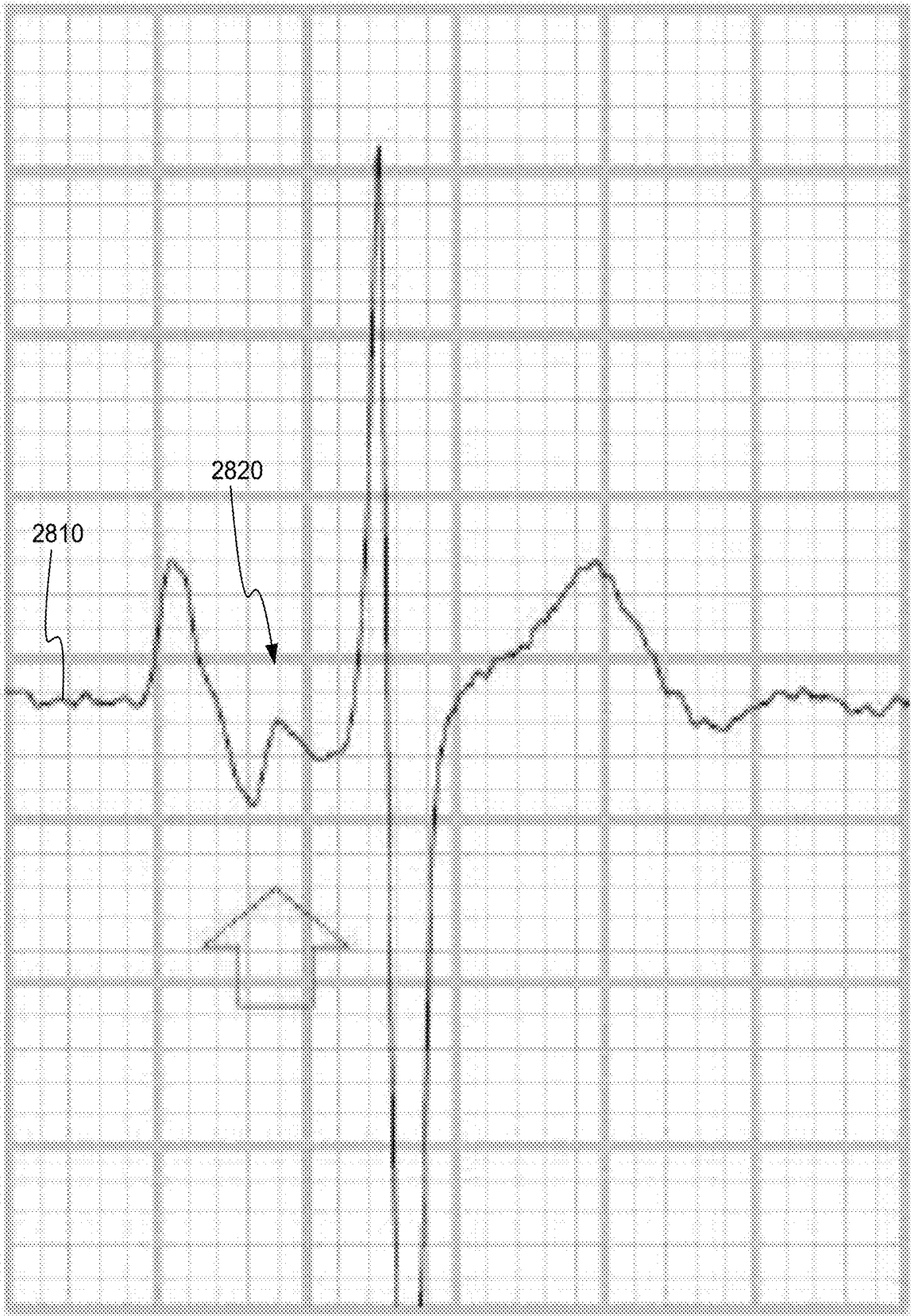
2600

FIG. 26



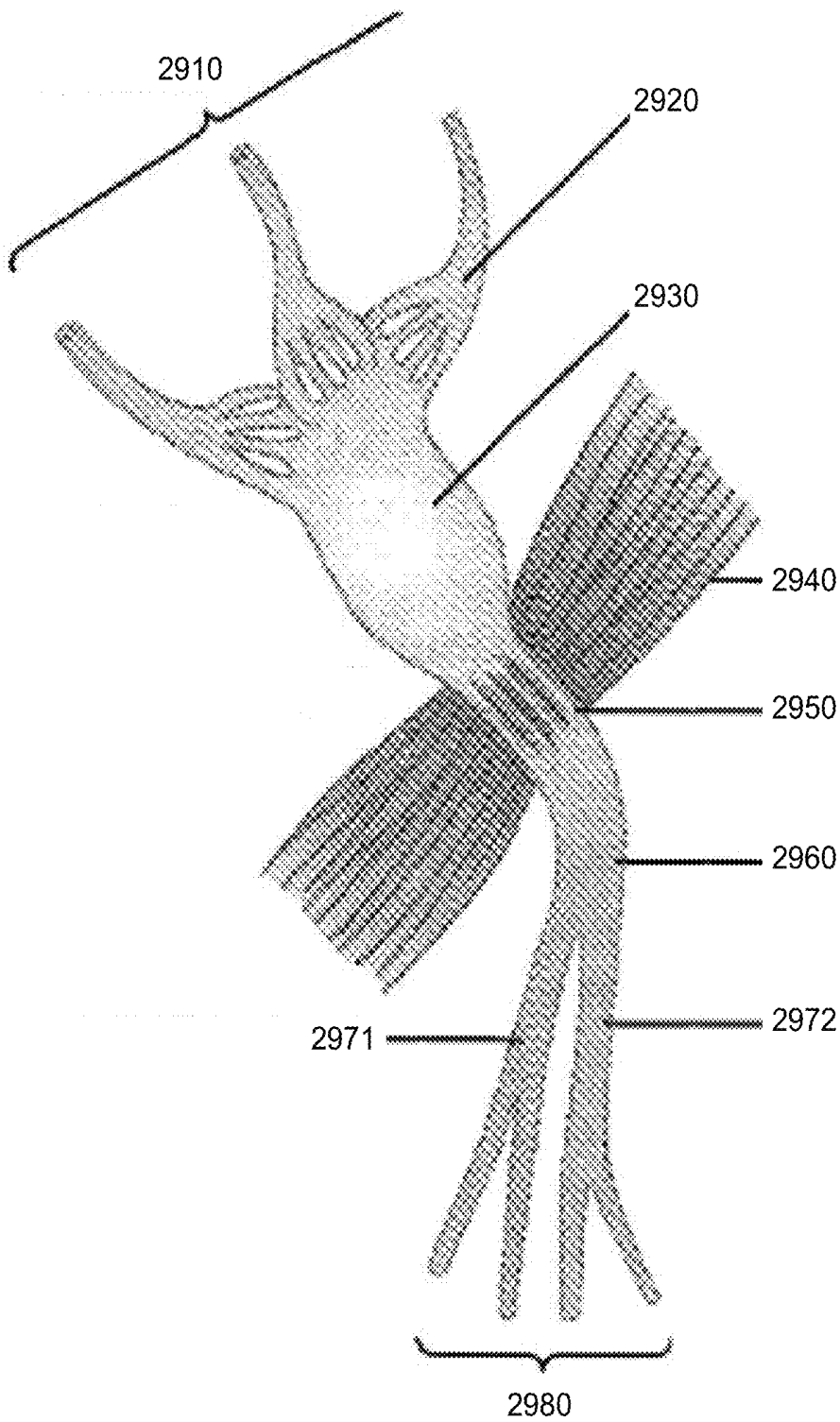
2700

FIG. 27



2800

FIG. 28



2900 ↗

FIG. 29

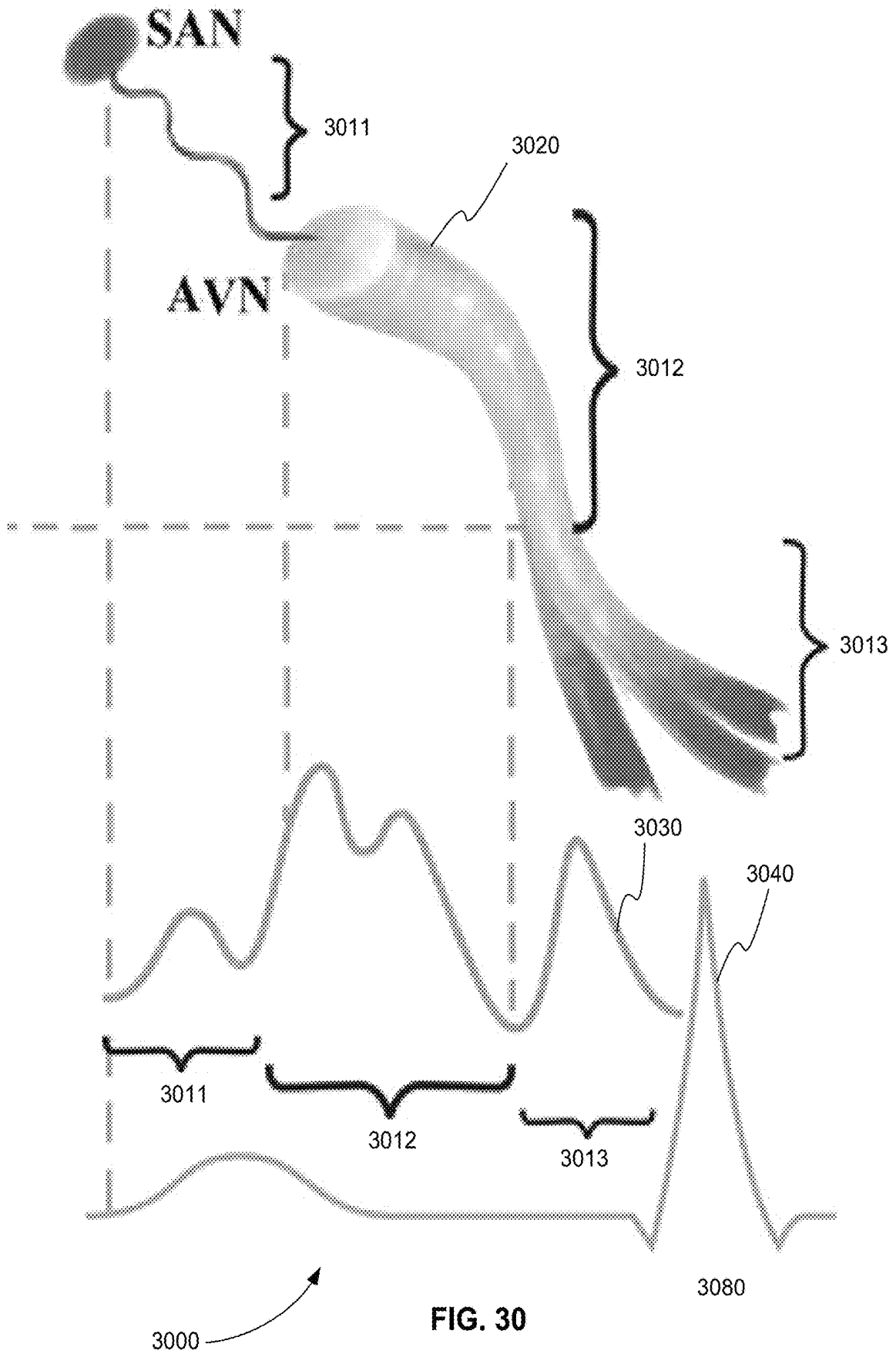


FIG. 30

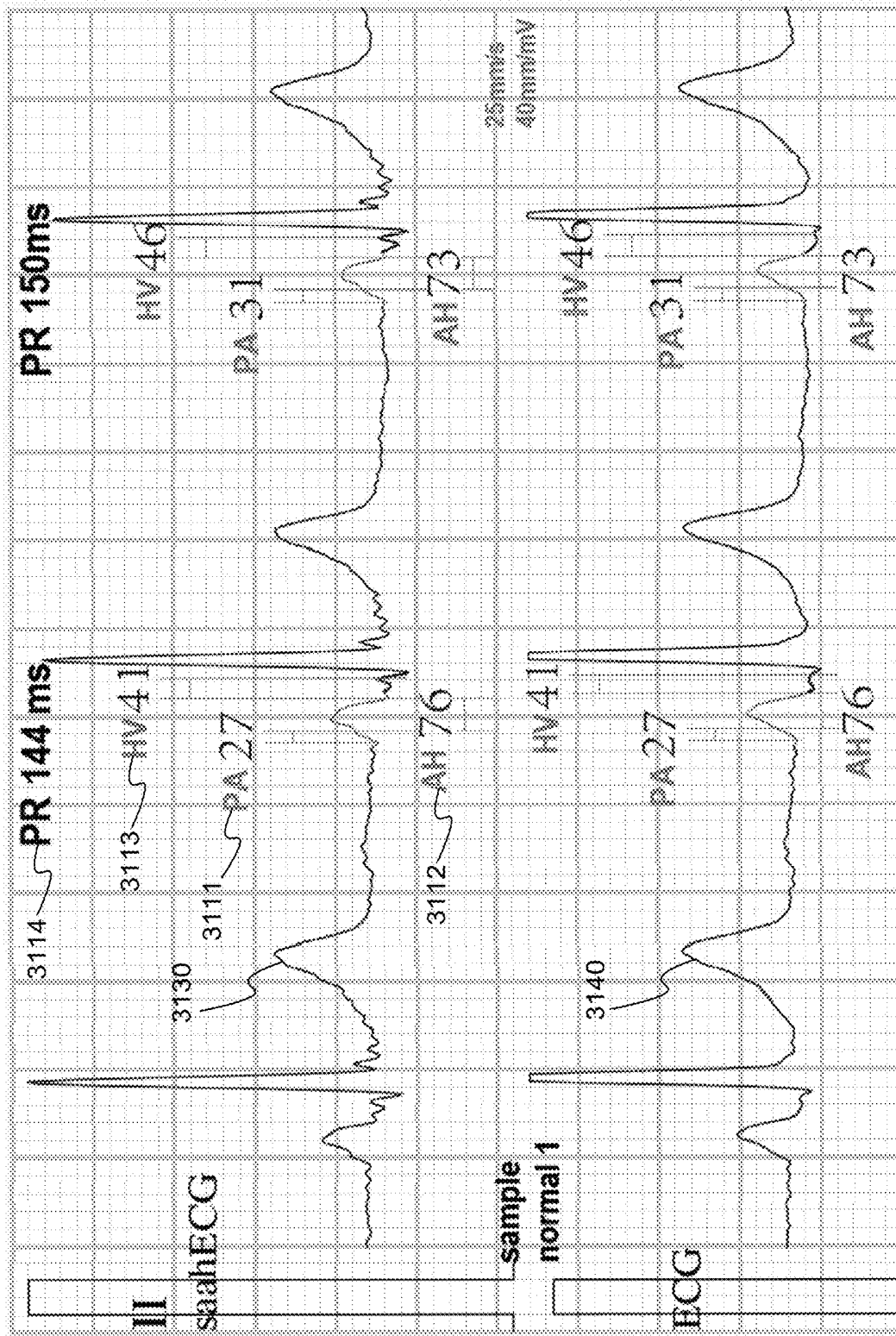
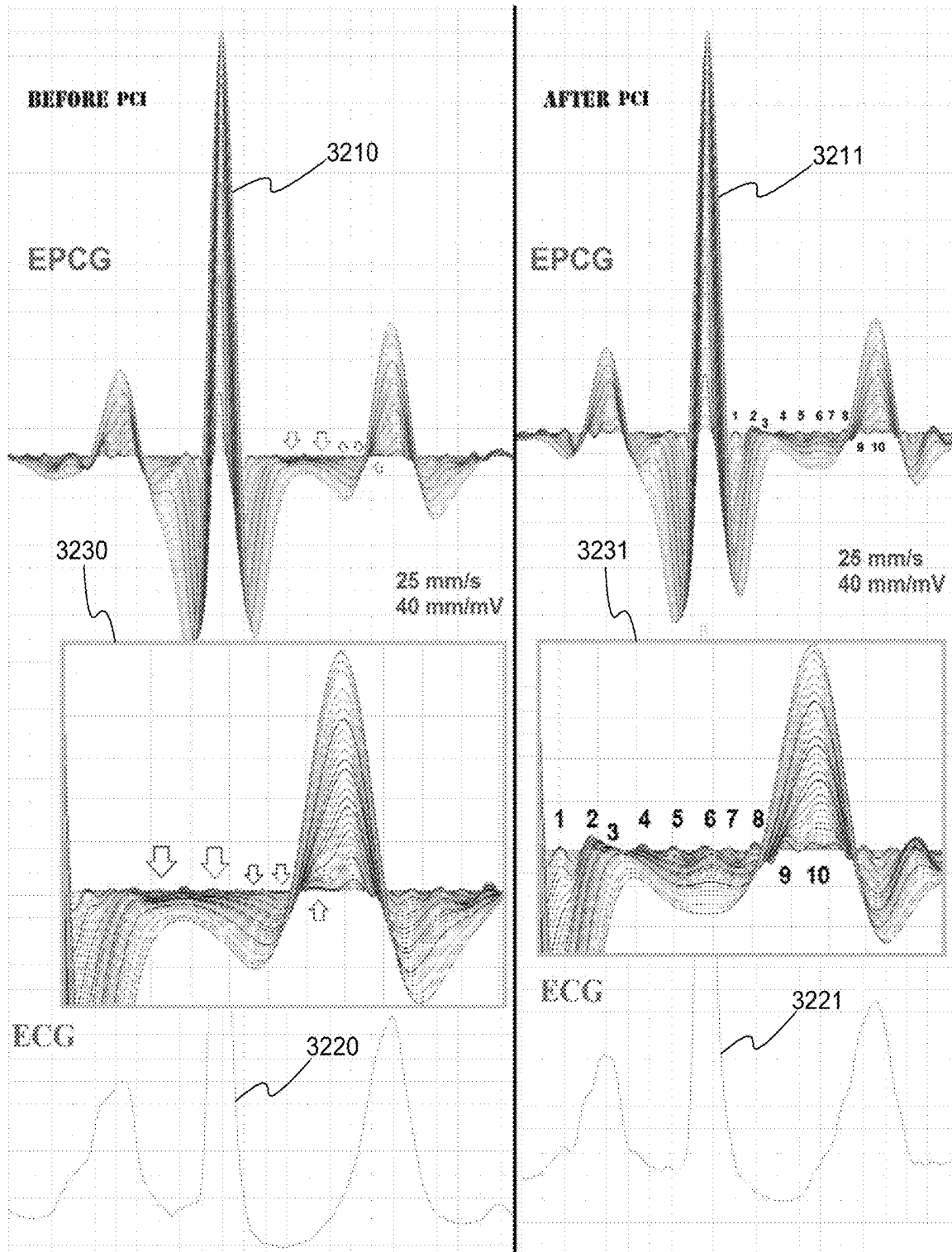


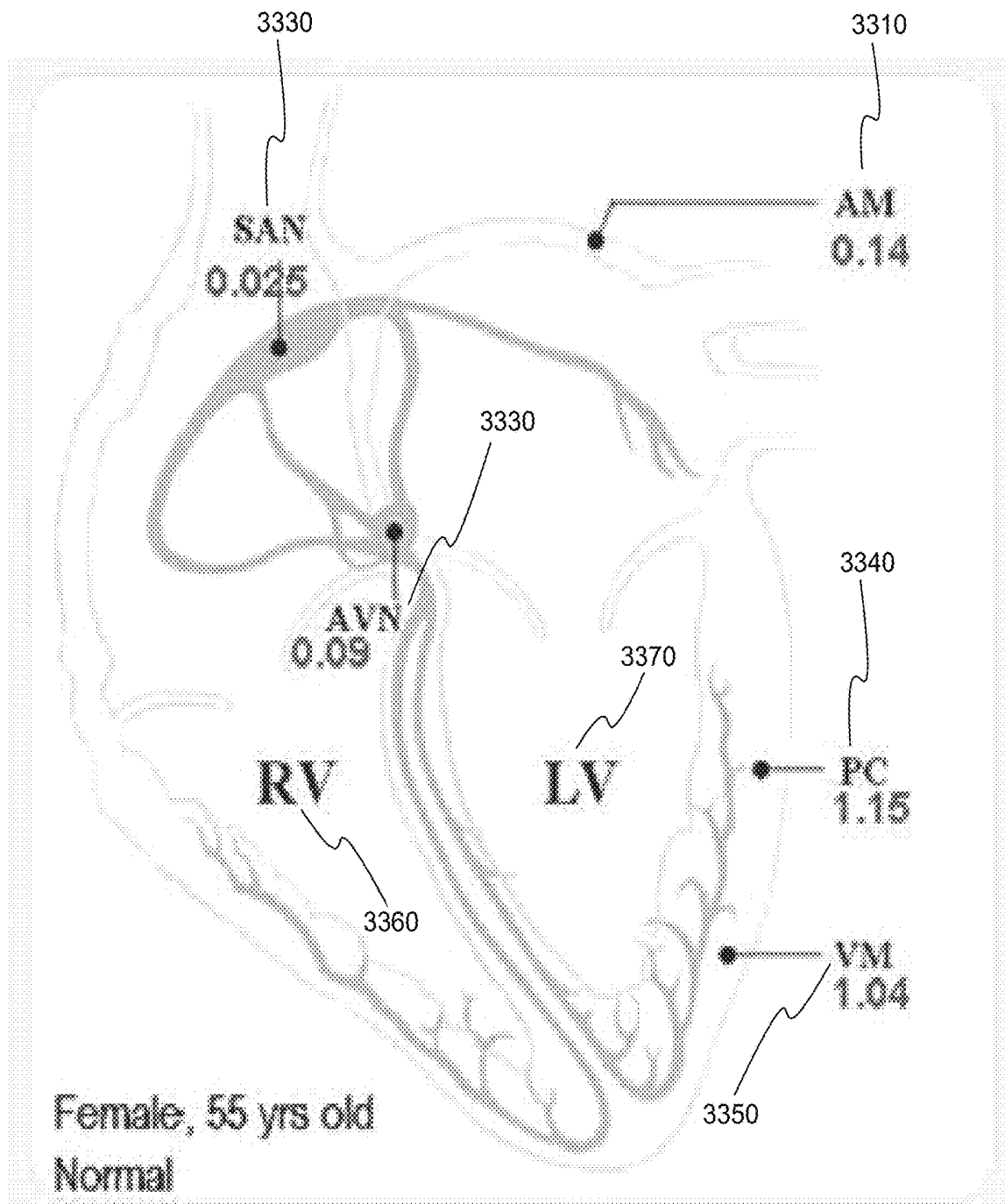
FIG. 31

3100



3200 →

FIG. 32



3300 ↗

FIG. 33

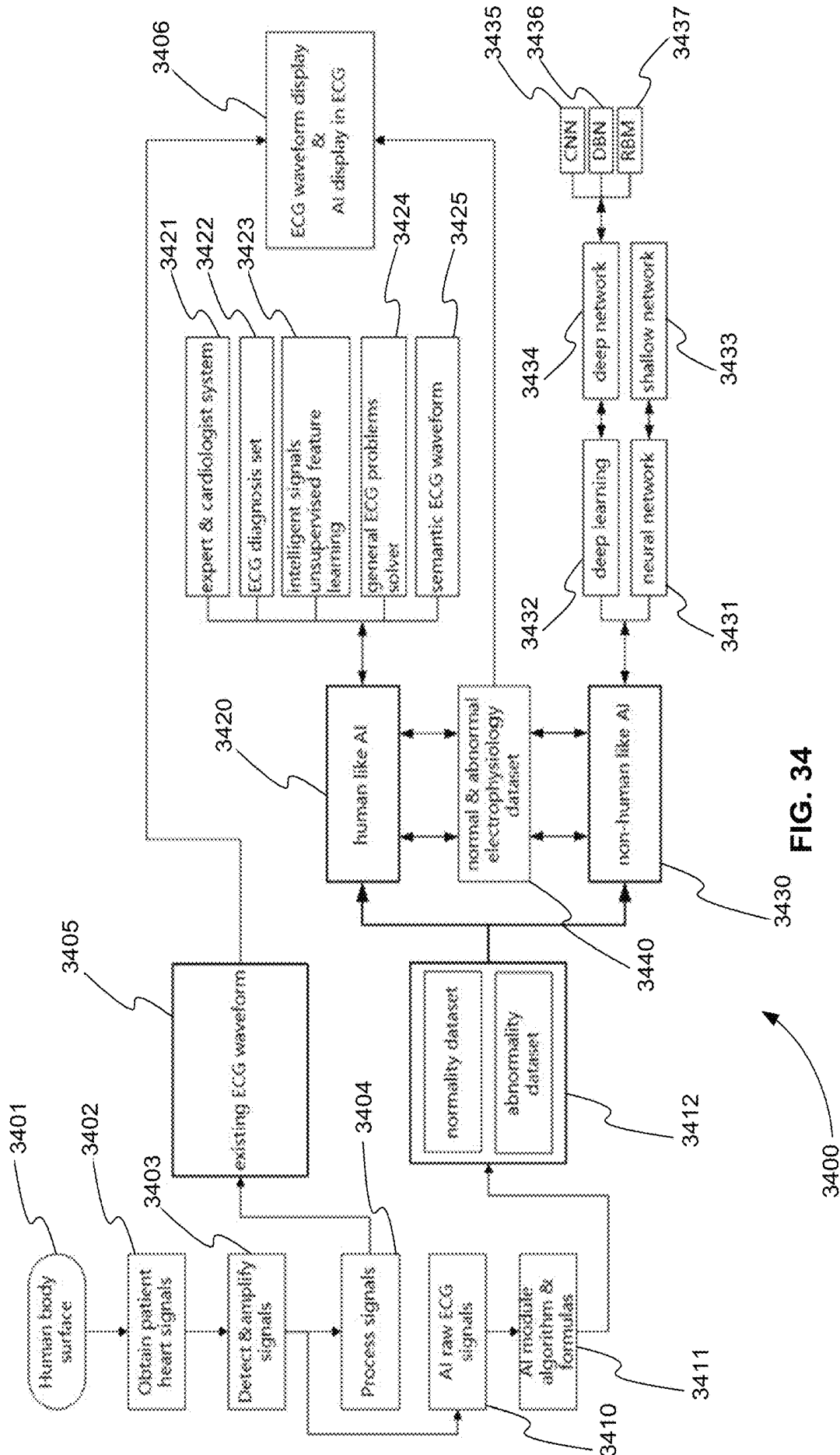


FIG. 34

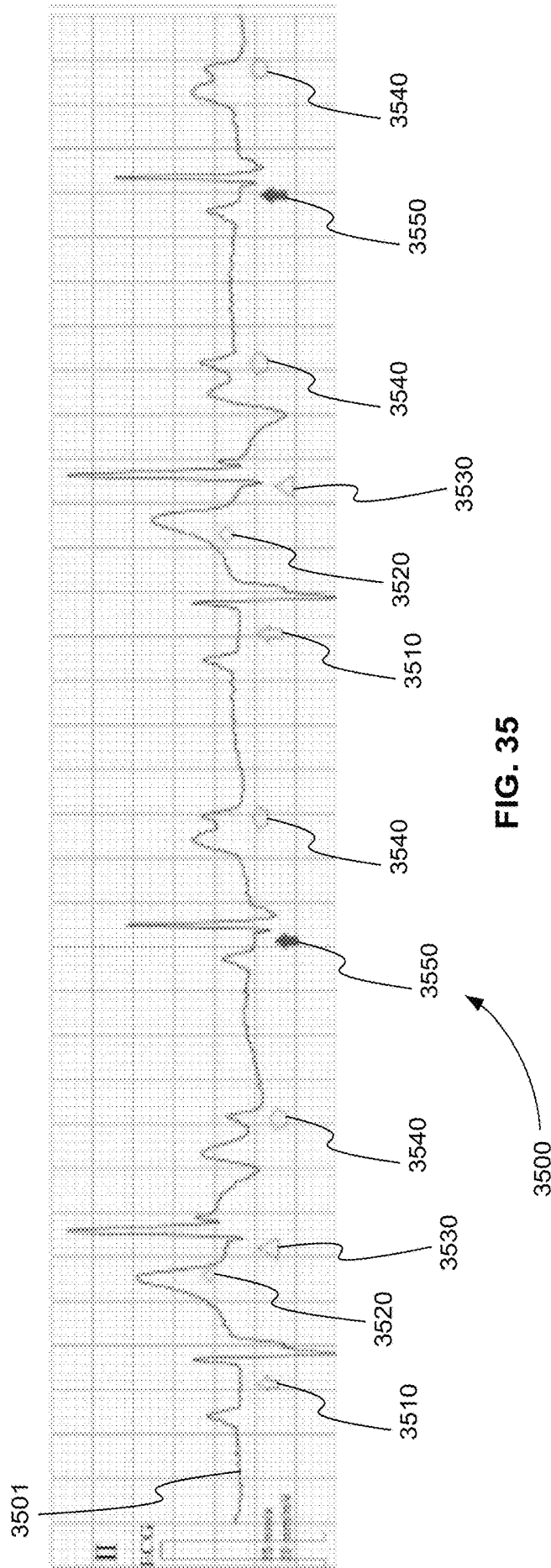


FIG. 35

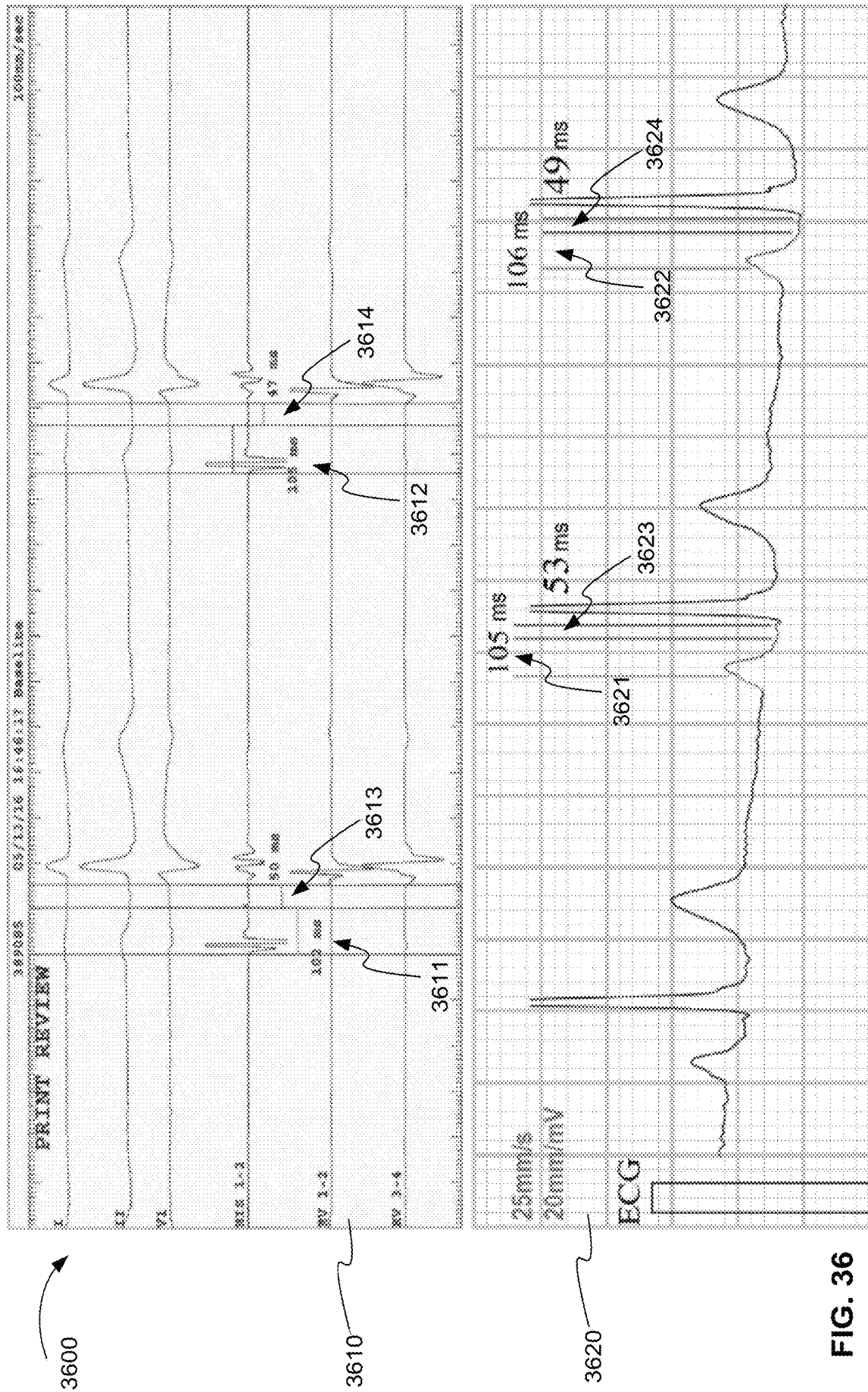


FIG. 36

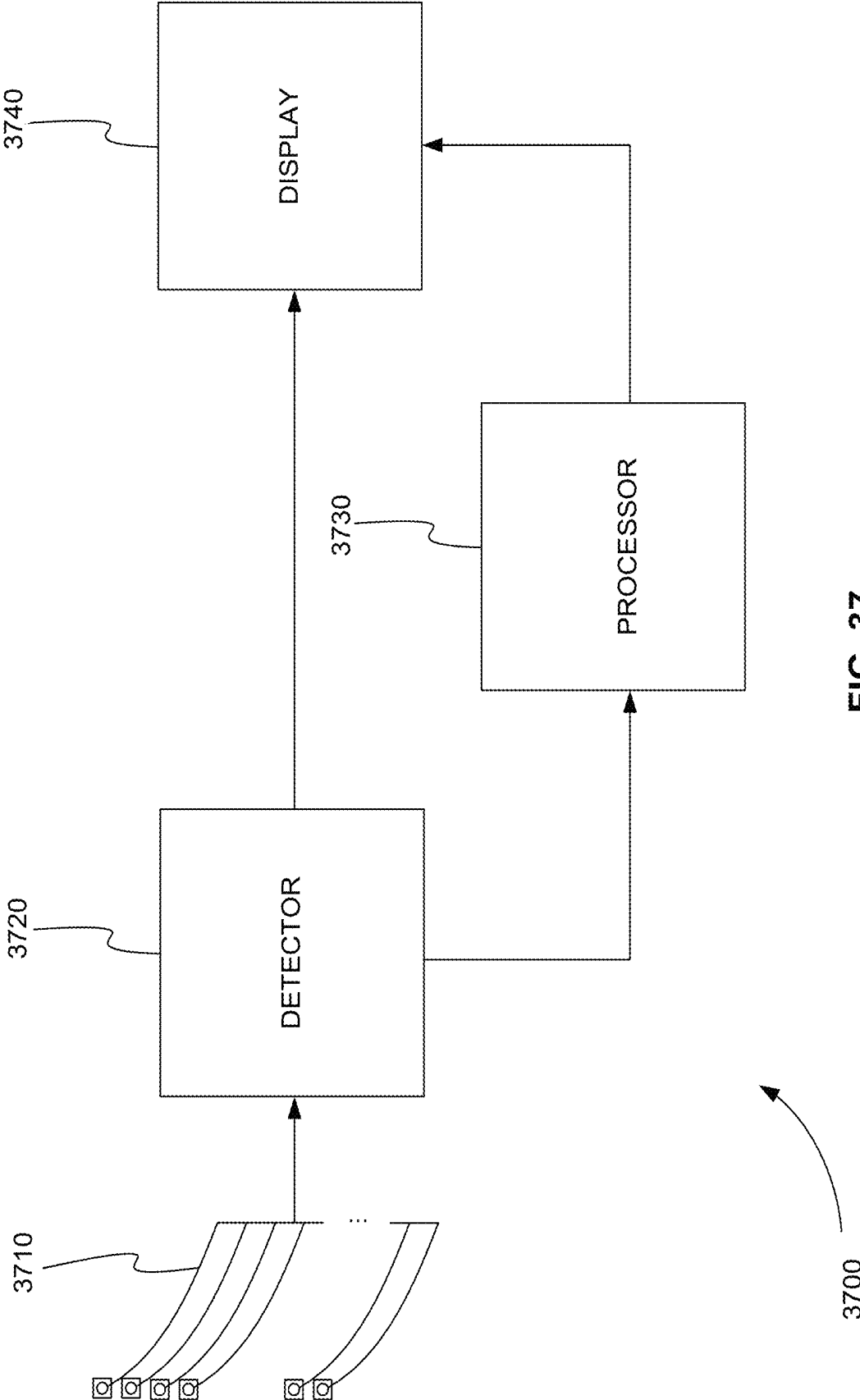
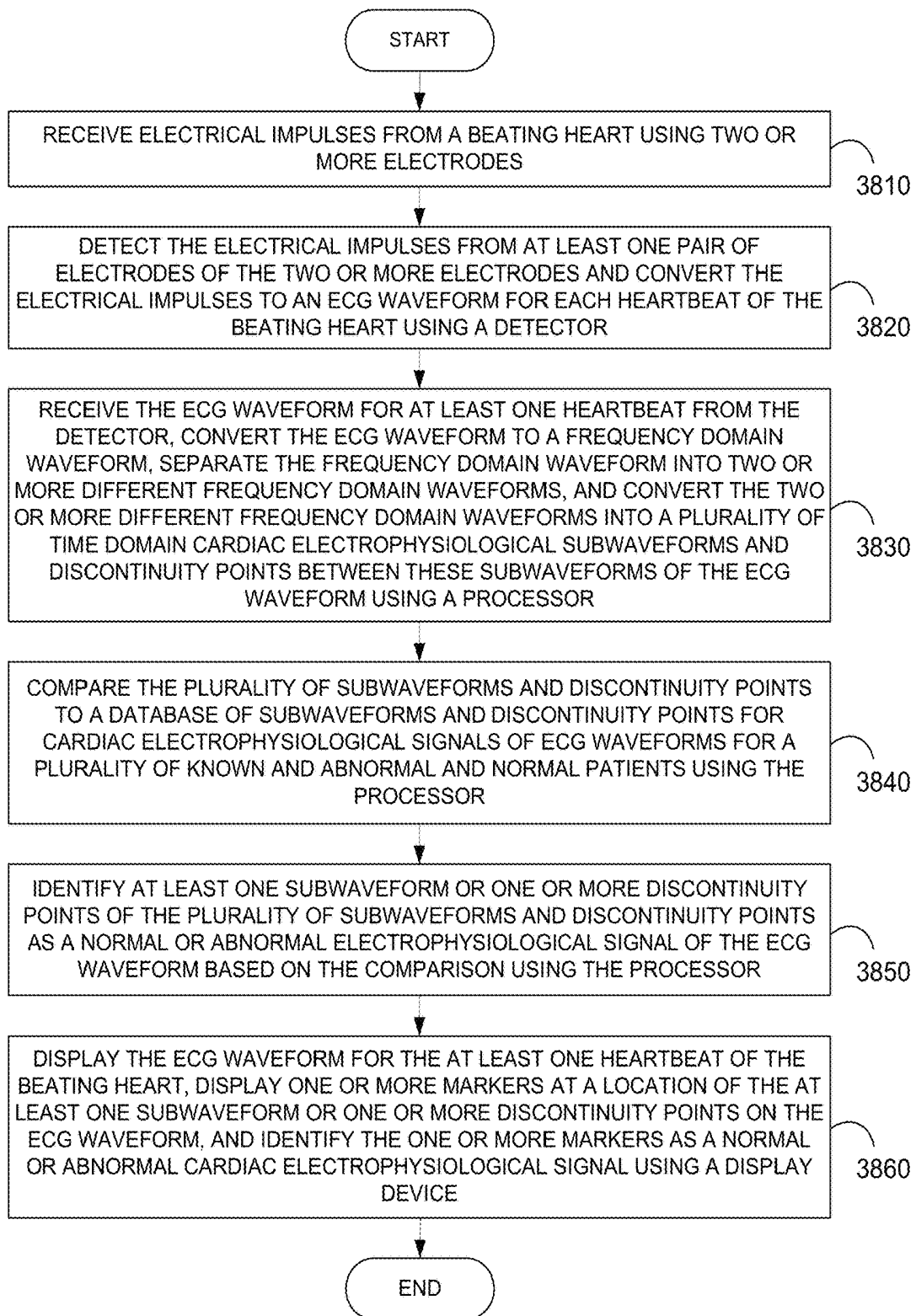


FIG. 37



3800 ↗

FIG. 38

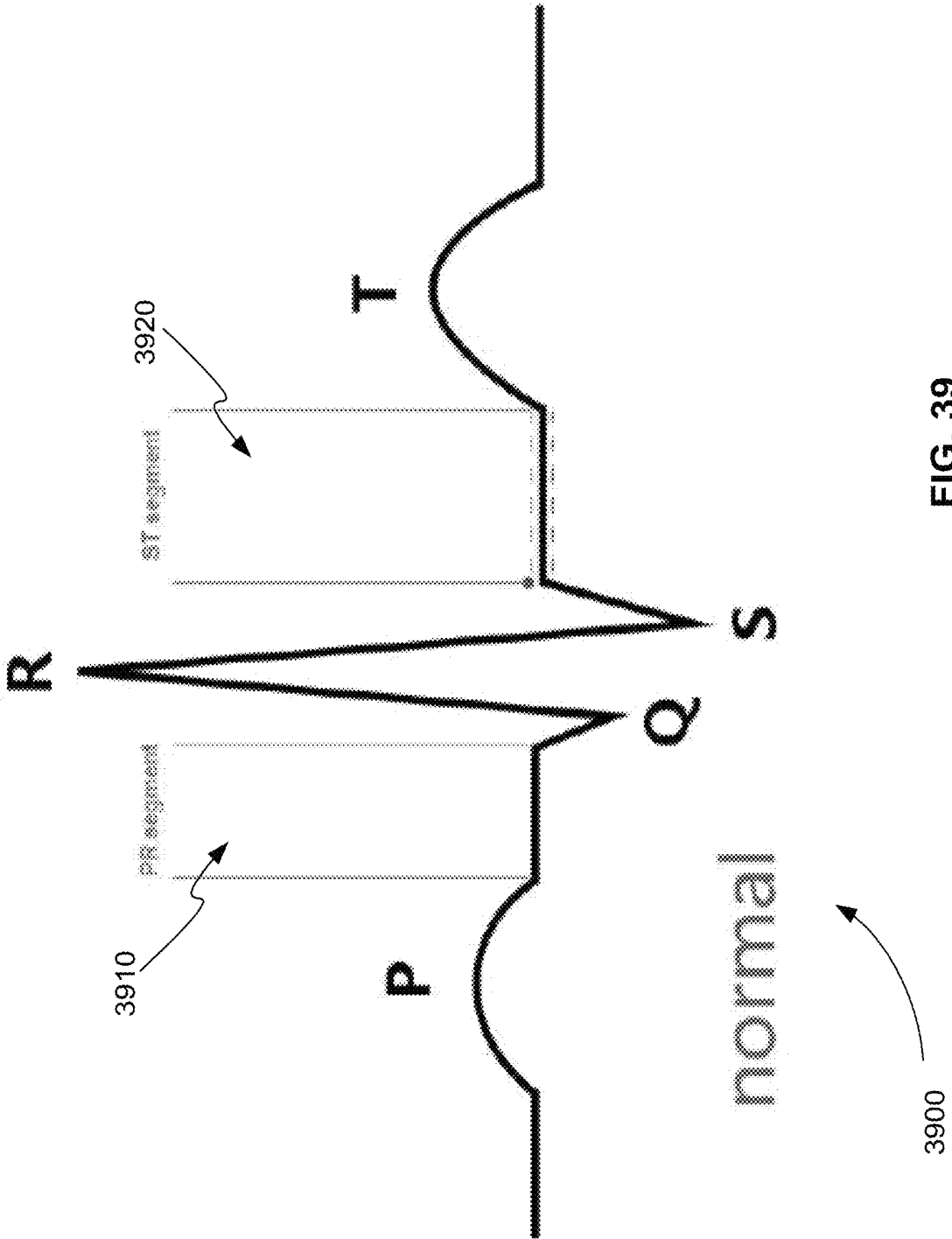
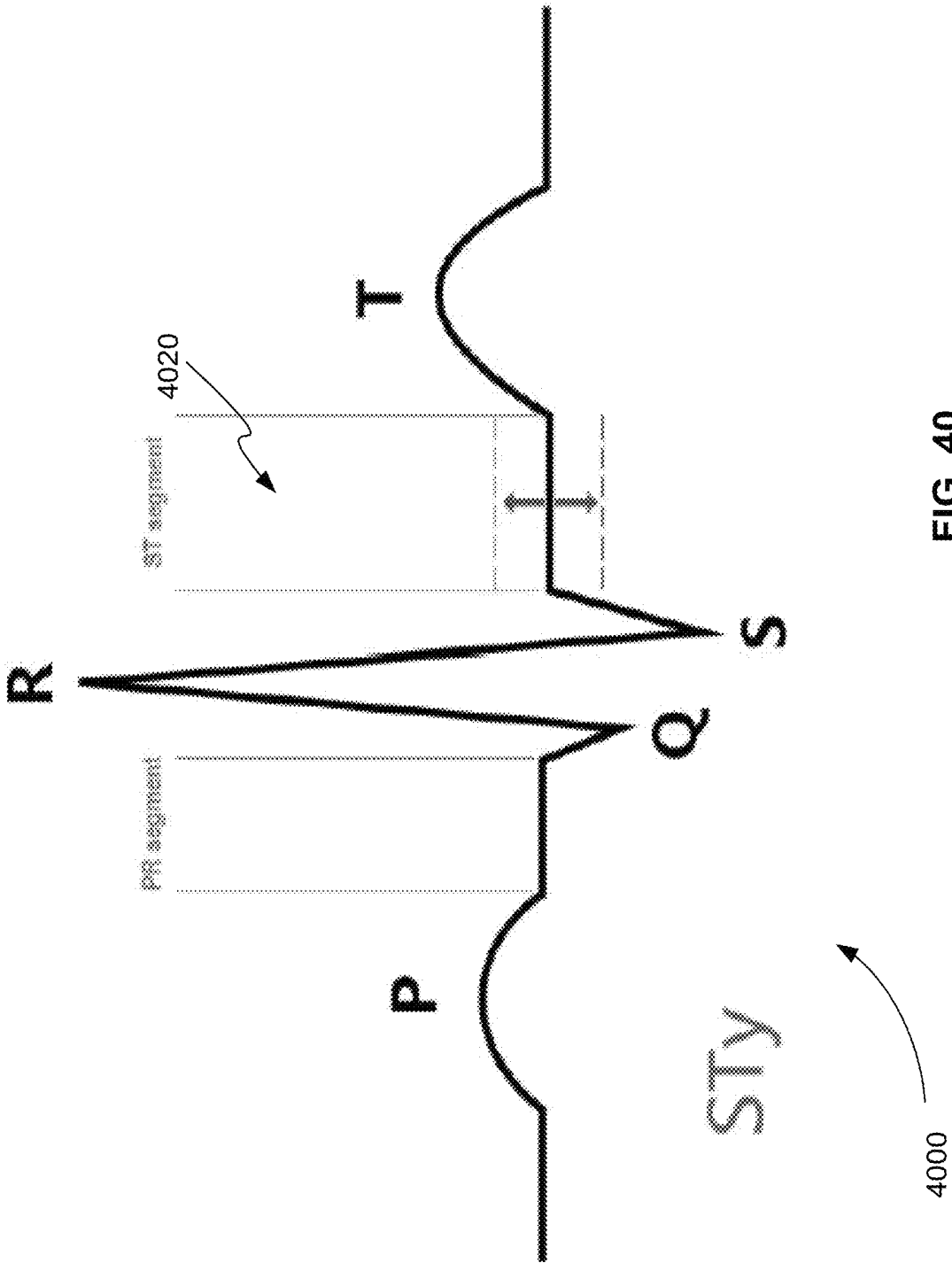


FIG. 39



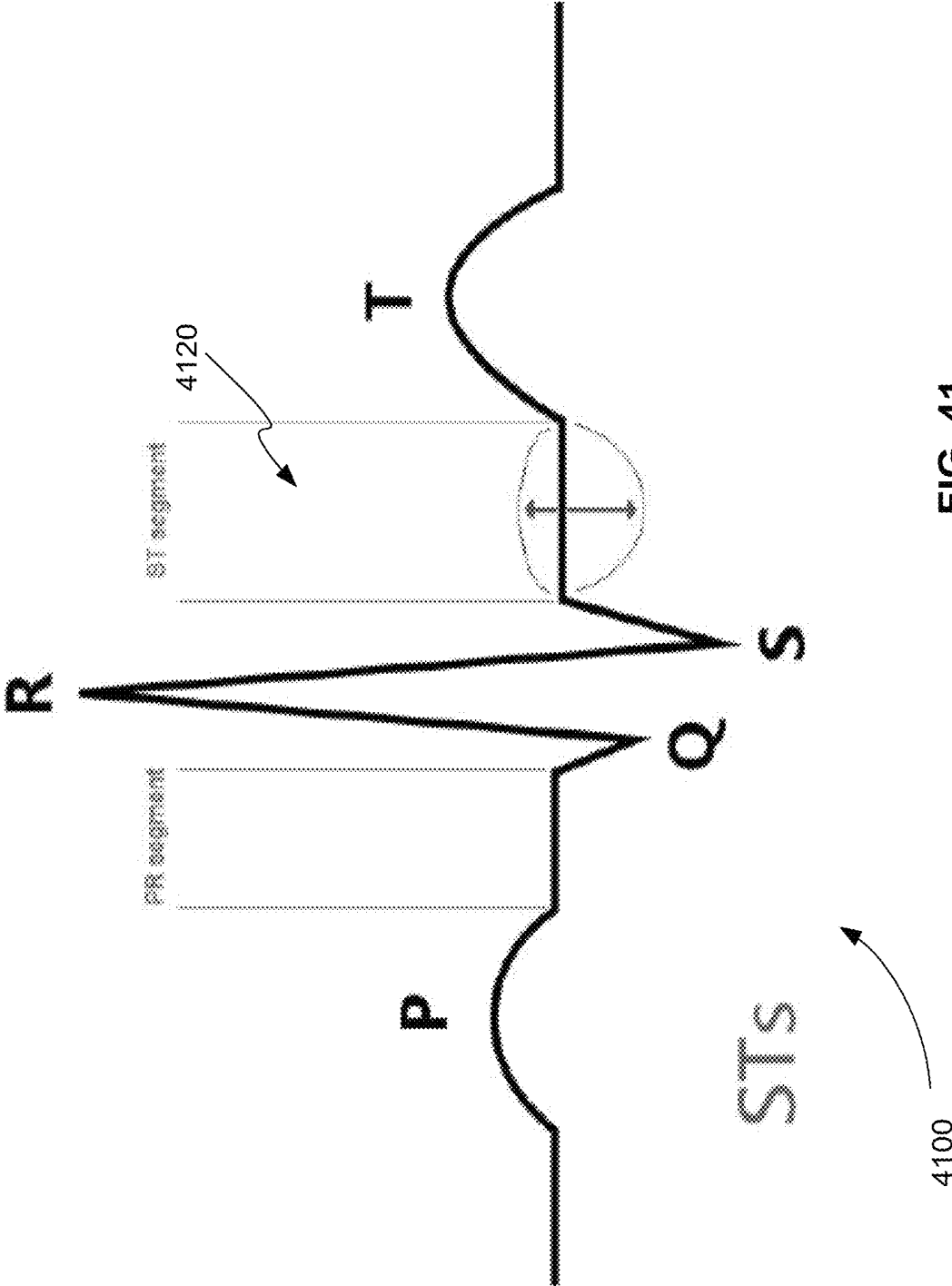


FIG. 41

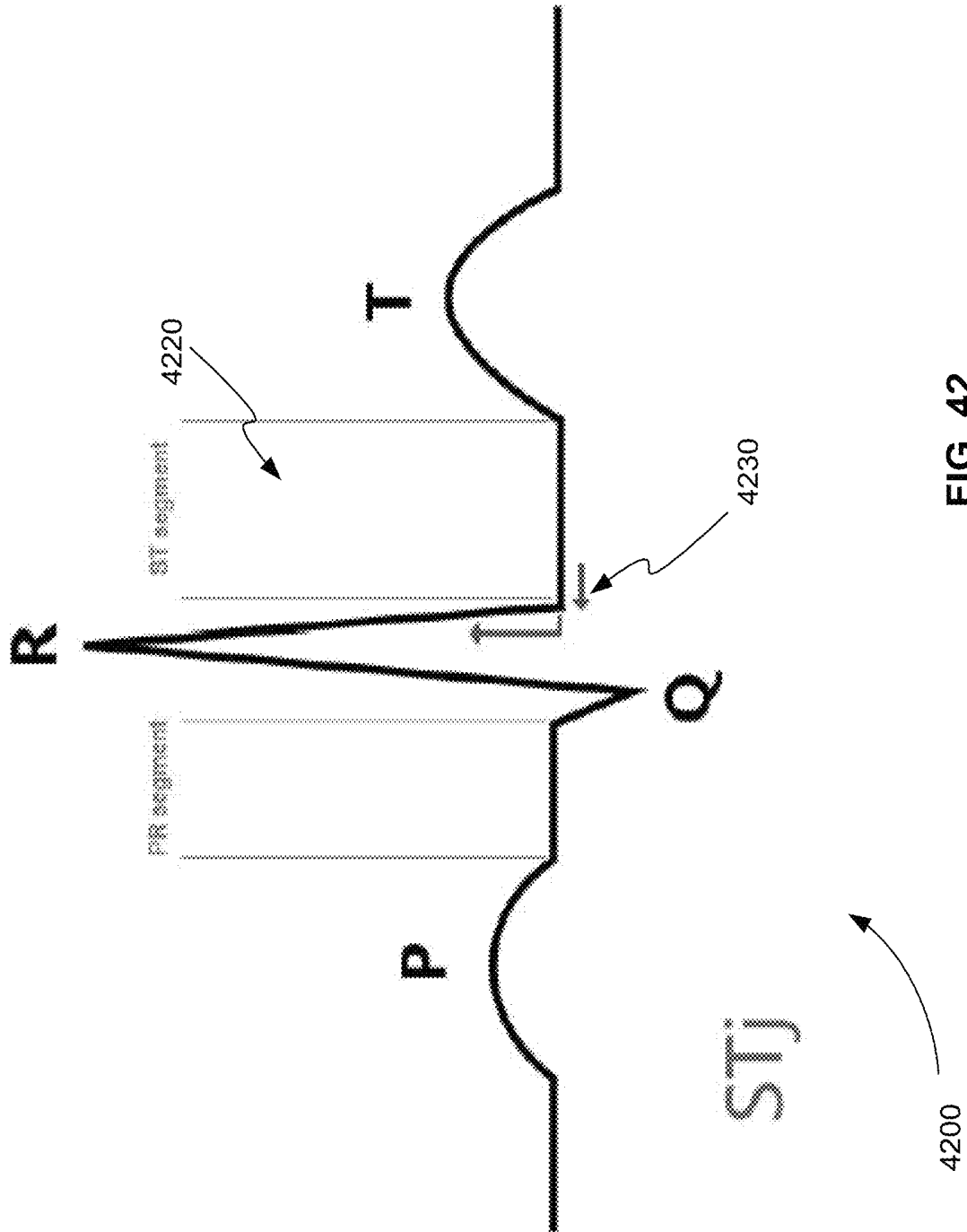


FIG. 42

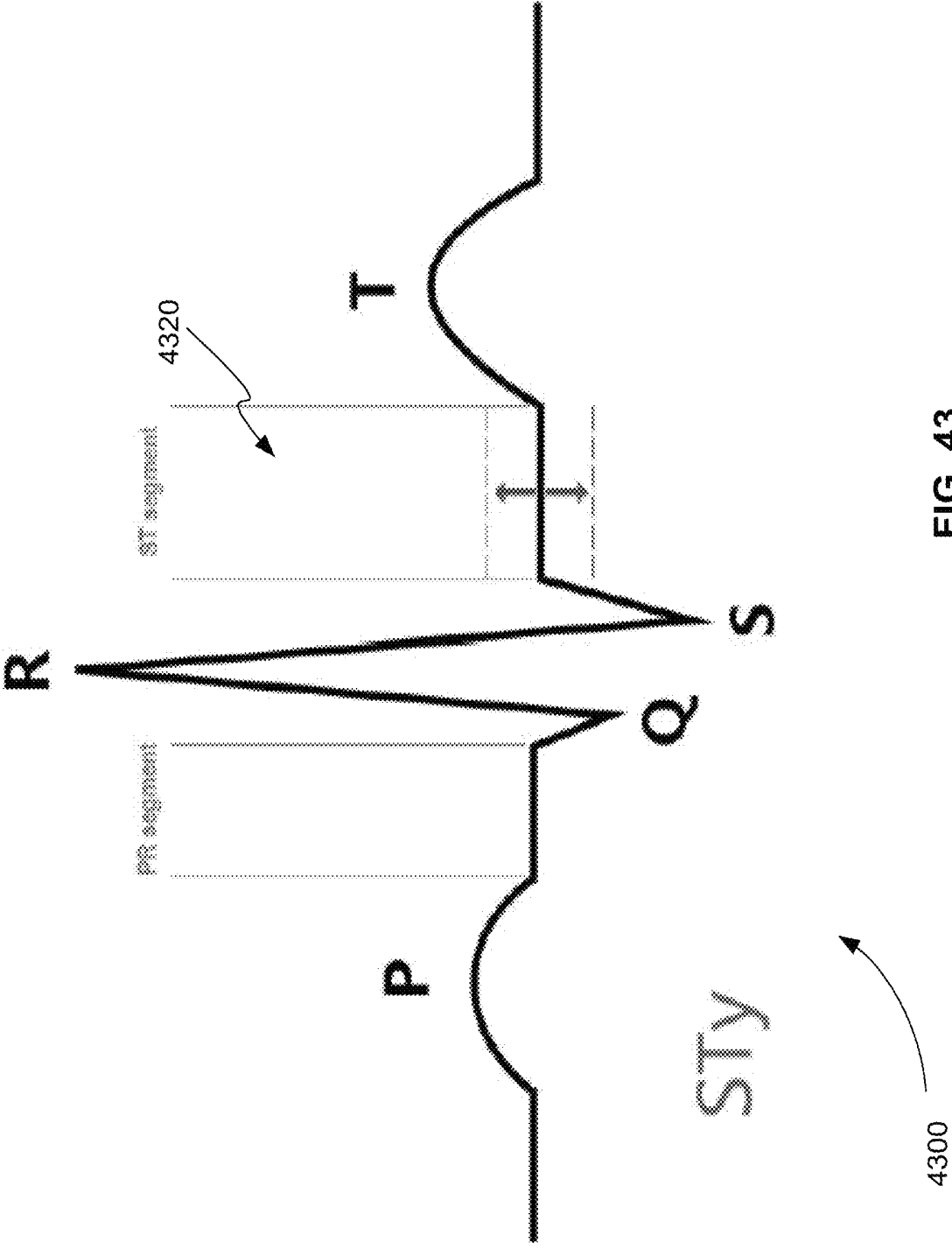


FIG. 43

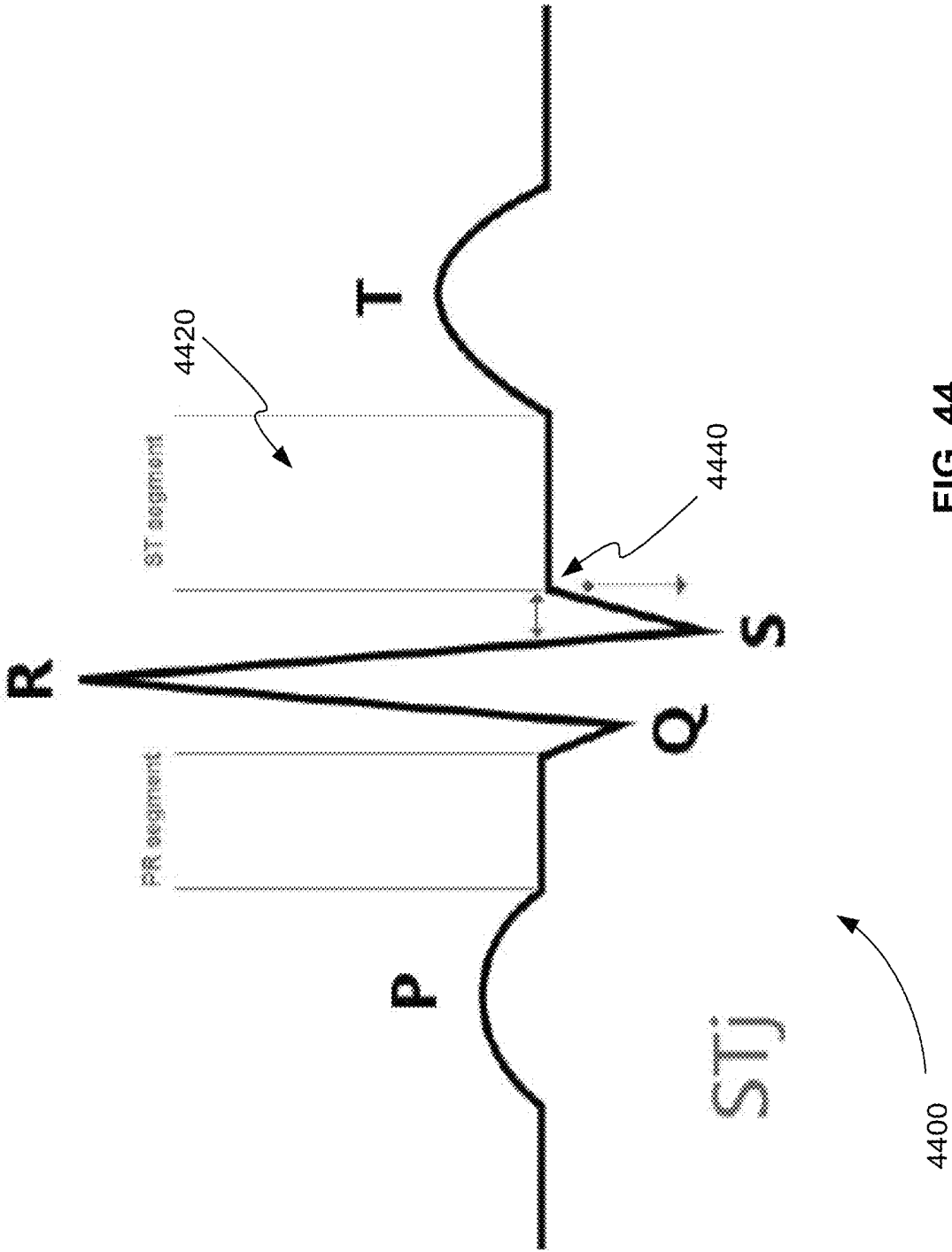
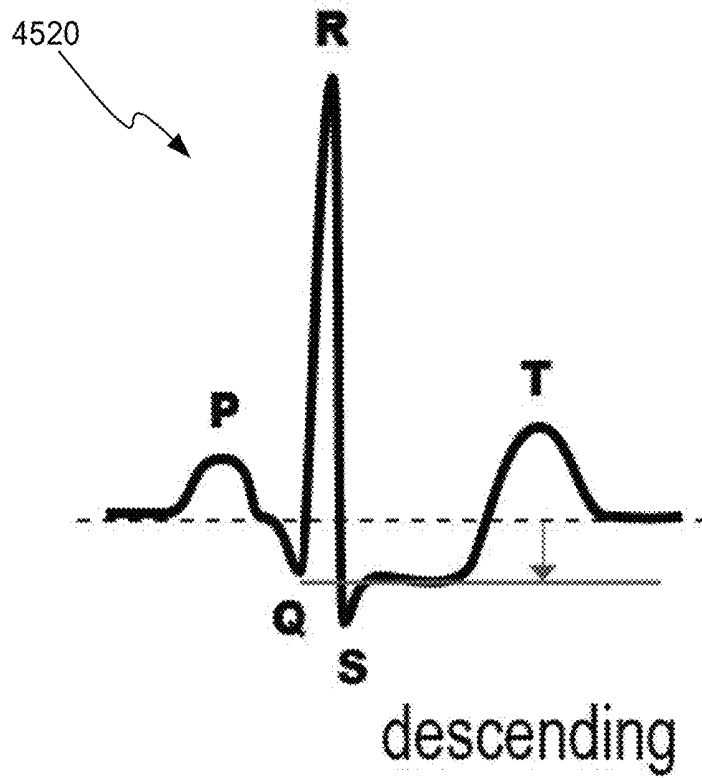
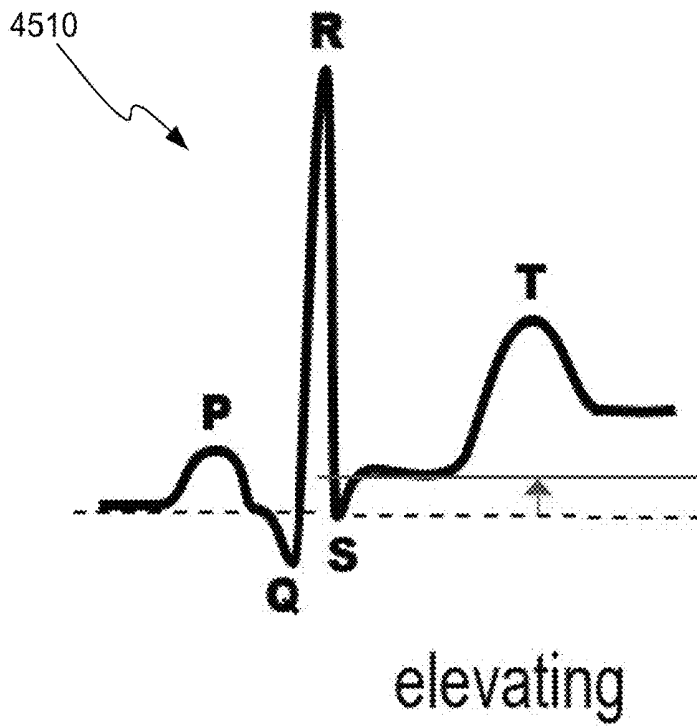
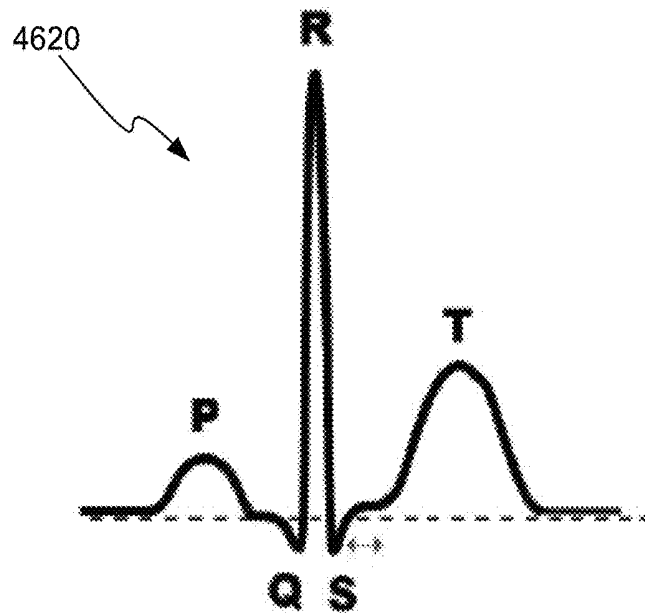
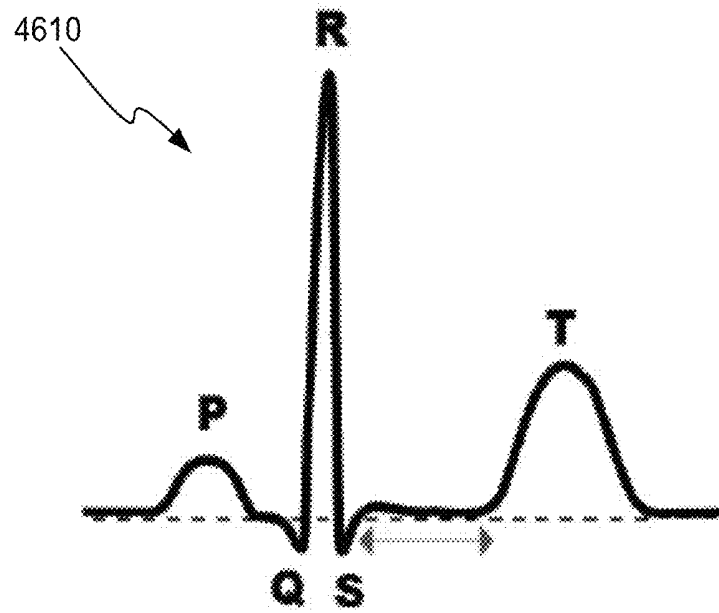


FIG. 44



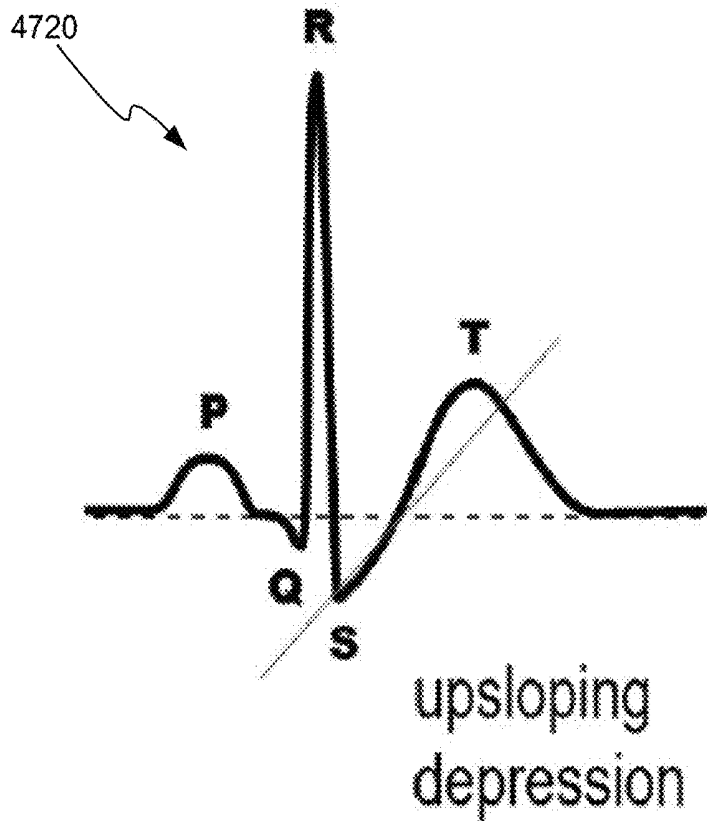
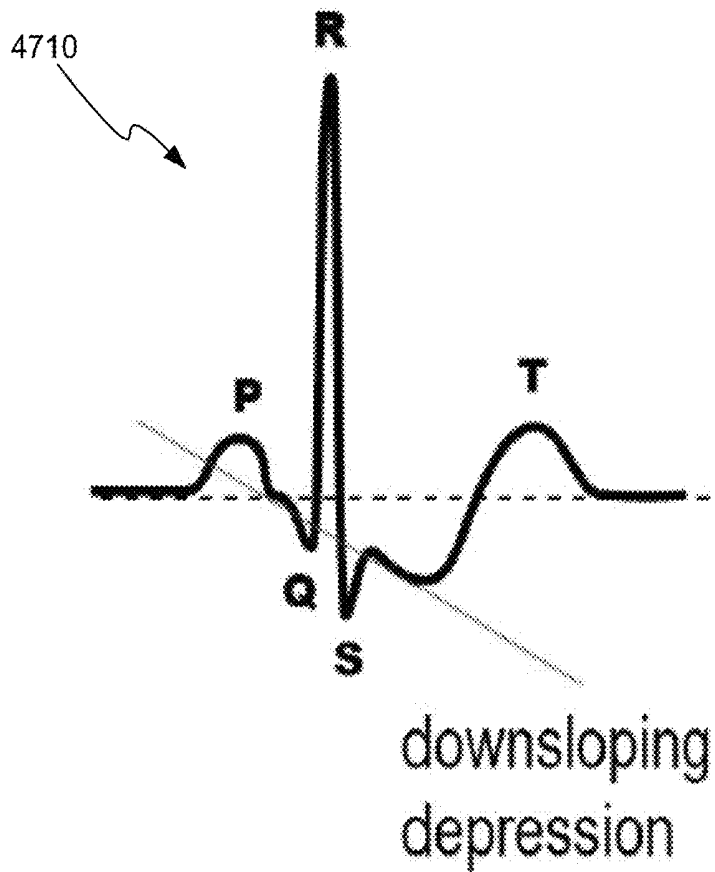
4500

FIG. 45



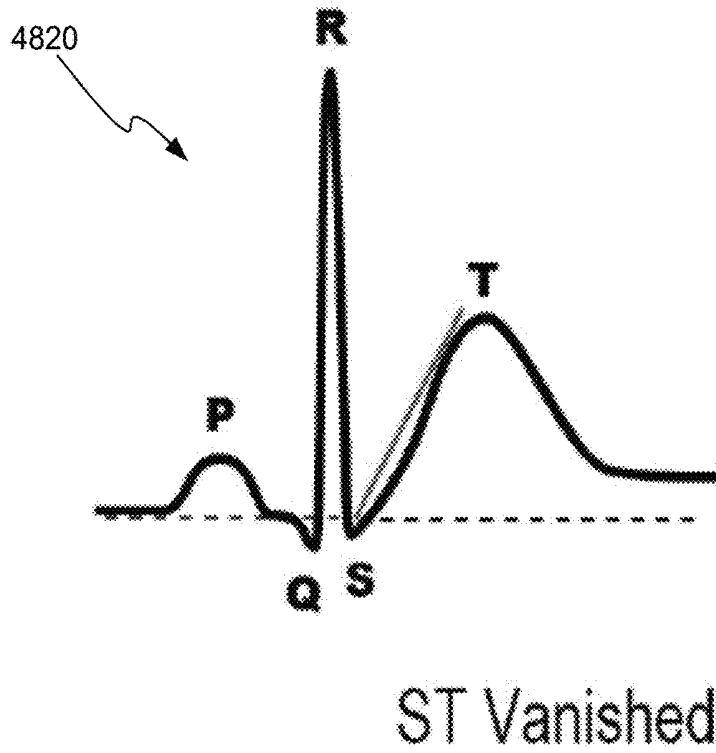
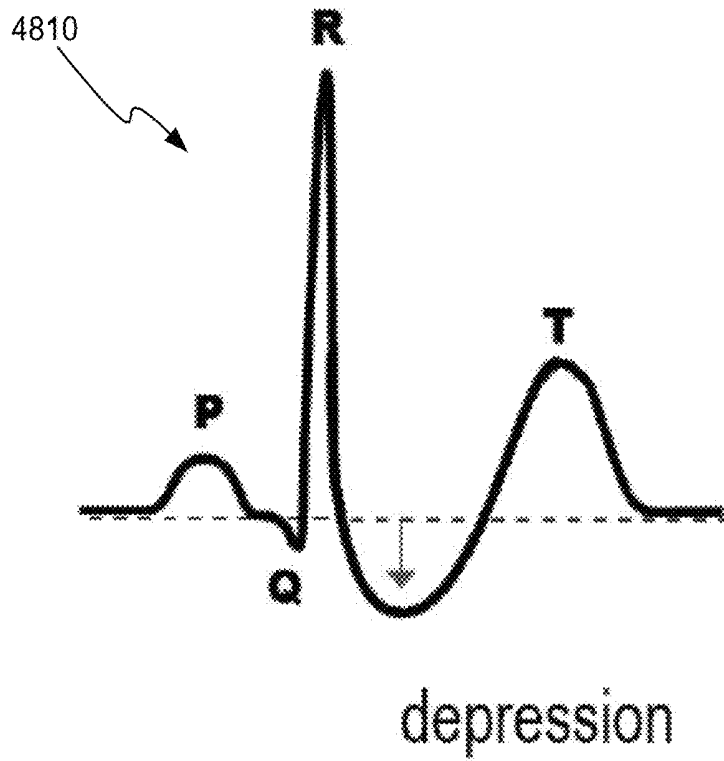
4600

FIG. 46



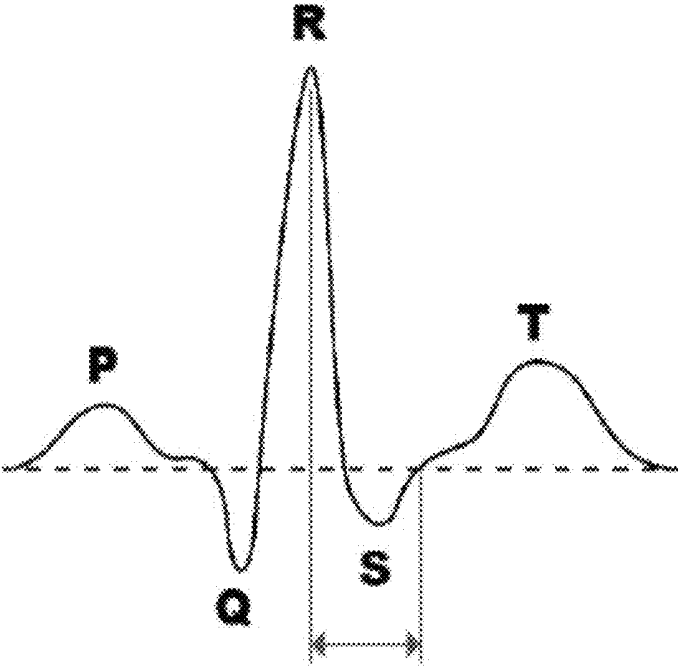
4700

FIG. 47



4800

FIG. 48



R-J interval
widened


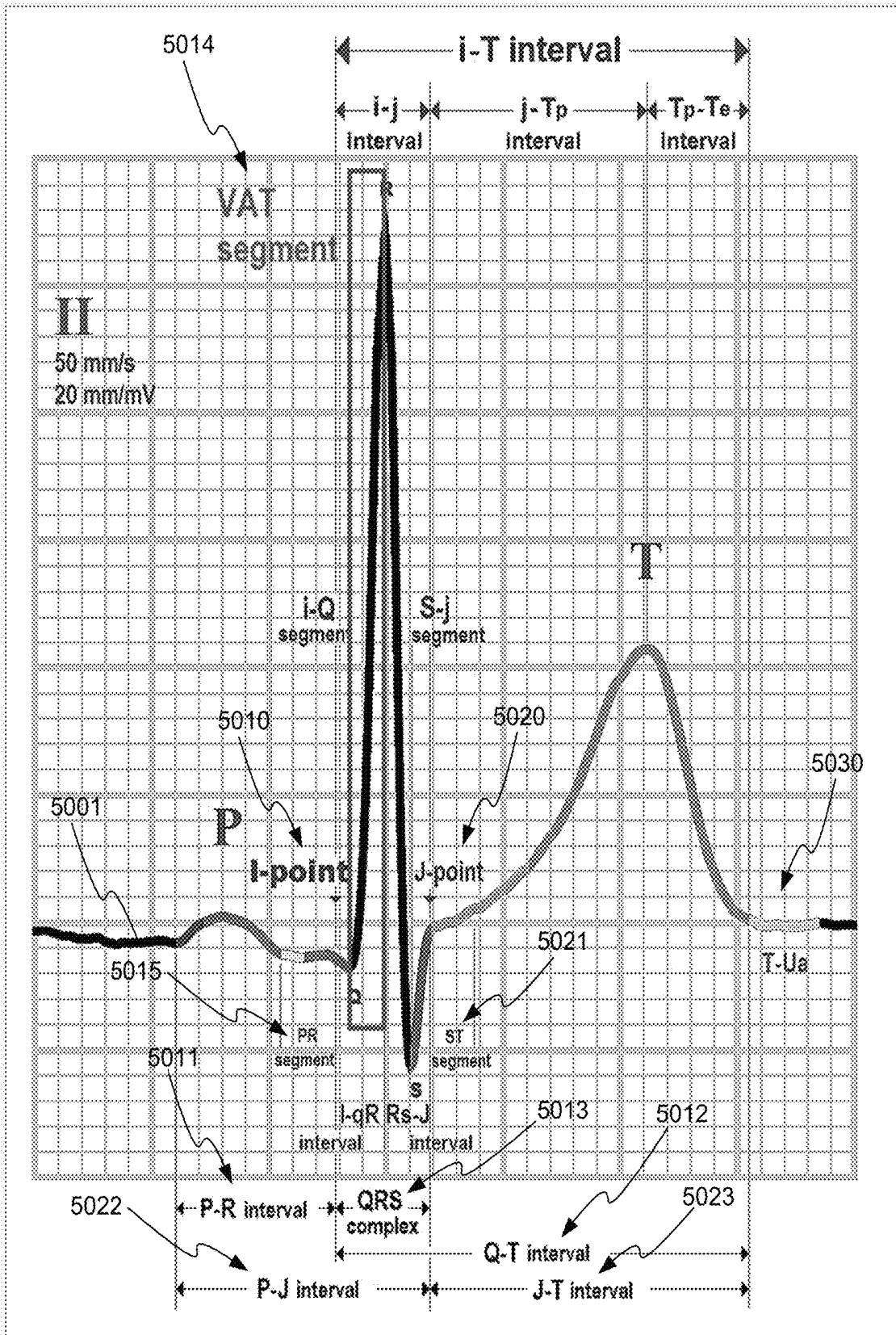
4900 

FIG. 49



5000 → **FIG. 50**

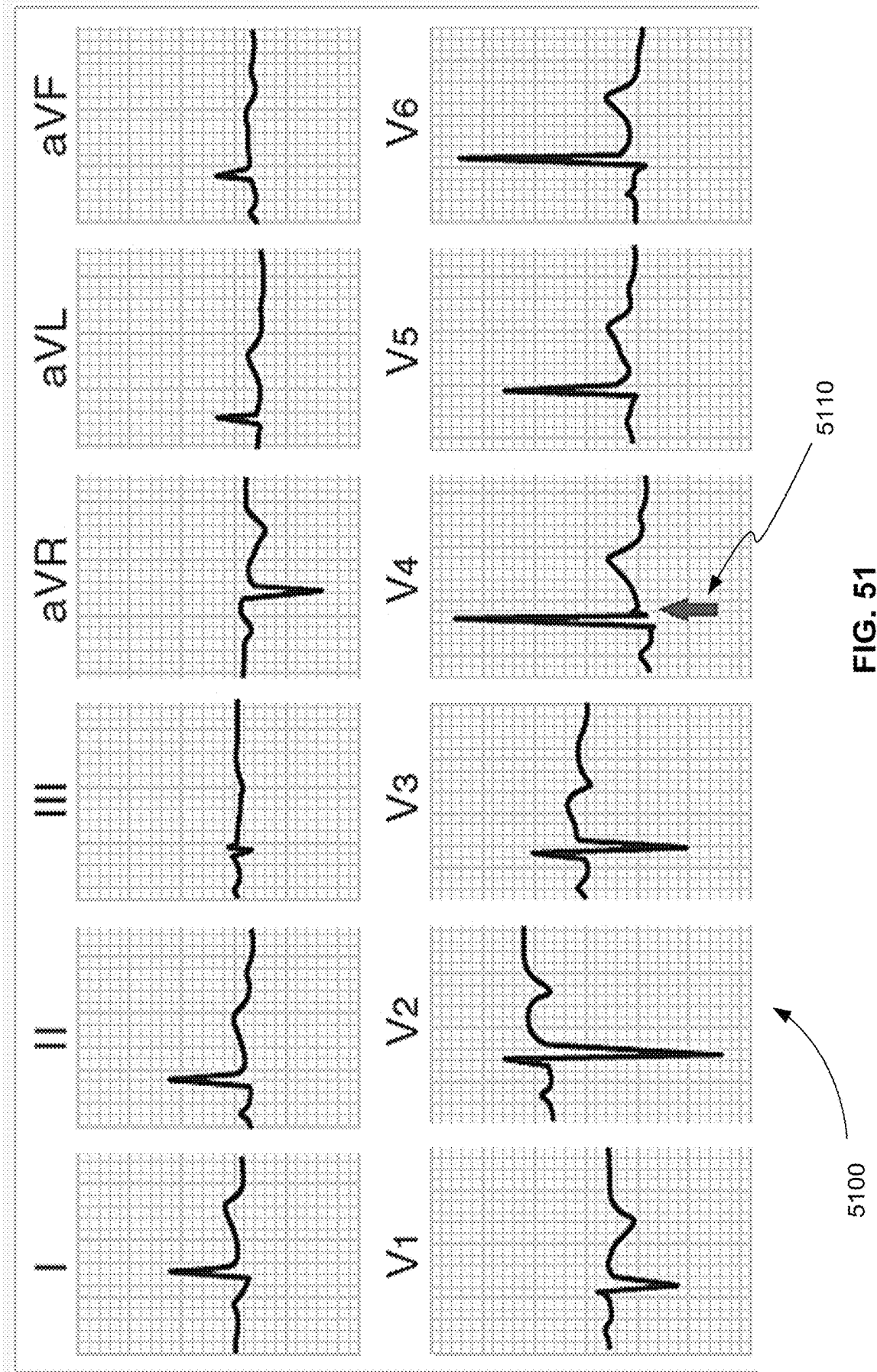
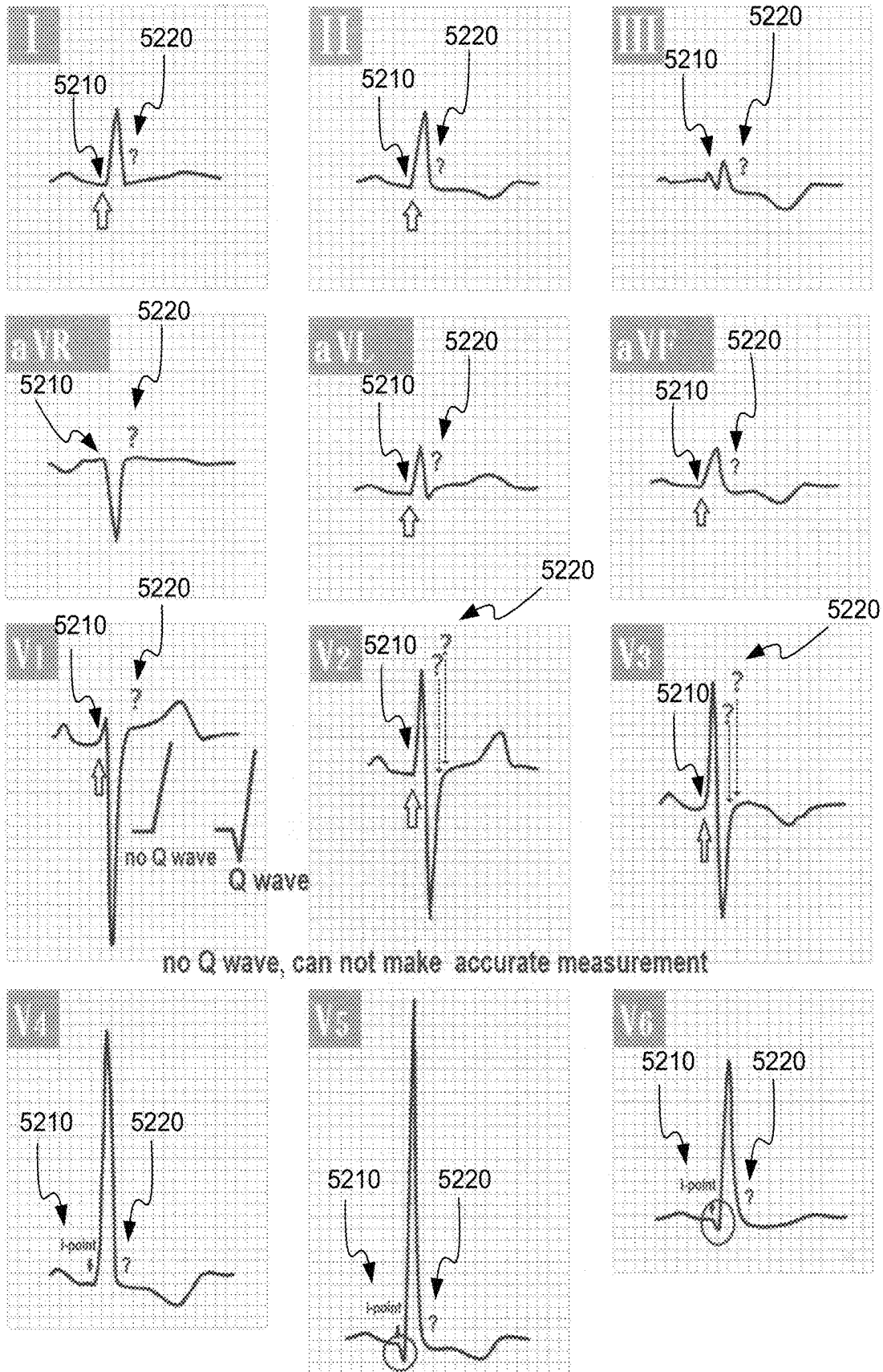


FIG. 51



5200

(PRIOR ART)
FIG. 52

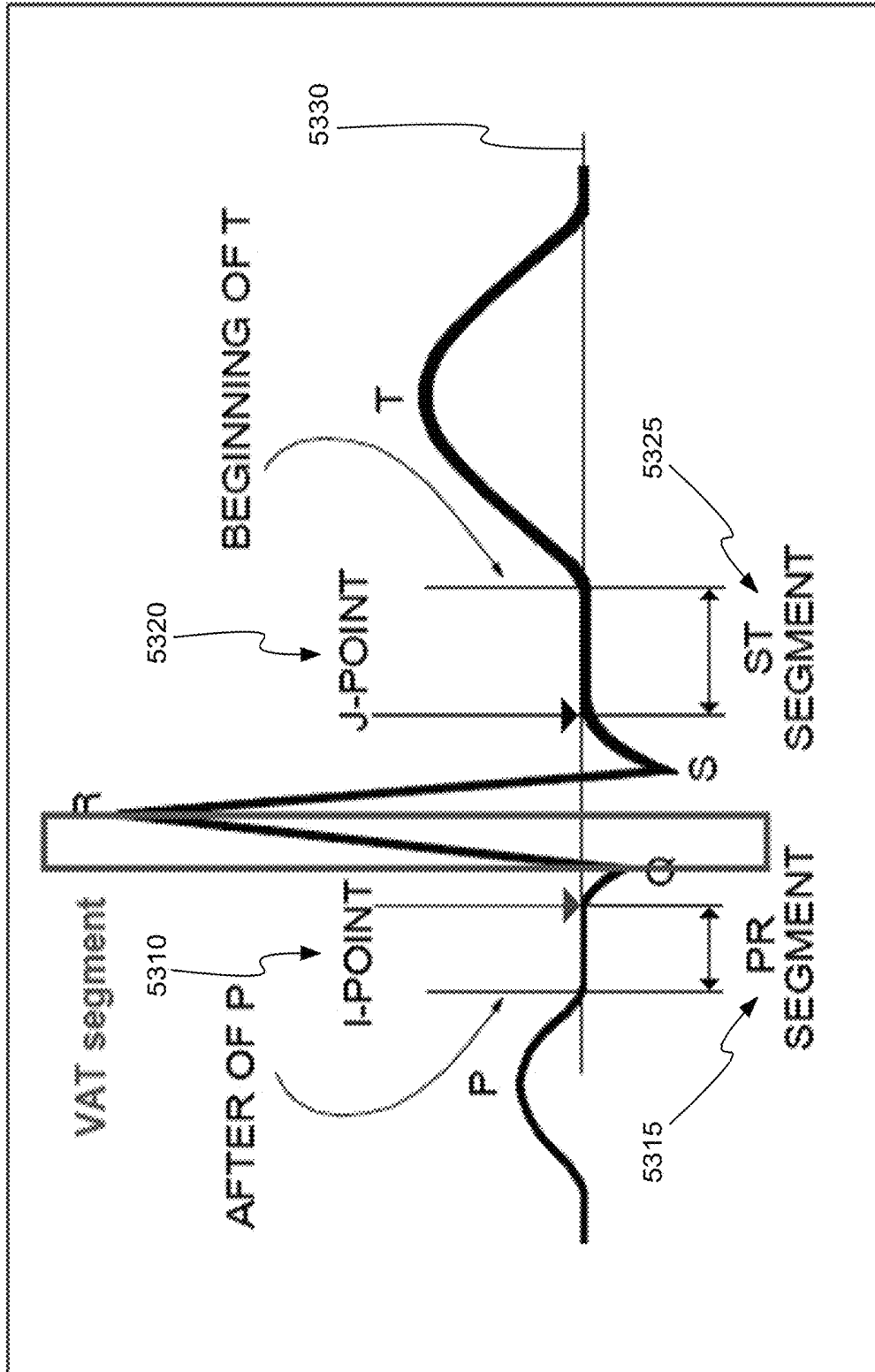


FIG. 53

5300

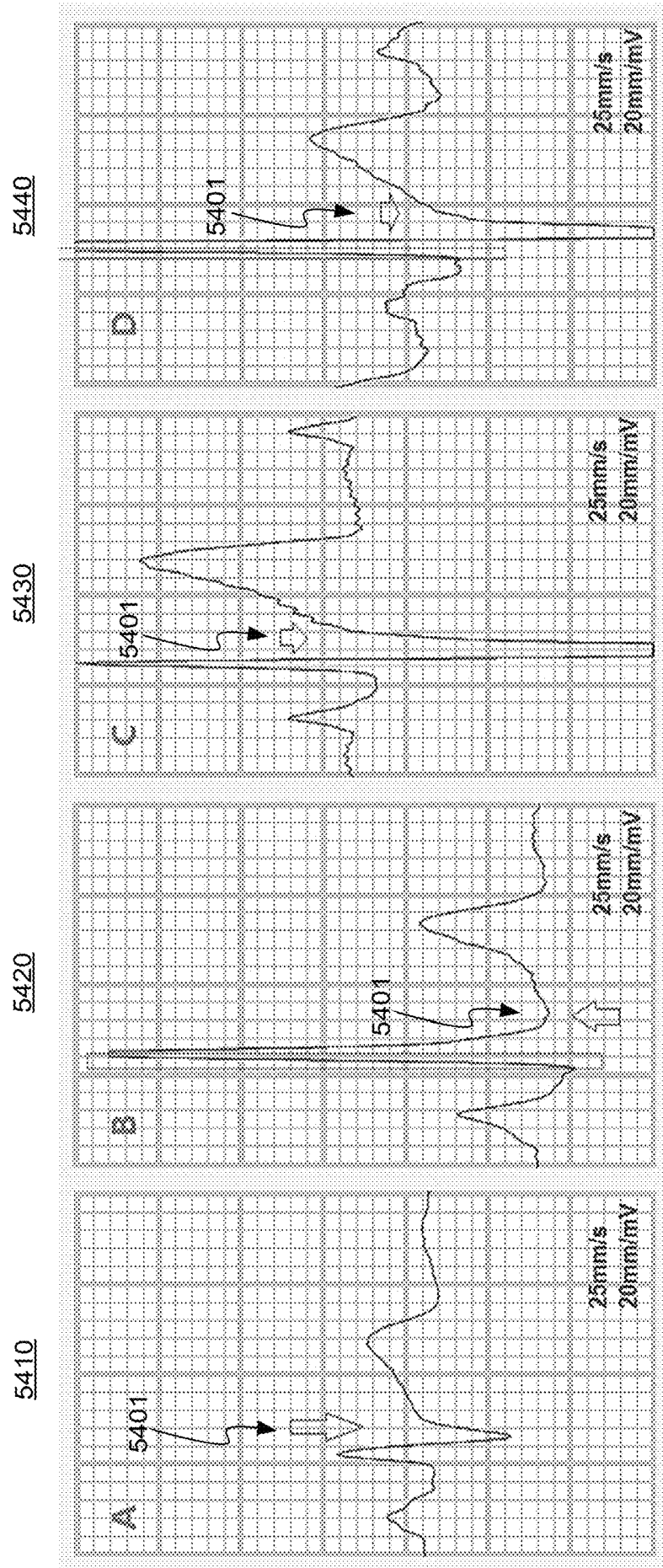


FIG. 54

5530

5520

5510

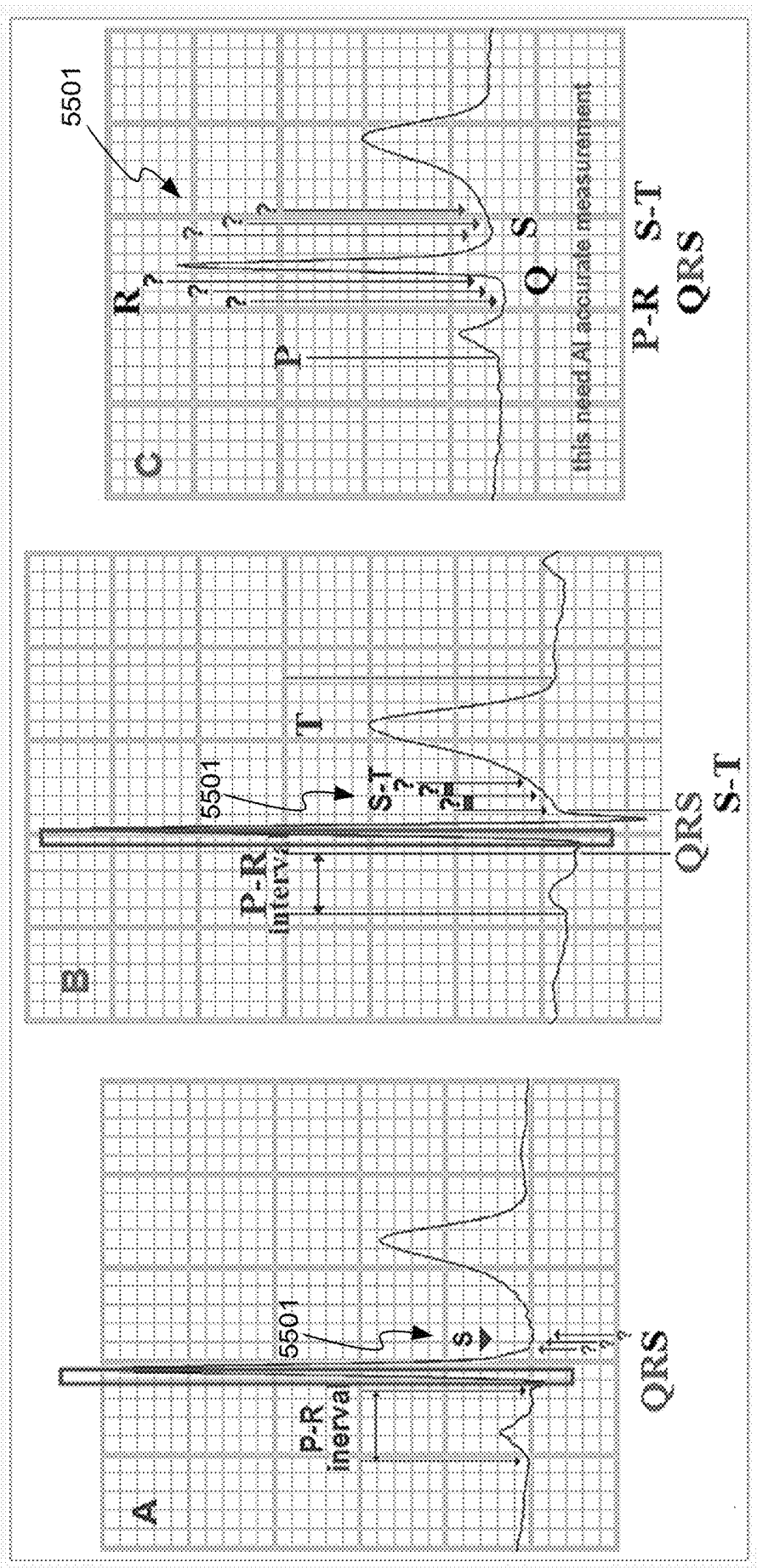
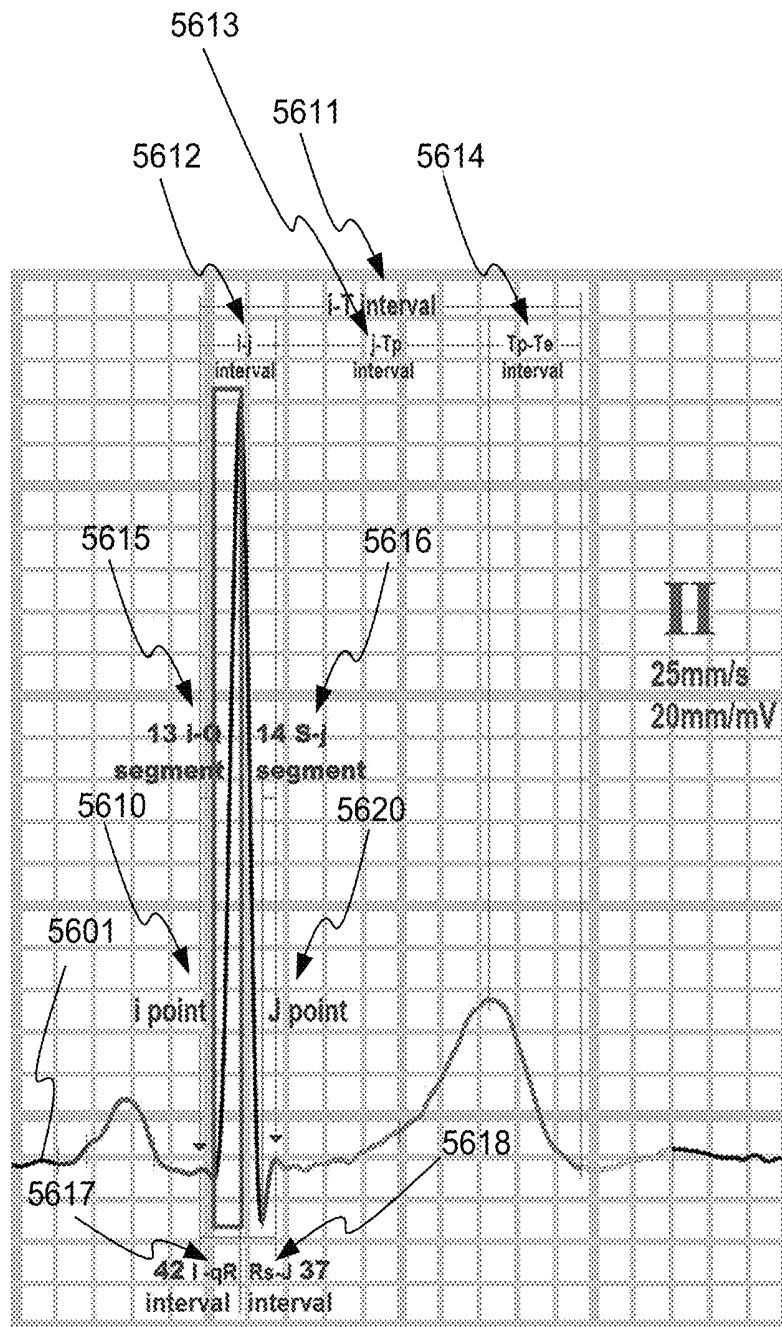


FIG. 55

5500



5600

FIG. 56

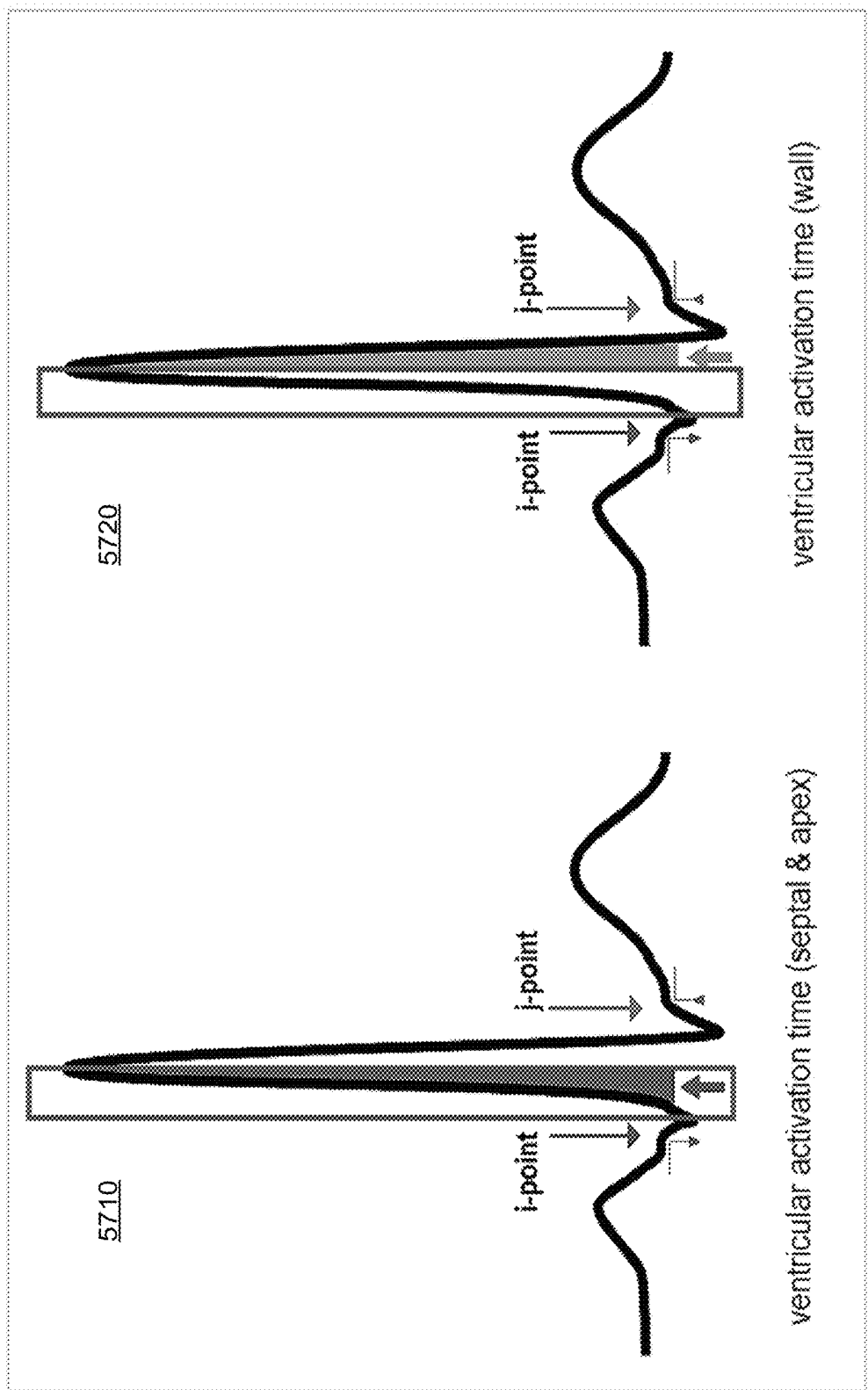
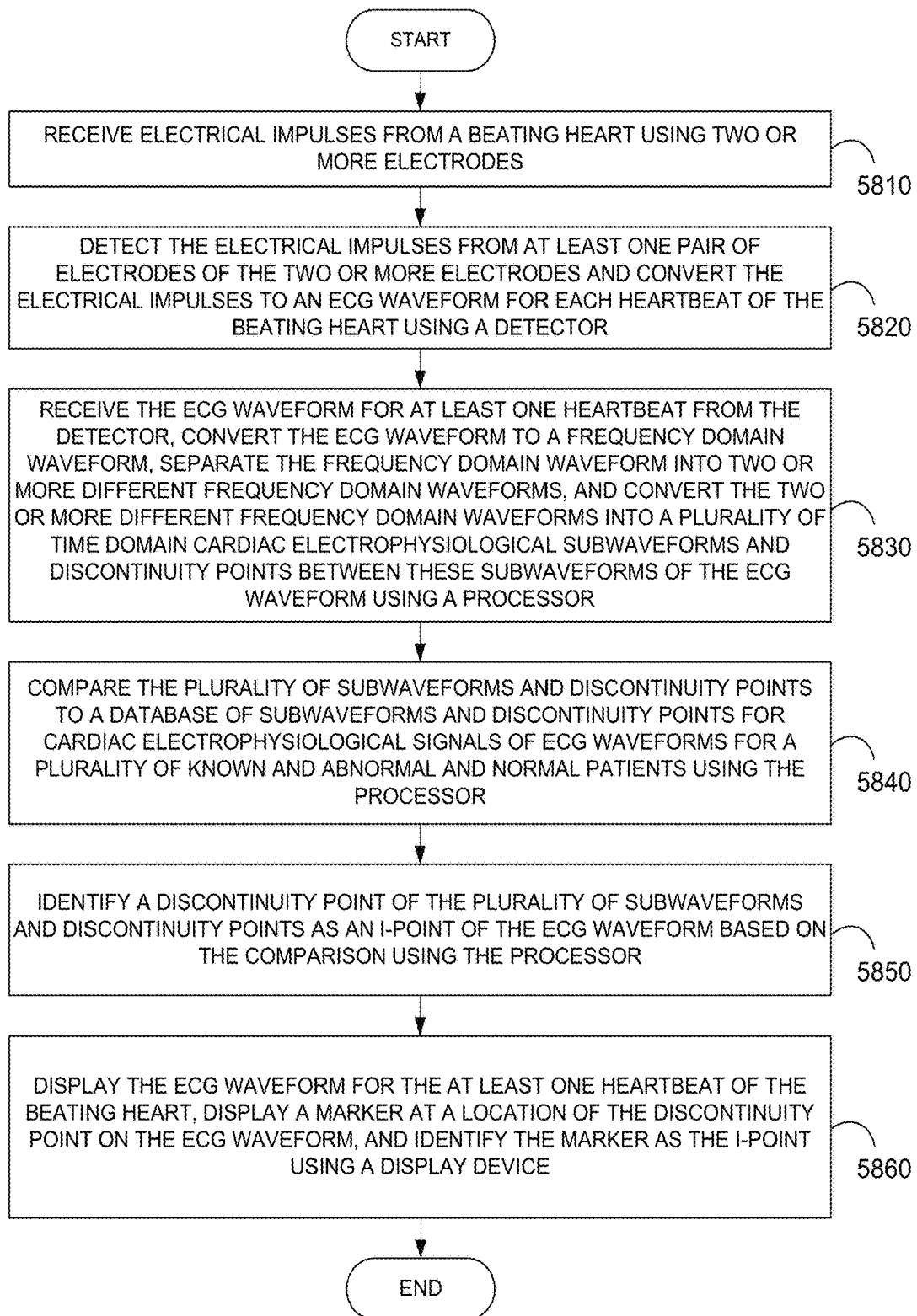


FIG. 57

5700



5800 ↗

FIG. 58

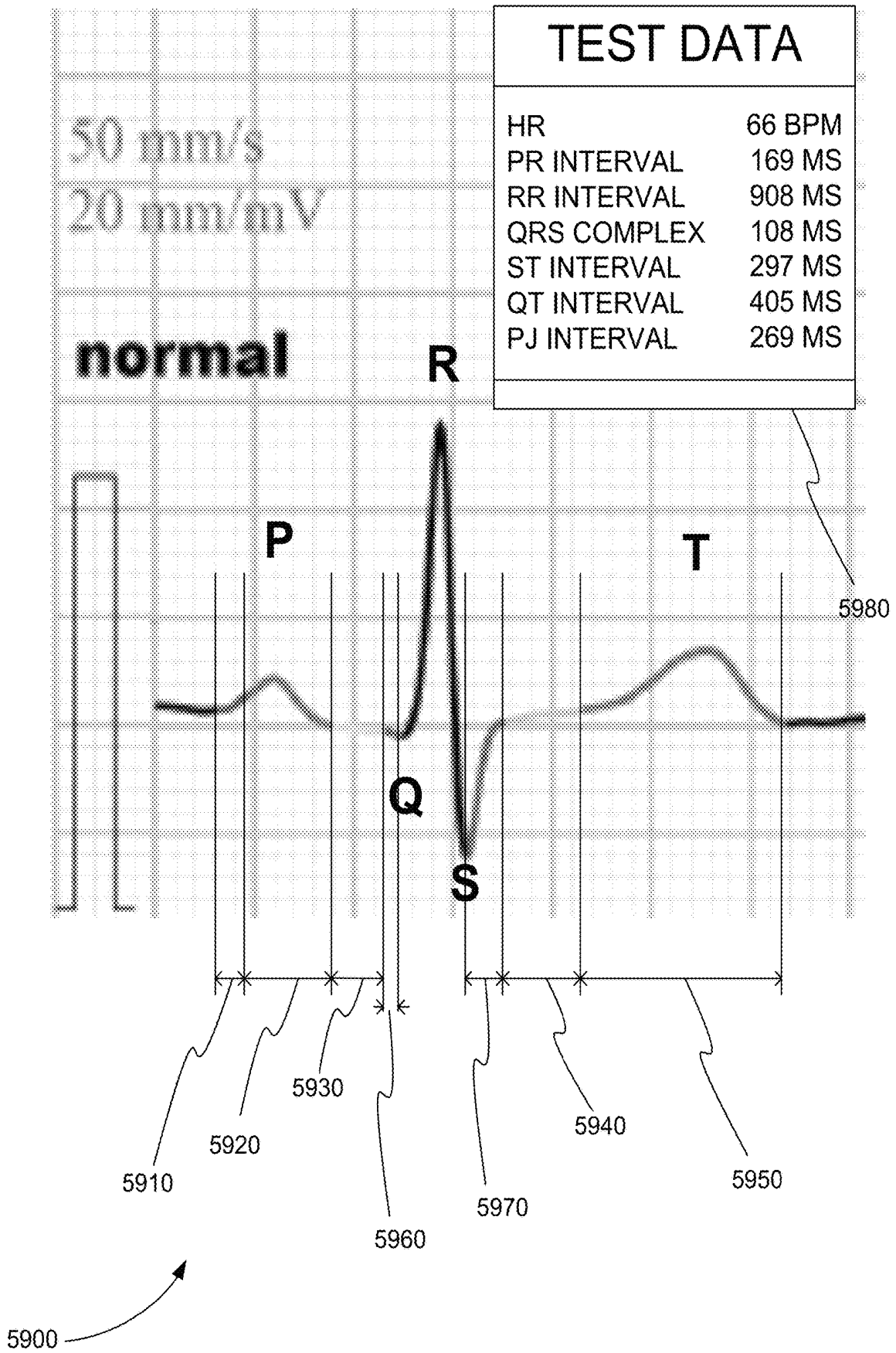


FIG. 59

6011 6012 6013

6010

PARAMETER	STANDARD	TEST DATA
HR	60-90 bpm	65
P-R interval	120-200 ms	155
PA interval	25-35 ms	30
AH interval	60-110 ms	84
HV interval	35-55 ms	41
RR interval	600-1000 ms	913
PP interval	600-1000 ms	917
qrs(QR+RS)	(QR+RS)	62
QRS complex	60-110 ms	111
ST segment	ST seg-T seg	84
T segment	T seg-ST seg	209
S-T interval	<380 ms	293
QT interval	<440 ms	404
P-J interval	<270 ms	266

6020

PA interval	Purkinje's
AH interval	ST segment
HV interval	T segment
QRS complex	S-T interval

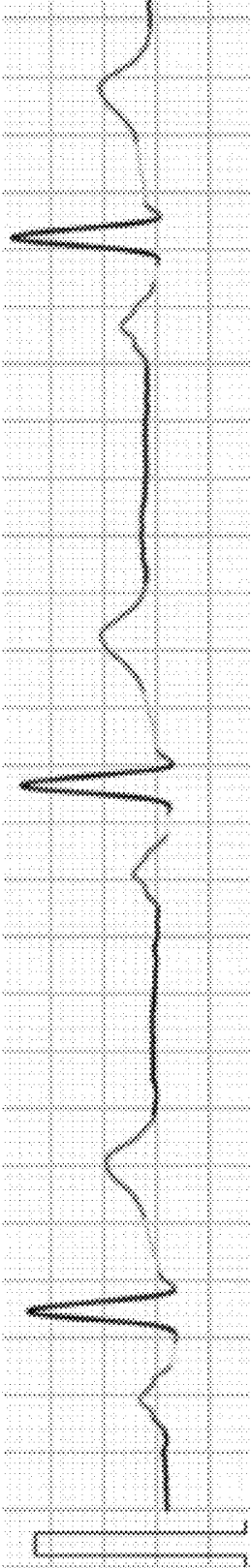
6021 6022 6023 6024 6025 6026

NORMAL

6000

FIG. 60

ABNORMAL
BEFORE PCI



6100

FIG. 61

PARAMETER STANDARD TEST DATA		
HR	60~90 bpm	63
P-R interval	120~200 ms	160
PA interval	25~35 ms	29
AH interval	60~110 ms	89
HV interval	35~55 ms	42
RR interval	600~1000 ms	940
PP interval	600~1000 ms	939
qrs(QR+RS)	(QR+RS)	61
QRS complex	60~110 ms	121
ST segment	ST seg<T seg	107
T segment	T seg>ST seg	189
S-T interval	<380 ms	286
QT interval	<440 ms	407
P-J interval	<270 ms	279

=====	PA interval	=====	Purkinje's
-----	AH interval	-----	ST segment
-----	HV interval	=====	T segment
=====	QRS complex	-----	S-T interval

ABNORMAL
BEFORE PCI


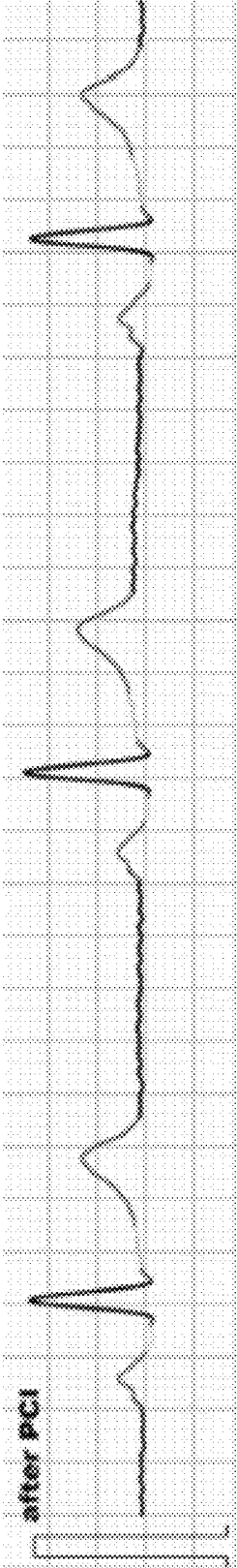
6200 

FIG. 62

ABNORMAL
AFTER PCI



6300

FIG. 63

PARAMETER	STANDARD	TEST DATA
HR	60-90 bpm	59
P-R interval	120-200 ms	158
PA interval	25-35 ms	26
AH interval	60-110 ms	94
HV interval	35-55 ms	40
RR interval	600-1000 ms	1006
PP interval	600-1000 ms	1005
QRS complex	60-110 ms	104
ST segment	ST seg < T seg	107
T segment	T seg > ST seg	184
S-T interval	<380 ms	291
QT interval	<440 ms	396
P-J interval	<270 ms	262
J-T interval	<380 ms	291

PA interval	Purkinje's
AH interval	ST segment
HV interval	T segment
QRS complex	S-T interval

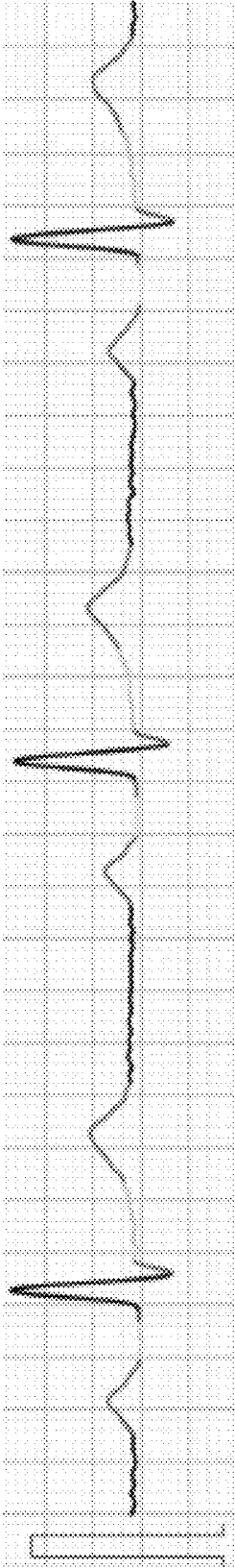
ABNORMAL

AFTER PCI

6400

FIG. 64

ABNORMAL
HIS BUNDLE BLOCK



6500

FIG. 65

PARAMETER	STANDARD	TEST DATA
HR	60-90 bpm	58
P-R interval	120-200 ms	321
PA interval	25-35 ms	32
AH interval	60-110 ms	107
HV interval	35-55 ms	82
RR interval	600-1000 ms	1013
PP interval	600-1000 ms	1014
qrs(QR+RS)	(QR+RS)	68
QRS complex	60-110 ms	112
ST segment	ST seg<T seg	152
T segment	T seg>ST seg	189
S-T interval	<380 ms	341
QT interval	<440 ms	452
P-J interval	<270 ms	333

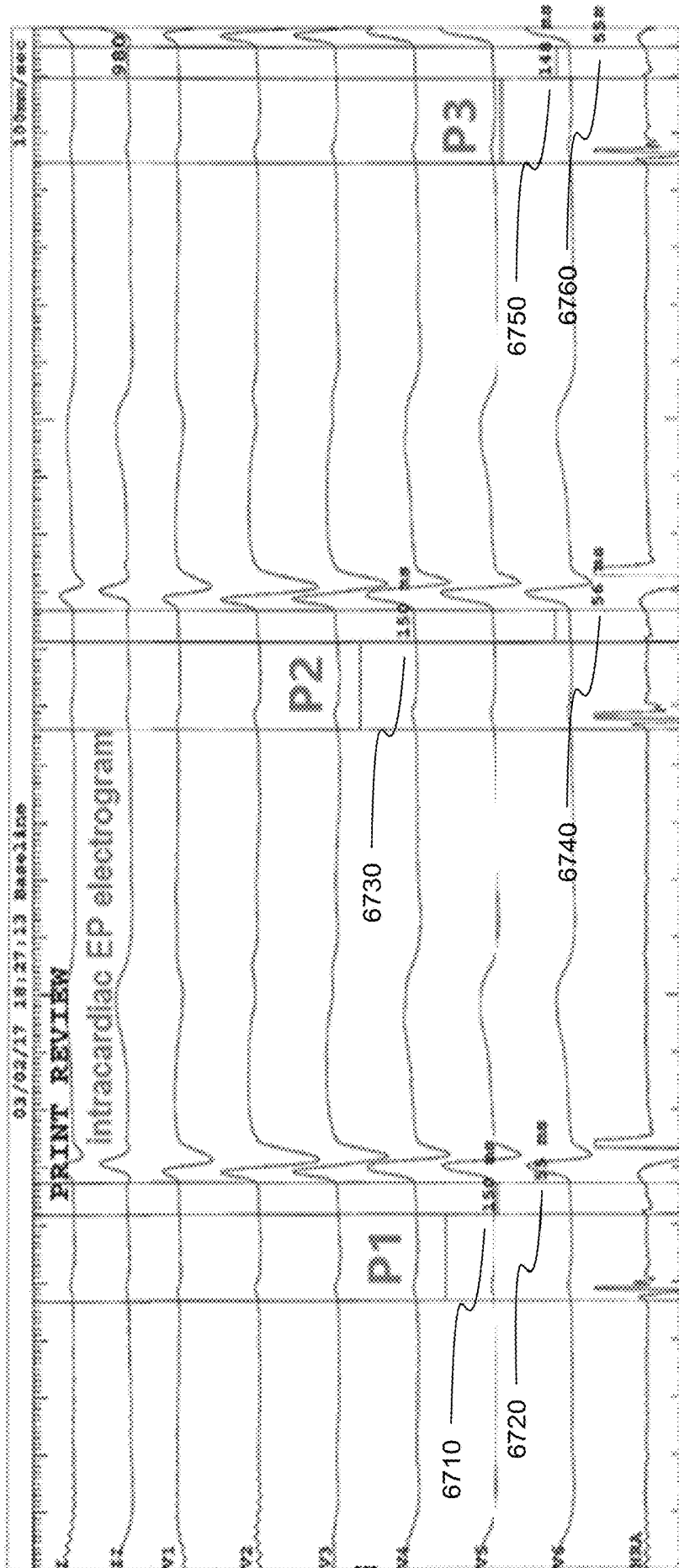
—————	PA interval	—————	Purkinje's
—————	AH interval	—————	ST segment
—————	HV interval	—————	T segment
—————	QRS complex	—————	S-T interval

ABNORMAL

HIS BUNDLE BLOCK

6600

FIG. 66



(PRIOR ART)

FIG. 67



6700

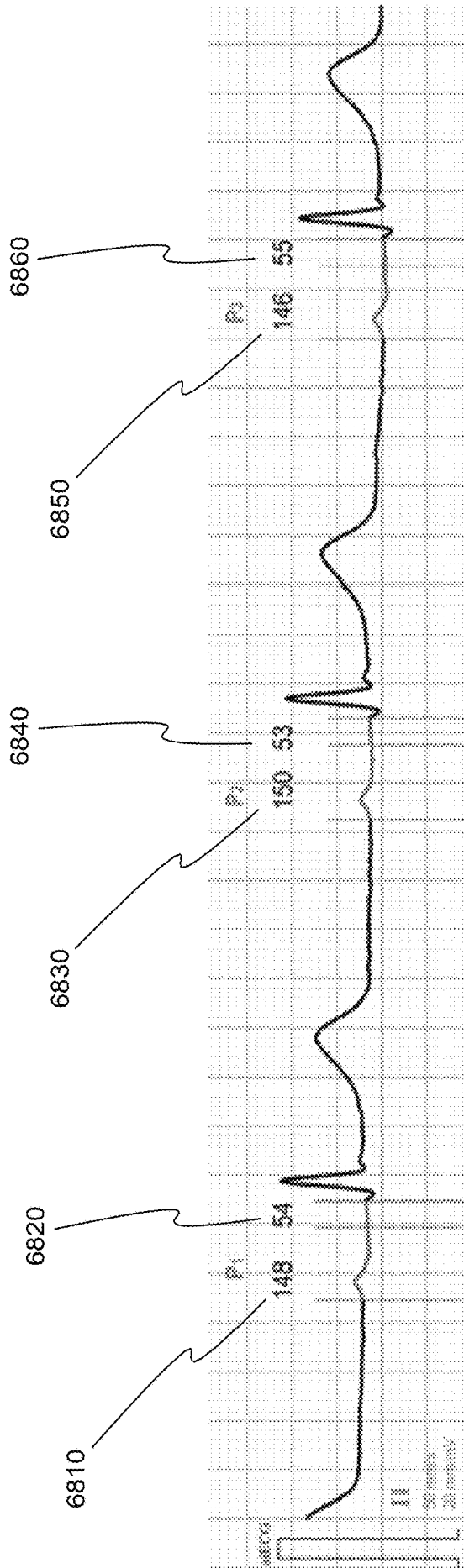
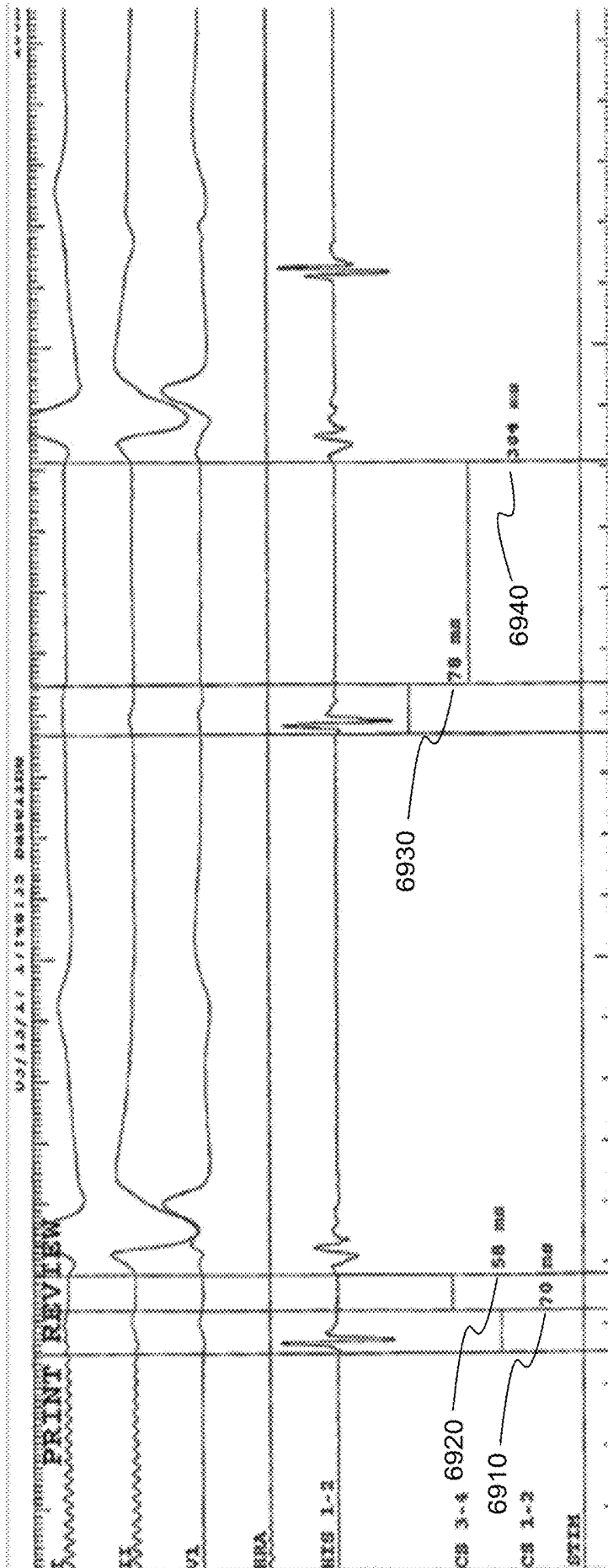


FIG. 68

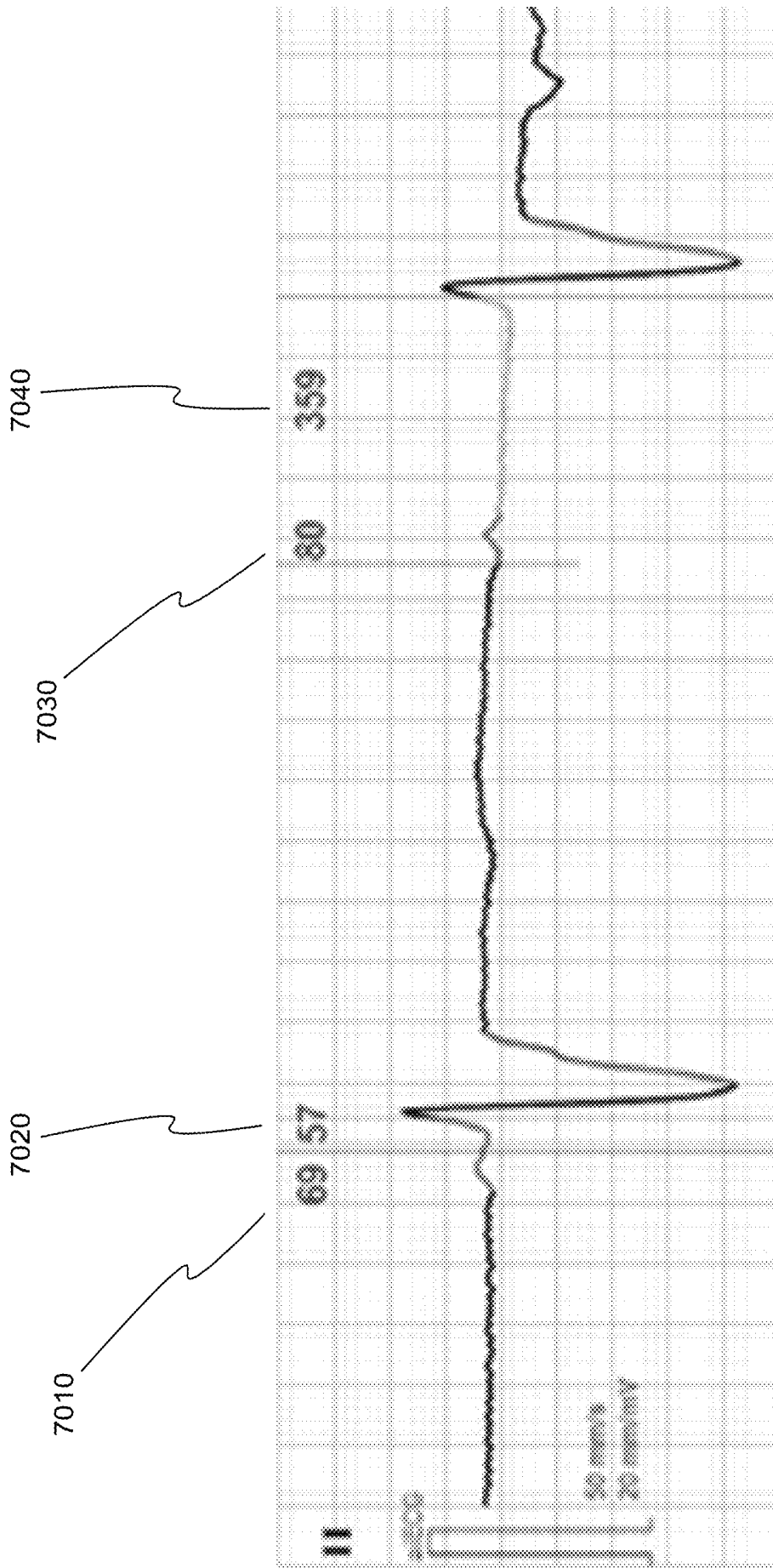




(PRIOR ART)

FIG. 69





7000

FIG. 70

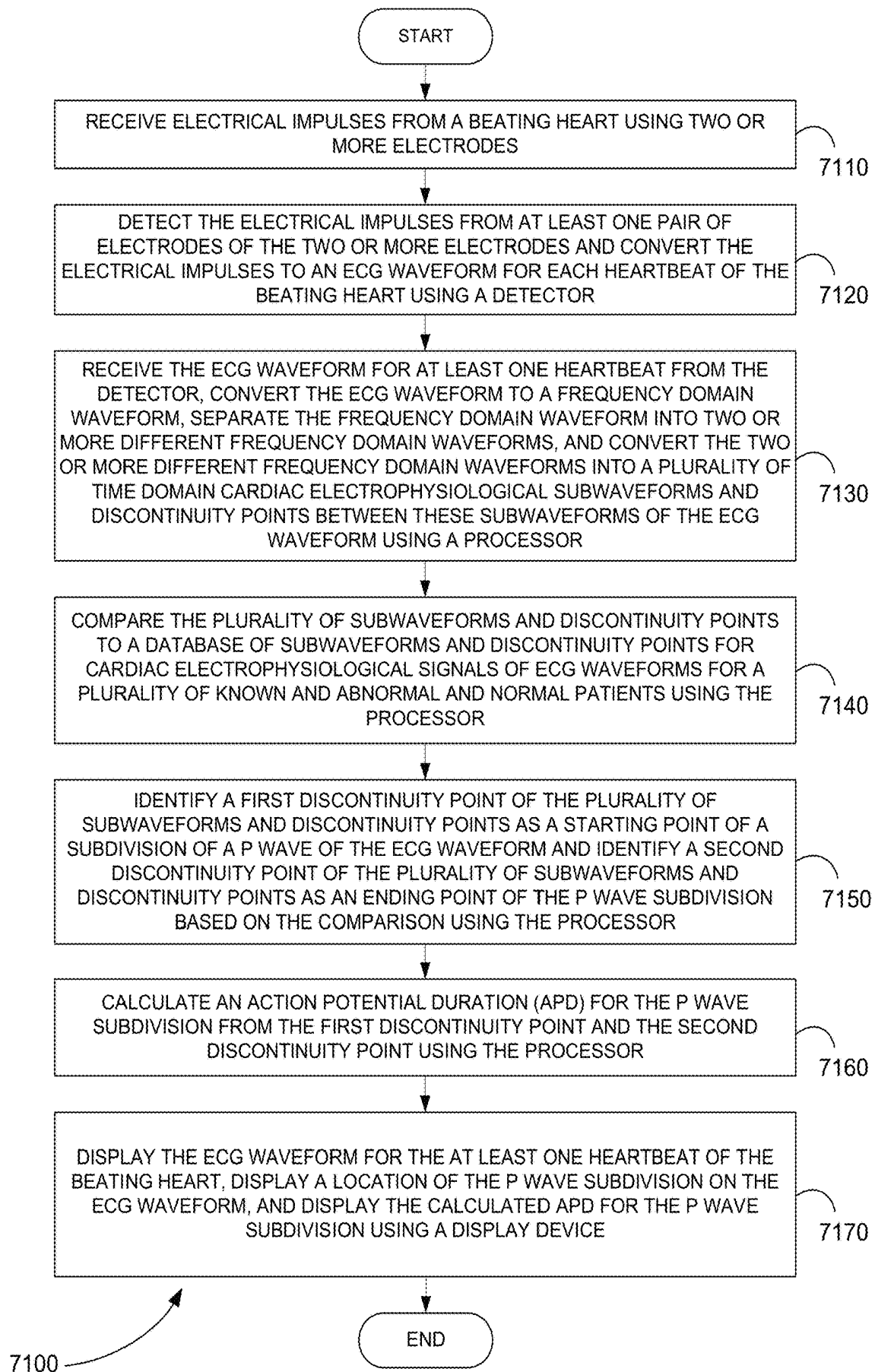
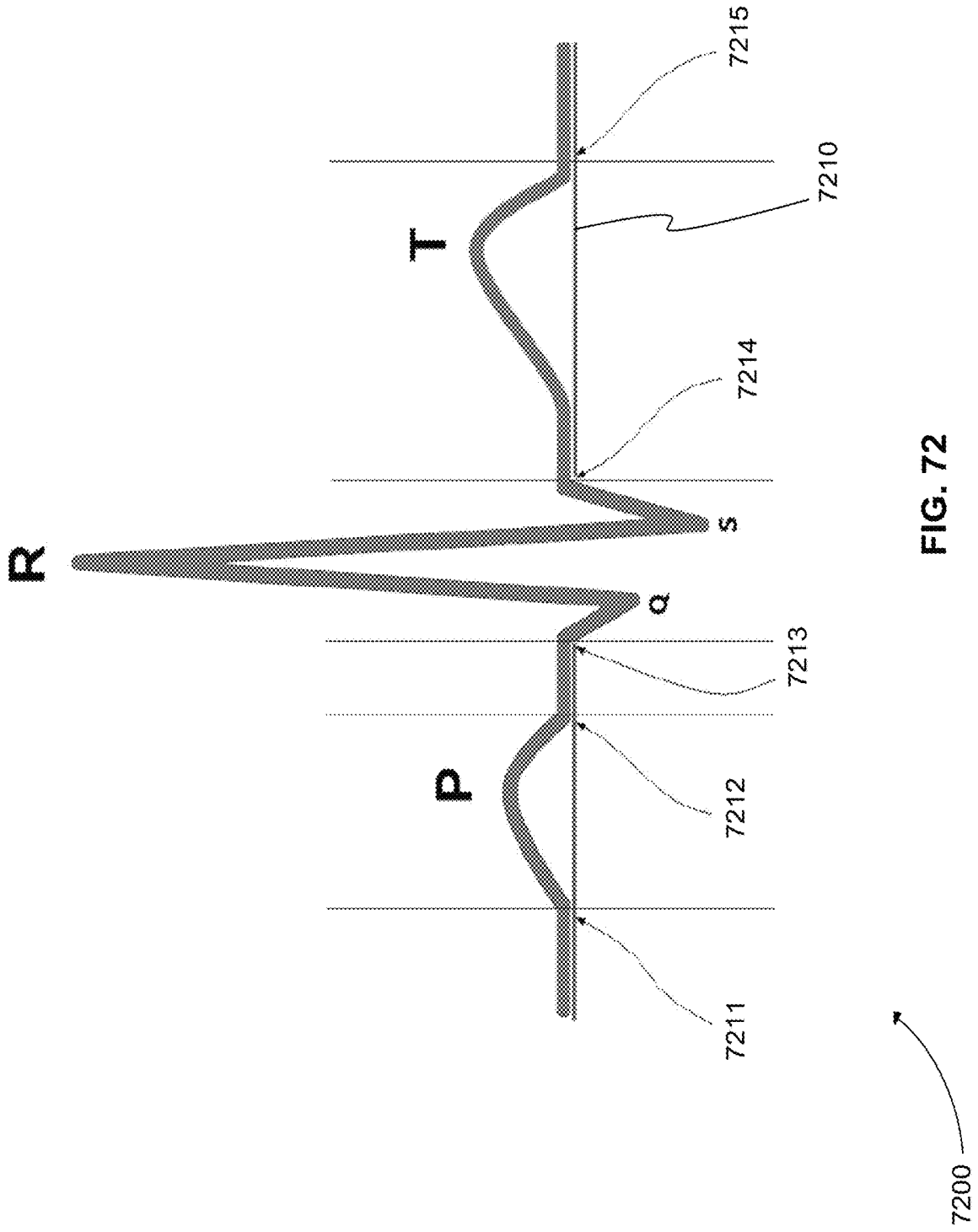
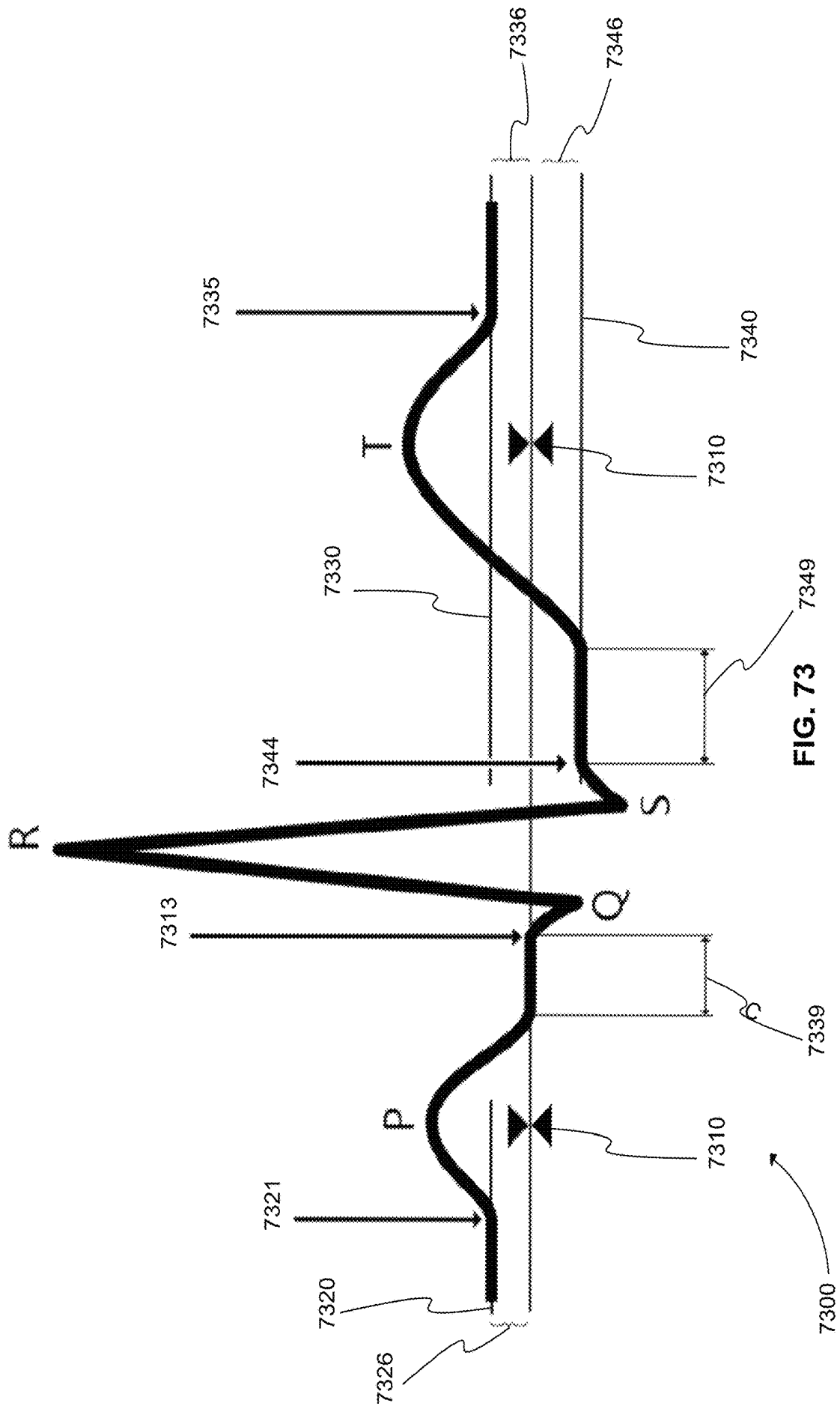


FIG. 71





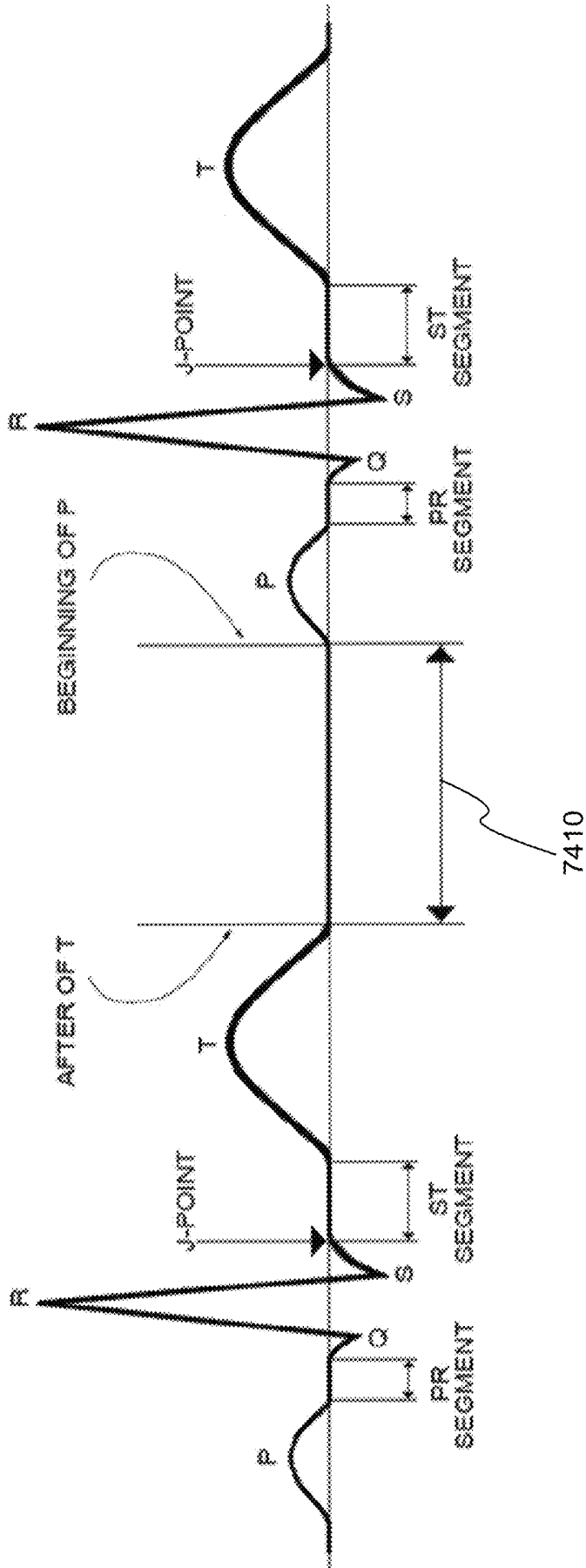


FIG. 74

7400

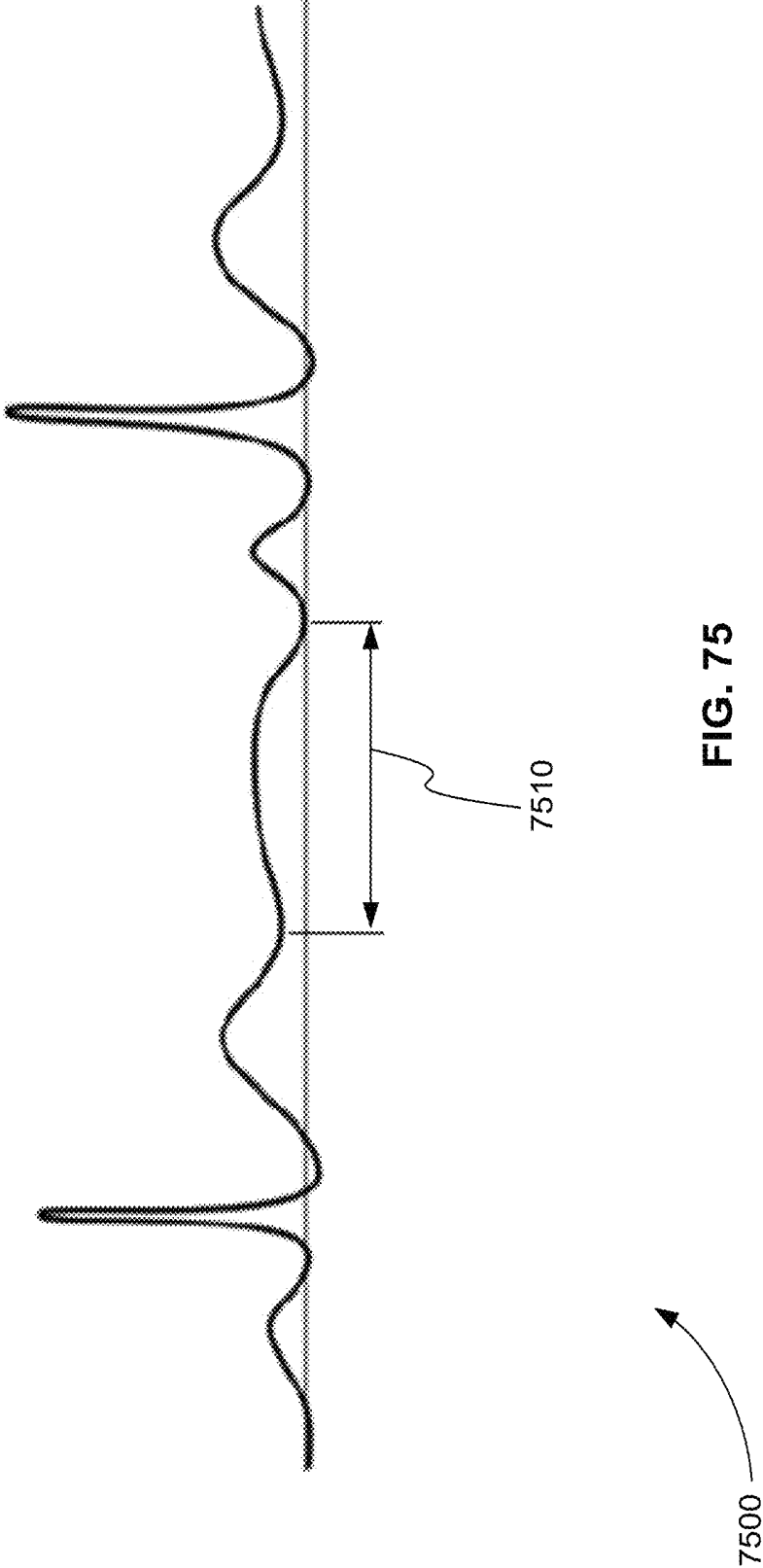
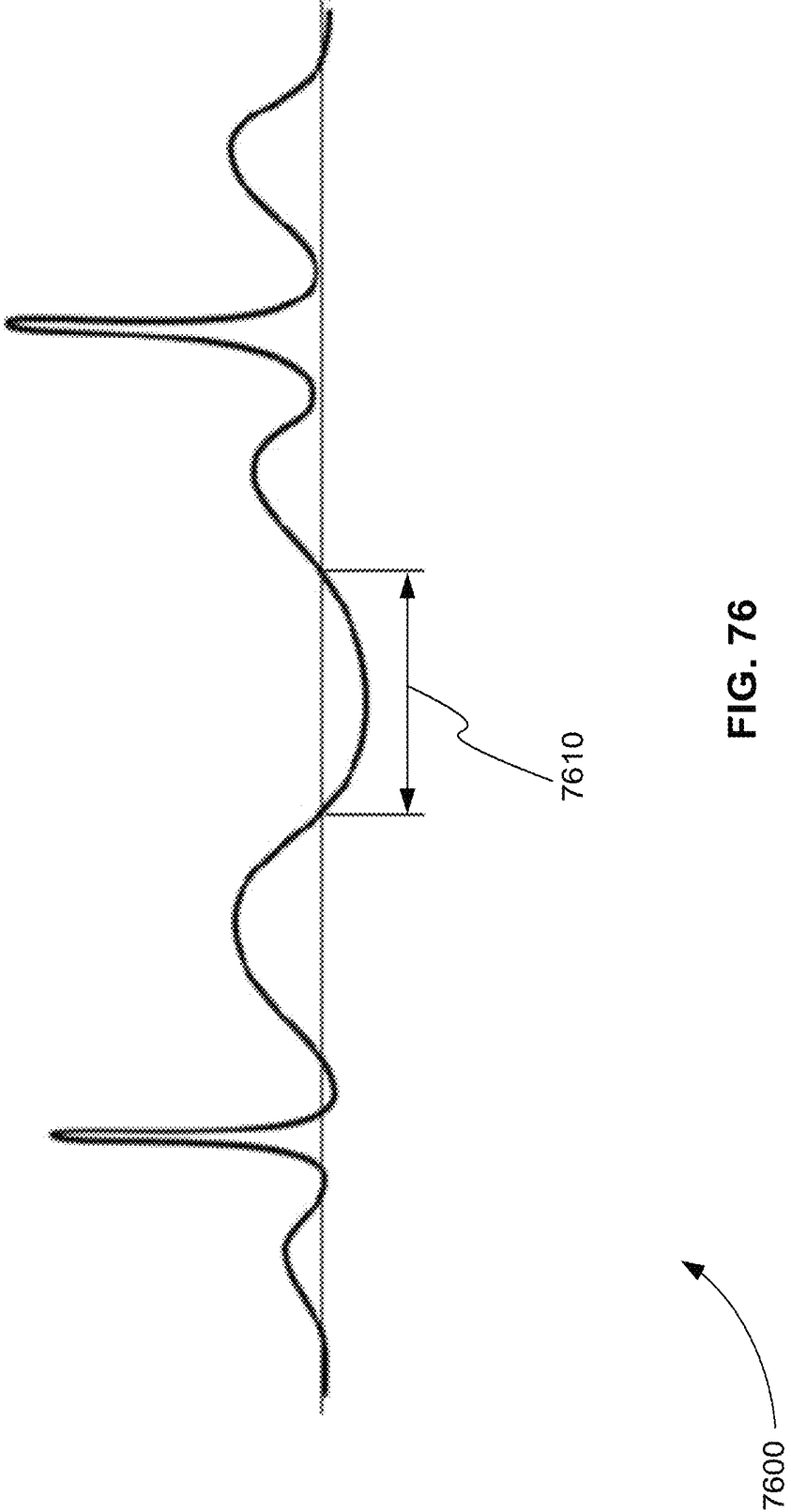


FIG. 75



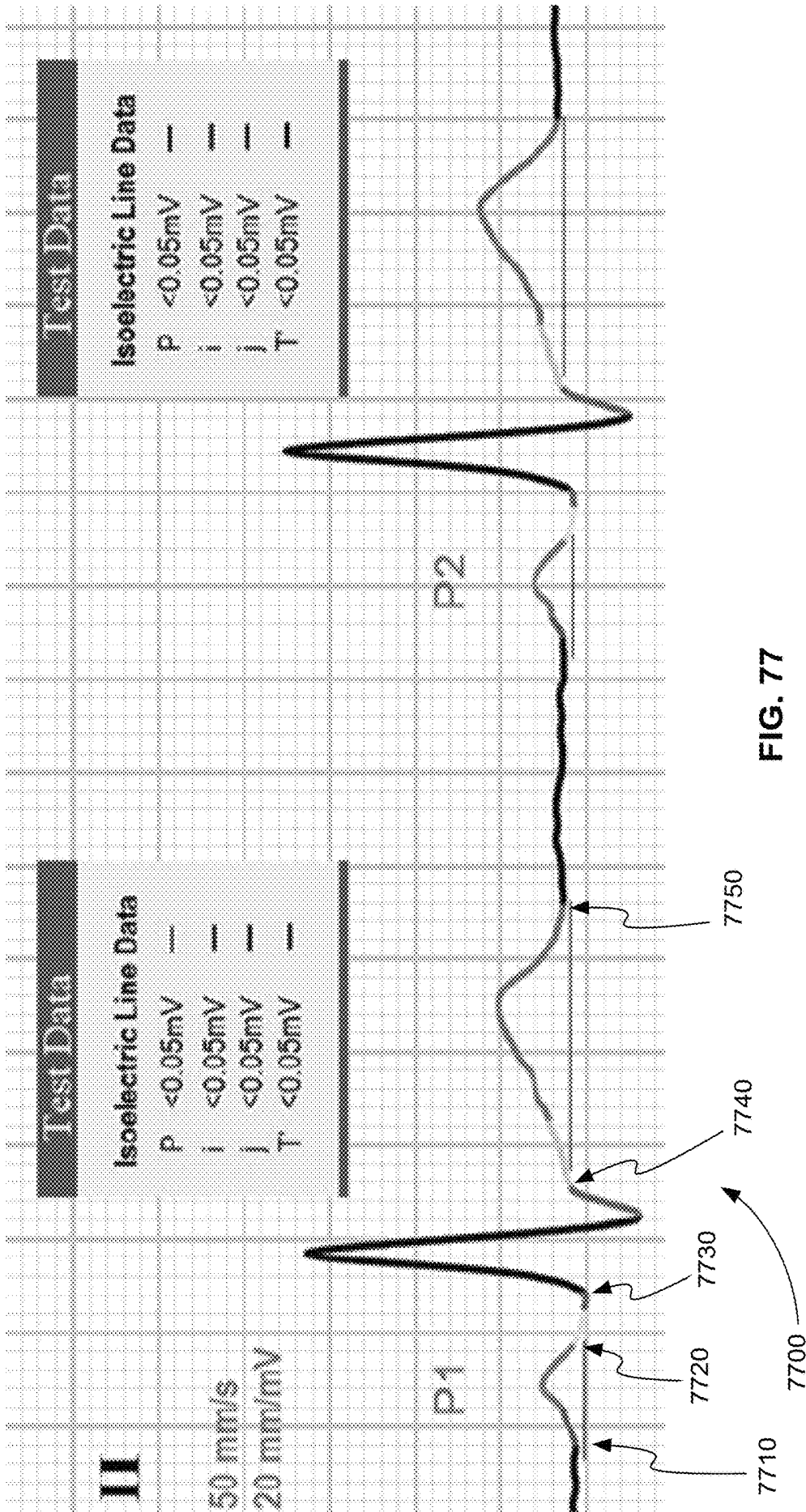


FIG. 77

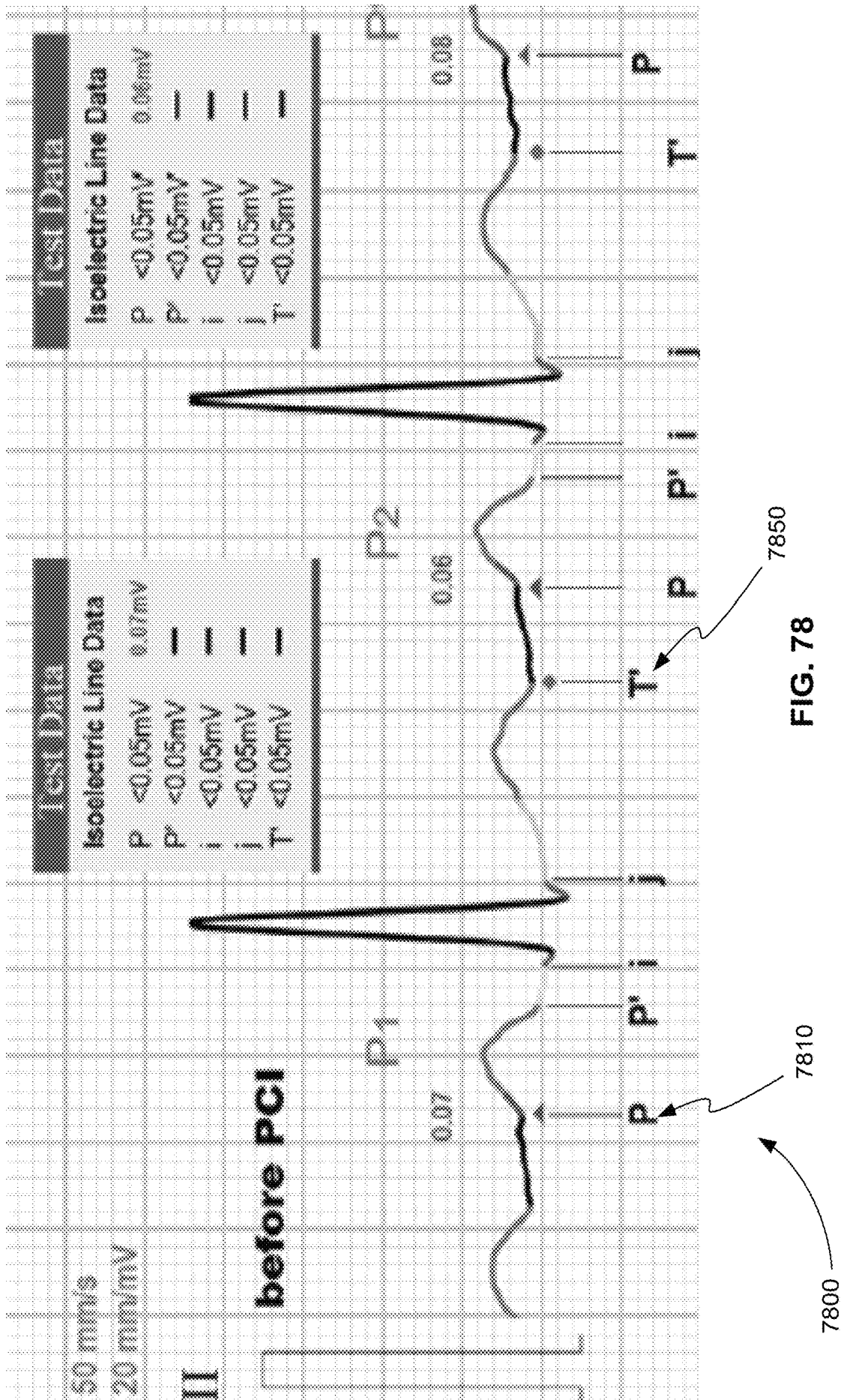


FIG. 78

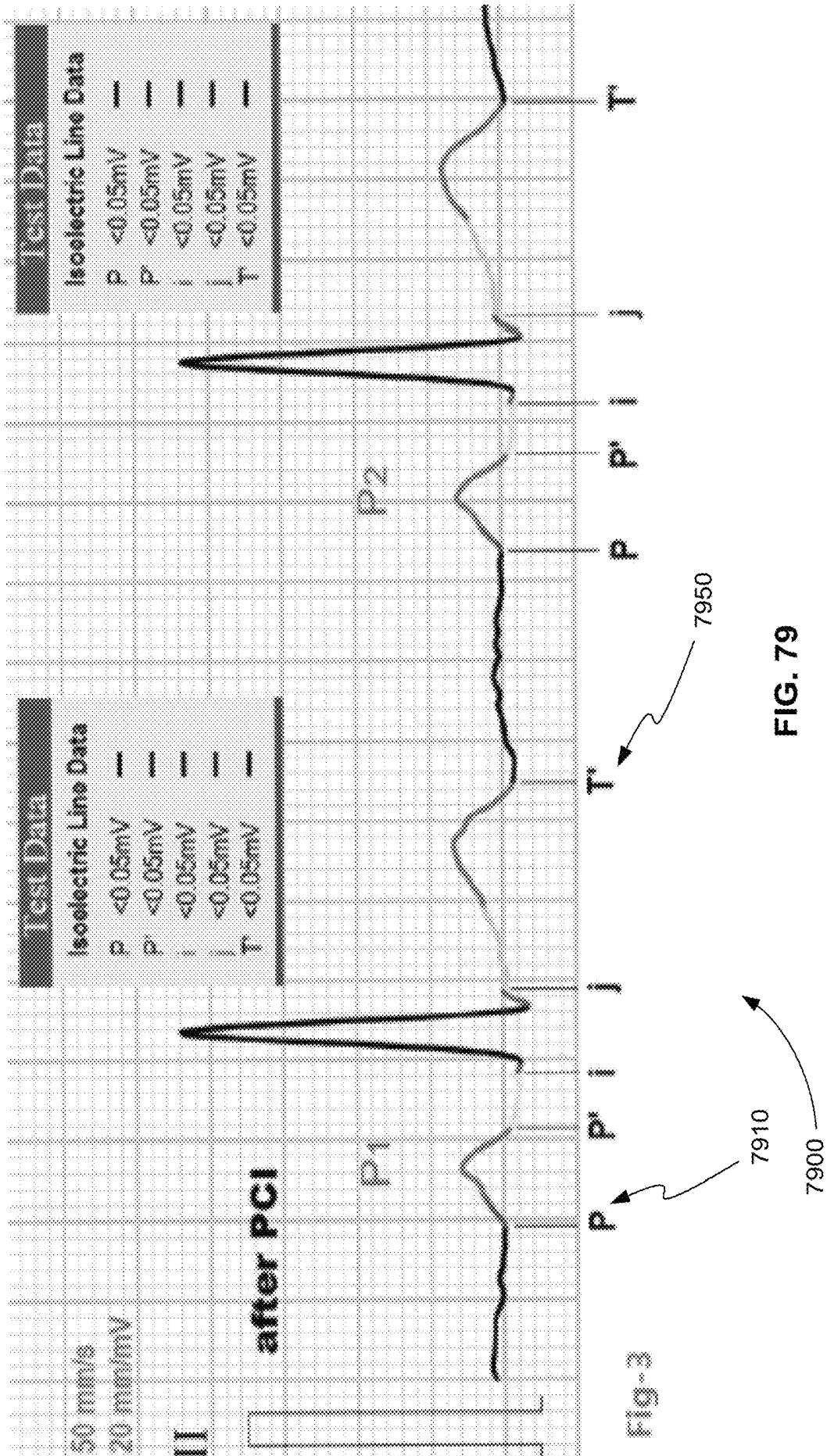


FIG. 79

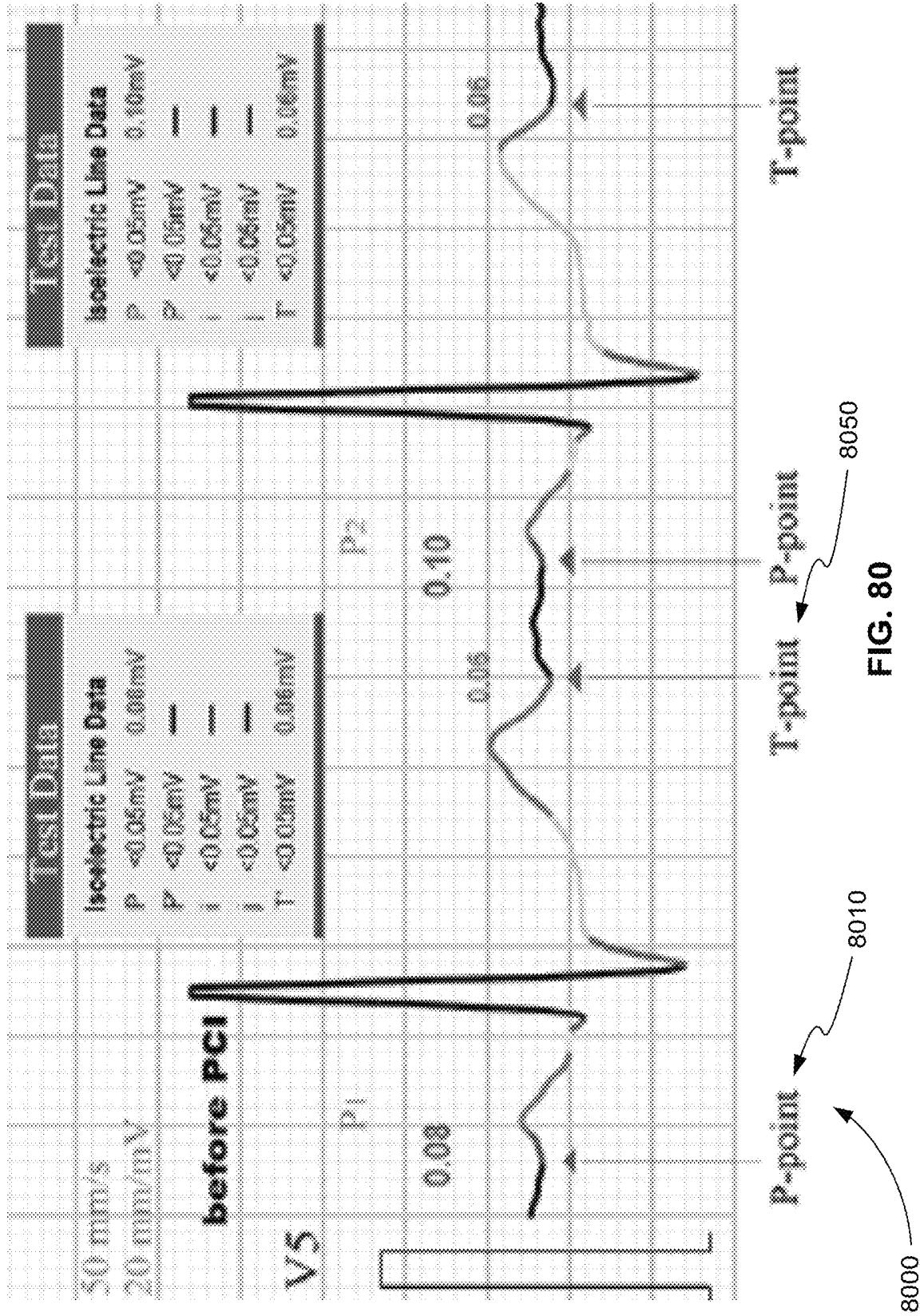
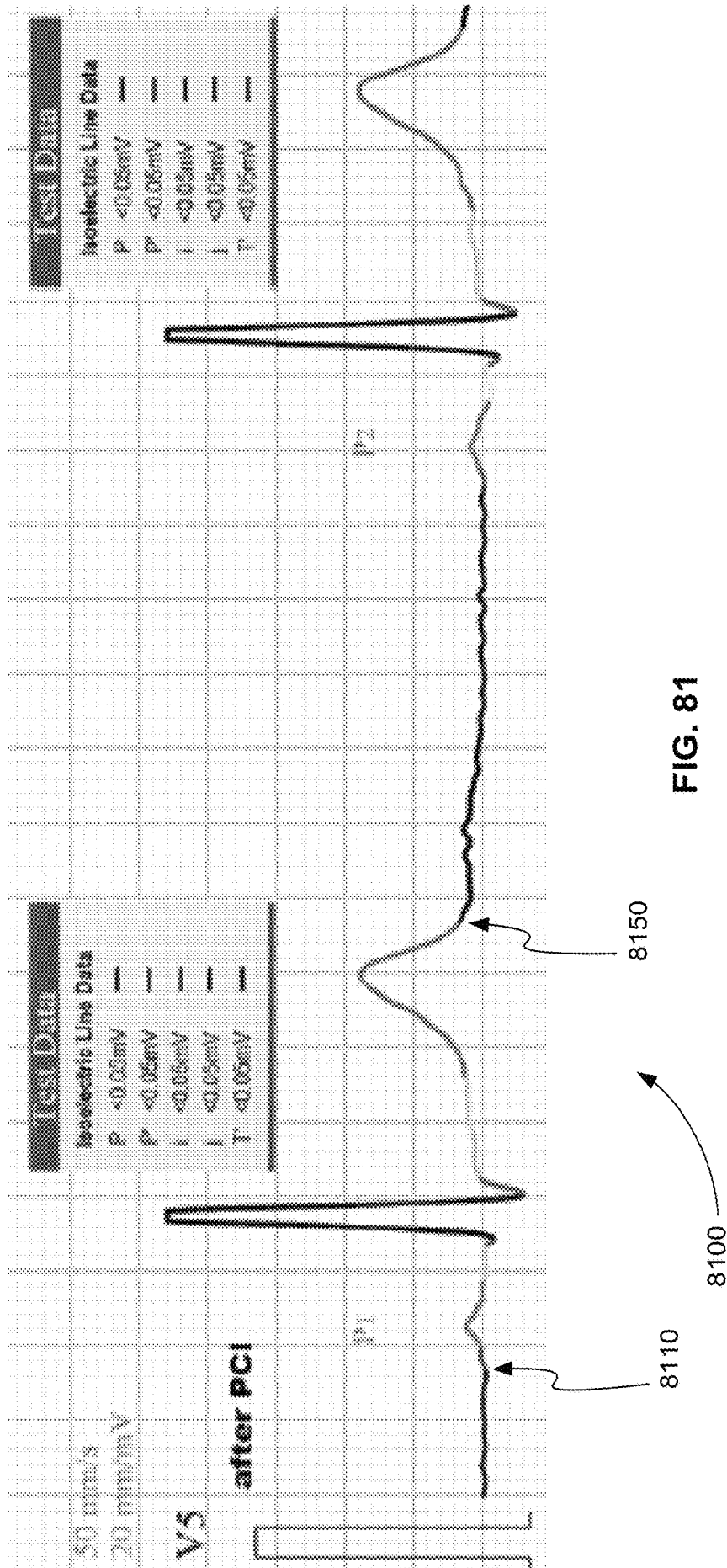
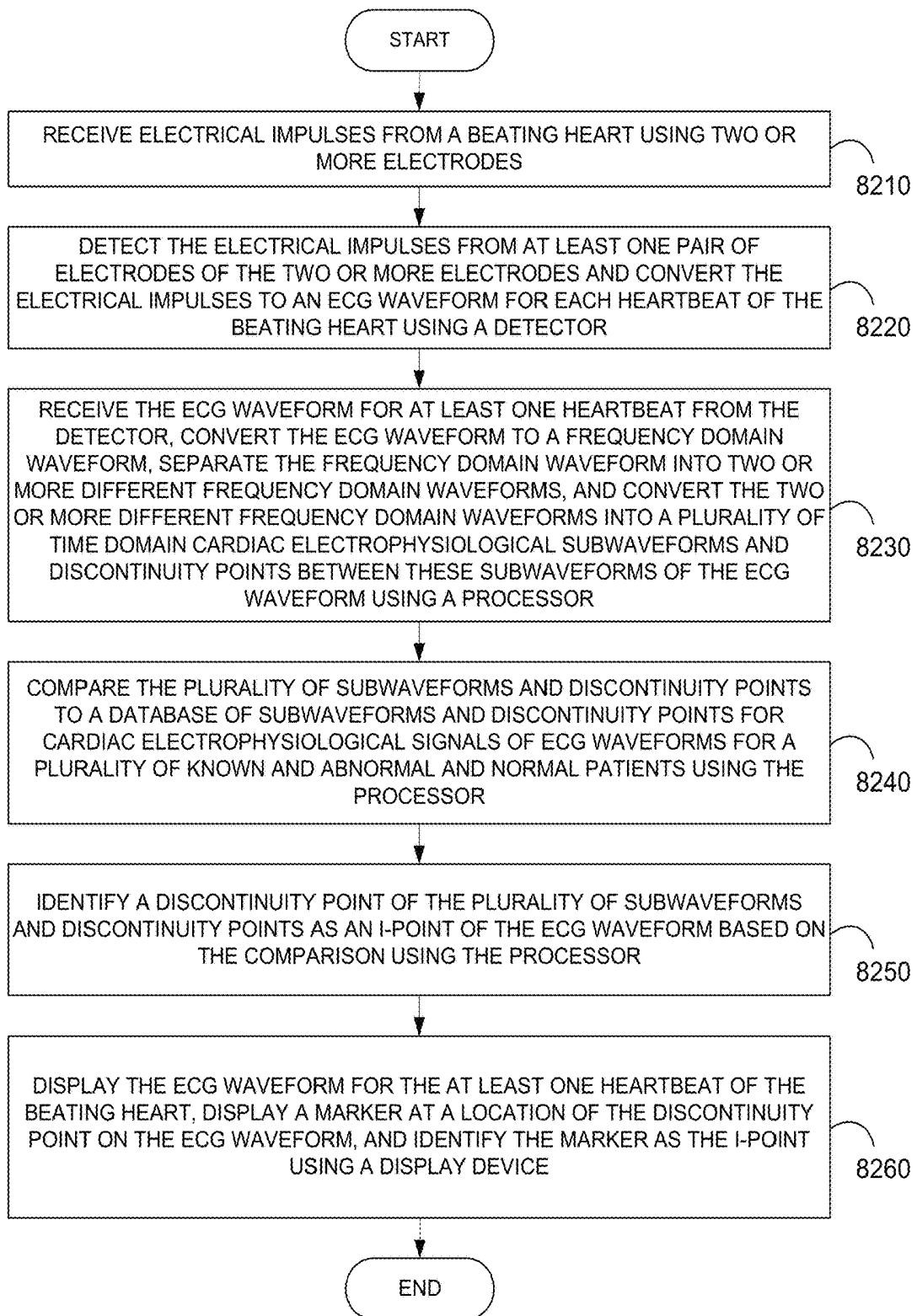


FIG. 80





8200

FIG. 82

**METHOD FOR RECOGNIZING POINT
QUANTIFICATION STANDARD ELEVATION
OR DEPRESSION NEAR THE
EQUIPOTENTIAL LINE OF EACH
HEARTBEAT**

CROSS-REFERENCE TO RELATED
APPLICATION

This application is a continuation in part of U.S. patent application Ser. No. 15/998,487, filed Aug. 16, 2018, which is a continuation in part of U.S. patent application Ser. No. 15/961,952, filed Apr. 25, 2018, which is a continuation in part of U.S. patent application Ser. No. 15/904,543, filed Feb. 26, 2018, which is a continuation in part of U.S. patent application Ser. No. 15/393,135, filed Dec. 28, 2016, which is a continuation in part of U.S. patent application Ser. No. 14/749,697, filed Jun. 25, 2015, now U.S. Pat. No. 9,538,930 (hereinafter the “930 Patent”), which is a continuation in part of U.S. patent application Ser. No. 14/662,996, filed Mar. 19, 2015, now U.S. Pat. No. 9,339,204 (hereinafter the “204 Patent”), which is a continuation of PCT application No. PCT/US15/20828, filed Mar. 16, 2015, which claims the benefit of U.S. Provisional Patent Application Ser. No. 62/008,435, filed Jun. 5, 2014; this application also claims the benefit of U.S. Provisional Patent Application Ser. No. 62/551,759, filed Aug. 29, 2017; U.S. patent application Ser. No. 15/998,487 claims the benefit of U.S. Provisional Patent Application Ser. No. 62/546,461, filed Aug. 16, 2018; U.S. patent application Ser. No. 15/961,952 claims the benefit of U.S. Provisional Patent Application Ser. No. 62/489,540, filed Apr. 25, 2017; U.S. patent application Ser. No. 15/904,543 claims the benefit of U.S. Provisional Patent Application Ser. No. 62/463,662, filed Feb. 26, 2017; U.S. patent application Ser. No. application Ser. No. 15/393,135 claims the benefit of U.S. Provisional Patent Application Ser. No. 62/271,704, filed Dec. 28, 2015, and U.S. Provisional Patent Application Ser. No. 62/271,699, filed Dec. 28, 2015; and U.S. patent application Ser. No. 14/749,697 claims the benefit of U.S. Provisional Patent Application Ser. No. 62/017,185, filed Jun. 25, 2014, the content of all of which is incorporated by reference herein in their entireties.

INTRODUCTION

The teachings herein relate to an automated electrocardiography (ECG) analysis system. More particularly, the teachings herein relate to systems and methods for measuring and annotating the P-point, P'-point, I-point, J-point, and T-point of an ECG waveform. These systems and methods use the harmonic signals of a conventional ECG waveform and previously recorded data from normal and abnormal patients to measure and annotate points. The distances from these points to the equipotential or isoelectric line of the ECG waveform are also calculated. These distances are used to diagnose blockages potentially leading to myocardial infarction.

The systems and methods herein can be performed in conjunction with a processor, controller, or computer system, such as the computer system of FIG. 1.

BACKGROUND

Non-ST Segment Elevation Myocardial Infarction Problem

Clinically, the current measuring method of myocardial infarction still requires elevation or depression ST segment in traditional ECG as the diagnostic criteria, and it has been

used for more than half a century. Among all heart-related diseases, CAD, AMI, and ACS attack rates amount to 60% to 70%. Noninvasive ECG examination is the only most common, convenient, and wide-spread method to detect arrhythmia, coronary vascular heart disease and all other cardiac disease; however, low detection rate of CAD and AMI by such examination is the major problem to be dealt with in the world at present.

According to many official sources, the waveforms of ST segment in ECG fall an additional 50% following 70% changes with myocardial ischemia. (See FIG. 7.) Therefore, sudden cardiac death and cardiovascular disease have always been the top causes of mortality and morbidity globally; the main reason may be that there are too many patients whose ST segments in traditional ECG fail to elevation or depression. So far, the change of ST segment has been taken as the standard to determine and diagnose MI & AMI; currently, for CAD and AMI patients whose ST segment does not change, they are all clinically categorized as NSTEMI (non-ST segment elevation myocardial infarction), but they can be deemed as patients with myocardial infarction by laboratory test or other test.

ECG itself is a “qualitative” diagnosis method based on changes of waveform morphology patterns. However, many characteristics of morphological waveform stay unchanged or have no patterns. In the case that the waveform stays unchanged at ST segment, there is a need to establish a standard for Myocardial Infarction without changes of ST segment.

A standard for Myocardial Infarction is established without changes of ST segment, indicating that there are no morphological features, no patterns can be recognize and data changes on such patients in the ECG morphological waveform. From this patent, it is found that there are signs of change on measuring “point” at other segments in traditional ECG images, instead of the ST segment elevation. (See FIGS. 1, 2, 5, and 6.) Please see the following detailed description.

ECG Quantitative Problem

Since the development of ECG, the electrophysiological signal separation of specific time periods of cardiac self-conduction system within the P wave, the QRS complex and the T wave has never been achieved. There is standardized data available in cardiac science, but such quantitative data has never been used in ECG for many reasons. Conventionally, only the character of an ECG waveform is read. As a result, only qualitative information is provided in clinical applications.

ECG is a noninvasive electrophysiological technology. It is able to scan and record cardiac electrical conduction signals. It is the only tracing image of cardiac “bioelectric conduction”, which is the character marker of the life of a heart. However, in the medical field, ECG is only a morphological technique, and the target of its reading, analyzing and determining is waveform character. It is a qualitative technology that does not have quantitative data, which is due to the ECG waveform being associated with deformation and instability. The standard measuring points frequently disappear, hide, overlap and shift. Consequently, they are frequently not shown in ECG, and thus cannot be used for making a determination.

Moreover, conventional ECG cannot measure all digital parameters. The established standards cannot be applied clinically, and cannot be measured. As a result, ECG is unable to achieve a data-based quantitative application. Hence, to date, ECG is still a qualitative application. The foregoing is the reason for which ECG is deemed as a

technology that needs experience. However, it is noted that such experience needs to be accumulated from a great number of cases with incorrect diagnosis.

The heart is the most important organ in human body. In addition to heart diseases, a variety of other diseases may also cause abnormalities in heart. Hence, not only cardiologists, but also all doctors in other departments need to read ECG. However, the morphological character changes in ECG cause difficulties for doctors to read ECG. Hence, the issue of how to use the ECG data has confused clinical practices for many years. In traditional ECG, diagnosis of diseases is still made according to morphological character changes in waveforms.

As a result, systems and methods are needed to add quantitative scientific indicators to ECG. Such systems and methods are needed to allow doctors to understand and utilize the knowledge saved in traditional ECG, as well as to reduce learning difficulties, reduce guesses in case diagnosis, reduce misjudgment rate, and improve reliability, diagnosis rate and accuracy, whenever waveform character changes.

ECG Accuracy Problem

Since the first ECG instrument was invented in 1903, its accuracy rate for diagnosis has always been a problem in clinical applications. For people with abnormal conditions, ECG waveform variations are not the same for the same person and are not completely identical even for the same disease. They are at most self-similar. Self-similarly, for example, refers to an object having a shape that is similar to the shape of one of its parts. As a result, ECG science is one of the most complicated disciplines in medicine.

It can be seen from numerous signal processing methods that, during a lifetime, each beat of a person's heart has different specific signal variation, and the difference is significant. However, generally one is unable to observe this from a conventional linear ECG waveform with the naked eye.

Since computers started to be widely used in ECG analysis the 1970s, people have been consistently exploring, searching, and studying how to automate ECG analysis and diagnosis. In the past half a century, thousands of scholars have made efforts in studying algorithms, exploring pattern recognition, and applying those in ECG mapping and automatic diagnosis.

However, wide clinical use of such systems has yet to be achieved. There are at least three technical reasons for this.

1. The ECG waveform is morphological, and generally no consistent mapping points can be found. In other words, the information in the ECG waveform is conveyed through its structure or form. Also, the waveform is abstractly self-similar. In particular, there is no rule for abnormal variations, the time axis signals interfere with each other on left and right sides of as well as above the x-axis, non-linear variations are invisible, and the same disease may have hundreds of millions of variations, but they are not clearly displayed on the ECG waveform. As a result, all ECG parameters are, in general, not accurate, and it is almost impossible to measure these parameters after the waveform changes. Therefore, the highest accuracy of automatic diagnosis by existing ECG software reaches around 38%. Also, this accuracy is only achieved for simple ECG waveform variations and not for many complex waveforms. This is because no mapping point can be found due to the loss or disappearance or deformation of the P-QRS-T waveform.

2. The second reason systems for automated ECG analysis and diagnosis have not been adopted clinically is related to how a conventional ECG waveform has been measured. As

described in the '204 Patent and below, the conventional ECG waveform is a single time domain waveform that represents a combination of many different frequency domain signals from different parts of the heart muscle. As a result, information specific to these different parts of the heart muscle are generally lost. In addition, the conventional ECG waveform is a linear waveform, while the heart is a nonlinear system, and the vast majority of variations as a result of abnormality are nonlinear.

3. The third reason systems for automated ECG analysis and diagnosis have not been adopted clinically is related to the high number of false positives found in normal and abnormal populations. For example, in many cases, conventional ECG waveforms show abnormal results in tests of normal people and also show normal results in tests of abnormal people, which makes it extremely difficult for clinical reading and understanding and makes it impossible to determine whether a result is normal or abnormal.

However, the heart is an electrified organ, and there is no doubt that the electrophysiological responses of a heart organ are the fastest and most sensitive measurements to diagnose heart problems. ECG remains one of the most extensively used clinical tools used at present along with blood tests and imaging, despite the lack of accurate systems for automated ECG analysis and diagnosis. As a result, there is a significant need for such systems.

Recent advancements have addressed one of the three technical problems. This is the conventional ECG waveform measurement problem. As described in the '204 Patent and below, an ECG device has been developed that uses signal processing to detect one or more subwaveforms within the P, Q, R, S, T, U, and J waveforms of a conventional ECG waveform and/or within the intervals between the P, Q, R, S, T, U, and J waveforms of a conventional ECG waveform. In other words, the device of the '204 Patent can provide information (subwaveforms) about different frequency domain signals from different parts of the heart muscle. A waveform displaying these subwaveforms is referred to as a saah ECG waveform, for example. In FIG. 30, described below, portions of a saah ECG waveform 3030 and a conventional or traditional ECG waveform 3040 are compared. FIG. 30 shows that saah ECG waveform 3030 relates ECG signals more closely to the anatomy of self-conducting system 3020 than traditional ECG waveform 3040.

As described in the '930 Patent and below, one way the different frequency domain signals from different parts of the heart muscle can be measured is through multi-domain ECG. In multi-domain ECG heart signals are measured using different frequency bands. These multi-domain ECG heart signals can be displayed in one diagram as an electrophysiocardiogram (EPCG) waveform. FIG. 32 shows EPCG waveforms before and after percutaneous coronary intervention (PCI), for example.

As a result of the systems of the '204 Patent and the '930 Patent, the technical problem of measuring the different frequency domain signals from different parts of the heart muscle has been addressed.

ECG Parameter Measurement Problem

The heart beats day and night from the first day of a human life to the last day of life. In a whole life, the heart beats about 2.5 billion to 3 billion times. In this regard, it could be calculated that the heart each time pumps 80 ml blood. Accordingly, based on the fact that the heart beats about 70 times per minute on average, the heart hence pumps 8,000 liters of blood per day, which is equivalent to the volume of 40 barrels of gasoline, and the total weight would be 8 tons. Therefore, the heart pumps 3,000 tons of

blood per year. If a person lives for 80 years, the number will reach 240,000 tons. It is noted that after the age of 60 years old, a person has a 45% chance of having the condition of arrhythmia, and about half of those cases become life threatening. According to a variety of different scientific predictions, some scientists believe that it is reasonable to predict that the average lifespan of a person is about 80 years old.

The heart is a charged elastic mucus organ, so an ECG instrument is the only instrument that is able to scan and record the physiological and pathological signs of the cardiac electrophysiology (heart ultrasound provides hemodynamic data, CT & MIR provide histological imaging data). ECG provides electrophysiological signals, in particular noninvasive electrophysiological data. It is able to scan and record cardiac electrical conduction signals. By far, it is the only tool that can record the scanning image of "bioelectric conduction," the identifier of a living heart.

On the other hand, however, in the medical field, ECG is also only a morphological signal. It needs to be read and analyzed to determine its various waveforms. In this regard, it is an area that highly relies on a practitioner's experience. In the history of ECG, there are many data-based parameter gold standards, such as P-R interval, Q-T interval, ST segment, QRS complex, P-J interval, J-T interval, VAT.

However, due to the fact that ECG waveforms are prone to certain issues such as deformation, instability, standard point loss, and so on, conventional ECG instruments are unable to accurately measure these ECG parameters. As a result, many established standards cannot be applied in clinical practice.

Furthermore, as for the data measured manually, a very small variation can result in a difference of tens of milliseconds. Clinically, only simple standards can be used at present, such as: HR, RR interval, PP interval. As a result, only a few very simple standards can be used in current clinical practice, including HR, RR interval, PP interval, etc.

As described above, the ECG systems of the '204 Patent and the '930 Patent have addressed the technical problem of accurately measuring the different frequency domain signals from different parts of the heart muscle.

Additional systems and methods, however, are needed to accurately measure ECG parameters such as the P-R interval, Q-T interval, ST segment, QRS complex, P-J interval, J-T interval, and VAT so that these standards can be used in clinical practice.

ECG History

Electrical signals produced by a human heart were observed through electrodes attached to a patient's skin as early as 1879. Between 1897 and 1911 various methods were used to detect these electrical signals and record a heartbeat in real-time. In 1924, Willem Einthoven was awarded the Nobel Prize in medicine for identifying the various waveforms of a heartbeat and assigning the letters P, Q, R, S, T, U, and J to these waveforms. Since the early 1900s, the equipment used for electrocardiography (ECG or EKG) has changed. However, the basic waveforms detected and analyzed have not changed.

An ECG device detects electrical impulses or changes in the electrical potential between two electrodes attached to the skin of a patient as the heart muscle contracts or beats. Electrically, the contraction of the heart is caused by depolarization and repolarization of various parts of the heart muscle. Initially, or at rest, the muscle cells of the heart have a negative charge. In order to cause them to contract, they receive an influx of positive ions Na^+ and Ca^{++} . This influx of positive ions is called depolarization. The return of

negative ions to bring the heart back to a resting state is called repolarization. Depolarization and repolarization of the heart affect different parts of the heart over time giving rise to the P, Q, R, S, T, U, and J waveforms.

FIG. 2 is an exemplary plot 200 of the P, Q, R, S, and T waveforms of a conventional ECG waveform of a heartbeat from a conventional ECG device. The P, Q, R, S, and T waveforms represent electrical conduction through a heart muscle. P waveform 210 represents the propagation of depolarization from the sinoatrial node, to the right and left atriums, and to the atrioventricular node. The sinoatrial node is also referred to as the sinus node, SA node, or SAN. The atrioventricular node is also referred to as the AV node or AVN. The right atrium is also referred to as the RA, and the left atrium is also referred to as the LA.

FIG. 3 is an exemplary diagram 300 of the depolarization of the muscle tissue of a heart that produces P waveform 210 of FIG. 2 as detected by a conventional ECG device. P waveform 210 of FIG. 2 is produced as depolarization propagates from SAN 310 to AVN 340 in FIG. 3. As depolarization propagates from SAN 310 to AVN 340, it also spreads from RA 320 to LA 340. P waveform 210 of FIG. 2 typically has a duration of 80 ms, for example.

PR segment 220 of FIG. 2 represents the propagation of depolarization from the AVN to the Bundle of His, and then to the Bundle Branches. PR segment 230 may also include depolarization to the Purkinje fibers of the inner ventricular walls. The Bundle of His is also referred to as the His Bundle or His. The Bundle Branches include the right bundle branches (RBB) and the left bundle branches (LBB). As shown in FIG. 2, in a conventional ECG, PR segment 220 shows up as a flat line or waveform with no amplitude.

FIG. 4 is an exemplary diagram 400 of the depolarization of the muscle tissue of a heart that produces PR segment 220 of FIG. 2 as detected by a conventional ECG device. PR segment 220 of FIG. 2 is produced as depolarization propagates from AVN 340 to His 450 and then to Bundle Branches 460 that include RBB 461 and LBB 462. PR segment 220 of FIG. 2 typically has a duration of between 50 and 120 ms, for example.

Waveforms Q 230, R 240, and S 250 of FIG. 2 form the QRS complex. The QRS complex represents the propagation of depolarization through the right and left ventricles. The right ventricle is also referred to as RV, and the left ventricle is referred to as LV.

FIG. 5 is an exemplary diagram 500 of the depolarization of the muscle tissue of a heart that produces Q waveform 230, R waveform 240, and S waveform 250 of FIG. 2 as detected by a conventional ECG device. Waveforms Q 230, R 240, and S 250 of FIG. 2 produced as depolarization propagates from Bundle Branches 460 through RV 571 and LV 572. RV 571 and LV 572 have the largest muscle mass in the heart. The QRS complex formed by waveforms Q 230, R 240, and S 250 of FIG. 2 typically has a duration of between 80 and 100 ms, for example.

ST segment 260 of FIG. 2 represents the period during which the ventricles remain depolarized and contracted. As shown in FIG. 2, in a conventional ECG, ST segment 260 shows up as a flat line or waveform with no amplitude. ST segment 260 typically has a duration of between 80 and 120 ms, for example.

The point in FIG. 2 at which the QRS complex ends and ST segment 260 begins is called J point 255. A J waveform (not shown) can sometimes appear as an elevated J point at J point 255 or as a secondary R waveform. A J waveform is usually characteristic of a specific disease. The J waveform is also referred to as the Osborn wave, camel-hump sign, late

delta wave, hathook junction, hypothermic wave, prominent J wave, K wave, H wave or current of injury.

T waveform 270 of FIG. 2 represents the repolarization or recovery of the ventricles. T waveform 270 typically has a duration of 160 ms, for example. The interval between the Q and T waveforms is referred to as the QT interval.

FIG. 6 is an exemplary diagram 600 of the repolarization of the muscle tissue of a heart that produces T waveform 270 of FIG. 2 as detected by a conventional ECG device. As shown in FIG. 6, RV 571 and LV 572 are repolarized.

Not shown in FIG. 2 is the U waveform. The U waveform sometimes appears after the T waveform. The U waveform is thought to represent repolarization of the interventricular septum, the papillary muscles, or the Purkinje fibers.

As shown in FIGS. 3 through 6, as a heart beats, electrical signals flow through all the different muscle tissues of the heart. As shown in FIG. 2, for the last 100 years conventional ECG devices have been able to detect some of these signals in the form of the P, Q, R, S, T, U, and J waveforms. These waveforms have aided in the diagnosis and treatment of many heart problems. Unfortunately, however, the P, Q, R, S, T, U, and J waveforms do not provide a complete picture of the operation of all the different muscle tissues of the heart. As a result, improved systems and methods are needed to detect and analyze more information from the electrical signals that flow through all the different muscle tissues of the heart as it is beating. This additional information can be used to diagnose and treat many more heart problems.

Artificial Intelligence

Artificial Intelligence (AI) generally refers to languages, algorithms, and operating systems that relate to how a computer system can carry out tasks that were previously only completed by relying on human intelligence. It is a general term and often does not include implementation or application. The definition of AI has evolved over time, however, and this phenomenon is referred to as the "AI effect." The AI effect can be summarized as the prescription that "AI intends to complete a collection of all tasks that cannot be implemented without relying on human intelligence at the present." In the 1940s and 1950s, a group of scientists from different fields (mathematics, psychology, engineering, economics and politics) began to explore the possibility of manufacturing an artificial brain. In 1956, AI was established as a discipline. The organizers of the 1956 Dartmouth Artificial Intelligence Conference were Marvin Minsky, John McCarthy, and two other senior scientists, Claude Shannon and Nathan Rochester, with the latter coming from IBM. At the 1956 Dartmouth Artificial Intelligence Conference, the name and tasks of AI were determined, and at the same time, initial achievements and the earliest group of researchers appeared. As a result, this event has been extensively acknowledged as a sign of the birth of AI. It is clear that AI is now a technological field, a second revolution since the invention of the computer, and a certain trend in the future. It is being applied in all industries, exists everywhere, and is used on almost everything on the earth. In the medical field, AI is now used in the following: medical imaging, sensor-based data analysis, conversion of bioinformatics, and development of public health policies. AI is also used in the clinical applications. These applications include cancer treatment: recognition of mitosis of cancerous tumor cells, identification of disease types and degrees of aggravation, shortening chemotherapy time, and mitigating damage caused by chemotherapy for cancer patients. These applications also include ophthalmological diagnosis: recognition of early signs of eye disease, such as senile macular

degeneration, and diabetic retinopathy and surgical treatment: AI surgical robots, etc. Google has also formed a team called DeepMind Health, which cooperated with the Imperial College London and the Royal Free Hospital in London, UK. They released a mobile application called Streams, and medical professionals can use Streams to observe treatment results in a faster manner. Overall, in the medical field, the AI system can be used on any job that previously required human thinking.

BRIEF DESCRIPTION OF THE DRAWINGS

FIG. 1 is a block diagram that illustrates a computer system, in accordance with various embodiments.

FIG. 2 is an exemplary plot of the P, Q, R, S, and T waveforms of a conventional electrocardiography (ECG) waveform of a heartbeat from a conventional ECG device.

FIG. 3 is an exemplary diagram of the depolarization of the muscle tissue of a heart that produces the P waveform of FIG. 2 as detected by a conventional ECG device.

FIG. 4 is an exemplary diagram of the depolarization of the muscle tissue of a heart that produces the PR segment of FIG. 2 as detected by a conventional ECG device.

FIG. 5 is an exemplary diagram of the depolarization of the muscle tissue of a heart that produces the Q waveform, the R waveform, and the S waveform of FIG. 2 as detected by a conventional ECG device.

FIG. 6 is an exemplary diagram of the repolarization of the muscle tissue of a heart that produces the T waveform of FIG. 2 as detected by a conventional ECG device.

FIG. 7 is a block diagram of a conventional ECG device.

FIG. 8 is a block diagram of an ECG device for detecting more information from the electrical signals that flow through all the different muscle tissues of the heart as it is beating, in accordance with various embodiments.

FIG. 9 is an exemplary plot of a saah ECG waveform of a heartbeat from a saah ECG device showing subwaveforms found within the P, Q, R, S, T, U, and J waveforms and/or within the intervals between the P, Q, R, S, T, U, and J waveforms, in accordance with various embodiments.

FIG. 10 is an exemplary block diagram showing a signal processing algorithm for detecting five subwaveforms within the PR interval of a conventional ECG waveform, in accordance with various embodiments.

FIG. 11 is an exemplary block diagram of a saah ECG device that displays conventional ECG waveforms, saah ECG waveforms, and saah ECG data, in accordance with various embodiments.

FIG. 12 is an exemplary plot of the information displayed by the saah ECG device of FIG. 10, in accordance with various embodiments.

FIG. 13 is an exemplary block diagram of a saah ECG device that displays conventional ECG waveforms, saah ECG waveforms, saah ECG data, and saah ECG automatic pattern recognition diagnosis information, in accordance with various embodiments.

FIG. 14 is an exemplary plot of a conventional ECG waveform showing how a small error in the starting point of the P wave can cause a large error in all subsequent time measurements, in accordance with various embodiments.

FIG. 15 is an exemplary plot of a conventional ECG waveform showing how the end of the PR interval cannot be confirmed due to an upward arc angle of the starting point of QRS wave, in accordance with various embodiments.

FIG. 16 is a flowchart showing a method for detecting subwaveforms within the P, Q, R, S, T, U, and J waveforms

of an ECG waveform of a heartbeat or in an interval between the P, Q, R, S, T, U, and J waveforms, in accordance with various embodiments.

FIG. 17 is a schematic diagram of a system that includes one or more distinct software modules that perform a method for detecting subwaveforms within the P, Q, R, S, T, U, and J waveforms of an ECG waveform of a heartbeat or in an interval between the P, Q, R, S, T, U, and J waveforms, in accordance with various embodiments.

FIG. 18 is an exemplary block diagram showing a system for performing multi-domain ECG using 16 different frequency bands or domains, in accordance with various embodiments.

FIG. 19 is an exemplary plot of a multi-domain ECG waveform that includes 10 different time domain signals, in accordance with various embodiments.

FIG. 20 is an exemplary plot of a multi-domain ECG waveform that includes 14 different time domain signals, in accordance with various embodiments.

FIG. 21 is an exemplary alignment of a multi-domain ECG waveform that includes 16 different time domain signals with a conventional ECG waveform, in accordance with various embodiments.

FIG. 22 is an exemplary plot of a conventional ECG waveform showing how the ST segment of a normal person can appear abnormal, in accordance with various embodiments.

FIG. 23 is an exemplary plot of a conventional ECG waveform showing how the T wave of an abnormal person can appear normal, in accordance with various embodiments.

FIG. 24 is an exemplary plot of a conventional ECG waveform showing how the section of an autonomic conduction system cannot be determined from a conduction block, in accordance with various embodiments.

FIG. 25 is an exemplary plot of a conventional ECG waveform showing how the QRS complex is widened in the waveform, in accordance with various embodiments.

FIG. 26 is an exemplary plot of a conventional ECG waveform showing how the atrial anatomical positions are difficult to identify, in accordance with various embodiments.

FIG. 27 is an exemplary plot of a conventional ECG waveform showing a premature ventricular beat, in accordance with various embodiments. In plot.

FIG. 28 is an exemplary plot of a conventional ECG waveform showing in atrial conduction block, in accordance with various embodiments.

FIG. 29 is an exemplary diagram of the anatomy of the self-conducting system of a heart, in accordance with various embodiments.

FIG. 30 is an exemplary diagram showing the anatomic sites that the PA, AH, and HV intervals represent and the corresponding PA, AH, and HV intervals in a saah ECG waveform and traditional ECG waveform, in accordance with various embodiments.

FIG. 31 is an exemplary comparison plot of a saah ECG waveform and a traditional ECG waveform with PA, AH, HV, and PR interval values obtained from aiECG processing for a patient with a normal heart, in accordance with various embodiments.

FIG. 32 is an exemplary comparison plot of a multi-domain ECG or electrophysiocardiogram (EPCG) waveform aligned with a traditional ECG waveform for a patient with acute coronary syndrome (ACS) before and after percutaneous coronary intervention (PCI), in accordance with various embodiments.

FIG. 33 is an exemplary diagram showing timing values of conduction calculated at various anatomic sites along the self-conduction system of a normal heart by further processing a traditional ECG waveform, in accordance with various embodiments.

FIG. 34 is an exemplary block diagram of a system for automated ECG analysis and diagnosis using AI, in accordance with various embodiments.

FIG. 35 is an exemplary plot of a conventional ECG waveform annotated with diagnosis marker information, in accordance with various embodiments.

FIG. 36 is an exemplary comparison of timing information from a conventional ECG waveform and from an ECG waveform produced and annotated using an automated analysis and diagnosis system, in accordance with various embodiments.

FIG. 37 is a block diagram of an ECG system for identifying and annotating cardiac electrophysiological signals in an ECG waveform as normal or abnormal during measurement of the ECG waveform, in accordance with various embodiments.

FIG. 38 is a flowchart showing a method for identifying and annotating cardiac electrophysiological signals in an ECG waveform as normal or abnormal during measurement of the ECG waveform, in accordance with various embodiments.

FIG. 39 is an exemplary ECG waveform plot showing the relative positions of the PR and ST segments for a normal heartbeat, in accordance with various embodiments.

FIG. 40 is an exemplary ECG waveform plot showing how the ST segment can shift vertically due to abnormal conditions, in accordance with various embodiments.

FIG. 41 is an exemplary ECG waveform plot showing how the ST segment can be deformed due to abnormal conditions, in accordance with various embodiments.

FIG. 42 is an exemplary ECG waveform plot showing how the vertical or horizontal movement of the end of an RS segment can affect the ST segment due to abnormal conditions, in accordance with various embodiments.

FIG. 43 is an exemplary ECG waveform plot showing how the ST segment can shift horizontally due to abnormal conditions, in accordance with various embodiments.

FIG. 44 is an exemplary ECG waveform plot showing how vertical or horizontal movement of the J point can affect the ST segment due to abnormal conditions, in accordance with various embodiments.

FIG. 45 is an exemplary comparison of two ECG waveform plots exhibiting ST segment changes that can be identified using the STy standard, in accordance with various embodiments.

FIG. 46 is an exemplary comparison of two ECG waveform plots exhibiting ST segment changes that can be identified using the STx standard, in accordance with various embodiments.

FIG. 47 is an exemplary comparison of two ECG waveform plots exhibiting ST segment changes that can be identified using the STs and STy standards (STs+STy), in accordance with various embodiments.

FIG. 48 is an exemplary comparison of two ECG waveform plots exhibiting ST segment changes that can be identified using the STj, STy, and STx standards (STj+STy+STx), in accordance with various embodiments.

FIG. 49 is an exemplary ECG waveform plot of an ST segment change that can be identified using the STx and STj standards (STx+STj), in accordance with various embodiments.

FIG. 50 is an exemplary plot of an ECG waveform showing the accurate detection and measurement of the I-point and J-point, in accordance with various embodiments.

FIG. 51 is a series of plots of conventional ECG waveforms from different ECG leads showing that the J-point can only be detected from one lead, in accordance with various embodiments.

FIG. 52 is a series of plots of conventional ECG waveforms from different ECG leads showing that difficulty in measuring the I-point and the J-point, in accordance with various embodiments.

FIG. 53 is a plot of an ideal ECG waveform showing the importance of the I-point to the PR segment and the importance of the J-point to the ST segment, in accordance with various embodiments.

FIG. 54 is a series of plots of abnormal ECG waveforms showing the difficulty in determining the J-point and, therefore, the ST segment, in accordance with various embodiments.

FIG. 55 is a series of plots of normal ECG waveforms showing the difficulty in determining the J-point and, therefore, the ST segment, in accordance with various embodiments.

FIG. 56 is a plot showing an ECG waveform for a normal subject using the systems of the present application, in accordance with various embodiments.

FIG. 57 is a series of plots of an ECG waveform showing depolarization of the ventricular septal and apical parts and the ventricular wall, in accordance with various embodiments.

FIG. 58 is a flowchart showing a method for measuring and annotating the I-point of an ECG waveform during measurement of the ECG waveform, in accordance with various embodiments.

FIG. 59 is an exemplary plot showing action potential duration (APD) subdivisions within the P wave, the T wave, and the QRS complex of an aiECG waveform for a normal heart, in accordance with various embodiments.

FIG. 60 is an exemplary table showing APD measurement data for a series of heartbeats for a normal heart, in accordance with various embodiments.

FIG. 61 is an exemplary plot showing APD subdivisions within the P wave, the T wave, and the QRS complex of an aiECG waveform for an abnormal patient before PCI treatment, in accordance with various embodiments.

FIG. 62 is an exemplary table showing APD measurement data corresponding to the aiECG waveform of FIG. 61, in accordance with various embodiments.

FIG. 63 is an exemplary plot showing APD subdivisions within the P wave, the T wave, and the QRS complex of an aiECG waveform for the abnormal patient of FIG. 61 after PCI treatment, in accordance with various embodiments.

FIG. 64 is an exemplary table showing APD measurement data corresponding to the aiECG waveform of FIG. 63, in accordance with various embodiments.

FIG. 65 is an exemplary plot showing APD subdivisions within the P wave, the T wave, and the QRS complex of an aiECG waveform for an abnormal patient with a His bundle block, in accordance with various embodiments.

FIG. 66 is an exemplary table showing APD measurement data corresponding to the aiECG waveform of FIG. 65, in accordance with various embodiments.

FIG. 67 is an exemplary electrogram from an intracardiac electrophysiology study (EPS) for a 58-year-old female with a first-degree atrioventricular block.

FIG. 68 is an exemplary plot of an aiECG waveform obtained for the same 58-year-old female with a first-degree atrioventricular block of FIG. 67, in accordance with various embodiments.

FIG. 69 is an exemplary electrogram from an intracardiac EPS for a 68-year-old female with a complete right bundle branch block and a left anterior fascicular block.

FIG. 70 is an exemplary plot of an aiECG waveform obtained for the same 68-year-old female with a complete right bundle branch block and a left anterior fascicular block of FIG. 69, in accordance with various embodiments.

FIG. 71 is a flowchart showing a method for measuring and annotating a subdivision of the P wave of an ECG waveform during measurement of the ECG waveform, in accordance with various embodiments.

FIG. 72 is a plot of an exemplary ECG waveform showing measurement points along the isoelectric line of the ECG waveform, in accordance with various embodiments.

FIG. 73 is a plot of an exemplary ECG waveform showing measurement points along elevated or descended lines with respect to the isoelectric line of the ECG waveform and in relation to the ST segment and PR segment of the ECG waveform, in accordance with various embodiments.

FIG. 74 is a plot of two exemplary ECG waveforms showing a TP segment between them, in accordance with various embodiments.

FIG. 75 is a plot of two exemplary ECG waveforms showing an elevated TP segment between them, in accordance with various embodiments.

FIG. 76 is a plot of two exemplary ECG waveforms showing a descended TP segment between them, in accordance with various embodiments.

FIG. 77 is a plot of an ECG for a normal 59-year-old male showing that even for normal people there can be a slight elevation of measurement points above the equipotential line, in accordance with various embodiments.

FIG. 78 is a plot of an ECG for a 55-year-old male with an LAD 90% blockage before PCI showing an elevated P-point and an elevated T-point but a normal ST segment, in accordance with various embodiments.

FIG. 79 is a plot of an ECG for the same patient shown in FIG. 78 after PCI showing that the P-point and the T-point have returned to the equipotential line, in accordance with various embodiments.

FIG. 80 is a plot of an ECG for a 62-year-old female with an LAD 60% blockage and RCA 90% blockage before PCI showing an elevated P-point and an elevated T-point but a normal ST segment, in accordance with various embodiments.

FIG. 81 is a plot of an ECG for the same patient shown in FIG. 80 after PCI showing that the P-point and the T-point have returned to the equipotential line, in accordance with various embodiments.

FIG. 82 is a flowchart showing a method for measuring and annotating the P-point of an ECG waveform during measurement of the ECG waveform, in accordance with various embodiments.

Before one or more embodiments of the invention are described in detail, one skilled in the art will appreciate that the invention is not limited in its application to the details of construction, the arrangements of components, and the arrangement of steps set forth in the following detailed description. The invention is capable of other embodiments and of being practiced or being carried out in various ways. Also, it is to be understood that the phraseology and terminology used herein is for the purpose of description and should not be regarded as limiting.

Computer-Implemented System

FIG. 1 is a block diagram that illustrates a computer system 100, upon which embodiments of the present teachings may be implemented. Computer system 100 includes a bus 102 or other communication mechanism for communicating information, and a processor 104 coupled with bus 102 for processing information. Computer system 100 also includes a memory 106, which can be a random access memory (RAM) or other dynamic storage device, coupled to bus 102 for storing instructions to be executed by processor 104. Memory 106 also may be used for storing temporary variables or other intermediate information during execution of instructions to be executed by processor 104. Computer system 100 further includes a read only memory (ROM) 108 or other static storage device coupled to bus 102 for storing static information and instructions for processor 104. A storage device 110, such as a magnetic disk or optical disk, is provided and coupled to bus 102 for storing information and instructions.

Computer system 100 may be coupled via bus 102 to a display 112, such as a cathode ray tube (CRT) or liquid crystal display (LCD), for displaying information to a computer user. An input device 114, including alphanumeric and other keys, is coupled to bus 102 for communicating information and command selections to processor 104. Another type of user input device is cursor control 116, such as a mouse, a trackball or cursor direction keys for communicating direction information and command selections to processor 104 and for controlling cursor movement on display 112. This input device typically has two degrees of freedom in two axes, a first axis (i.e., x) and a second axis (i.e., y), that allows the device to specify positions in a plane.

A computer system 100 can perform the present teachings. Consistent with certain implementations of the present teachings, results are provided by computer system 100 in response to processor 104 executing one or more sequences of one or more instructions contained in memory 106. Such instructions may be read into memory 106 from another computer-readable medium, such as storage device 110. Execution of the sequences of instructions contained in memory 106 causes processor 104 to perform the process described herein. Alternatively, hard-wired circuitry may be used in place of or in combination with software instructions to implement the present teachings. Thus implementations of the present teachings are not limited to any specific combination of hardware circuitry and software.

In various embodiments, computer system 100 can be connected to one or more other computer systems, like computer system 100, across a network to form a networked system. The network can include a private network or a public network such as the Internet. In the networked system, one or more computer systems can store and serve the data to other computer systems. The one or more computer systems that store and serve the data can be referred to as servers or the cloud, in a cloud computing scenario. The other computer systems that send and receive data to and from the servers or the cloud can be referred to as client or cloud devices, for example.

The term “computer-readable medium” as used herein refers to any media that participates in providing instructions to processor 104 for execution. Such a medium may take many forms, including but not limited to, non-volatile media, volatile media, and transmission media. Non-volatile media includes, for example, optical or magnetic disks, such as storage device 110. Volatile media includes dynamic

memory, such as memory 106. Transmission media includes coaxial cables, copper wire, and fiber optics, including the wires that comprise bus 102.

Common forms of computer-readable media or computer program products include, for example, a floppy disk, a flexible disk, hard disk, magnetic tape, or any other magnetic medium, a CD-ROM, digital video disc (DVD), a Blu-ray Disc, any other optical medium, a thumb drive, a memory card, a RAM, PROM, and EPROM, a FLASH-EPROM, any other memory chip or cartridge, or any other tangible medium from which a computer can read.

Various forms of computer-readable media may be involved in carrying one or more sequences of one or more instructions to processor 104 for execution. For example, the instructions may initially be carried on the magnetic disk of a remote computer. The remote computer can load the instructions into its dynamic memory and send the instructions over a telephone line using a modem. A modem local to computer system 100 can receive the data on the telephone line and use an infra-red transmitter to convert the data to an infra-red signal. An infra-red detector coupled to bus 102 can receive the data carried in the infra-red signal and place the data on bus 102. Bus 102 carries the data to memory 106, from which processor 104 retrieves and executes the instructions. The instructions received by memory 106 may optionally be stored on storage device 110 either before or after execution by processor 104.

In accordance with various embodiments, instructions configured to be executed by a processor to perform a method are stored on a computer-readable medium. The computer-readable medium can be a device that stores digital information. For example, a computer-readable medium includes a compact disc read-only memory (CD-ROM) as is known in the art for storing software. The computer-readable medium is accessed by a processor suitable for executing instructions configured to be executed.

The following descriptions of various implementations of the present teachings have been presented for purposes of illustration and description. It is not exhaustive and does not limit the present teachings to the precise form disclosed. Modifications and variations are possible in light of the above teachings or may be acquired from practicing of the present teachings. Additionally, the described implementation includes software but the present teachings may be implemented as a combination of hardware and software or in hardware alone. The present teachings may be implemented with both object-oriented and non-object-oriented programming systems.

Subwaveform Detection of the P, Q, R, S, T, U, and J Waveforms

As described above, electrical signals flow through all the different muscle tissues of the heart. For the last 100 years, conventional ECG devices have been able to detect some of these signals in the form of the P, Q, R, S, T, U, and J waveforms. These waveforms have aided in the diagnosis and treatment of many heart problems.

Unfortunately, however, the P, Q, R, S, T, U, and J waveforms do not provide a complete picture of the operation of all the different muscle tissues of the heart. As a result, improved systems and methods are needed to detect and analyze more information from the electrical signals that flow through all the different muscle tissues of the heart as it is beating. This additional information can be used to diagnose and treat many more heart problems.

In various embodiments, additional information is obtained from the electrical signals produced by a heart through signal processing. More specifically, signal process-

ing is added to an ECG device in order to detect more information from the electrical signals that flow through all the different muscle tissues of the heart as it is beating.

FIG. 7 is a block diagram 700 of a conventional ECG device. The conventional ECG device includes two or more leads or electrodes 710. Electrodes 710 are typically attached to the skin of a patient. Electrical signals produced by a beating heart are detected between pairs of electrodes 710. Because the heart is three-dimensional, electrodes are attached at different locations on a body to detect signals at different corresponding locations or angles from the heart. In other words, the electrodes are placed on a body to partially surround the heart. One typical type of ECG includes 12 electrodes, for example.

A voltage signal is detected between two electrodes 710 by detector 720. Detector 720 also typically amplifies the voltage signal. Detector 720 can also convert the voltage signal to a digital voltage signal using an analog to digital converter (A/D).

Detector 720 provides the detected and amplified voltage signal from each pair of electrodes 710 to display 730. Display 730 can be an electronic display device including, but not limited to, a cathode ray tube (CRT) device, light emitting diode (LED) device, or Liquid crystal display (LCD) device. Display 730 can also be a printer device. Additionally, display 730 can include a memory device to record detected signals. The memory device can be, but is not limited to, a volatile electronic memory, such as random access memory (RAM), a non-volatile electronic memory, such as electrically erasable programmable read-only memory (EEPROM or Flash memory), or a magnetic hard drive.

Display 730 displays a continuous loop of the detected P, Q, R, S, T, U, and J waveforms as shown in FIG. 2 for each pair of electrodes 710. Modern ECG devices can also include a processor (not shown), such as the processor shown in FIG. 1, to analyze the P, Q, R, S, T, U, and J waveforms. For example, the processor can calculate the time periods of the P, Q, R, S, T, U, and J waveforms and the times between the P, Q, R, S, T, U, and J waveforms. The processor can also compare this timing information to stored normal information. Based on the comparison, the processor can determine differences from the normal data. All information calculated by the processor can also be displayed on display 730.

FIG. 8 is a block diagram 800 of an ECG device for detecting more information from the electrical signals that flow through all the different muscle tissues of the heart as it is beating, in accordance with various embodiments. Electrodes 810 are attached to the skin of a patient, for example. Electrical signals produced by a beating heart are detected between pairs of electrodes 810.

A voltage signal is detected between two electrodes 810 by detector 820. Detector 820 also amplifies the voltage signal. Detector 820 also converts the voltage signal to a digital voltage signal using an analog to digital converter (A/D).

Detector 820 provides the detected and amplified voltage signal from each pair of electrodes 810 to signal processor 830. Detector 820 can also provide the detected and amplified voltage signal from each pair of electrodes 810 directly to display device 840 to display the conventional P, Q, R, S, T, U, and J waveforms.

Signal processor 830 detects or calculates one or more subwaveforms within and/or in the interval between the P, Q, R, S, T, U, and J waveforms of each detected and amplified voltage signal. A waveform is a shape or form of

a signal. A subwaveform is a shape or form of a signal that is within or part of another signal.

Signal processor 830 can be a separate electronic device that can include, but is not limited to, an application specific integrated circuit (ASIC), a field programmable gate array (FPGA), or a general purpose processor. Signal processor 830 can be software implemented on another processor of the ECG device, such as a processor of display device 840. Signal processor 830 can also be a remote server that receives the detected and amplified voltage signal from detector 820, detects or calculates one or more subwaveforms within and/or in the interval between the P, Q, R, S, T, U, and J waveforms, and sends the detected and amplified voltage signal and the one or more subwaveforms to display device 840.

Signal processor 830 sends one or more subwaveforms of each detected and amplified voltage signal to display device 840. Signal processor 830 can also calculate and send to the display device 840 the time periods of the one or more subwaveforms, the times between the one or more subwaveforms, and the times of the one or more subwaveforms in relation to the P, Q, R, S, T, U, and J waveforms and or the intervals between the P, Q, R, S, T, U, and J waveforms. Signal processor 830 can also compare this timing information to stored normal timing information. Based on the comparison, signal processor 830 can determine differences from the normal data and send this difference information and any of the timing information to display device 840.

Display device 840 displays a continuous loop of the one or more subwaveforms for each pair of electrodes 810. Display device 840 can also display part or all of the conventional P, Q, R, S, T, U, and J waveforms for comparison with the one or more subwaveforms. Like display 730 of FIG. 7, display device 840 of FIG. 8 can be an electronic display device, a printer, or any combination of the two.

In various embodiments, an ECG device using signal processing to detect one or more subwaveforms within the P, Q, R, S, T, U, and J waveforms and/or within the intervals between the P, Q, R, S, T, U, and J waveforms is herein referred to as a saah ECG device. The voltage difference signals produced by a saah ECG device are referred to as saah ECG waveforms. The term "saah" is an acronym for some of the anatomically distinct portions of muscle tissue that produce subwaveforms. Specifically, saah stands for sinoatrial node (SAN), atria (right atrium (RA) and left atrium (LA)), atrioventricular node (AVN), and bundle of His (HIS). However, a saah ECG waveform is not limited to including subwaveforms representing the SAN, the atria, the AVN, and the HIS. A saah ECG waveform can include any subwaveform the P, Q, R, S, T, U, and J waveforms and/or within the intervals between the P, Q, R, S, T, U, and J waveforms.

FIG. 9 is an exemplary plot 900 of a saah ECG waveform of a heartbeat from a saah ECG device showing subwaveforms found within the P, Q, R, S, T, U, and J waveforms and/or within the intervals between the P, Q, R, S, T, U, and J waveforms, in accordance with various embodiments. For example, five subwaveforms 910-950 of FIG. 9 are detected within the P waveform and the PR segment. The time period that includes the P waveform and the PR segment is also called the PR interval. Subwaveform 910 represents the depolarization of the SAN. Subwaveform 920 represents the depolarization of RA and LA. Subwaveform 930 represents the depolarization of the AVN. Subwaveform 940 represents the depolarization HIS. Finally, subwaveform 950 represents the depolarization of the bundle branches (BB).

In various embodiments, the subwaveforms of a saah ECG waveform are detected using signal processing. Electrodes **810** of the saah ECG of FIG. **8**, for example, receive electrical impulses from anatomically distinct portions of muscle tissue or cells. The electrical impulses of anatomically distinct portions of muscle tissue of the heart have distinct frequencies. Through animal and human experimentation, the distinct frequency, frequency range, or frequency band of the anatomically distinct portions of muscle tissue of the heart are found. These distinct frequency bands of anatomically distinct portions of muscle tissue of the heart provide predetermined data or information for signal processing. In other words, the band pass frequency filtering of the signal processing is determined from the experimental data collected. A saah ECG device then employs one or more frequency band pass filters to detect the one or more subwaveforms.

FIG. **10** is an exemplary block diagram **1000** showing a signal processing algorithm for detecting five subwaveforms within the PR interval of a conventional ECG waveform, in accordance with various embodiments. Sampling block **1010** samples the electrical impulses in the PR interval time period of each heart. This is shown graphically in FIG. **1000** by separating PR interval **1020** from ECG waveform **200**. The electrical impulses in the PR interval time period are sampled using electrodes **810** and detector **820** of FIG. **8**, for example. Detector **820** of FIG. **8** can also amplify and convert the analog signal into a digital signal for digital processing.

The signal processing can be performed directly on the time domain signal received from a detector or the time domain signal received from a detector can be converted to the frequency domain for algorithmic processing. In FIG. **10**, block **1030** converts the PR interval time domain signal to a PR interval frequency domain signal. The time domain signal is converted into a frequency domain signal using a Fourier transform, for example.

As described above, through animal and/or human experimentation, the frequency bands associated with depolarization of the SAN, atria, AVN, HIS, and BB of the heart are determined. Based on these frequency bands, band pass filters are created. Blocks **1041-1045** represent the band pass filters created to filter the PR interval frequency domain signal for frequency bands of the SAN, atria, AVN, HIS, and BB of the heart, respectively.

In block **1050**, the frequency domain subwaveforms detected from the band pass filtering the frequency bands of the SAN, atria, AVN, HIS, and BB of the heart are summed. In block **1060**, the filtered and summed frequency domain signal of the PR interval is converted back to a time domain signal. The frequency domain signal is converted into a time domain signal using a Fourier transform, for example.

The PR interval filtered and summed time domain signal **1070** includes five time domain subwaveforms **910-950**. Subwaveforms **910-950** represent depolarization of the SAN, atria, AVN, HIS, and BB of the heart, respectively. Time domain signal **1070** can be used to replace PR interval **1020** in ECG waveform **200**, for example. As a result, a saah ECG waveform is produced.

FIG. **10** shows a signal processing algorithm for detecting five subwaveforms. However, similar steps can be applied to detect fewer than five waveforms or more than five waveforms. Also, the steps of FIG. **10** describe detecting subwaveforms within the PR interval. However, similar steps can be applied to detect subwaveforms within the P, Q, R, S, T, U, and J waveforms and/or within one or more of the intervals between the P, Q, R, S, T, U, and J waveforms. In

addition, the steps of FIG. **10** describe converting time signals to the frequency domain and then back to the time domain. One of ordinary skill in the art can appreciate that band pass filters can be applied directly to the time domain signal to provide the same result.

FIG. **11** is an exemplary block diagram **1100** of a saah ECG device that displays conventional ECG waveforms, saah ECG waveforms, and saah ECG data, in accordance with various embodiments. In block **1110**, patient heart signals are obtained. These heart signals can be obtained through noninvasive electrodes placed on the skin, such as electrodes **810** shown in FIG. **8**. In various embodiments, heart signals may also be obtained using invasive electrodes placed directly on the heart. In block **1120**, the heart signals are detected using a detector and amplified.

In block **1130**, the detected and amplified heart signals are processed using a signal processor. The signal processor detects the conventional P, Q, R, S, T, U, and J waveforms and sends them to the display of block **1160**. The signal processor also detects or calculates subwaveforms within the conventional P, Q, R, S, T, U, and J waveforms and/or within intervals between the conventional P, Q, R, S, T, U, and J waveforms. The signal processor sends the subwaveforms to block **1140** for further processing. The processor of block **1140** produces the saah ECG waveform that includes the subwaveforms and sends the saah ECG waveform to the display of block **1160**. The processor of block **1140** calculates additional information or new data from the saah ECG waveform. This new data can include, but is not limited to, timing information about the subwaveforms, timing information about the intervals between the subwaveforms, and timing information about the subwaveforms and their relation to the conventional P, Q, R, S, T, U, and J waveforms. In block **1150**, this new data is sent to the display of block **1160**.

The display of block **1160** displays a continuous loop of the conventional ECG waveform, the saah ECG waveform, and the new data from the subwaveforms. The display of block **1160** can display this information on an electronic display or print it on paper. The display of block **1160** can also record this information. The display of block **1160** can record this information on any type of memory device.

FIG. **12** is an exemplary plot **1200** of the information displayed by the saah ECG device of FIG. **11**, in accordance with various embodiments. Plot **1200** includes conventional ECG waveform **1210** and saah ECG waveform **1220**. Saah ECG waveform **1220**, for example, includes, among others, five subwaveforms A-E representing the depolarization of the SAN, the RA and LA, the AVN, the HIS, and the BB, respectively.

Plot **1200** also shows new data or timing information about the subwaveforms and their relation to the conventional P, Q, R, S, T, U, and J waveforms. For example, the time interval between line **1231** and line **1232** relates subwaveform A of saah ECG waveform **1220** to P waveform **1240** of conventional ECG waveform **1210**. The time interval between line **1232** and line **1233** relates subwaveforms B and C of saah ECG waveform **1220** to P waveform **1240** conventional ECG waveform **1210**. The time interval between line **1233** and line **1234** relates subwaveforms D and E of saah ECG waveform **1220** to PR segment **1250** conventional ECG waveform **1210**.

FIG. **13** is an exemplary block diagram **1300** of a saah ECG device that displays conventional ECG waveforms, saah ECG waveforms, saah ECG data, and saah ECG automatic pattern recognition diagnosis information, in accordance with various embodiments. In block **1310**,

patient heart signals are obtained. These heart signals can be obtained through noninvasive electrodes placed on the skin, such as electrodes **810** shown in FIG. **8**. In various embodiments, heart signals may also be obtained using invasive electrodes placed directly on the heart. In block **1320**, the heart signals are sampled or detected using a detector. The heart signals may also be amplified.

In block **1330**, the sampled heart signals are processed using a signal processor. The signal processor produces four different types of information from the sampled heart signals. As shown in block **1340**, the signal processor produces conventional ECG waveforms including the conventional P, Q, R, S, T, U, and J waveforms and sends them to display **1380**. As shown in block **1350**, the signal processor produces saah ECG waveforms. These saah ECG waveforms include subwaveforms of the conventional P, Q, R, S, T, U, and J waveforms and the intervals between them. Note that the arrow between blocks **1330** and **1350** show information following in both directions. This shows that information from the saah ECG waveforms is further analyzed by the signal processor.

As shown in block **1360**, the signal processor further analyzes the saah ECG waveforms to produce saah ECG data. This saah ECG data is sent to display **1380**. Additionally, as shown in block **1370**, the signal processor further analyzes the saah to obtain endocardium and epicardium data. This data is compared to recorded normal and abnormal data. The signal processor then produces automatic pattern recognition diagnosis (APD) information, and this information is sent to display **1380**. APD information is, for example, patterns and/or colors that allow a user to easily and quickly determine that normal or abnormal endocardium and/or epicardium data was found.

Systems and methods for detecting ECG subwaveforms are described in the '204 Patent, which is incorporated by reference in its entirety.

System for Detecting ECG Subwaveforms

In various embodiments, an electrocardiography (ECG) system for detecting one or more subwaveforms within the P, Q, R, S, T, U, and J waveforms or in an interval between the P, Q, R, S, T, U, and J waveforms is provided. Returning to FIG. **8**, the ECG system includes two or more electrodes **810**, a detector **820**, a signal processor **830**, and a display device **840**.

Two or more electrodes **810** are placed near a beating heart and receive electrical impulses from the beating heart. Two or more electrodes **810** are shown in FIG. **8** as noninvasive electrodes that are attached to the skin of a patient. In various embodiments, two or more electrodes **810** can be invasive electrodes placed directly on or within heart tissue.

Detector **820** is electrically connected to two or more electrodes **810**. Detector **820** detects the electrical impulses from at least one pair of electrodes of the two or more electrodes **810**. Detector **820** converts the electrical impulses to an ECG waveform for each heartbeat of the beating heart. Detector **820**, for example, samples the electrical impulses. In various embodiments, detector **820** further amplifies the ECG waveform. In various embodiments, detector **820** further performs analog to digital (A/D) conversion on the ECG waveform. In various embodiments, detector **820** provides an ECG waveform with a higher signal-to-noise (S/N) ratio than conventional ECG devices.

Signal processor **830** is electrically connected to detector **820**. Signal processor **830** receives the ECG waveform from detector **820**. Signal processor **830** detects or calculates one or more subwaveforms within P, Q, R, S, T, U, and J waveforms of the ECG waveform or in an interval between

the P, Q, R, S, T, U, and J waveforms that represent the depolarization or repolarization of anatomically distinct portions of muscle tissue of the beating heart. Signal processor **830** produces a processed ECG waveform that includes the one or more subwaveforms for each heartbeat.

Signal processor **830** can be a separate device, can be software running on a device of detector **820** or display device **840**, or can be software running on a remote server and communicating with detector **820** and display device **840** through one or more communication devices. Signal processor **830** can be a separate device that includes, but is not limited to, an application specific integrated circuit (ASIC) or a field programmable gate array (FPGA) or a general purpose processor. A general purpose processor can include, but is not limited to, a microprocessor, a microcontroller, or a computer such as the system shown in FIG. **1**. Signal processor **830** can be software implemented on another processor of the ECG device, such as a processor of display device **840**. Signal processor **830** can also be a remote server that receives the detected and amplified difference voltage signal from detector **820**, detects or calculates one or more subwaveforms within and/or in the interval between the P, Q, R, S, T, U, and J waveforms, and sends the detected and amplified different voltage signal and the one or more subwaveforms to display device **840**.

Display device **840** receives the processed ECG waveform for each heartbeat and displays the processed ECG waveform for each heartbeat. The processed ECG waveform is called a saah ECG waveform, for example. As described above, display device **840** can be an electronic display device including, but not limited to, a cathode ray tube (CRT) device, light emitting diode (LED) device, or Liquid crystal display (LCD) device. Display device **840** can also be a printer device or any combination of an electronic display device and a printer. Additionally, display device **840** can include a memory device to record saah ECG waveforms, saah ECG data and conventional ECG waveforms and data. The memory device can be, but is not limited to, a volatile electronic memory, such as random access memory (RAM), a non-volatile electronic memory, such as electrically erasable programmable read-only memory (EEPROM or Flash memory), or a magnetic hard drive.

In various embodiments, the detected one or more subwaveforms include at least one subwaveform representing depolarization of the sinoatrial node (SAN), the atria (right atrium (RA) and left atrium (LA)), the atrioventricular node (AVN), the bundle of His (HIS), or the bundle branches (BB) of the beating heart.

In various embodiments, the display device **840** further displays the ECG waveform for comparison with the processed ECG waveform.

In various embodiments, signal processor **830** further calculates timing information about the one or more subwaveforms, timing information about the intervals between the one or more subwaveforms, and timing information about the one or more subwaveforms and their relation to the P, Q, R, S, T, U, and J waveforms of the ECG waveform for each heartbeat. Display device **840** further receives this timing information from signal processor **830**. Display device **840** displays the timing information about the one or more subwaveforms, the timing information about the intervals between the one or more subwaveforms, and the timing information about the one or more subwaveforms and their relation to the P, Q, R, S, T, U, and J waveforms of the ECG waveform for each heartbeat.

In various embodiments, the ECG system further includes a memory device (not shown). The memory device receives the ECG waveform and the processed ECG waveform from the signal processor.

In various embodiments, the memory device further includes normally processed ECG waveform data. Normally processed ECG waveform data is stored on the memory device using signal processor **830** or a general-purpose processor (not shown). Signal processor **830** further compares the processed ECG waveform to the normally processed ECG waveform data and calculates a status condition based on the comparison. The status conditions are, for example, normal, suspicious, or abnormal.

In various embodiments, the ECG system includes a second display device (not shown) surrounding a rotating button (not shown). Signal processor **830** further sends a colored pattern to the second display device based on the status condition. The second display device provides automatic pattern recognition diagnosis (APD).

Method for Detecting ECG Subwaveforms

FIG. **16** is a flowchart showing a method **1600** for detecting subwaveforms within the P, Q, R, S, T, U, and J waveforms of an ECG waveform of a heartbeat or in an interval between the P, Q, R, S, T, U, and J waveforms, in accordance with various embodiments.

In step **1610** of method **1600**, electrical impulses are detected between at least one pair of electrodes of two or more electrodes placed proximate to a beating heart using a detector. The electrical impulses are converted to an ECG waveform for each heartbeat of the beating heart using the detector.

In step **1620**, the ECG waveform for each heartbeat is received from the detector using a signal processor. One or more subwaveforms within P, Q, R, S, T, U, and J waveforms of the ECG waveform for each heartbeat or in an interval between the P, Q, R, S, T, U, and J waveforms that represent the depolarization or repolarization of an anatomically distinct portion of muscle tissue of the beating heart are detected using the signal processor. A processed ECG waveform that includes the one or more subwaveforms for each heartbeat is produced using the signal processor.

In step **1630**, the processed ECG waveform is received from the signal processor and the processed ECG waveform is displayed using a display device.

Computer Program Product for Detecting ECG Subwaveforms

In various embodiments, computer program products include a tangible computer-readable storage medium whose contents include a program with instructions being executed on a processor so as to perform a method for detecting subwaveforms within the P, Q, R, S, T, U, and J waveforms of an ECG waveform of a heartbeat or in an interval between the P, Q, R, S, T, U, and J waveforms. This method is performed by a system that includes one or more distinct software modules.

FIG. **17** is a schematic diagram of a system **1700** that includes one or more distinct software modules that perform a method for detecting subwaveforms within the P, Q, R, S, T, U, and J waveforms of an ECG waveform of a heartbeat or in an interval between the P, Q, R, S, T, U, and J waveforms, in accordance with various embodiments. System **1700** includes detection module **1710**, processing module **1720**, and display module **1730**.

Detection module **1710** detects electrical impulses between at least one pair of electrodes of two or more electrodes placed proximate to a beating heart. Detection

module **1710** converts the electrical impulses to an ECG waveform for each heartbeat of the beating heart.

Processing module **1720** receives the ECG waveform for each heartbeat. Processing module **1720** detects one or more subwaveforms within P, Q, R, S, T, U, and J waveforms of the ECG waveform for each heartbeat or in an interval between the P, Q, R, S, T, U, and J waveforms that represent the depolarization or repolarization of an anatomically distinct portion of muscle tissue of the beating heart. Processing module **1720** produces a processed ECG waveform that includes the one or more subwaveforms for each heartbeat.

Display module **1730** receives the processed ECG waveform. Display module **1730** displays the processed ECG waveform.

Multi-Domain ECG

The heart muscle, like other muscles, is activated by biologically generated electrical signals. Electrocardiography (ECG or EKG) has long been used to measure and record these electrical signals. Essentially, in ECG the electrical activity of the heart is measured from a number of different points on the body and plotted over time. As a result, ECG traces out each cardiac cycle or heartbeat as a voltage versus time waveform.

A human heart has two functional systems. The first system, referred to as a self-conduction system, is part of the atrium (including left and right atria). In a traditional ECG, the self-conduction system is represented by the P wave or PR interval. The excitation, rhythm, and conduction of every beat are completed by the collaboration of all parts of the heart, which is an axis system, including: sinoatrial node (SAN)-atrial-atrioventricular node (AVN)-Bundle of His-Bundle Branches (left and right). The Bundle of His is a collection of heart muscle cells specialized for electrical conduction that transmits the electrical impulses from the AVN to the point of the apex of the fascicular branches. Complex arrhythmias disease typically occurs in these different areas. However, ECG is only half of a sine wave.

The second system, referred to as a cardiac work system, is a pump system (one for each complete contraction and relaxation of the heart), which is done by the heart muscles. The main part of the second system is the left ventricle. In the traditional ECG, it is represented by the T wave or QT interval. There are about 10 million ventricular myocardial cells, without nerves or tracts.

Features or waves of each heartbeat waveform have been known for more than a century to correspond to electrical signals activating various parts of the heart. For example, the P wave is known to result from an electrical signal directed from the SAN to the AV node activating the atrium of the heart, to the Bundle of His to the left and right Bundle Branches, and the T wave is known to result from a recovery electrical signal (ventricular depolarization and repolarization) sent to the ventricles of the heart after they have contracted. As a result, physicians are able to diagnose specific heart problems by analyzing the shapes and time of these waves.

It is thought that an ECG heartbeat waveform includes much more information about the anatomy of the heart that is not being used (scanning and displaying). In particular, it is thought that at least some of the waves in an ECG heartbeat waveform include subwaveforms that provide more detailed information about parts of the heart, as described above. Consequently, there is a need for systems and methods for processing biological electrical signals, such as signals read by ECG, in order to provide additional information about anatomical structures.

Also, electrocardiogram information itself contains a lot of information that has not been discovered so far, leaving numerous puzzles in a clinical application.

In various embodiments, new waveforms are created from a conventional ECG waveform. New indexes and new parameters are obtained from the new waveforms, so that it is possible to have a breakthrough in electrocardiogram diagnostics.

In various embodiments, heart signals are divided into different frequency bands, and then convolved or combined in one diagram. For example, 16 different frequency bands can be used. This procedure is based on the study of ergonomics and analysis procedures for frequently used information in cybernetics and nonlinear theory. The procedure makes use of the theory and analysis index of an “electrocardiogram multi-phase signal,” and by using a new method of frequency division and dimension division, according to the display method of P, Q, R, S, T, U, and J waveforms P-QRS-T in a conventional ECG waveform. Heart diseases are also related to and/or complicated by different other diseases. Therefore, different numbers of frequency ranges are required to be displayed as a diagnostic requirement, because the frequency shifts of various diseases are different. In the multi-domain frequency division method, 8, 9, 10, 11, 12, 13, 14, 15, or 16 roots of multi-domain linear waveforms are displayed, and a total of 12 leads are individually displayed. If each lead is divided into 16 waveforms, there are totally 192 ECG waveforms, providing much more information. In various embodiments, multi-domain ECG (mdECG) can be used as a very valuable and new diagnostic technique for combined heart diseases. This technique can be applied in electrocardiograph, monitor, echocardiography, and invasive electrophysiological instrument.

Since the invention of ECG, the linear waveform shaped like a rope has been used. Its frequency response range is 0-150 Hz and all subwaveforms are convolved or combined together. However, heart signals are formed by combining different ultra-low frequency, low frequency, intermediate frequency, high frequency, and ultra-high frequency signals. Because in ECG all frequencies are convolved together, many fine, weak, and very valuable signals are usually submerged or overlapped by the high frequency; especially at ventricle (ECG at T-wave, ECG ‘T’ wave duration) and atrium (ECG at P-wave, ECG ‘P’ wave duration), and numerous signals accumulate within a very small time axis range, causing problems and confusion in the accuracy of the ECG diagnosis rate. As a result, the detection rate of ECG for acute myocardial infarction (AMI), acute coronary syndrome (ACS), coronary artery disease (CAD), myocardial infarction (MI), heart failure (HF), etc., with the highest incidence of cardiovascular disease is only 17%-25%. Based on a large number of research reports, for the CAD/MI/ACS patient, ECG begins to change only after ischemia reaches 70%, and only about half of the electrocardiograms show abnormality. There are 7 billion people in the world, and the percentage of people who die of cardiovascular diseases or complicated cardiovascular diseases is about 42.86% (3/7). An electrocardiogram is the most fundamental clinical assessment instrument, and it is simple, fast and economical. Therefore, it is important to improve the clinical ECG diagnosis rate, which is possible only by improving the waveform display rate of ECG.

In various embodiments, systems and methods improve the waveform display rate of ECG and clinical diagnosis rate using a 16 linear multi-domain electrocardiogram. Because the heart signals are separated according to different fre-

quency bands with frequency bands being recombined, many high frequency signals, ultra-high frequency signal, low frequency signals, and ultra-low frequency signals are displayed with the raw heart signals at different frequency band according to the heart transduction pathway and electrophysiological rule, without the electrocardiogram being altered, i.e., at X-transverse axis and Y-vertical axis of P-QRS-T. Because the frequency bands of ECG are combined signals, mdECG separates the signals, i.e., separates them into independent waveforms consisting of different frequency bands. In this way, those frequency bands with the one linear waveform invisible and obscure in traditional ECG can be displayed clearly with different frequency bands one by one, assisting the doctor in reading, analyzing, judging and basic clinical assessment.

FIG. 18 is an exemplary block diagram 1800 showing a system for performing multi-domain ECG using 16 different frequency bands or domains, in accordance with various embodiments. Sampling block 1810 samples the electrical impulses at one electrode for one heartbeat, for example. This is shown graphically in FIG. 1800 by converting ECG waveform 200 to sampled ECG waveform 1820 using block 1810. The electrical impulses for the entire ECG waveform 200 are sampled using electrodes 810 and detector 820 of FIG. 8, for example. Detector 820 of FIG. 8 can also amplify and convert the analog signal into a digital signal for digital processing.

The signal processing can be performed directly on the time domain signal received from a detector or the time domain signal received from a detector can be converted to the frequency domain for algorithmic processing. In FIG. 18, block 1830 converts sampled ECG waveform 1820 to a frequency domain signal. The time domain signal is converted into a frequency domain signal using a Fourier transform, for example.

As described above, through animal and/or human experimentation, the frequency bands associated with different muscles of the heart can be determined. The frequency bands used here can be based on those bands determined experimentally, for example. Alternatively, the 16 frequency bands can be found by dividing the total frequency bands 16 ways. The different band can have the same bandwidth or can have different bandwidths.

In block 1840, 16 different band pass filters filter sampled ECG waveform 1820’s frequency domain signal into 16 different frequency domain signal. These 16 different 16 different frequency domain signals are then converted back to the time domain. The result of block 1840 is 16 different time domain signals.

In block 1850, the 16 different time domain signals are combined or plotted together in the time domain as one multi-domain ECG waveform 1860. In FIG. 1800, a conventional ECG signal from one electrode is processed into a multi-domain ECG waveform that includes 16 different time domain signals. In various embodiments, a conventional ECG signal from one electrode, however, can be processed into a multi-domain ECG waveform that includes any number of different time domain signals.

FIG. 19 is an exemplary plot 1900 of a multi-domain ECG waveform that includes 10 different time domain signals, in accordance with various embodiments.

FIG. 20 is an exemplary plot 2000 of a multi-domain ECG waveform that includes 14 different time domain signals, in accordance with various embodiments.

FIG. 21 is an exemplary alignment 2100 of a multi-domain ECG waveform 2110 that includes 16 different time domain signals with a conventional ECG waveform 2120, in

accordance with various embodiments. Multi-domain ECG waveform **2110** is produced from conventional ECG waveform **2120** using the system depicted in FIG. **18**, for example. As shown in FIG. **21**, multi-domain ECG waveform **2110** can display data with negative values while conventional ECG waveform **2120** cannot.

Systems and methods for detecting multi-domain ECG waveforms are described in the '930 Patent, which is incorporated by reference in its entirety.

Example saah ECG Waveforms and EPCG Waveforms

FIG. **29** is an exemplary diagram **2900** of the anatomy of the self-conducting system of a heart, in accordance with various embodiments. The self-conducting system begins with S-A node (SAN) **2910**. Conduction moves from SAN **2910** through transitional fibers **2920** to A-V node (AVN) **2930**. Conduction then moves from AVN **2930** past atrioventricular fibrous tissue **2940** and through penetrating portion of A-V bundle (His bundle) **2950** to distal portion of A-V bundle **2960**. From distal portion of A-V bundle **2960** conduction moves through right bundle branch **2971** and left bundle branch **2972** to ventricular septum **2960**.

FIG. **30** is an exemplary diagram **3000** showing the anatomic sites that the PA, AH, and HV intervals represent and the corresponding PA, AH, and HV intervals in a saah ECG waveform and traditional ECG waveform, in accordance with various embodiments. PA interval **3011**, AH interval **3012**, and HV interval **3013** are depicted with respect to anatomic sites along self-conducting system **3020** of the heart. The same intervals, PA interval **3011**, AH interval **3012**, and HV interval **3013**, are also shown with respect to saah ECG waveform **3030** and traditional ECG waveform **3040**. FIG. **30** shows that processed or calculated information like PA interval **3011**, AH interval **3012**, HV interval **3013**, and saah ECG waveform **3030** relate ECG signals more closely to the anatomy of self-conducting system **3020** than traditional ECG waveform **3040**.

FIG. **31** is an exemplary comparison plot **3100** of a saah ECG waveform and a traditional ECG waveform with PA, AH, HV, and PR interval values obtained from aiECG processing for a patient with a normal heart, in accordance with various embodiments. Timing values for PA interval **3111**, AH interval **3112**, HV interval **3113** and PR interval **3114** are shown with respect to saah ECG waveform **3130** and aligned traditional ECG waveform **3140**. As described above, PR interval **3114** refers to the time period that includes the P waveform and the PR segment of traditional ECG waveform **3140**. FIG. **31** shows that processed or calculated information like the timing values for PA interval **3111**, AH interval **3112**, HV interval **3113**, and PR interval **3113** and saah ECG waveform **3130** provide much more information than traditional ECG waveform **3140** on its own.

FIG. **32** is an exemplary comparison plot **3200** of a portion of a multi-domain ECG or electrophysiocardiogram (EPCG) waveform aligned with a portion of a traditional ECG waveforms for a patient with acute coronary syndrome (ACS) before and after percutaneous coronary intervention (PCI), in accordance with various embodiments. EPCG waveform **3210** is aligned with traditional ECG waveform **3220** for the patient with ACS before PCI treatment. EPCG waveform **3211** is aligned with traditional ECG waveform **3221** for the patient with ACS after PCI treatment. A comparison of magnified portions **3230** and **3231** of EPCG waveforms **3211** and **3211**, respectively, shows that all small waveforms are not apparent in waveform portion **3210** before PCI treatment are back to normal after PCI treatment

in waveform portion **3211**. Similar information cannot be found in a comparison of traditional ECG waveforms **3220** and **3221**.

FIG. **33** is an exemplary diagram **3300** showing timing values of conduction calculated at various anatomic sites along the self-conduction system of a normal heart by further processing a traditional ECG waveform, in accordance with various embodiments. For example, timing values are provided for the atrial myocardium (AM) **3310**, the sino atrial node (SAN) **3320**, the atrioventricular node (AVN) **3330**, Purkinje's cell (PC) **3340**, and the ventricular myocardium (VM) **3350**. The right ventricle (RV) **3360** and the left ventricle (LV) **3370** are also labeled in diagram **3300**. Automated ECG Analysis and Diagnosis

As described above, to date the accuracy rate of automated ECG analysis and diagnosis systems has been a problem in clinical applications. There are at least three technical reasons for this. 1. The conventional ECG waveform is morphological and generally no consistent mapping points can be found. 2. Conventional ECG measurements have not provided information specific different parts of the heart muscle. 3. Automated ECG waveform analysis has generally resulted in a high number of false positives for both normal and abnormal populations. However, ECG remains one of the most extensively used clinical tools, despite the lack of accurate systems for automated ECG analysis and diagnosis. As a result, there is a significant need for such systems. Recent advancements have addressed the conventional ECG waveform measurement problem. Specifically, the systems of the '204 Patent and the '930 Patent have allowed the different frequency domain signals from different parts of the heart muscle to be measured.

Additional systems, however, are needed to further address the technical problems of analyzing the shape and form of these frequency domain signals and distinguishing disease conditions from false positives in normal and abnormal populations.

Conventional ECG Waveform Analysis Problems

Analysis of conventional ECG waveforms for clinical diagnosis has been limited by a number of problems for more than a century. (1) It has been difficult to correctly confirm the start point of the P wave. The reason for this is that the start point of the P wave is on "a parallel equipotential line," which needs to be determined. This has traditionally been determined through guessing. If the starting point of each heartbeat cannot be correctly identified, then all subsequent parameter measurements will be wrong. The normal value for the conduction time from the SA node (the starting point of the P wave) to the atrium is only around 30 ms. As a result, a small mistake in the location of the starting point can make a big difference in the measurement of this conduction time.

FIG. **14** is an exemplary plot **1400** of a conventional ECG waveform showing how a small error in the starting point of the P wave can cause a large error in all subsequent time measurements, in accordance with various embodiments. The starting point of P wave **1430** of conventional ECG waveform **1410** is somewhere on parallel equipotential line **1420**. Each square of the grid of plot **1400** represents a time of 40 milliseconds (ms). Parallel equipotential line **1420** spans about one square of the grid of plot **1400**. As a result, picking four different closely spaced points along parallel equipotential line **1420** produces starting point times that vary among 8 ms, 16 ms, 24 ms, and 32 ms within the one square of the grid of plot **1400**. In other words, small differences in the selection of the starting point of P wave **1430** can mean large differences in the timing values used

for P wave **1430**. It can also affect all of the other components of ECG waveform **1410**. This is because the starting point of P wave **1430** is also the starting point of the entire ECG waveform **1410**.

(2) At the PR interval, it has been difficult to identify the specific PA, AH, or HV intervals within PR interval. When the PR interval is abnormal, in particular, it can only be estimated and cannot be measured. Also, often the end of the PR interval cannot be confirmed, as there is no equipotential and the starting point of QRS wave appears to be an upward arc angle.

FIG. **15** is an exemplary plot **1500** of a conventional ECG waveform showing how the end of the PR interval cannot be confirmed due to an upward arc angle of the starting point of QRS wave, in accordance with various embodiments. The timing measurement of PR interval **1520** of conventional ECG waveform **1510** is a very important measurement since it is the only measurement for the atrium. As described above, it is difficult to measure the starting point of the P wave, which is also the start of PR interval **1520**. It turns out it is just as difficult if not more difficult to measure the ending point of PR interval **1520**. This is due to changes to parallel equipotential line **1530** at the ending point of PR interval **1520** as shown in plot **1500**. Parallel equipotential line **1530** is not parallel at all but rather is shaped like an upward arc angle. Therefore, it is very difficult to accurately map PR interval **1520**. The standard value for PR interval **1520** is 120-200 ms, for example. In contrast, PR segment **220** of ideal conventional ECG waveform of FIG. **2** has a parallel equipotential line just before a downward arc angle to the QRS wave.

(3) It has been difficult to identify a difference between the ST segment of a normal person and the ST segment of an abnormal person. In other words, the ST segment appears to be exactly abnormal for normal people and exactly normal for abnormal people. Also, and the J point often disappears, making it impossible to determine. As a result, the standards for the ST segment often cannot be applied.

FIG. **22** is an exemplary plot **2200** of a conventional ECG waveform showing how the ST segment of a normal person can appear abnormal, in accordance with various embodiments. Plot **2200** shows the conventional ECG waveform **2210** of a normal person. However, ST segment **2220** has lifted or arc shape. As a result, ST segment **2220** is difficult to measure. The normal morphological waveform is exactly like abnormal, while abnormal is exactly like normal.

(4) It has been difficult to identify the main peak of the T wave. Often it appears to be exactly abnormal (inverted) for normal people and exactly normal for abnormal people, making it almost impossible to determine.

FIG. **23** is an exemplary plot **2300** of a conventional ECG waveform showing how the T wave of an abnormal person can appear normal, in accordance with various embodiments. Plot **2300** shows the conventional ECG waveform **2310** of an abnormal person. However, the T wave **2320** appears normal.

(5) It has been difficult to identify which section of an autonomic conduction system is blocked.

FIG. **24** is an exemplary plot **2400** of a conventional ECG waveform showing how the section of an autonomic conduction system cannot be determined from a conduction block, in accordance with various embodiments. In plot **2400**, conduction in the PR interval **2420** of conventional ECG waveform **2410** is blocked. However, from conventional ECG waveform **2410** it is impossible to tell how the signal was conducted down through the conduction system.

(6) It has been difficult to identify the section of an autonomic conduction system that causes a QRS complex to widen or narrow.

FIG. **25** is an exemplary plot **2500** of a conventional ECG waveform showing how the QRS complex is widened in the waveform, in accordance with various embodiments. In plot **2500**, although QRS complex **2520** is widened in conventional ECG waveform **2510**, it is not possible to determine if this is caused by the atrium or the ventricle.

(7) It has been difficult to identify atrial anatomical positions, such as SA node, AV node, Bundle of His, and Purkinje's, from a conventional ECG waveform, as described above.

FIG. **26** is an exemplary plot **2600** of a conventional ECG waveform showing how the atrial anatomical positions are difficult to identify, in accordance with various embodiments. In plot **2600**, the entire PR interval **2620** of conventional ECG waveform **2610** is abnormal and cannot be measured. A calibration point cannot be mapped. For the patient in this case, the elevated ST segment also cannot be measured. Clinically, an elevated ST segment is also often measured for normal people.

(8) It has been difficult to identify when a premature ventricular beat occurs. It is almost impossible to determine the position of an ectopic premature beat, especially when the premature ventricular beat is accompanied with an aberrant conduction.

FIG. **27** is an exemplary plot **2700** of a conventional ECG waveform showing a premature ventricular beat, in accordance with various embodiments. In plot. In plot **2700**, conventional ECG waveform **2710** includes premature ventricular beat **2720**. When premature ventricular beat **2720** occurs, it is not possible to determine whether it is benign or malignant. Not all premature ventricular beats are malignant. In general, a conventional ECG waveform can only show that a premature ventricular beat or premature atrial contraction has occurred.

(9) It has been difficult to identify a malignant arrhythmia.

FIG. **28** is an exemplary plot **2800** of a conventional ECG waveform showing in atrial conduction block, in accordance with various embodiments. In plot **2800**, conventional ECG waveform **2810** includes conduction block **2820**. However, it is not possible to determine the specific block location of conduction block **2820**. The position can determine whether or not the block is malignant. For example, if it is below the His bundle, the block is malignant.

In summary, at an abnormal moment, signals of a conventional ECG waveform often shift positions, and the waveform is changed to a different shape, making it difficult or impossible to estimate. If a conventional ECG waveform is changed in such a way and human intelligence or experience is still relied on to diagnose, a large amount of accuracy is lost.

Automated ECG Analysis and Diagnosis using AI

As described above, additional systems are needed to further address the technical problems of analyzing the shape and form of the frequency domain signals of a conventional ECG waveform and distinguishing disease conditions from false positives in normal and abnormal populations using the conventional ECG waveform.

In various embodiments, these technical problems are addressed by 1. applying artificial intelligence (AI) algorithms to characterize the shape and form of the frequency domain signals of a conventional ECG waveform; 2. comparing the characterized shape and form of the frequency domain signals to a database of characterized signals from normal and abnormal populations using human like AI

algorithms and non-human like AI algorithms; and 3. annotating the conventional ECG waveform with diagnosis information based on the comparison.

FIG. 34 is an exemplary block diagram 3400 of a system for automated ECG analysis and diagnosis using AI, in accordance with various embodiments. In step 3401 of the system of FIG. 34, two or more electrodes are attached to the skin of a patient to obtain electrical signals from the heart muscle. In various alternative embodiments, the two or more electrodes may be attached directly and invasively to the heart muscle. The two or more electrodes are, for example, conventional ECG leads.

In step 3402, electrical heart signals are obtained from the two or more electrodes.

In step 3403, the electrical heart signals are detected and amplified.

In step 3404, the amplified signals are processed. For example, the signals from a number of different conventional ECG leads are combined.

In step 3405, the combined signals form a conventional ECG waveform.

In step 3406, the conventional ECG waveform is displayed or printed, for example.

In step 3410, the detected signals of step 3403 are obtained and processed to produce two or more frequency domain signals.

In step 3411, the two or more frequency domain signals are processed for characteristics of cardiac electrophysiological signals using one or more AI algorithms.

In step 3412, the cardiac electrophysiological characteristics of the two or more frequency domain signals are compared to databases of similar cardiac electrophysiological characteristics for normal and abnormal populations using the system of FIG. 34.

In step 3420, the cardiac electrophysiological characteristics of the two or more frequency domain signals are compared to the databases using human like AI algorithms. These human like AI algorithms can include, but are not limited to, an expert and cardiologist system 3421, an ECG diagnosis system 3422, an intelligent signals unsupervised feature learning system 3423, a general ECG problem solver 3424, and a semantic ECG waveform system 3425.

In step 3430, the cardiac electrophysiological characteristics of the two or more frequency domain signals are compared to the databases using non-human like AI algorithms. These human like AI algorithms can include, but are not limited to, a neural network algorithm 3431 and a deep learning algorithm 3432. The neural network algorithm 3431 can include a shallow network 3433. The deep learning algorithm 3432 can include a deep network 3434. This deep network 3434 can include, but is not limited to, a convolution all neural network (CNN) 3435, a deep belief net (DBN) 3436, or a restricted Boltzmann machine (RBM).

In step 3440, the results from steps 3420 and 3430 are combined to provide diagnosis information for the conventional ECG waveform.

In step 3406, this diagnosis information is displayed on the conventional ECG waveform.

The system of FIG. 34 provides a number of advantages over conventional automated analysis and diagnosis systems. First of all, it reduces medical and insurance expenses. As a result of the automated diagnosis information patients can avoid invasive and expensive examinations. Secondly, the quick and accurate diagnosis information allows prompt and accurate treatment. In other words, the shortened time for diagnosis allows treatment to occur without delay. Thirdly, the quick and accurate diagnosis helps train doctors

more efficiently and can significantly reduce misdiagnosis rates. Fourthly, the quick and accurate diagnosis information can help in the research and development of new target drugs for cardiac treatments. Finally, the use of these AI algorithms in ECG makes these instruments intelligent systems.

In various embodiments, the diagnosis information presented in step 3406 can include, but is not limited to, diagnosis markers or more accurate timing information.

Automated Diagnosis Markers and Timing Information

FIG. 35 is an exemplary plot 3500 of a conventional ECG waveform annotated with diagnosis marker information, in accordance with various embodiments. In plot 3500, conventional ECG waveform 3501 is annotated with five different diagnosis markers or prompts. Unfilled arrow marker 3510 represents a specific conduction block position. Unfilled diamond marker 3520 represents a hidden P wave. Unfilled triangle marker 3530 represents a premature ventricular beat position. Unfilled pentagon marker 3540 represents a position where a heartbeat is not conducted. Filled arrow marker 3550 represents a normal heartbeat.

FIG. 36 is an exemplary comparison 3600 of timing information from a conventional ECG waveform and from an ECG waveform produced and annotated using an automated analysis and diagnosis system, in accordance with various embodiments. Comparison 3600 includes timing information from conventional ECG waveform 3610 and timing information from ECG waveform 3620 produced and annotated using an automated analysis and diagnosis system.

Conventional ECG waveform 3610 measures first AH interval 3611 to be 102 ms and second AH interval 3612 to be 105 ms. In contrast, annotated ECG waveform 3620 measures first AH interval 3621 to be 105 ms and second AH interval 3622 to be 106 ms.

Similarly, conventional ECG waveform 3610 measures first HV interval 3613 to be 50 ms and second HV interval 3612 to be 47 ms. In contrast, annotated ECG waveform 3620 measures first HV interval 3623 to be 53 ms and second HV interval 3624 to be 49 ms.

Comparison 3600 shows that an automated analysis and diagnosis system can produce more accurate timing information than a conventional ECG system.

System for Identifying and Annotating Cardiac Electrophysiological Signals

The conventional ECG's P-QRS-T waveform records the normal atrial and ventricular muscles, which is composed of high frequency (HF), ultra high frequency (UHF), and super high frequency (SHF) signals. The heart is a micro-current organ. The atrium has two electrical channels, while the ventricle has multilayer channels. In conventional ECG systems the majority of the high frequency signals of the ECG waveform are convoluted with other signals. Besides the normal atrial muscle, there also exists a special conduction system. In addition to the normal Ventricular muscle, there are multilayer characteristic cellular groups. These specific signals are not accurately displayed in the conventional ECG P and T waves. This is the reason why the conventional ECG waveform has not evolved and has been difficult to change.

The reason why the conventional ECG waveform has not evolved is related to the developmental history of mathematics. Since its invention, ECG has only had an empirical formula, which is basically a guide, such as: III lead link is equal to II lead minus I lead. However, no mathematical formula proof for this formula exists. Galvani founded electrophysiology in 1791. Matteucci discovered heart elec-

trical activity in 1842. In 1898, Waller proposed the electrocardiogram dipole distribution theory, in 1912 recorded the electrical waveform by electrocardiogram, and named this sinusoidal line the P-QRS-T. A conventional ECG system scans and records this sinusoidal wave.

Harmonics and Discontinuities

Since as early as the 17th century, however, there has been a huge controversy in the scientific-mathematical world. In the academic world, an argument arose between Fourier and Lagrange, which focused on whether the sine wave curve contained minute, harmonic frequency signals. It wasn't until 1898 (ECG theory proposed the same year) that Nobel Prize winner Albert Abraham Michelson successfully developed the harmonic analyzer. Using this method, the American mathematical physicist Josiah Willard Gibbs confirmed that a sinusoidal wave can contain a harmonic image, which was later called the Gibbs phenomenon. The pioneers of the traditional ECG did not mean to discover this confirmation of a great theory of mathematics and, until this day, this discovery has not been taken seriously. Harmonics are cycles. The signal can be the sum of many sine waves because the frequency of the ECG sine wave is different, and there are harmonic (wavelet or subwaveforms) signals between and within the P-QRS-T waveforms. For more than a century, scientists have been studying the ECG waveform, ignoring basic signal processing (mathematics) and ignoring the fact that sine waves are convolutions of multitudes of discontinuities.

In various embodiments, a complete set of signal processing systems have been developed to measure these subwaveforms and discontinuities. For example, the visual EPCG waveform has been confirmed within the P-QRS-T waveform. It contains many small subwaveforms (harmonics). These are located in the conventional ECG waveform in front of the P wave, in the P wave itself, after the P wave, to the right and left side of the QRS, in the ST segment, in the T wave, and after the T wave, for example. In other words, it has been confirmed that the conventional ECG periodic signal is composed of the sum of its harmonics. ST Segment Harmonics and Discontinuity Points

Most recently and in various embodiments, new subwaveforms and discontinuity points have been discovered in relation to the ST segment. Exemplary ST segment 260 is shown in FIG. 2, for example. The ST segment is one of the least understood elements of a conventional ECG waveform.

FIG. 39 is an exemplary ECG waveform plot 3900 showing the relative positions of the PR and ST segments for a normal heartbeat, in accordance with various embodiments. In plot 3900, PR segment 3910 and ST segment 3920 have the same position vertically.

Conventionally, there is only one standard for accessing the ST segment: either elevation or descent.

FIG. 40 is an exemplary ECG waveform plot 4000 showing how the ST segment can shift vertically due to abnormal conditions, in accordance with various embodiments. In plot 4000, ST segment 4020 can elevate or descend vertically depending on the abnormal condition. This standard or rule can be referred to as STy.

According to the STy standard, one or more (mV) movements upward from the baseline x-axis (isoelectric line) equate to an elevation. Similarly, one or more mV movements downward from the baseline x-axis equate to descent or depression. The problem with this ST segment standard, is that 90% of normal data for healthy people usually shows an ST segment elevation. In addition, abnormal data for unhealthy people is usually not represented as a simple elevation or a descent.

FIG. 41 is an exemplary ECG waveform plot 4100 showing how the ST segment can be deformed due to abnormal conditions, in accordance with various embodiments. In plot 4100, ST segment 4120 can be deformed so that it forms a concavity or convexity vertically, for example.

FIG. 42 is an exemplary ECG waveform plot 4200 showing how the vertical or horizontal movement of the end of the RS segment can affect the ST segment due to abnormal conditions, in accordance with various embodiments. In plot 4200, the movement of end 4230 of RS segment removes the difference between the S point and J point of ST segment 4220, for example.

FIG. 43 is an exemplary ECG waveform plot 4300 showing how the ST segment can shift horizontally due to abnormal conditions, in accordance with various embodiments. In plot 4300, the length of ST segment 4320 can shorten or widen horizontally depending on the abnormal condition.

FIG. 44 is an exemplary ECG waveform plot 4400 showing how vertical or horizontal movement of the J point can affect the ST segment due to abnormal conditions, in accordance with various embodiments. In plot 4400, the movement of J point 4440 can change the length or slope of ST segment 4420, for example.

In various embodiments, new standards or rules are developed to assess the ST segment based on harmonic waveforms and points of discontinuity. These standards or rules are used in AI algorithms, for example.

In one embodiment, an STx standard is developed. A conventional ECG system cannot measure the sum of the ST segment and the T segment (x-axis time parameter). The STx standard measures the sum of the ST segment and the T segment. This sum is typically <380 ms. This STx standard is extremely important and can be compared to the borderlines between counties. It represents time value changes. The following are times changes which can occur. (1) The time value change may be >100 ms. (2) The time value change may be <40 ms. (3) The time value change may be =0 ms. (4) The ST-T segment may also be represented as a negative curve (lower than the isoelectric line). (5) These time changes are all based on relation to the x-axis.

In another embodiment, an STa standard is developed. The "a" relates to amplitude. (1) The top peak of the T wave may be lower than the P wave's top peak, or the two waves are equal. (2) The starting point of the P wave is greater than the isoelectric line. (3) T wave terminal point is greater than the isoelectric line. (4) The T wave's time value is less than P wave's time value (reversed). All of these changes will cause the ST segment to deform.

In another embodiment, an STs standard is developed. The "s" relates to the slope. This is only related to the terminal slope of the ST segment in relation to the initial slope of the T wave. The following are new pattern recognition rules. (1) This slope shrinks or shortens. (2) This slope is represented as the isoelectric line. (3) This slope is lower than the isoelectric line. (4) The ST slope is upside-down, but the T wave is normal. (5) This slope takes on an upward slope but looks convex instead of the traditional concave slope. (6) The ST segment slope completely disappears, and the T wave begins directly after the QRS segment (this happens very often). (7) The ST segment is completely horizontal with the isoelectric line; the two halves of the T wave are complete mirrors of each other in both angle and slope.

In another embodiment, an STj standard is developed. The "j" relates to the J-point. (1) The S point to the J-point

time is increased. (2) S-point and J-point disappear; there is almost a 90° angle between the RS end and ST segment start. (3) The S-point and J-point are concealed within the RS segment; the J-point is above the isoelectric line. (4) The J-point falls below the isoelectric point, concealed deep into RS.

FIG. 45 is an exemplary comparison 4500 of two ECG waveform plots exhibiting ST segment changes that can be identified using the STy standard, in accordance with various embodiments. In plot 4510, the ST segment is identified as elevating according to the STy standard. In plot 4520, the ST segment is identified as descending according to the STy standard.

FIG. 46 is an exemplary comparison 4600 of two ECG waveform plots exhibiting ST segment changes that can be identified using the STx standard, in accordance with various embodiments. In plot 4610, the ST segment is identified as widened according to the STx standard. In plot 4620, the ST segment is identified as shortened according to the STx standard.

FIG. 47 is an exemplary comparison 4700 of two ECG waveform plots exhibiting ST segment changes that can be identified using the STs and STy standards (STs+STy), in accordance with various embodiments. In plot 4710, the ST segment is identified as a down-sloping depression according to the STs and STy standards (STs+STy). In plot 4720, the ST segment is identified as an up-sloping depression according to the STs and STy standards (STs+STy).

FIG. 48 is an exemplary comparison 4800 of two ECG waveform plots exhibiting ST segment changes that can be identified using the STj, STy, and STx standards (STj+STy+STx), in accordance with various embodiments. In plot 4810, the ST segment is identified as a depression according to the STj, STy, and STx standards (STj+STy+STx). In plot 4820, the ST segment is identified as vanishing according to the STj, STy, and STx standards (STj+STy+STx) the STs and STy standards (STs+STy).

FIG. 49 is an exemplary ECG waveform plot 4900 of an ST segment change that can be identified using the STx and STj standards (STx+STj), in accordance with various embodiments. In plot 4900, the ST segment is identified as having a widened RJ interval according to the STx and STj standards (STx+STj).

Analysis and Diagnosis System

The systems of the '204 Patent and the '930 Patent have used different signal processing methods to detect the harmonic signals and discontinuity points of a conventional ECG waveform. In various embodiments, artificial intelligence (AI) in conjunction with a database of normal and abnormal ECG data is used to detect the harmonic signals and discontinuity points of a conventional ECG waveform and to annotate cardiac electrophysiological signals in the ECG waveform as normal or abnormal.

FIG. 37 is a block diagram 3700 of an ECG system for identifying and annotating cardiac electrophysiological signals in an ECG waveform as normal or abnormal during measurement of the ECG waveform, in accordance with various embodiments. Electrodes 3710 are attached to the skin of a patient in a noninvasive measurement, for example. In an alternative embodiment, electrodes 3710 are attached directly on the surface of a beating heart of a patient. Electrical signals produced by a beating heart are detected between pairs of electrodes 3710.

A voltage signal is detected between two electrodes 3710 by detector 3720. Detector 3720 also amplifies the voltage signal. Detector 3720 converts the electrical impulses to an ECG waveform for each heartbeat of the beating heart.

Detector 3720 converts the voltage signal to a digital voltage signal using an analog to digital converter (A/D), for example. Detector 3720 provides the detected and amplified voltage signal from each pair of electrodes 3710 directly to display device 3740 to display the ECG waveform. The ECG waveform includes conventional P, Q, R, S, T, U, and J waveforms, for example. Detector 3720 also provides the detected and amplified voltage signal from each pair of electrodes 3710 directly to processor 3730.

Processor 3730 can be a separate electronic device that can include, but is not limited to, an application specific integrated circuit (ASIC), a field programmable gate array (FPGA), or a general purpose processor or computer, such as the system of FIG. 1. Processor 3730 can be software implemented on another processor of the ECG device, such as a processor of display device 3740. Processor 3730 can also include a remote server computer.

Processor 3730 receives the ECG waveform for at least one heartbeat from detector 3720. Processor 3730 converts the ECG waveform to a frequency domain waveform. Processor 3730 separates the frequency domain waveform into two or more different frequency domain waveforms. Processor 3730 converts the two or more different frequency domain waveforms into a plurality of time domain cardiac electrophysiological subwaveforms and discontinuity points between these subwaveforms of the ECG waveform.

Processor 3730 compares the plurality of subwaveforms and discontinuity points to a database (not shown) of subwaveforms and discontinuity points for cardiac electrophysiological signals of ECG waveforms for a plurality of known and normal and abnormal patients. Processor 3730 identifies at least one subwaveform or one or more discontinuity points of the plurality of subwaveforms and discontinuity points as a normal or abnormal electrophysiological signal of the ECG waveform based on the comparison.

Display device 3740 is an electronic display device, a printer, or any combination of the two. Display device 3740 displays the ECG waveform for the at least one heartbeat of the beating heart. Display device 3740 also displays one or more markers at the location of the at least one subwaveform or the one or more discontinuity points on the ECG waveform and identifies the one or more markers as a normal or abnormal cardiac electrophysiological signal. For example, FIGS. 35 and 36 show how one or more markers are displayed on ECG waveforms to indicate normal or abnormal cardiac electrophysiological signals. The one or more markers can be identified as a normal or abnormal cardiac electrophysiological signal using symbols, colors, or text, for example.

In various embodiments, processor 3730 converts the ECG waveform to a frequency domain waveform, separates the frequency domain waveform into two or more different frequency domain waveforms, and converts the two or more different frequency domain waveforms into a plurality of time domain cardiac electrophysiological subwaveforms and discontinuity points using an artificial intelligence algorithm. The artificial intelligence algorithm includes a multivariable calculus algorithm, for example.

In various embodiments, processor 3730 compares the plurality of subwaveforms and discontinuity points to a database of subwaveforms and discontinuity points using a human like artificial intelligence algorithm.

In various embodiments, the human like artificial intelligence algorithm includes an expert and cardiologist system. This system evaluates the comparison based on morphological rules developed from cardiologists. In other words, the

shape differences are compared using rules based on pattern recognition and doctors' experiences.

In various embodiments, the human like artificial intelligence algorithm includes an ECG diagnosis system. This system evaluates the comparison based on morphological patterns and their correlation to specific diseases.

In various embodiments, the human like artificial intelligence algorithm includes an intelligent signals unsupervised feature learning system. This system evaluates the comparison based on morphological patterns learned over time by the system.

In various embodiments, the human like artificial intelligence algorithm includes a general ECG problem solver. This system evaluates the comparison based on one or more known conditions or conflicting conditions including, but not limited to, heart failure (HF), atrium fibrillation (AF), atrial conductor block, premature atrial contraction (PAC), premature ventricular contraction (PVC), atrial tachycardia, and ventricular tachycardia.

In various embodiments, the human like artificial intelligence algorithm includes a semantic ECG waveform system. This system evaluates the comparison based on additional signal processing rather than pattern recognition.

In various embodiments, processor **3730** compares the plurality of subwaveforms and discontinuity points to a database of subwaveforms and discontinuity points using a non-human like artificial intelligence algorithm.

In various embodiments, the human like artificial intelligence algorithm includes a neural network. The neural network can be a shallow network, for example.

In various embodiments, the human like artificial intelligence algorithm includes a deep learning algorithm. The deep learning algorithm can include a deep network, for example. The deep network can include, but is not limited to, convolution all neural network (CNN), a deep belief net (DBN), or a restricted Boltzmann machine (RBM). Method for Identifying and Annotating Cardiac Electrophysiological Signals

FIG. **38** is a flowchart showing a method **3800** for identifying and annotating cardiac electrophysiological signals in an ECG waveform as normal or abnormal during measurement of the ECG waveform, in accordance with various embodiments.

In step **3810** of method **3800**, electrical impulses are received from a beating heart using two or more electrodes.

In step **3820**, the electrical impulses are detected from at least one pair of electrodes of the two or more electrodes and converted to an ECG waveform for each heartbeat of the beating heart using a detector.

In step **3830**, the ECG waveform for at least one heartbeat is received from the detector, the ECG waveform is converted to a frequency domain waveform, the frequency domain waveform is separated into two or more different frequency domain waveforms, and the two or more different frequency domain waveforms are converted into a plurality of time domain cardiac electrophysiological subwaveforms and discontinuity points between these subwaveforms of the ECG waveform using a processor.

In step **3840**, the plurality of subwaveforms and discontinuity points are compared to a database of subwaveforms and discontinuity points for cardiac electrophysiological signals of ECG waveforms for a plurality of known and normal and abnormal patients using the processor.

In step **3850**, at least one subwaveform or one or more discontinuity points of the plurality of subwaveforms and discontinuity points are identified as a normal or abnormal

electrophysiological signal of the ECG waveform based on the comparison using the processor.

In step **3860**, the ECG waveform for the at least one heartbeat of the beating heart is displayed, one or more markers at a location of the at least one subwaveform or one or more discontinuity points is displayed on the ECG waveform, and the one or more markers are identified as a normal or abnormal cardiac electrophysiological signal using a display device.

I-Point and J-Point Detection and Measurement

As described above, ECG waveforms are prone to certain issues such as deformation, instability, standard point loss, and so on. Consequently, conventional ECG instruments are unable to accurately measure ECG parameters, such as the P-R interval, Q-T interval, ST segment, QRS complex, P-J interval, J-T interval, and VAT. Furthermore, as for the data measured manually, a very small variation can result in a difference of tens of milliseconds. Clinically, only simple standards can be used at present.

As described above, the ECG systems of the '204 Patent and the '930 Patent have addressed the technical problem of accurately measuring the different frequency domain signals from different parts of the heart muscle. Additional methods, however, are needed to employ the ECG systems of the '204 Patent and the '930 Patent to accurately measure ECG parameters such as the P-R interval, Q-T interval, ST segment, QRS complex, P-J interval, J-T interval, and VAT so that these standards can be used in clinical practice.

In various embodiments, systems and methods are provided to accurately detect the I-point, which is the point in an ECG waveform that demarks the location of the electrical connection between atrium and ventricle. These systems and methods are also able to accurately detect the J-point, which is the starting point for repolarization of the ventricle. From accurate I-point and the J-point measurements, other ECG parameters such as the P-R interval, Q-T interval, ST segment, QRS complex, P-J interval, J-T interval, and VAT are accurately measured. Also, new parameters are developed and measured.

FIG. **50** is an exemplary plot **5000** of an ECG waveform showing the accurate detection and measurement of the I-point and J-point, in accordance with various embodiments. In ECG waveform **5001**, I-point **5010** and J-point **5020** are accurately detected and measured. From accurate I-point **5010** and the J-point **5020** measurements, other ECG parameters such as P-R interval **5011**, Q-T interval **5012**, ST segment **5021**, QRS complex **5013**, P-J interval **5022**, J-T interval **5023**, and ventricular activation (VAT) segment **5014** are accurately measured. I-point **5010** measurement is important to the following parameters: Q-T interval **5012**, QRS complex **5013**, VAT segment **5014**, P-R interval **5011**, and PR segment **5015**. J-point **5020** measurement is important to the following parameters: ST segment **5021**, P-J interval **5022**, J-T interval **5023**, and QRS complex **5013**.

It is noted that the detection of the J-point and the I-point in most of the waveforms of traditional ECG are in an arc shape, from which it is hard to identify an accurate measurement point. As a result, even if a measurement itself is accurate, the result still cannot be utilized in clinical practice.

FIG. **51** is a series of plots **5100** of conventional ECG waveforms from different ECG leads showing that the J-point can only be detected from one lead, in accordance with various embodiments. For example, J-point **5110** is detected from lead V_4 . However, as shown in FIG. **51**, although J-point **5110** can be detected, it is not possible to accurately measure it even in lead V_4 .

FIG. 52 is a series of plots 5200 of conventional ECG waveforms from different ECG leads showing that difficulty in measuring the I-point and the J-point, in accordance with various embodiments. For example, it is not possible to even detect I-point 5210 and J-point 5220 in leads I, II, III, aVR, aVL, aVF, V₁, V₂, and V₃. In leads V₄, V₅, and V₆, I-point 5210 can be detected but J-point 5220 cannot. Further, in these last three leads, although I-point 5210 can be detected, it is not possible to accurately measure it.

FIGS. 51 and 52 illustrate the biggest problem in the ECG field, namely inaccuracy. For example, the ST segment is still used in practice. It is a standard used for determining myocardial ischemia and myocardial infarction.

FIG. 53 is a plot 5300 of an ideal ECG waveform showing the importance of the I-point to the PR segment and the importance of the J-point to the ST segment, in accordance with various embodiments. For example, I-point 5310 is the ending point of PR segment 5315. Similarly, J-point 5320 is the starting point of ST segment 5325.

However, it is noted that in many patients, their ST segments do not show any elevation or depression, or show a slant line, or absence of the J point, and the like, which makes the ST segment unmeasurable.

FIG. 54 is a series of plots 5400 of abnormal ECG waveforms showing the difficulty in determining the J-point and, therefore, the ST segment, in accordance with various embodiments. Plots 5410, 5420, 5430, and 5440 all exhibit abnormal heart conditions. J-point 5401 is difficult to determine, making the ST segment unmeasurable.

Also, in many normal people, there may also be an elevation in the ST segment. In other words, in traditional ECG, normal results can be very similar to an abnormal condition; while in some cases, the measurement results of people with the condition are so close to that of a normal person; or sometimes, the ST segment cannot be measured, or the obtained measurement result is useless in a determination.

FIG. 55 is a series of plots 5500 of normal ECG waveforms showing the difficulty in determining the J-point and, therefore, the ST segment, in accordance with various embodiments. Plots 5510, 5520, and 5530 all exhibit normal heart conditions. J-point 5501, however, is still difficult to determine, making the ST segment unmeasurable.

As a result, the clinical practice has been confused by the correlation between the traditional ECG and disease and the validity of a determination based thereon. There are some digitalized standards, but they either cannot be measured, or the measurement cannot be applied in clinical practice, and it becomes even more complex when the image is deformed. For example, there are ST segment elevations in both abnormal patients and normal people. In various embodiments, by way of I-point extension, even if the J-point is lost, it is possible the J-point position can still be determined. As a result, even in the case in which the J-point is lost, certain detection points for determination and analysis can still be acquired.

Since the invention of traditional ECG in 1903, on the left and right sides of the QRS there are always two semicircular sinusoidal waves, which are referred to as the P wave and T wave. There is a pulse wave, which is referred to as QRS wave group. Also, there is a half sinusoidal wave after the T wave, which is referred to as the U wave. It is noted that the foregoing waves are named in an alphabetic order based on the order of their appearances; for each heartbeat, the waves repeatedly appear in the following P→QRS→T→U.

As for J-point, it is the starting point of ST segment intersection from the ending point of ventricular depolar-

ization to the starting point of ventricular repolarization. This intersection point is the beginning of ST segment, which is critical for determining the elevation or depression of the ST segment. In this regard, it is reasonable to first determine and establish the J-point. However, it is noted that the J point may be completely lost in many people with abnormal conditions, as shown in FIGS. 51 and 54. On the other hand, it is also lost in many normal people, as shown in FIG. 55. Accordingly, it is the weakest part in the traditional ECG.

The cardiac conduction system is the control center for cardiac electrical activity and an important portion for impulse conduction. Its special tissue structure and cell type determine that its cardiac electrical pacing and conduction functions are different from normal myocardia. In addition, it is closely related to the initiation and development of a variety types of arrhythmia. In this regard, it is important and necessary to study the cardiac conduction system.

It is noted that the traditional ECG signal acquisition range is from 0 to 150 Hz; and about 95% of the image signal convolution is actually ordinary atrial and ventricular myoelectric signals. Accordingly, many delicate electrical signals have been buried under those high frequency and ultra-high frequency signals. As a result, the I-point and J-point in most traditional ECG are not clearly shown, which causes the problem that certain standard digital parameters cannot be applied clinically.

Therefore, currently, the field lacks a digitalized uniform standard to verify whether a determination based on morphological waveforms is correct. It frequently occurs that for the same ECG image, different people can get different determination results, or a lot of different determinations can be derived therefrom.

Concerning the relationship between the positions of I-point and J-point in each heartbeat, it is noted that these two detection points are the most important determination points for QRS complex. The points Q and S of QRS interval in an accurate image should show sharp angles. In addition, on each of the left and right sides of QS, there is a reverse line reaching a parallel axis of the X axis. And, after the end of P wave, there is an equipotential line parallel to the X axis. The intersection of the distance between the ending point of the equipotential line and the q' point is the I-point. It has the following features: the line between the I-point and point q' is in a direction downward from the X axis. Moreover, there is another equipotential line parallel to the X axis before the starting point of the T wave, the intersection of the distance between the starting point of the equipotential line and the point s' is the J-point. It has the following features: the line between point s' and J-point is in a direction upward towards the X axis. The relationship between the positions of I-point and J-point in each heartbeat is illustrated in FIG. 53, for example.

Referring to FIG. 53, I-point 5310 is the starting point of the QRS complex, and at the same time, I-point 5310 is also the ending point of PR segment 5315 and P-R interval, that is to say, the starting point of the Q-T interval and the VAT segment. J-point 5320 is located at the intersection of equipotential line 5330 after the QRS interval and the starting point of ST segment 5325.

J-point 5320 is also the starting point of ST segment 5325 and the ending point of the QRS complex. It is the same in both the atrium and ventricle that the starting point P wave is the starting point of each heartbeat, and after P wave there is an equipotential line 5330. The portion from the ending point of P wave to I-point 5310 is referred to as PR segment 5315. The portion from the starting point of P wave to the

ending point of PR segment **5315** (I-point **5310**) is referred to as the PR interval. They have extraordinary significance in cardiac physiology and pathology.

In most of the traditional ECGs, a signal loss causes an arc-shaped portion. In a traditional ECG, the clear position of the I-point and J-point are rarely determined, as shown in FIGS. **51**, **52**, **54**, and **55**. The accuracy of most of the traditional ECGs is not high enough and cannot be measured. However, to provide a gold standard for ECG, these points cannot be ignored. In particular, because the I-point is the entrance of the connection between the atrium and the ventricle, it is critically important.

In various embodiments, the I-point is considered in the atrium, while the J-point is in the ventricle. It is noted that the process of a heartbeat is in the order from the atrium to the ventricle, and in the alphabetic order, the letter before J is I. Accordingly, the atrium point is named as I-point. Also, most normal people have this point. In many people, especially with abnormal conditions, the J-point is not detectable.

In various embodiments, 50,000 normal subjects were selected in normal physical examinations, and ECG waveforms were found using the systems of the present application. 95% of the normal people were found to have an I-point, and 89% of the normal people were found to have a J-point.

FIG. **56** is a plot **5600** showing an ECG waveform for a normal subject using the systems of the present application, in accordance with various embodiments. In ECG waveform **5601** for the normal subject, an I-point **5610** and a J-point **5620** were detected and measured. Note that the high-precision ECG instrument of various embodiments has a sampling rate of 50,000/s.

The I-point has a very important physiological significance and clinical application value. From the point of view of anatomy, it is the connection portion between the ends of left and right bundles and the starting point of the Purkinje's fibrous network. After the I-point, there is the Purkinje's network, while before the J-point, it is the ending portion of the Purkinje's fibrous network. It is noted that the I-point and the J-point are a pair of key points that should be presented at the same time.

The I-point is the starting point of Purkinje's, and the starting point of an instantaneous vector. Hence, it is the only way from Purkinje's fibrous network 360° towards the entire endocardial wall of the heart. On the other hand, the J-point is located in the connection portion from the ending point of Purkinje's network to the starting point of ST segment. Hence, it is the only way from Purkinje's fibrous network towards the depth of endocardium.

In various embodiments, once the I-point is accurately positioned, new I-point related parameters are detected and measured. Referring to FIG. **56**, these new parameters include I-T interval **5611**, I-J interval **5612**, J-Tp interval **5613**, Tp-Te **5614**, I-Q segment **5615**, S-J segment **5616**, I-qR interval **5617**, and Rs-J interval **5618**.

I-J interval **5612** extends from the starting point of the QRS wave group to J-point **5620**, with 0-1 phase. Ventricular depolarization QR ascending branch reaches ventricular septal and apical parts, while the RS descending branch reaches the front part of the ventricular wall.

FIG. **57** is a series of plots **5700** of an ECG waveform showing depolarization of the ventricular septal and apical parts and the ventricular wall, in accordance with various embodiments. Plot **5710** depicts depolarization of the ventricular septal and apical parts. Plot **5720** depicts depolarization of the ventricular wall.

Returning to FIG. **56**, J-Tp interval **5613** depicts repolarization of the ventricular. J-Tp interval **5613** extends from J-point **5620** to the highest peak of the T wave. It has 2 phases, from ventricular repolarization to the front and middle portions of the ventricular wall.

Tp-Te **5614** extends from the highest peak of T wave to the end of T wave. It has 3 phases, from ventricular repolarization to the posterior part of the ventricular wall.

The entire I-T interval **5611** is equal to that of Q-T interval. However, I-T interval **5611** is able to distinguish various stages of ventricular contraction. I-J interval **5612** is the early stage of ventricular contraction. J-Tp interval **5613** is the mid-stage of ventricular contraction. Tp-Te **5614** is the late stage of ventricular contraction. As a result, within the entire I-T interval **5611**, data analysis is carried out; and according to the specific anatomical location, certain important analysis and determination on local cardiac information can be conducted, especially for the atrioventricular junctions.

Referring to FIG. **50**, T-Ua interval **5030** represents ventricular myocyte M cell APD and partial Purkinje's cell repolarization.

Returning to FIG. **56**, I-Q segment **5615** is at the junction of the left and right bundles and the starting point of the Purkinje's. S-J segment **5616** is at the junction of the Purkinje's end and the endocardium. Hence the foregoing two data are very important. Their locations are equivalent to the intersections of complex highways. It is noted that the traditional ECG cannot detect this pair of data, because the images of the I-point and J-point are unclear, and most of the waveforms are shown as arcs. As a result, this pair of data cannot be detected. Therefore, their measurement requires an ECG instrument with very, very high precision.

I-qR interval **5617** is equivalent to the I-Q segment plus the VAT segment, yet I-qR interval has a correction formula. It is able to distinguish between left and right ventricles, so different data can be obtained from left and right ventricles. The VAT segment extends from the peak of the Q wave to the peak of the R wave.

The data for Rs-J interval **5618** interval is very complex, and accordingly, its normal value needs to be further studied in the clinical.

These new parameters have critical functions in clinical applications. They are the parameters concerning the connection part between atrium and ventricle and specific locations in ventricle. They not only can detect the starting and ending parts of the Purkinje's, but also can identify and diagnose the cause of certain primary and secondary diseases, in other word, whether the disease is caused by a primary lesion in atrium or a primary lesion in ventricle. In particular, for many coronary artery disease (CAD), myocardial infarction (MI) or CAD/MI patients, their traditional ECG result show no change in ST-T, this technique can show abnormal changes in atrial parts.

It is even more important for patients with Non-ST-elevation myocardial infarction (NSTEMI), or patients with non-coronary artery stenosis diffusive small blood vessel obstruction ischemia, hypertrophic cardiomyopathy, and heart failure disease, etc. In the case when a traditional ECG detection image does not show any change, both the established standard parameters and the new parameters and new detection points disclosed in the present application can be detected, which will bring in novel, effective, and convenient applications to clinical practice.

Normal ventricular activation (VAT) is a complex process that is dependent on interactions between the physiology and

anatomy of both the specialized ventricular conducting system and the ventricular myocardium.

VAT is the product of two temporally overlapping events—endocardial activation and transmural activation. Endocardial activation is guided by the anatomic distribution and physiology of the His-Purkinje system. The broadly dispersed ramifications of this treelike (fractal) system and the rapid conduction within it result in the near-simultaneous activation of multiple endocardial sites and the depolarization of most of the endocardial surfaces of both ventricles within several milliseconds. The sequence of ventricular endocardial activation is dependent upon the fanlike distribution of the left bundle branch system across the endocardium.

Earliest activity begins in three sites: (1) the anterior paraseptal wall of the left ventricle, (2) the posterior paraseptal wall of the left ventricle, and (3) the center of the left side of the septum. These loci correspond to the sites of insertion of the fascicles of the left bundle branch. Septal activation begins on the left side and spreads across the septum from left to right and from apex to base. Wave fronts sweep from these initial sites of activation in anterior and inferior and then superior directions to activate the anterior and lateral walls of the left ventricle. The posterobasal areas of the left ventricle are the last to be activated.

Excitation of the right ventricle begins near the insertion point of the right bundle branch near the base of the anterior papillary muscle and spreads to the free wall. The final areas to be activated are the pulmonary conus and the posterobasal areas. Thus, in both ventricles, the overall endocardial excitation pattern begins on septal surfaces and sweeps down toward the apex and then around the free walls to the posterior and basal regions in an apex-to-base direction. The activation fronts then move from endocardium to epicardium. Excitation of the endocardium begins at sites of Purkinje—ventricular muscle junctions and proceeds by muscle cell to muscle cell conduction in an oblique direction toward the epicardium.

Normal QRS Complex

The sequence of endocardial and transmural activation results in the characteristic waveforms of the QRS complex. QRS patterns are described by the sequence of waves constituting the complex. An initial negative deflection is called the Q wave, the first positive wave is the R wave, and the first negative wave after a positive wave is the S wave. A second upright wave following an S wave is an R' as in R' wave. Tall waves are denoted by uppercase letters and smaller ones by lowercase letters. A monophasic negative complex is referred to as a QS complex. Thus, for example, the overall QRS complex may be described as qRS if it consists of an initial small negative wave (the q wave) followed by a tall upright one (the R wave) and a deep negative one (an S wave). In an RSr' complex, initial tall R and S waves are followed by a small positive wave (the r' wave). In each case, the deflection must cross the baseline to be designated a discrete wave; changes in waveform direction that do not cross the baseline result in notches. Early QRS Patterns.

The complex pattern of activation described earlier can be simplified into two vectors, the first representing septal activation and the second representing left ventricular free wall activation. Initial activation of the interventricular septum corresponds to a vector oriented from left to right in the frontal plane and anteriorly in the horizontal plane, corresponding to the anatomic position of the septum within the chest. This vector produces an initial positive wave in leads with axes directed to the right (lead aVR) or anteriorly

(lead V1). Leads with axes directed to the left (leads I, aVL, V5, and V6) will register initial negative waves known as septal q waves. These initial forces are normally of low amplitude and are brief (less than 30 milliseconds in duration). The absence of these septal q waves, with QS complexes evident in the right precordial leads or seen as initial R waves in leads I, V5, and V6, typically is a normal variant and not associated with any cardiac disease.

Mid- and Late QRS Patterns

Subsequent parts of the QRS complex reflect activation of the free walls of the left and right ventricles. Because right ventricular muscle mass is considerably smaller than that of the left ventricle, it contributes little to normal QRS complexes. Thus the normal QRS can be considered to represent only septal and left ventricular activity, with little meaningful oversimplification. The complex interrelationships among cardiac position, conduction system function, and ventricular geometry result in a wide range of normal QRS patterns in the limb leads. The QRS pattern in leads II, III, and aVF may be predominantly upright with qR complexes, or these leads may show rS or RS patterns. Lead I may record an isoelectric RS pattern or a predominantly upright qR pattern.

The wide range of QRS patterns, especially in the inferior leads, can be interpreted by referring to the hexaxial reference system. The normal mean QRS axis in adults lies between -30 degrees and $+90$ degrees. If the mean axis is near 90 degrees, the QRS complex in leads II, III, and aVF will be predominantly upright, with qR complexes; lead I will record an isoelectric RS pattern because the heart vector lies perpendicular to the lead axis. If the mean axis is near 0 degrees, the patterns will be reversed; leads I and aVL will register predominantly upright qR pattern, and leads II, III, and aVF will show rS or RS patterns.

Mean QRS axes more positive than $+90$ degrees (usually with an rS pattern in lead I) represent right axis deviation. Axes between $+90$ and $+120$ degrees are referred to as moderate and those between $+120$ and $+180$ degrees are referred to as marked right axis deviation. Axes more negative than -30 degrees (with an rS pattern in lead II) represent left axis deviation, with axes between -30 and -45 degrees called moderate and those between -45 and -90 degrees called marked left axis deviation. Mean QRS axes of approximately -80 to -90 degrees are sometimes referred to as superior axis deviation and have been reported in cases of severe chronic obstructive lung disease.

Mean axes lying between -90 degrees and -180 degrees (or, equivalently, between $+180$ degrees and $+270$ degrees) are referred to as extreme axis deviations or, alternatively, as right superior axis deviations. The term indeterminate axis is applied when all six extremity leads show biphasic (QR or RS) patterns, indicating a mean axis that is perpendicular to the frontal plane. This finding can occur as a normal variant or may be seen in a variety of pathologic conditions. Normal QRS patterns in the precordial leads follow an orderly progression from right (V1) to left (V6).

In leads V1 and V2, leftward and posterior activation of the left ventricular free wall generates S waves following the initial r waves generated by septal activation (an rS pattern). These S waves are produced by the spread of activation in the free wall to the left and posteriorly, with generation of a heart vector directed away from the axes of these leads. Patterns in the midprecordial leads V3 and V4 reflect the activation front in the ventricular free wall. It first approaches the exploring electrode and then moves leftward and posteriorly to more remote regions of the left ventricle and away from the exploring electrode. In leads V3 and V4,

this generates an R or r wave as it moves toward the electrode, followed by an S wave as it moves away from the electrode to produce rS or RS complexes.

As the exploring electrode moves laterally to the left, the R wave becomes more dominant and the S wave becomes smaller (or is totally lost) because of the longer time period during which the activation front moves toward the positive end of the electrode. In the leftmost leads (i.e., leads V5 and V6), the normal pattern also includes the septal q wave, to produce a qR or qRs pattern. Thus, in the precordial leads, the QRS complex usually is characterized by a consistent progression from an rS complex in the right precordial leads to an RS pattern in the midprecordial leads, and to a qR pattern in the left precordial leads. The site at which the pattern changes from an rS to an Rs configuration—the lead in which an isoelectric RS pattern is present—is known as the transition zone and normally occurs in lead V3 or V4. An altered location of the transition zone may occur for a variety of reasons; transition zones that are shifted to the right to lead V2 are early transitions, and those that are shifted leftward to V5 or V6 are delayed transitions.

Normal variability in QRS amplitudes, axes, and duration QRS are related to demographic and physiologic factors. QRS amplitudes are greater in men than in women, with higher amplitudes in African Americans than in those of other races. In addition, the location of the mitral papillary muscles in relation to the septum affects the duration and frontal plane axis, and left ventricular mass (within the normal range) affects both QRS amplitude and duration. Higher-than-normal amplitudes are characteristic of chamber hypertrophy and conduction defects, as discussed later on. Low-amplitude QRS complexes—that is, complexes with overall amplitudes of less than 0.5 mV in all frontal plane leads and less than 1.0 mV in the precordial leads—may occur as a normal variant or as a result of cardiac (e.g., multiple infarctions, infiltrative cardiomyopathies, myocarditis) or extracardiac (e.g., pericardial effusion, chronic obstructive pulmonary disease, pneumothorax) conditions.

QRS Duration

The upper normal value for QRS duration traditionally is set at less than 120 milliseconds (and often at less than 110 milliseconds), measured in the lead with the widest QRS complex. Women, on average, have somewhat shorter QRS durations than men (by approximately 5 to 8 milliseconds).

The Intrinsicoid Deflection.

An additional feature of the QRS complex is the intrinsicoid deflection. An electrode overlying the ventricular free wall will record a rising R wave as transmural activation proceeds toward it. Once the activation front reaches the epicardium, the full thickness of the wall under the electrode will be in an active state. At that moment, the electrode will register negative potentials as activation proceeds in remote cardiac areas. The sudden reversal of potential produces a sharp downslope—the intrinsicoid deflection—that approximates the timing of activation of the epicardium under the electrode. The term ventricular activation time (VAT) is sometimes used with reference to the surface ECG.

The foregoing disclosure of the preferred embodiments of the present invention has been presented for purposes of illustration and description. It is not intended to be exhaustive or to limit the invention to the precise forms disclosed. Many variations and modifications of the embodiments described herein will be apparent to one of ordinary skill in the art in light of the above disclosure. The scope of the invention is to be defined only by the claims appended hereto, and by their equivalents.

I-Point Detection and Measurement System

The systems of the '204 Patent and the '930 Patent have used different signal processing methods to detect the harmonic signals and discontinuity points of a conventional ECG waveform. In various embodiments, artificial intelligence (AI) in conjunction with a database of normal and abnormal ECG data is used to measure and annotate the I-point of an ECG waveform during measurement of the ECG waveform. This system is referred to as an aiECG system or a system for performing aiECG, for example.

Returning to FIG. 37, electrodes 3710 are attached to the skin of a patient in a noninvasive measurement, for example. In an alternative embodiment, electrodes 3710 are attached directly on the surface of a beating heart of a patient. Electrical signals produced by a beating heart are detected between pairs of electrodes 3710.

A voltage signal is detected between two electrodes 3710 by detector 3720. Detector 3720 also amplifies the voltage signal. Detector 3720 converts the electrical impulses to an ECG waveform for each heartbeat of the beating heart. Detector 3720 converts the voltage signal to a digital voltage signal using an analog to digital converter (A/D), for example. Detector 3720 provides the detected and amplified voltage signal from each pair of electrodes 3710 directly to display device 3740 to display the ECG waveform. The ECG waveform includes conventional P, Q, R, S, T, U, and J waveforms, for example. Detector 3720 also provides the detected and amplified voltage signal from each pair of electrodes 3710 directly to processor 3730.

Processor 3730 can be a separate electronic device that can include, but is not limited to, an application specific integrated circuit (ASIC), a field programmable gate array (FPGA), or a general-purpose processor or computer, such as the system of FIG. 1. Processor 3730 can be software implemented on another processor of the ECG device, such as a processor of display device 3740. Processor 3730 can also include a remote server computer.

Processor 3730 receives the ECG waveform for at least one heartbeat from detector 3720. Processor 3730 converts the ECG waveform to a frequency domain waveform. Processor 3730 separates the frequency domain waveform into two or more different frequency domain waveforms. Processor 3730 converts the two or more different frequency domain waveforms into a plurality of time domain cardiac electrophysiological subwaveforms and discontinuity points between these subwaveforms of the ECG waveform.

Processor 3730 compares the plurality of subwaveforms and discontinuity points to a database (not shown) of subwaveforms and discontinuity points for cardiac electrophysiological signals of ECG waveforms for a plurality of known and normal and abnormal patients. Processor 3730 identifies a discontinuity point of the plurality of subwaveforms and discontinuity points as an I-point of the ECG waveform based on the comparison.

Display device 3740 is an electronic display device, a printer, or any combination of the two. Display device 3740 displays the ECG waveform for the at least one heartbeat of the beating heart. Display device 3740 also displays a marker at a location of the discontinuity point on the ECG waveform and identifies the marker as the I-point.

In various embodiments, processor 3730 further identifies a second discontinuity point of the plurality of subwaveforms and discontinuity points as a J-point of the ECG waveform based on the comparison. Display device 3740 further displays a second marker at a location of the second discontinuity point on the ECG waveform and identifies the second marker as the J-point.

In various embodiments, display device **3740** further displays a marker between the first marker and the second marker on the ECG waveform and identifies the marker as the I-J interval.

In various embodiments, processor **3730** further identifies a third discontinuity point of the plurality of subwaveforms and discontinuity points as an endpoint of a T wave (Te) of the ECG waveform based on the comparison. Display device **3740** further displays a third marker at a location of the third discontinuity point on the ECG waveform and identifies the third marker as the endpoint of a T wave (Te).

In various embodiments, display device **3740** further displays a marker between the first marker and the third marker on the ECG waveform and identifies the marker as the I-T interval.

In various embodiments, processor **3730** further identifies a fourth discontinuity point of the plurality of subwaveforms and discontinuity points as a peak of a T wave (Tp) of the ECG waveform based on the comparison. Display device **3740** further displays a fourth marker at a location of the fourth discontinuity point on the ECG waveform and identifies the fourth marker as the peak of a T wave (Tp).

In various embodiments, display device **3740** further displays a marker between the second marker and the fourth marker on the ECG waveform and identifies the marker as the J-Tp interval.

In various embodiments, display device **3740** further displays a marker between the fourth marker and the third marker on the ECG waveform and identifies the marker as the Tp-Te interval.

In various embodiments, processor **3730** further identifies a fifth discontinuity point of the plurality of subwaveforms and discontinuity points as a start point of a T wave (Ts) of the ECG waveform based on the comparison. Display device **3740** further displays a fifth marker at a location of the fifth discontinuity point on the ECG waveform and identifies the fifth marker as the start point of a T wave (Ts).

In various embodiments, display device **3740** further displays a marker between the second marker and the fifth marker on the ECG waveform and identifies the marker as the S-T segment.

In various embodiments, display device **3740** further displays a marker between the second marker and the third marker on the ECG waveform and identifies the marker as the S-T interval.

In various embodiments, processor **3730** further identifies a third discontinuity point of the plurality of subwaveforms and discontinuity points as a peak of a Q wave (Q) of the ECG waveform based on the comparison. Display device **3740** further displays a third marker at a location of the third discontinuity point on the ECG waveform and identifies the third marker as the peak of a Q wave (Q).

In various embodiments, display device **3740** further displays a marker between the first marker and the third marker on the ECG waveform and identifies the marker as the I-Q segment.

In various embodiments, processor **3730** further identifies a fourth discontinuity point of the plurality of subwaveforms and discontinuity points as a peak of a R wave (R) of the ECG waveform based on the comparison. Display device **3740** further displays a fourth marker at a location of the fourth discontinuity point on the ECG waveform and identifies the fourth marker as the peak of a R wave (R).

In various embodiments, display device **3740** further displays a marker between the first marker and the fourth marker on the ECG waveform and identifies the marker as the I-qR interval.

In various embodiments, display device **3740** further displays a marker between the fourth marker and the second marker on the ECG waveform and identifies the marker as the Rs-J interval.

In various embodiments, processor **3730** further identifies a fifth discontinuity point of the plurality of subwaveforms and discontinuity points as a peak of an S wave (S) of the ECG waveform based on the comparison. Display device **3740** further displays a fifth marker at a location of the fifth discontinuity point on the ECG waveform and identifies the fifth marker as the peak of an S wave (S).

In various embodiments, display device **3740** further displays a marker between the fifth marker and the second marker on the ECG waveform and identifies the marker as the S-J segment.

Method for Measuring and Annotating the I-point

FIG. **58** is a flowchart showing a method **5800** for measuring and annotating the I-point of an ECG waveform during measurement of the ECG waveform, in accordance with various embodiments.

In step **5810** of method **5800**, electrical impulses are received from a beating heart using two or more electrodes.

In step **5820**, the electrical impulses are detected from at least one pair of electrodes of the two or more electrodes and converted to an ECG waveform for each heartbeat of the beating heart using a detector.

In step **5830**, the ECG waveform for at least one heartbeat is received from the detector, the ECG waveform is converted to a frequency domain waveform, the frequency domain waveform is separated into two or more different frequency domain waveforms, and the two or more different frequency domain waveforms are converted into a plurality of time domain cardiac electrophysiological subwaveforms and discontinuity points between these subwaveforms of the ECG waveform using a processor.

In step **5840**, the plurality of subwaveforms and discontinuity points are compared to a database of subwaveforms and discontinuity points for cardiac electrophysiological signals of ECG waveforms for a plurality of known and normal and abnormal patients using the processor.

In step **5850**, a discontinuity point of the plurality of subwaveforms and discontinuity points is identified as an I-point of the ECG waveform based on the comparison using the processor.

In step **5860**, the ECG waveform for the at least one heartbeat of the beating heart is displayed, a marker at a location of the discontinuity point is displayed on the ECG waveform, and the marker is identified as the I-point using a display device.

ECG Quantitative Parameters

As described above, the electrophysiological signal separation of specific time periods of cardiac self-conduction system within the P wave, the QRS complex and the T wave was not previously possible. As a result, only qualitative information was provided by conventional ECG.

Consequently, systems and methods are needed to add quantitative scientific indicators to ECG. Such systems and methods are needed to allow doctors to understand and utilize the knowledge saved in traditional ECG, as well as to reduce learning difficulties, reduce guesses in case diagnosis, reduce misjudgment rate, and improve reliability, diagnosis rate and accuracy, whenever waveform character changes.

In various embodiments, using the systems and methods described above, one or more quantitative cardiac electrical markers within the half sinusoidal wave of the P wave and the T wave are found. Specifically, the time course of the P

wave and time course of the T wave are divided to form cardiac electrical signal segments of different anatomical locations of the heart. For example, the time course of the P wave is divided into an action potential duration (APD) for the sino atrial node (SAN), an APD for the atrioventricular node (AVN), and an APD for the His bundle (HIS).

In various embodiments, the time course of the T wave is divided into an APD for the ST segment and an APD for the T segment. Recall, that the T wave represents the repolarization of the ventricles.

In various embodiments, the time course of the QRS complex is also subdivided. For example, an APD for the Purkinje's fibrous network in the Q wave is measured and an APD for the Purkinje's fibrous network in the S wave is measured.

FIG. 59 is an exemplary plot 5900 showing action potential duration (APD) subdivisions within the P wave, the T wave, and the QRS complex of an aiECG waveform for a normal heart, in accordance with various embodiments. The P wave is subdivided into APD 5910 for the SAN, APD 5920 for the AVN, and APD 5930 for the HIS. The T wave is subdivided into APD 5940 for the ST segment and APD 5950 the T segment. In the QRS complex, the Q wave is subdivided to include APD 5960 for the Purkinje's fibrous network and the S wave is subdivided to include APD 5970 for the Purkinje's fibrous network.

The APD subdivisions in plot 5900 can be distinguished using color. For example, APD 5910, APD 5920, APD 5930, APD 5940, APD 5950, APD 5960, and APD 5970 are shown in red, blue, yellow, pink, brown, purple, and purple, respectively. In other words, the red-colored starting point is the APD starting point of SAN; the blue-colored starting point is the APD starting point of AVN; the yellow-colored starting point is the APD starting point of the His bundle; the purple-colored starting point is the APD starting point of Purkinje's; in addition, after the QRS ending point, the purple-colored ending point is the APD ending point of Purkinje's; the pink-colored starting point is the APD starting point of the J-point, and the starting point of the ST segment; and the brown-colored starting point is the APD starting point of the T segment.

In various embodiments, for each heartbeat, one or more APD measurements are shown in a table. For example, table 5980 shows the measured heart rate (HR), PR interval, RR interval, QRS complex interval, ST interval, QT interval, and PJ interval.

In various embodiments, for a series of heartbeats, one or more APD measurements are shown in another table. This table includes, for example, a first column showing the name of the parameter, a second column showing the range of the standard data, and a third column showing the average data of the test.

FIG. 60 is an exemplary table 6000 showing APD measurement data for a series of heartbeats for a normal heart, in accordance with various embodiments. Table 6000 includes section 6010 that includes APD measurements, and section 6020 that includes a key relating some of the anatomical measurements in 6010 to the ECG waveform. Column 6011 of section 6010 shows the name of the parameter, column 6012 shows the range of the standard data, and column 6013 shows the average data for each parameter.

Section 6020 is a color-coded key for relating some of the anatomical measurements in 6010 to the ECG waveform. For example, PA interval 6021, AH interval 6021, and HV interval 6023 of FIG. 60 are related to APD 5910 for the SAN, APD 5920 for the AVN, and APD 5930 for the HIS of

FIG. 59, respectively, through color coding. Also, ST segment 6024, T segment 6025, and Purkinje's 6026 of FIG. 60 are related to APD 5940 for the ST segment, APD 5950 the T segment, and APD 5960 and APD 5970 for the Purkinje's fibrous network, respectively, through color coding.

In various embodiments, the aiECG system described above with regard to I-Point detection and measurement is also used for APD measurement. It is a technology of integrated signal processing. It does not divide according to respective waveforms; instead, it measures each cell of APD potential, membrane potential, frequency rage, size, orientation, current, voltage, time range, and so on.

It has qualitative and quantitative data, including half sinusoidal wave signals, which cannot be identified by a user's eyes, such as shifted, buried, concerted, overlapped or lost signals. It is able to accurately navigate and detect locations of abnormal signals on the timeline.

It is able to show the signals other than the cardiac signals within the P-QRS-T-U waveform, so as to have automatic data, automatic measurement parameters within the entire ECG waveform.

Conventionally, the ST segment is the criterion used to determine myocardial ischemia and myocardial infarction. However, the ST segments of many patients do not show any elevation or drop, or disappear altogether, or the J point may disappear. Hence, the ST segments of many patients cannot be detected. More importantly, the ST segments of many people in normal condition show elevations. In traditional ECG, the ST segments of many individuals in normal condition are very similar to that of a patient; as for the ST segments of patients, they are either similar to that of a normal person or cannot be detected or measured. In addition, traditional ECG has standard digital parameters, yet they cannot be applied clinically. Traditional ECG lacks a digital unified standard to confirm the identification and determination of individual morphological waveform. In many cases, it is unknown if the identification and determination are correct. For the same ECG detection image, different reviewers may reach different conclusions, or various determinations are made for the same ECG result. Therefore, the object of the present application is to solve the clinical issues mentioned above.

The present invention is able to solve the biggest current clinical ECG ambiguities, and can be used in many medical devices related to cardiac electric signal, such as Vital Signs Monitor, Holter, treadmill exercise testing (TET), noninvasive ECG, invasive method of intracardiac electrogram and so on. It is mainly used to detect ECG abnormal morphological changes that are invisible to the human eye, as well as waveforms without significant changes, waveforms that cannot be measured by ECG, a half sinusoidal waveforms that are within the borderline between normal condition and abnormal condition, and so on. It is able to improve the accuracy rate, detection rate, correlation, and diagnosis rate. It is therefore the first re-creation of the ECG waveform since the development of ECG.

FIG. 61 is an exemplary plot 6100 showing APD subdivisions within the P wave, the T wave, and the QRS complex of an aiECG waveform for an abnormal patient before PCI treatment, in accordance with various embodiments. The abnormal patient in this case is a 55 year-old male with an 80% left anterior descending (LAD) blockage and an 80% left circumflex artery (LCX) blockage.

FIG. 62 is an exemplary table 6200 showing APD measurement data corresponding to the aiECG waveform of FIG. 61, in accordance with various embodiments.

FIG. 63 is an exemplary plot 6300 showing APD subdivisions within the P wave, the T wave, and the QRS complex of an aiECG waveform for the abnormal patient of FIG. 61 after PCI treatment, in accordance with various embodiments.

FIG. 64 is an exemplary table 6400 showing APD measurement data corresponding to the aiECG waveform of FIG. 63, in accordance with various embodiments.

Before PCI treatment, the aiECG test of FIGS. 61 and 62 shows no change of ST-T. However, the APD measurement of the QRS complex 6210 in FIG. 62 is higher than the normal range and the APD measurement of the P-J interval 6220 is also a little bit higher. The P-J interval represents the interval from atrium to ventricular depolarization at the J-point. The PA, AH, and HV intervals all showed normal in P-R interval. Therefore, the abnormal position could be at the point of ventricular depolarization.

After PCI treatment, the aiECG test of FIGS. 63 and 64, show that all the abnormal parameters of the same patient are back to the normal. Specifically, the APD measurement of the QRS complex 6410 in FIG. 64 is back in the normal range and the APD measurement of the P-J interval 6420 is also back in the normal range. The similarity of the aiECG waveforms in FIGS. 61 and 63 show that even a comparison of aiECG waveforms does not easily detect an abnormality. However, a comparison of the APD measurements in FIGS. 62 and 64 does show that the measured APD quantities from aiECG are able to detect an abnormality. In other words, an abnormality can be detected using the quantitative data of aiECG, while the traditional ECG waveform does not show any abnormal characteristic. It is evidence that the quantitative data diagnosis of various embodiments can be better than a qualitative one.

FIG. 65 is an exemplary plot 6500 showing APD subdivisions within the P wave, the T wave, and the QRS complex of an aiECG waveform for an abnormal patient with a His bundle block, in accordance with various embodiments.

FIG. 66 is an exemplary table 6600 showing APD measurement data corresponding to the aiECG waveform of FIG. 65, in accordance with various embodiments. Table 6600 shows seven abnormal average APD values 6610, 6620, 6630, 6640, 6650, 6660, and 6670. Although all seven values are outside of the normal range, PR interval 6610, HV interval 6620, and PJ interval 6670 deviate from normal much more than the other values. Since HV interval 6620 is a subset of both PR interval 6610 and PJ interval 6670, it seems likely that this is location of the block.

However, it is not clear what part of HV interval 6620 is causing the abnormality. HV interval 6620 is composed of the His bundle and bundle branches. It is known that if the bundle branches are abnormal, the QRS complex would show an abnormality. But, the APD 6650 of the QRS complex is just slightly outside of the normal range. This means that the large deviation of HV interval 6620 is caused by abnormality in the His bundle.

In various embodiments, obtaining APD measurements from aiECG can provide similar results to an intracardiac electrophysiology study (EPS). In an EPS, catheters are placed inside a heart. Some of the catheters are used to stimulate the heart muscles, while other catheters record the result of the stimulation. In this way, the location of arrhythmias, for example, can be determined.

FIG. 67 is an exemplary electrogram 6700 from an intracardiac electrophysiology study (EPS) for a 58-year-old female with a first-degree atrioventricular block. Electrogram 6700 shows a P1 AH interval measurement 6710 of 150 ms and HV interval measurement 6720 of 55 ms, a P2

AH interval measurement 6730 of 150 ms and HV interval measurement 6740 of 56 ms, and a P3 AH interval measurement 6750 of 148 ms and HV interval measurement 6760 of 55 ms.

FIG. 68 is an exemplary plot 6800 of an aiECG waveform obtained for the same 58-year-old female with a first-degree atrioventricular block of FIG. 67, in accordance with various embodiments. Plot 6800 shows a P1 AH interval measurement 6810 of 148 ms and HV interval measurement 6820 of 54 ms, a P2 AH interval measurement 6830 of 150 ms and HV interval measurement 6840 of 53 ms, and a P3 AH interval measurement 6850 of 146 ms and HV interval measurement 6860 of 55 ms. A comparison of FIG. 67 and FIG. 68 shows that aiECG can provide the same quantitative data as an intracardiac EPS.

FIG. 69 is an exemplary electrogram 6900 from an intracardiac electrophysiology study (EPS) for a 68-year-old female with a complete right bundle branch block and a left anterior fascicular block. Electrogram 6900 shows a first beat AH interval measurement 6910 of 70 ms and HV interval measurement 6920 of 58 ms and a second beat AH interval measurement 6930 of 78 ms and blocked measurement 6940 to QRS of 364 ms.

FIG. 70 is an exemplary plot 7000 of an aiECG waveform obtained for the same 68-year-old female with a complete right bundle branch block and a left anterior fascicular block of FIG. 69, in accordance with various embodiments. Plot 7000 shows a first beat AH interval measurement 7010 of 69 ms and HV interval measurement 7020 of 57 ms and a second beat AH interval measurement 7030 of 80 ms and blocked measurement 7040 to QRS of 359 ms. Again, a comparison of FIG. 69 and FIG. 70 shows that aiECG can provide the same quantitative data as an intracardiac EPS. P Wave Subdivision Detection and Measurement System

The systems of the '204 Patent and the '930 Patent have used different signal processing methods to detect the harmonic signals and discontinuity points of a conventional ECG waveform. In various embodiments, artificial intelligence (AI) in conjunction with a database of normal and abnormal ECG data is used to measure and annotate a subdivision of the P wave of an ECG waveform during measurement of the ECG waveform. This system is referred to as an aiECG system or a system for performing aiECG, for example.

Returning to FIG. 37, electrodes 3710 are attached to the skin of a patient in a noninvasive measurement, for example. In an alternative embodiment, electrodes 3710 are attached directly on the surface of a beating heart of a patient. Electrical signals produced by a beating heart are detected between pairs of electrodes 3710.

A voltage signal is detected between two electrodes 3710 by detector 3720. Detector 3720 also amplifies the voltage signal. Detector 3720 converts the electrical impulses to an ECG waveform for each heartbeat of the beating heart. Detector 3720 converts the voltage signal to a digital voltage signal using an analog to digital converter (A/D), for example. Detector 3720 provides the detected and amplified voltage signal from each pair of electrodes 3710 directly to display device 3740 to display the ECG waveform. The ECG waveform includes conventional P, Q, R, S, T, U, and J waveforms, for example. Detector 3720 also provides the detected and amplified voltage signal from each pair of electrodes 3710 directly to processor 3730.

Processor 3730 can be a separate electronic device that can include, but is not limited to, an application specific integrated circuit (ASIC), a field programmable gate array (FPGA), or a general-purpose processor or computer, such

as the system of FIG. 1. Processor 3730 can be software implemented on another processor of the ECG device, such as a processor of display device 3740. Processor 3730 can also include a remote server computer.

Processor 3730 performs a number of steps. In step (a), processor 3730 receives the ECG waveform for at least one heartbeat from detector 3720. Processor 3730 converts the ECG waveform to a frequency domain waveform. Processor 3730 separates the frequency domain waveform into two or more different frequency domain waveforms. Processor 3730 converts the two or more different frequency domain waveforms into a plurality of time domain cardiac electrophysiological subwaveforms and discontinuity points between these subwaveforms of the ECG waveform.

In step (b), processor 3730 compares the plurality of subwaveforms and discontinuity points to a database (not shown) of subwaveforms and discontinuity points for cardiac electrophysiological signals of ECG waveforms for a plurality of known and normal and abnormal patients. In step (c), processor 3730 identifies a first discontinuity point of the plurality of subwaveforms and discontinuity points as a starting point of a subdivision of a P wave of the ECG waveform and identifies a second discontinuity point of the plurality of subwaveforms and discontinuity points as an ending point of the P wave subdivision based on the comparison. In step (d) processor 3730 calculates an APD for the P wave subdivision from the first discontinuity point and the second discontinuity point.

Display device 3740 is an electronic display device, a printer, or any combination of the two. Display device 3740 displays the ECG waveform for the at least one heartbeat of the beating heart. Display device 3740 also displays a location of the P wave subdivision on the ECG waveform and displays the calculated APD for the P wave subdivision. The P wave subdivision can be, but is not limited to, an AH interval, a PH interval, or an HV interval.

In various embodiments, processor 3730 further identifies a first discontinuity point of the plurality of subwaveforms and discontinuity points as a starting point of a subdivision of a T wave of the ECG waveform and identifies a second discontinuity point of the plurality of subwaveforms and discontinuity points as an ending point of the T wave subdivision based on the comparison. Processor 3730 then calculates an APD for the T wave subdivision from the first discontinuity point and the second discontinuity point. Display device 3740 further displays a location of the T wave subdivision on the ECG waveform and displays the calculated APD for the T wave subdivision. The T wave subdivision can be, but is not limited to, an ST segment or a T segment.

In various embodiments, processor 3730 further identifies a first discontinuity point of the plurality of subwaveforms and discontinuity points as a starting point of a subdivision of a QRS complex of the ECG waveform and identifies a second discontinuity point of the plurality of subwaveforms and discontinuity points as an ending point of the QRS complex subdivision based on the comparison. Processor 3730 then calculates an APD for the QRS complex subdivision from the first discontinuity point and the second discontinuity point. Display device 3740 further displays a location of the QRS complex subdivision on the ECG waveform and displays the calculated APD for the QRS complex subdivision. The QRS complex subdivision can be, but is not limited to, a subdivision of a Q wave that represents conduction through a Purkinje's fibrous network or a subdivision of an S wave that represents conduction through a Purkinje's fibrous network.

In various embodiments, display device 3740 displays a location of the P wave subdivision on the ECG waveform, a location of the T wave subdivision on the ECG waveform, or a location of the QRS complex subdivision on the ECG waveform by color coding the location by color coding the location.

In various embodiments, processor 3730 further, for each of two or more heartbeats, performs steps (a)-(d), producing two or more APDs for the P wave subdivision, calculates an average APD from the two or more APDs and the display device further displays the average APD along with a range of normal values for the P wave subdivision.

Similarly, in various embodiments, processor 3730 further, for each of two or more heartbeats, performs steps (a)-(d), producing two or more APDs for the T wave subdivision, calculates an average APD from the two or more APDs and the display device further displays the average APD along with a range of normal values for the T wave subdivision.

Also, in various embodiments, processor 3730 further, for each of two or more heartbeats, performs steps (a)-(d), producing two or more APDs for the QRS complex subdivision, calculates an average APD from the two or more APDs and the display device further displays the average APD along with a range of normal values for the QRS complex subdivision.

Method for Measuring and Annotating a P Wave Subdivision

FIG. 71 is a flowchart showing a method 7100 for measuring and annotating a subdivision of the P wave of an ECG waveform during measurement of the ECG waveform, in accordance with various embodiments.

In step 7110 of method 5800, electrical impulses are received from a beating heart using two or more electrodes. In step 7120, the electrical impulses are detected from at least one pair of electrodes of the two or more electrodes and converted to an ECG waveform for each heartbeat of the beating heart using a detector.

In step 7130, the ECG waveform for at least one heartbeat is received from the detector, the ECG waveform is converted to a frequency domain waveform, the frequency domain waveform is separated into two or more different frequency domain waveforms, and the two or more different frequency domain waveforms are converted into a plurality of time domain cardiac electrophysiological subwaveforms and discontinuity points between these subwaveforms of the ECG waveform using a processor.

In step 7140, the plurality of subwaveforms and discontinuity points are compared to a database of subwaveforms and discontinuity points for cardiac electrophysiological signals of ECG waveforms for a plurality of known and normal and abnormal patients using the processor.

In step 7150, a first discontinuity point of the plurality of subwaveforms and discontinuity points is identified as a starting point of a subdivision of a P wave of the ECG waveform and a second discontinuity point of the plurality of subwaveforms and discontinuity points is identified as an ending point of the P wave subdivision based on the comparison using the processor.

In step 7160, an APD for the P wave subdivision is calculated from the first discontinuity point and the second discontinuity point using the processor

In step 7170, the ECG waveform for the at least one heartbeat of the beating heart is displayed, a location of the P wave subdivision is displayed on the ECG waveform, and the calculated APD for the P wave subdivision is displayed using a display device.

MI Standard without Changes to ST Segment

As described above, ECG itself is a “qualitative” diagnosis method based on changes of waveform morphology patterns. However, many characteristics of morphological waveform stay unchanged or have no patterns. In the case that the waveform stays unchanged at the ST segment, there is a need to establish a standard for myocardial infarction (MI) without changes in the ST segment.

In various embodiments, systems and methods measure points between other segments in traditional ECG images to establish a standard for diagnosing MI without using changes in the ST segment.

FIG. 72 is a plot 7200 of an exemplary ECG waveform showing measurement points along the isoelectric line of the ECG waveform, in accordance with various embodiments. Isoelectric line 7210 includes P-point 7211, P'-point 7212, I-point 7213, J-point 7214, and T'-point 7215.

In various embodiments, in order to determine the measurement points, systems and methods first make a comprehensive analysis of the ST segment and analyze the time periods of other ECG waveforms. Electro physiologically, the ST segment is located at the repolarized area of ventricular septum and the apex of the heart, it also partly overlaps the depolarized area of middle-and-posterior ventricular free wall. Anatomically, the ST segment is the joint of Purkinje fibers end and endocardium. It is part of the repolarized ventricular muscle.

FIG. 73 is a plot 7300 of an exemplary ECG waveform showing measurement points along elevated or descended lines with respect to the isoelectric line of the ECG waveform and in relation to the ST segment and PR segment of the ECG waveform, in accordance with various embodiments. FIG. 73 shows elevated line 7320, elevated line 7330, and descended line 7340 with respect to isoelectric base line 7310. Elevated line 7320 includes elevated P-point 7321. Elevated P-point 7321 has a P-point value 7326. Elevated line 7330 includes elevated T'-point 7335. Elevated T'-point 7335 has a T'-point value 7336. Descended line 7340 includes descended J-point 7344. Descended J-point 7344 has a J-point value 7346. Isoelectric base line 7310 includes I-point 7313. J-point 7344 is the starting point of ST segment 7349. I-point 7313 is the ending point of PR segment 7339.

The ventricular free wall is a 360° cone-shaped myocardial tissue. During the conductive process, myocardial cells observe the following conductive order: from the ventricular septum, the front, middle and rear part of apex of heart to the anterior, central and posterior part of the ventricular free wall. According to ionic theory, it is located at phase II where sodium and potassium have the most active exchanges during loading the ion pump.

Physiologically and anatomically, the QRS of an ECG is a depolarization process, the QR time-course is the depolarization of the corresponding ventricular septum and apex of heart, and the RS time-course is the depolarization of corresponding anterior ventricular wall. J-point 7344 is the starting point of ST segment 7349, which refers to a resting potential after the depolarization of ventricular and before the repolarization of ventricular, corresponding to the heart apex of ventricular septum. The time course from the end of ST segment 7349 to the T peak corresponds to the anterior part of ventricular free wall. The time course from the T peak to the end of the T wave corresponds to the middle and posterior part of ventricular wall. The portion between the end of T wave and the start of P wave at the next heartbeat corresponds to the time course when negative after-potentials are produced by each part and Purkinje's fibers are repolarized.

There are two equipotential lines on the right and left sides of the QRS. On the left side of the QRS is PR segment 7339, which is shown as one equipotential line. On the right side of the QRS is S-T segment 7349, which is shown as another equipotential line. PR segment 7339 and the start of P wave (pacemaker of each heartbeat) are normally on the same equipotential line, but not FIG. 73. ST segment 7349 and the end of T wave (pace-ending of each heartbeat) are normally on the same equipotential line after the T wave to beginning of the next P wave, but not in FIG. 73.

FIG. 74 is a plot 7400 of two exemplary ECG waveforms showing a TP segment between them, in accordance with various embodiments. TP segment 7410 is shown along the equipotential or isoelectric line in FIG. 74. TP segment 7410 can be elevated or descended, however.

FIG. 75 is a plot 7500 of two exemplary ECG waveforms showing an elevated TP segment between them, in accordance with various embodiments. TP segment 7510 is elevated above the equipotential or isoelectric line in FIG. 75.

FIG. 76 is a plot 7600 of two exemplary ECG waveforms showing a descended TP segment between them, in accordance with various embodiments. TP segment 7610 is descended below the equipotential or isoelectric line in FIG. 76.

According to the rules described above, as well as anatomy and electrophysiology combined with the distribution of ECG waveforms on the time axis, the equipotential not only exists on the ST segment in each heartbeat, but also at measuring points of other parts. And the time course for the ST segment relates to a slope (left to right; low to high) instead of a uniform zero potential line.

The myocardium's excitement, pacing, conduction, and acting go from depolarization to repolarization, by way of ventricular septum, apex of heart, the anterior, middle and posterior parts of myocardial free wall successively. Not all of these parts will show during the time course of the ST segment, characteristic changes will show not only at the repolarized the ST segment, and the abnormality of ventricular muscle occurs not only at the repolarized ST segment either. As for the ST segment, only 25% is covered by ventricular free wall. The American Heart Association (AHA) website shows that normal ECG detection rates for the first time and repetitions are respectively at 17% and 25%, which is based on comprehensive patterns analysis.

In the long history of ECG discipline, ECG refers to the scanning record diagram of electrophysiological signals at each heartbeat within a specified period. It is necessary to state that the ST segment and the T segment are the repolarized parts during the conduction of ventricular muscle. According to clinical application guidelines on standard values in cardiovascular field, as well as all other books, only the ST interval standard normal value is less than 380 ms. The ST interval consists of the ST segment and the T segment, but no specific reference value has yet been found for ST segment and T segment. As the ECG cannot be measured, ST-T is a sine wave from the parallel equipotential line to the half arc. ECG is a linear wave with continuous potential, there is no small wave or incisures in the middle of the ST-T, and it cannot separate ST segment from T segment.

For years, there are no ST segment changes (elevation or depression) in many CAD and AMI patients. In various embodiments, the measuring point for trend diagnostic criteria turns to the J-point which is the starting point of ST segment, so it is easier to determine whether there is elevation or depression between X axis and Y axis. It is

easier to determine J-point characteristics, while that is not true for the ST segment. Not all the myocardial cells with rotational structure of layers in clockwise or anti-clockwise direction will suffer from myocardial infarction, because the damaged areas of myocardial wall may be at different positions, such as the front, rear, left, right, upper and lower parts, as well as different layers, such as the inner, middle and outer layers. Myocardial infarction occurs when the amount of ischemic myocardial cells is more than 30%. So, the point changes on the equipotential line may occur not only at the J-point (ST segment), but also are related to ventricular muscle structure three-dimensional orientations and spatial relationships, etc.

With a lot of research results from animal experiments on MI Model as well as the comparison of a large number of clinical CAD and AMI patients before and after the PTCA or PCI treatment, 3 addition quantitative testing points were found located at the intersection points between Y axis and the equipotential line, and the TP segment.

FIG. 77 is a plot 7700 of an ECG for a normal 59-year-old male showing that even for normal people there can be a slight elevation of measurement points above the equipotential line, in accordance with various embodiments. In FIG. 77, P-point 7710, P'-point 7720, and I-point 7730 are generally along the equipotential line. J-point 7740 and T'-point 7750 are slightly elevated about the equipotential line.

FIG. 78 is a plot 7800 of an ECG for a 55-year-old male with an LAD 90% blockage before PCI showing an elevated P-point and an elevated T'-point but a normal ST segment, in accordance with various embodiments. P-point 7810 and T'-point 7850 are shown elevated in FIG. 78.

FIG. 79 is a plot 7900 of an ECG for the same patient shown in FIG. 78 after PCI showing that the P-point and the T'-point have returned to the equipotential line, in accordance with various embodiments. P-point 7910 and T'-point 7950 have now returned to the equipotential line.

FIG. 80 is a plot 8000 of an ECG for a 62-year-old female with an LAD 60% blockage and RCA 90% blockage before PCI showing an elevated P-point and an elevated T'-point but a normal ST segment, in accordance with various embodiments. P-point 8010 and T'-point 8050 are shown elevated in FIG. 80.

FIG. 81 is a plot 8100 of an ECG for the same patient shown in FIG. 80 after PCI showing that the P-point and the T'-point have returned to the equipotential line, in accordance with various embodiments. P-point 8110 and T'-point 8150 have now returned to the equipotential line.

From experiments like these, it was found that within the waveforms of the traditional ECG at each heartbeat, there are 4 points on X axis zero potential line crossed by Y axis, among them J-point had previously be described. Hence the four points are named as P, I, J, and T'. The basis for the forgoing naming is as follows: P is the starting point of each pace-making process, and there is one segment on the left of pace-making, which is close to zero potential line, which is named as P-point.

I was the ending point of P-R segment, and there is one segment on the left of QRS, which is close to the parallel zero potential line. It and the J point on the right of QRS correspond to each other to form the equilibrium potential. J-point has been named in ECG discipline and the letter J comes after I, so this is the reason why I-point receives its name.

J-point was named previously, which is the starting point of ST segment. It is the only parameter with reference and

identification characteristic regarding the elevation or decline along the Y axis in the traditional ECG.

T' is the ending point of the main peak of T wave, and there is one segment after this point, which is close to the parallel zero potential line, which is named as T'-point. TP is one segment of potential between the end of one heartbeat and the start of next heartbeat, which is named as TP segment. And not only do those four points (P-point, I-point, J-point, T'-point) change but other points also change, including the P'-point.

These signals of electric potential energy at junction of X axis and Y axis relate to different anatomical sites, and have their own characteristics and significance. P-point is the pace of each heartbeat, and it may relate to (1) the front U wave which relates to coronary artery wave; (2) the atrium, wherein the blood supply in SAN and AVN is from coronary arteries of LCX and RCA; (3) the depolarization and repolarization of the atrium.

The following points may be easily neglected: the anatomical structure of I-point is a one-way passage, and is the ending point of P-R segment, as well as the ending point of P-R interval; in addition, it is also the starting point of Purkinje's fibers, and is the point with the most changes. In traditional ECG, J-point is the starting point of ST segment. It is also the starting point of ventricular repolarization, but it often changes even in normal people, and disappears or shifts in abnormal people, for it is strongly affected by the link-up of powerful Purkinje's fiber potential and ventricular intima.

T'-point is the ending point of T wave, of each heartbeat and ventricular repolarization. It corresponds to the back portion of the ventricular wall, which is thus easy to neglect. TP segment refers to the portion from the end of T wave and the start of the next pacing; if the detecting target is elevated or lowered on the equipotential line of TP segment, the reason for such changes varies from pathological effect, drugs to electrolyte effect, because the potential after T'-point not only relates to the negative after-potential produced by each part during the auxocardia (diastolic), but also to the repolarization of Purkinje's fibers.

Regarding the TP segment, Chikamir, et al. find that the occurrence rate for elevation is higher when the TP segment (i.e., the TP segment in this patent) is taken as the baseline, with the occurrence rate (33%) for increased lesion of the left anterior descending of coronary artery, the occurrence rate (52%) of left circumflex artery, and the occurrence rate (59%) of right coronary artery. This prediction makes sense anatomically and physiologically, because 90% of the blood supply for AVN comes from the right coronary artery (RCA), and 10% comes from the left circumflex (LCX). 55~60% of the blood supply for SAN comes from the right coronary artery (RCA), and 40~45% comes from the left circumflex (LCX). Therefore, potential anomaly in TP segment closely relates to the vasculopathy of RCA & LCX. Besides, the elevation at both T'-point and P-point directly relates to the TP segment, which can be taken as a useful reference to diagnose the stenosis in right coronary artery and left circumflex artery.

The specific site refers to the myocardial ischemia of wide inferior wall, or the myocardial ischemia of the combination of inferior wall and back wall. It is inconclusive that to what extent the T'-point and P-point are lowered should be taken as abnormal. But it is visible in the patients with ventricular hypertrophy, coronary heart disease, heart failure, cerebrovascular accident, and ones before their death. A lot of cases,

combined with early clinical diagnosis, treatment, and prevention are needed in order to lower the rate of myocardial infarction.

Regarding the normal values of these equipotential lines, there will be slight changes even for normal people along upper and lower vicinities of Y axis, with the changes ranging less than 0.05 mV. A large number of clinical studies have confirmed that the 3 equipotential measuring points and 1 interphase invented in this patent can bring clinical effect for the patients with changes of equipotential line, especially the patients with insignificant changes at P-QRS-T-U, including the patients with no change in the ST segment and the patients with disappearance or shift of J-point. They relate to the anatomical sites, the special structure of ventricle, the characteristics of excitable cells, the law of electrophysiological conduction, the synchronization of atrium and ventricle, the space phase, the negative after-potential, the repolarization potential, and so on. These new measuring methods might make up for traditional ECG measurement and judgment in which currently only J-point (ST segment) is applied clinically; more importantly, they are of diagnostic value to those patients with no changes at ST segment.

When there is no change in the traditional ECG waveform or a slight change which is difficult to determine, especially when the morphology waveform characteristics can't be analyzed "qualitatively," or when a critical condition between normal and abnormal, so that all characteristics of the traditional ECG can't be determined, the new measuring methods in this patent can make sure of enough "quantitative analysis," and improve the identification rate of ECG, as well as the detection rate, relevance, and accuracy. Especially for those CAD, AMI and ACS patients with no changes at ST segment or J point, the characteristics parts and measuring methods described herein have practical and clinical value. Applications include: traditional ECG (3/5/12/18-lead ECG), Vital Sign Monitoring, treadmill exercise testing, ECG treadmill test, Holter, invasive intracardiac electrophysiology electrograph, aiECG, cardiac ultrasonography, etc.

P-Point Detection and Measurement System

The systems of the '204 Patent and the '930 Patent have used different signal processing methods to detect the harmonic signals and discontinuity points of a conventional ECG waveform. In various embodiments, artificial intelligence (AI) in conjunction with a database of normal and abnormal ECG data is used to measure and annotate the P-point, P'-point, I-point, J-point, and T'-point, of an ECG waveform during measurement of the ECG waveform. Measurement of the I-point, J-point, and T'-point is also described above. This system is referred to as an aiECG system or a system for performing aiECG, for example.

Returning to FIG. 37, electrodes 3710 are attached to the skin of a patient in a noninvasive measurement, for example. In an alternative embodiment, electrodes 3710 are attached directly on the surface of a beating heart of a patient. Electrical signals produced by a beating heart are detected between pairs of electrodes 3710.

A voltage signal is detected between two electrodes 3710 by detector 3720. Detector 3720 also amplifies the voltage signal. Detector 3720 converts the electrical impulses to an ECG waveform for each heartbeat of the beating heart. Detector 3720 converts the voltage signal to a digital voltage signal using an analog to digital converter (A/D), for example. Detector 3720 provides the detected and amplified voltage signal from each pair of electrodes 3710 directly to display device 3740 to display the ECG waveform. The

ECG waveform includes conventional P, Q, R, S, T, U, and J waveforms, for example. Detector 3720 also provides the detected and amplified voltage signal from each pair of electrodes 3710 directly to processor 3730.

Processor 3730 can be a separate electronic device that can include, but is not limited to, an application specific integrated circuit (ASIC), a field programmable gate array (FPGA), or a general-purpose processor or computer, such as the system of FIG. 1. Processor 3730 can be software implemented on another processor of the ECG device, such as a processor of display device 3740. Processor 3730 can also include a remote server computer.

Processor 3730 receives the ECG waveform for at least one heartbeat from detector 3720. Processor 3730 converts the ECG waveform to a frequency domain waveform. Processor 3730 separates the frequency domain waveform into two or more different frequency domain waveforms. Processor 3730 converts the two or more different frequency domain waveforms into a plurality of time domain cardiac electrophysiological subwaveforms and discontinuity points between these subwaveforms of the ECG waveform.

Processor 3730 compares the plurality of subwaveforms and discontinuity points to a database (not shown) of subwaveforms and discontinuity points for cardiac electrophysiological signals of ECG waveforms for a plurality of known and normal and abnormal patients. Processor 3730 identifies a discontinuity point of the plurality of subwaveforms and discontinuity points as a P-point starting point of a P wave of the ECG waveform based on the comparison.

Display device 3740 is an electronic display device, a printer, or any combination of the two. Display device 3740 displays the ECG waveform for the at least one heartbeat of the beating heart. Display device 3740 also displays a marker at a location of the discontinuity point on the ECG waveform and identifies the marker as the P-point.

In various embodiments, processor 3730 further measures a distance from the P-point to an isoelectric line of the ECG waveform as a P-point value. This distance is measured in millivolts, for example, as shown in FIG. 78.

In various embodiments, processor 3730 identifies a second discontinuity point of the plurality of subwaveforms and discontinuity points as a T'-point end point of a T wave of the ECG waveform based on the comparison and display device 3740 further displays a second marker at a location of the second discontinuity point on the ECG waveform and identifies the second marker as the T'-point.

In various embodiments, processor 3730 further measures a distance from the T'-point to the isoelectric line of the ECG waveform as a T'-point value.

In various embodiments, display device 3740 further displays a marker between the first marker and the second marker on the ECG waveform and identifies the marker as a TP segment.

In various embodiments, processor 3730 further identifies a third discontinuity point of the plurality of subwaveforms and discontinuity points as a P'-point end point of the P wave of the ECG waveform based on the comparison and display device 3740 further displays a third marker at a location of the third discontinuity point on the ECG waveform and identifies the third marker as the P'-point.

In various embodiments, processor 3730 further measures a distance from the P'-point to the isoelectric line of the ECG waveform as a P'-point value.

In various embodiments, processor 3730 further identifies a fourth discontinuity point of the plurality of subwaveforms and discontinuity points as an I-point starting point of a QRS complex of the ECG waveform based on the comparison and

display device **3740** further displays a fourth marker at a location of the fourth discontinuity point on the ECG waveform and identifies the fourth marker as the I-point.

In various embodiments, processor **3730** further measures a distance from the I-point to the isoelectric line of the ECG waveform as an I-point value.

In various embodiments, processor **3730** further identifies a fifth discontinuity point of the plurality of subwaveforms and discontinuity points as a J-point ending point of the QRS complex of the ECG waveform based on the comparison and display device **3740** further displays a fifth marker at a location of the fifth discontinuity point on the ECG waveform and identifies the fifth marker as the J-point.

In various embodiments, processor **3730** further measures a distance from the J-point to the isoelectric line of the ECG waveform as a J-point value.

In various embodiments, if the P-point value is above a threshold elevated P-point value, the first marker is identified as elevated and if the P-point value is below a threshold descended P-point value, the first marker is identified as descended.

In various embodiments, if the first marker is identified as elevated or if the first marker is identified as descended, display device **3740** further displays a warning of a potential blockage.

In various embodiments, if the T'-point value is above a threshold elevated T'-point value, the second marker is identified as elevated and if the T'-point value is below a threshold descended T'-point value, the second marker is identified as descended.

In various embodiments, if the second marker is identified as descended, display device **3740** further displays a warning of a potential blockage.

In various embodiments, if the P'-point value is above a threshold elevated P'-point value, the third marker is identified as elevated and if the P'-point value is below a threshold descended P'-point value, the third marker is identified as descended.

In various embodiments, if the I-point value is above a threshold elevated I-point value, the fourth marker is identified as elevated and if the I-point value is below a threshold descended I-point value, the fourth marker is identified as descended.

In various embodiments, if the J-point value is above a threshold elevated J-point value, the fifth marker is identified as elevated and if the J-point value is below a threshold descended J-point value, the fifth marker is identified as descended.

Method for Measuring and Annotating the P-Point

FIG. **82** is a flowchart showing a method **8200** for measuring and annotating the P-point of an ECG waveform during measurement of the ECG waveform, in accordance with various embodiments.

In step **8210** of method **8200**, electrical impulses are received from a beating heart using two or more electrodes.

In step **8220**, the electrical impulses are detected from at least one pair of electrodes of the two or more electrodes and converted to an ECG waveform for each heartbeat of the beating heart using a detector.

In step **8230**, the ECG waveform for at least one heartbeat is received from the detector, the ECG waveform is converted to a frequency domain waveform, the frequency domain waveform is separated into two or more different frequency domain waveforms, and the two or more different frequency domain waveforms are converted into a plurality of time domain cardiac electrophysiological subwaveforms

and discontinuity points between these subwaveforms of the ECG waveform using a processor.

In step **8240**, the plurality of subwaveforms and discontinuity points are compared to a database of subwaveforms and discontinuity points for cardiac electrophysiological signals of ECG waveforms for a plurality of known and normal and abnormal patients using the processor.

In step **8250**, a discontinuity point of the plurality of subwaveforms and discontinuity points is identified as a P-point starting point of a P wave of the ECG waveform based on the comparison using the processor.

In step **8260**, the ECG waveform for the at least one heartbeat of the beating heart is displayed, a marker at a location of the discontinuity point is displayed on the ECG waveform, and the marker is identified as the P-point using a display device.

Further, in describing representative embodiments of the present invention, the specification may have presented the method and/or process of the present invention as a particular sequence of steps. However, to the extent that the method or process does not rely on the particular order of steps set forth herein, the method or process should not be limited to the particular sequence of steps described. As one of ordinary skill in the art would appreciate, other sequences of steps may be possible. Therefore, the particular order of the steps set forth in the specification should not be construed as limitations on the claims. In addition, the claims directed to the method and/or process of the present invention should not be limited to the performance of their steps in the order written, and one skilled in the art can readily appreciate that the sequences may be varied and still remain within the spirit and scope of the present invention.

What is claimed is:

1. A noninvasive electrocardiography (ECG) system for measuring and annotating the P-point of an ECG waveform during measurement of the ECG waveform, comprising:

two or more electrodes adapted to be located near a beating heart of a patient and attached to the skin of the patient that receive electrical impulses from the beating heart;

a detector that detects the electrical impulses from at least one pair of electrodes of the two or more electrodes and converts the electrical impulses to an ECG waveform for each heartbeat of the beating heart;

a processor that

receives the ECG waveform for at least one heartbeat from the detector, converts the ECG waveform to a frequency domain waveform, separates the frequency domain waveform into two or more different frequency domain waveforms, and converts the two or more different frequency domain waveforms into a plurality of time domain cardiac electrophysiological subwaveforms and discontinuity points between these subwaveforms of the ECG waveform,

compares the plurality of subwaveforms and discontinuity points to a database of subwaveforms and discontinuity points for cardiac electrophysiological signals of ECG waveforms for a plurality of known and normal and abnormal patients, and identifies a discontinuity point of the plurality of subwaveforms and discontinuity points as a P-point starting point of a P wave of the ECG waveform based on the comparison; and

a display device that displays the ECG waveform for the at least one heartbeat of the beating heart, displays a

first marker at a location of the discontinuity point on the ECG waveform, and identifies the first marker as the P-point.

2. The ECG system of claim 1, wherein the processor further measures a distance from the P-point to an isoelectric line of the ECG waveform as a P'-point value.

3. The ECG system of claim 2, wherein the processor further identifies a second discontinuity point of the plurality of subwaveforms and discontinuity points as a T'-point end point of a T wave of the ECG waveform based on the comparison and the display device further displays a second marker at a location of the second discontinuity point on the ECG waveform and identifies the second marker as the T'-point.

4. The ECG system of claim 3, wherein the processor further measures a distance from the T'-point to the isoelectric line of the ECG waveform as a T'-point value.

5. The ECG system of claim 4, wherein the processor further identifies a third discontinuity point of the plurality of subwaveforms and discontinuity points as a P'-point end point of the P wave of the ECG waveform based on the comparison and the display device further displays a third marker at a location of the third discontinuity point on the ECG waveform and identifies the third marker as the P'-point.

6. The ECG system of claim 5, wherein the processor further measures a distance from the P'-point to the isoelectric line of the ECG waveform as a P'-point value.

7. The ECG system of claim 6, wherein the processor further identifies a fourth discontinuity point of the plurality of subwaveforms and discontinuity points as an I-point starting point of a QRS complex of the ECG waveform based on the comparison and the display device further displays a fourth marker at a location of the fourth discontinuity point on the ECG waveform and identifies the fourth marker as the I-point.

8. The ECG system of claim 7, wherein the processor further measures a distance from the I-point to the isoelectric line of the ECG waveform as an I-point value.

9. The ECG system of claim 8, wherein the processor further identifies a fifth discontinuity point of the plurality of subwaveforms and discontinuity points as a J-point ending point of the QRS complex of the ECG waveform based on the comparison and the display device further displays a fifth marker at a location of the fifth discontinuity point on the ECG waveform and identifies the fifth marker as the J-point.

10. The ECG system of claim 9, wherein the processor further measures a distance from the J-point to the isoelectric line of the ECG waveform as a J-point value.

11. The ECG system of claim 10, wherein, if the P-point value is above a threshold elevated P-point value, the first marker is identified as elevated and if the P-point value is below a threshold descended P-point value, the first marker is identified as descended.

12. The ECG system of claim 11, wherein, if the first marker is identified as elevated or if the first marker is identified as descended, the display device further displays a warning of a potential blockage.

13. The ECG system of claim 10, wherein, if the T'-point value is above a threshold elevated T'-point value, the second marker is identified as elevated and if the T'-point value is below a threshold descended T'-point value, the second marker is identified as descended.

14. The ECG system of claim 13, wherein, if the second marker is identified as elevated or if the second marker is identified as descended, the display device further displays a warning of a potential blockage.

15. The ECG system of claim 10, wherein, if the P'-point value is above a threshold elevated P'-point value, the third marker is identified as elevated and if the P'-point value is below a threshold descended P'-point value, the third marker is identified as descended.

16. The ECG system of claim 10, wherein, if the I-point value is above a threshold elevated I-point value, the fourth marker is identified as elevated and if the I-point value is below a threshold descended I-point value, the fourth marker is identified as descended.

17. The ECG system of claim 3, wherein the display device further displays a marker between the first marker and the second marker on the ECG waveform and identifies the marker as a TP segment.

18. The ECG system of claim 10, wherein, if the J-point value is above a threshold elevated J-point value, the fifth marker is identified as elevated and if the J-point value is below a threshold descended J-point value, the fifth marker is identified as descended.

19. A method for detecting and annotating the P-point of an electrocardiography (ECG) waveform during measurement of the ECG waveform, comprising:

receiving electrical impulses from a beating heart using two or more electrodes;

detecting the electrical impulses from at least one pair of electrodes of the two or more electrodes and converting the electrical impulses to an ECG waveform for each heartbeat of the beating heart using a detector;

receiving the ECG waveform for at least one heartbeat from the detector, converting the ECG waveform to a frequency domain waveform, separating the frequency domain waveform into two or more different frequency domain waveforms, and converting the two or more different frequency domain waveforms into a plurality of time domain cardiac electrophysiological subwaveforms and discontinuity points between these subwaveforms of the ECG waveform using a processor;

comparing the plurality of subwaveforms and discontinuity points to a database of subwaveforms and discontinuity points for cardiac electrophysiological signals of ECG waveforms for a plurality of known and normal and abnormal patients using the processor;

identifying a discontinuity point of the plurality of subwaveforms and discontinuity points as a P-point starting point of a P wave of the ECG waveform based on the comparison using the processor; and

displaying the ECG waveform for the at least one heartbeat of the beating heart, displaying a marker at a location of the discontinuity point on the ECG waveform, and identifying the markers as the P-point using a display device.

20. An invasive electrocardiography (ECG) system for measuring and annotating the P-point of an ECG waveform during measurement of the ECG waveform, comprising:

two or more electrodes placed directly on the surface of a beating heart of a patient that receive electrical impulses from the beating heart;

a detector that detects the electrical impulses from at least one pair of electrodes of the two or more electrodes and converts the electrical impulses to an ECG waveform for each heartbeat of the beating heart;

a processor that receives the ECG waveform for at least one heartbeat from the detector, converts the ECG waveform to a frequency domain waveform, separates the frequency domain waveform into two or more different frequency domain waveforms, and converts the two

or more different frequency domain waveforms into a plurality of time domain cardiac electrophysiological subwaveforms and discontinuity points between these subwaveforms of the ECG waveform, compares the plurality of subwaveforms and discontinuity points to a database of subwaveforms and discontinuity points for cardiac electrophysiological signals of ECG waveforms for a plurality of known and normal and abnormal patients, and identifies a discontinuity point of the plurality of subwaveforms and discontinuity points as a P-point starting point of a P wave of the ECG waveform based on the comparison; and a display device that displays the ECG waveform for the at least one heartbeat of the beating heart, displays a marker at a location of the discontinuity point on the ECG waveform, and identifies the marker as the P-point.

* * * * *

专利名称(译)	每个心跳等电位线附近的点量化标准升高或降低的识别方法		
公开(公告)号	US10646130	公开(公告)日	2020-05-12
申请号	US16/114025	申请日	2018-08-27
[标]申请(专利权)人(译)	陈广仁 杨荣		
申请(专利权)人(译)	陈, 广仁 杨, 荣		
当前申请(专利权)人(译)	陈, 广仁 杨, 荣		
[标]发明人	CHEN GUANGREN YANG RONG		
发明人	CHEN, GUANGREN YANG, RONG		
IPC分类号	A61B5/04 A61B5/044 A61B5/0408 A61B5/0402 A61B5/00 A61B5/0452 A61B5/0245 A61B5/0468 A61B5/0464 A61B5/0472 A61B5/0456		
CPC分类号	A61B5/0452 A61B5/725 A61B5/0408 A61B5/7257 A61B5/04012 A61B5/04023 A61B5/044 A61B5/ /7267 A61B5/0245 A61B5/6823 A61B5/0464 A61B5/0472 A61B5/0456 A61B5/0468		
代理人(译)	卡莎, JOHN R.		
优先权	15/393135 2018-06-19 US 62/008435 2014-06-05 US 62/017185 2014-06-25 US 62/271699 2015-12-28 US 62/271704 2015-12-28 US 62/463662 2017-02-26 US 62/489540 2018-04-25 US 62/546461 2017-08-16 US 62/551759 2017-08-29 US		
其他公开文献	US20190015006A1		
外部链接	Espacenet		

摘要(译)

ECG系统从谐波波形中测量并注释ECG波形的P点。从跳动的心脏接收电脉冲。电脉冲被转换为ECG波形。ECG波形被转换为频域波形，该波形又被分离为两个或多个不同的频域波形，这些波形又被转换为多个时域心脏电生理子波形以及这些子波形之间的不连续点。将多个子波形和不连续点与正常和异常患者的子波形和不连续点的数据库进行比较。通过比较，将不连续点标识为ECG波形的P点。对P点，I点，J点和T点进行了类似的测量。计算从这些点到等电位线的距离，并将其用于检测导致心肌梗塞的阻塞。

